

**ANTI-INFLAMMATORY MECHANISMS OF THE
ALKYL-LYSOPHOSPHOLIPID EDELFOSE IN THE MURINE EXPERIMENTAL
AUTOIMMUNE ENCEPHALOMYELITIS AND IN HUMAN CELLS**

Dissertation

zur Erlangung der Würde des Doktors der Naturwissenschaften
des Fachbereichs Biologie, der Fakultät für Mathematik, Informatik
und Naturwissenschaften der Universität Hamburg

vorgelegt von

Pierre Abramowski

aus Peine

Hamburg 2012

Genehmigt vom Fachbereich Biologie
der Fakultät für Mathematik, Informatik und Naturwissenschaften
an der Universität Hamburg
auf Antrag von Professor Dr. R. MARTIN
Weiterer Gutachter der Dissertation:
Professor Dr. M. KNEUSSEL
Tag der Disputation: 30. März 2012

Hamburg, den 15. März 2012



Professor Dr. J. Fromm
Vorsitzender des Promotionsausschusses
Biologie

Alan Hodgkinson, MA
Grillparzerstraße 41
31224 Peine
Ehem. Englischlehrer am Ratsgymnasium Peine
Englischlehrer am Freien Gymnasium Hannover
Allgemein beeidigter Dolmetscher für das Landgericht Hildesheim

Universität Hamburg
Department Biologie
Departmentleitung
Prof. Dr. Axel Temming
Martin-Luther-King-Platz 2
20146 Hamburg

02.02.2012

Bestätigung der Korrektheit der englischen Sprache

Sehr geehrter Herr Prof. Temming,

hiermit bestätige ich, dass die Dissertation von Herrn Pierre Abramowski in korrekter englischer Sprache abgefasst ist.

Mit freundlichem Gruß,

A. Hodgkinson

Content

1	Introduction	1
1.1	<i>The immune system</i>	1
1.1.1	Innate immunity	1
1.1.2	Adaptive immunity	3
1.1.3	Immunology of the central nervous system	5
1.2	<i>Multiple Sclerosis</i>	6
1.2.1	Epidemiology and etiology of MS	7
1.2.2	Pathogenesis	8
1.2.3	Clinical course	10
1.2.4	Therapy	11
1.3	<i>Experimental autoimmune encephalomyelitis</i>	15
1.4	<i>Apoptosis</i>	17
1.5	<i>Edelfosine</i>	20
2	Aims	26
3	Materials and Methods	27
3.1	<i>Materials</i>	27
3.1.1	Reagents	27
3.1.2	Kits	30
3.1.3	ELISA	30
3.1.4	Software	30
3.1.5	Laboratory animals	31
3.1.6	Equipment	31
3.1.7	Consumables	32
3.1.8	Cell culture media	33
3.1.9	Buffers and solutions	33
3.1.10	Antibodies	35
3.2	<i>Methods</i>	37
3.2.1	Preparation of edelfosine	37
3.2.2	Active induction of EAE	37
3.2.3	Organ preparation and cell isolation from mice	38
3.2.4	Histological analysis	39
3.2.5	Flow cytometry	41
3.2.6	Isolation of human cells from blood	44
3.2.7	<i>In vitro</i> cell-culture experiments	44
3.2.8	RNA isolation, cDNA synthesis and microarray analysis	47
3.2.9	ELISA	48
3.2.10	Analysis of cytokine production by flow cytometry	49
3.2.11	Statistical analysis	49

4	Results	51
4.1	<i>Reduced proliferation of T lymphocytes in vitro in the presence of edelfosine</i>	51
4.2	<i>Edelfosine treatment influences clinical symptoms in the EAE-mouse model</i>	53
4.2.1	Preventive oral edelfosine administration reveals dose-dependent treatment effects in EAE-induced C57BL/6 mice (dose finding).....	53
4.2.2	Preventive treatment of EAE in SJL mice with edelfosine every other day has no influence on disease course.....	53
4.2.3	Preventive treatment of EAE in SJL mice with edelfosine on a daily basis ameliorates disease course	54
4.2.4	Investigation of the therapeutic effectiveness of edelfosine on EAE in SJL mice.....	54
4.3	<i>Analysis of preventive edelfosine-treatment effects in RR-EAE</i>	56
4.3.1	Preventive edelfosine treatment increases activated caspase-3 expression in the preclinical phase of RR-EAE	56
4.3.2	The proliferative capacity of T cells is not compromised after preventive edelfosine treatment in RR-EAE	68
4.3.3	CNS-infiltrating T cells appear at lower frequencies and show a higher expression of activated caspase-3 upon preventive edelfosine treatment.....	68
4.3.4	The preventive edelfosine treatment prohibits neuronal loss in acute RR-EAE	78
4.4	<i>Edelfosine interferes with human T-cell proliferation and modulates distinct signaling pathways</i>	78
4.4.1	Edelfosine induces cell death in a concentration-dependent manner in CD4+ and CD8+ T cells	78
4.4.2	Edelfosine interferes with proliferation of human PBMCs after mitogenic activation, but also with proliferation of antigen-specific T-cell lines	81
4.4.3	Whole genome expression analysis of CD4+ T cells reveals impact of edelfosine on a distinct set of signaling pathways	84
4.4.4	Edelfosine-induced downmodulation of MHC class II-surface expression of B-cell subsets	90
4.4.5	Edelfosine reduces IFN- γ secretion of stimulated CD4+ T cells.....	92
5	Discussion	95
6	Summary	119
7	Abbreviations	120
8	References	123
9	Acknowledgments	153

1 Introduction

1.1 The immune system

In 1796, Edward Jenner reported that vaccination conferred protection against smallpox infection. These pioneering observations are usually referred to as the beginning of immunological research. Nevertheless, the infectious agent was not known until Robert Koch identified microorganisms to be responsible for triggering infectious diseases. In 1890, Emil von Behring and Shibasaburo Kitasato isolated proteins with antitoxic, neutralizing activity, nowadays designated as antibodies. As recently as 1911, the word “immunology” was invented (1). At that time, Paul Ehrlich had already developed the concept claiming the co-existence of humoral and cellular immunity (2). According to his “side-chain theory” antigens interact with antibodies, but also with cellular receptors. Instead, cells were denied to participate in antibody formation and Ehrlich’s concept was rejected. This condensed retrospect of the evolution of immunological research already points to the central role of developing concepts. The acceptance and rejection of postulates promotes the progress, not exclusively in immunological sciences. Notably, Ehrlich was rehabilitated as biological research was increasingly consulted, and in 1948 the word “lymphocyte” was coined for the first time (3). In vertebrates, these seminal investigations have established the concepts of innate and adaptive immunity that interact to ensure the body’s defense against pathogens.

1.1.1 Innate immunity

Pluripotent hematopoietic stem cells (HSCs) of the bone marrow differentiate into red blood cells (erythrocytes), platelets and white blood cells (leukocytes). Leukocytes are classified as members of the myeloid or lymphoid lineage. They execute their functioning in the body’s protection from pathogens by targeted migration and residence in tissues (spleen, lymph nodes, gut etc.), circulation in the blood and the lymphatic system. The innate immune system comprises both members of the myeloid (monocytes/macrophages, granulocytes, dendritic cells (DCs)) and lymphoid (natural killer (NK) cells) lineage. Innate immunity is the first-line defense of a host against infection with a pathogen. It is non-specific and does not confer long-lasting immunity, i.e. an immunological memory. Monocytes as circulating myeloid precursors possess remarkable plasticity. In response to cytokines, they can differentiate *in vitro* into myeloid DCs (mDCs) in presence of granulocyte-macrophage colony stimulating factor (GM-CSF) and interleukin (IL)-4 (4–6) as well as macrophages by co-culture with macrophage colony-stimulating factor (M-CSF) (7). *In vivo* monocytes differentiate into macrophages after migration into the target tissue. Together with

lymphocytes and DCs, macrophages constitute mononuclear leukocytes. Monocytes and macrophages act as phagocytes of pathogens and infected/aberrant cells. Activated macrophages induce inflammation by cytokine secretion, e.g. tumor necrosis factor (TNF)- α , IL-1 β , IL-6 (8, 9). The expression of anti-inflammatory cytokines, e.g. IL-10, IL-4, tumor growth factor (TGF)- β (10), is involved in the downmodulation of the immune response. As antigen-presenting cells (APCs), they present antigenic peptides in the context of MHC class II/HLA class II to T cells thereby linking innate immunity to specific, adaptive immunity. Recruitment of monocytes/macrophages to inflammatory sites depends among other factors on very late antigen 4 (VLA-4) expression on these cells and vascular cell-adhesion molecule-1 (VCAM-1) on the surface of endothelial cells. The *de novo* expression requires several hours. Granulocytic phagocytes comprise eosinophils, basophils and neutrophils with the latter being the most abundant leukocytes in blood, circa 60% in humans (11). The selectin CD62L and integrins CD11a/b on neutrophils as well as the immunoglobulin-superfamily members intercellular adhesion molecule (ICAM)-1 and ICAM-2 are constitutively expressed or can be rapidly upregulated. Endothelial cells also possess a preformed pool of the chemokine IL-8 for neutrophil recruitment. Therefore, neutrophils are considered to be among the earliest cell types recruited to sites of inflammation, e.g. in the case of central nervous system (CNS)-inflammation in the course of experimental autoimmune encephalomyelitis (EAE) (12). Neutrophils may induce endothelial cells to secrete monocyte chemoattractant protein-1 (MCP-1), which results in enhanced macrophage recruitment (13). Besides pathogen engulfment and intracellular degradation, effector mechanisms of neutrophils are the production of reactive oxygen species (ROS) for formation of oxidative burst and neutrophil extracellular traps to fight bacterial and fungal infections. Neutrophils require a first activation step, e.g. by TNF- α , IL-8 and platelet activating factor (PAF), a process that is reported to be altered in multiple sclerosis (MS)-patients (14). DCs represent a third cell type with phagocytic activity. Derived from myeloid precursor cells, mDCs within non-lymphoid tissue and the blood take up extracellular fluid, and their encounter with pathogens (whole bacterial cells, bacterial lipopolysaccharide (LPS), viral RNA) or necrotic cell debris initiates the migration into lymph nodes. Pathogens are recognized by pattern-recognition receptors, e.g. toll-like receptors (TLRs), c-type lectin receptors and heat shock protein receptors. mDCs present degraded proteins (immunogens) in the context of MHC class I and II and upregulated co-stimulatory molecules on their surface (CD80, CD86). Besides interactions of MHC class I/II peptide and T-cell receptor (TCR) as well as co-receptors (CD4, CD8) and co-stimulatory molecules, surface adhesion molecules, e.g. DC-SIGN and LFA-1, mediate binding to antigen-specific T cells and their activation to initiate adaptive immune responses. T-cell responses (tolerance or immunity, T helper (Th) 1 or 2 differentiation) are influenced by cytokines secreted by DCs (15–17).

Activated mDCs produce, among others, IL-12 that induces Th1 differentiation but also IL-10 in favor of Th2 differentiation (18). IL-10 is not secreted by plasmacytoid DCs (pDCs). Instead, pDCs are able to produce large amounts of type I interferons. NK cells are of lymphoid origin and are considered to be cells of the innate system as they are not antigen-specific. They are effective in immune responses against intracellular pathogens and viruses. According to the “missing self” hypothesis NK cells mediate target-cell lysis of infected or mutated cells by the release of cytoplasmic granules containing perforin and granzyme as a consequence of the lack of MHC class I expression or an overexpression of ligands for NK cell receptor activation (19). NK-cell receptors specific for MHC class I comprise CD94/NKG2 (20, 21), human killer cell Ig-like receptors (KIR) (22, 23) and murine Ly49 receptors (24).

1.1.2 Adaptive immunity

The concept of T- and B-lymphocyte lineages, which are the main components of the adaptive immune system, was established in 1965 (25). Adaptive immunity is characterized by specific recognition of antigens by receptors on the surface of T cells, i.e. cellular immunity, and by antibodies, which are secreted by B cells and constitute humoral immunity. Secondly, T and B cells encode an “immunological memory” that develops during the individual’s life after encountering many different pathogens.

T cells develop in the thymus as naïve T cells. During maturation, T cells undergo several stages of selection. Immature T cells are positively selected if their TCR is able to engage self-peptide:self-MHC complexes on thymic epithelium. If the T cell is not able to recognize this complex, it is subjected to “death by neglect”, e.g. by growth-factor deprivation. The positively selected population is restricted to self-MHC and shows intermediate affinity TCRs for self-peptide:self-MHC complexes. Negative selection removes T cells with high affinity TCRs for self-peptide:self-MHC complexes via activation-induced cell death (AICD) (potentially self-reactive cells). In this way a self-tolerant population of T cells is established. Self-tolerance is a prerequisite for preserving the host’s integrity by avoiding pathological autoimmunity. Mature T cells express TCRs on the cell surface specific for a particular antigen in the context of self-MHC. As they are released from the thymus naïve T cells circulate in blood, lymph and accumulate in lymphoid tissues. If T cells encounter their specific antigen, e.g. presented by DCs, they proliferate and give rise to clones with identical receptor specificity. The TCR consists of two distinct transmembrane polypeptide chains, TCR α and TCR β , joined by a disulfide bond. Each chain consists of a variable (V) and a constant (C) domain. For recognition, antigens are displayed to T cells on MHC molecules as processed peptides. Antigens can be presented to CD8+ T cells by MHC class I molecules, which are expressed on nearly all nucleated cells. APCs as macrophages, DCs but also B lymphocytes express MHC class II molecules for the presentation of antigens to CD4+

T cells. The ability to recognize a wide range of antigenic peptides is made possible by recombination of a selected number of germline encoded TCR α and β chain gene segments that form a large number of TCR α and β chains. Polygeny, polymorphism, somatic recombination of gene segments (variable, diversity in the case of TCR β chain, and joining regions to a constant region) and the addition/deletion of nucleotides at segment junctions contribute to the diversity of TCRs and MHC molecules.

Naïve CD4⁺ T-cell differentiation into effector Th cells is triggered by the interaction of the TCR with antigen and MHC class II. The T cell:APC-complex formation is consolidated by adhesion molecules (e.g. CD2/LFA-2:CD58/LFA-3 in humans) and co-receptors (e.g. CD4:MHC class II, CD28:CD80/CD86, CTLA-4:CD80/CD86) to establish immunological synapse formation. Innate immunity shapes adaptive immunity responses by inducing and modulating complex signaling events and effector functions. Cytokines produced by cells of innate and adaptive immunity also determine the effector phenotype of a CD4⁺ T cell, for instance Th1, Th2 (26, 27), induced regulatory T cells (iTregs) (28–30) and Th17 cells (31–33). By expression of distinct surface receptors and cytokines CD4⁺ effector T cells themselves can migrate to sites of inflammation and influence the local immune response. Th1 cells produce interferon (IFN)- γ and mediate cellular immunity against intracellular pathogens. They activate macrophages also by GM-CSF and TNF- α . Th2 cells produce IL-4, IL-13 and IL-25/IL-17E and mediate the clearance of extracellular pathogens. They activate B cells but can also secrete IL-10 to dampen humoral immunity. The concept of either Th1 or Th2 differentiation of CD4⁺ T cells has been advanced following the description of Th17 cells. These cells are characterized by their production of IL-17A (in the following chapters: IL-17), IL-17F, IL-6 and IL-22. They are involved in clearing extracellular pathogens and act early in the course of an immune response thereby contributing to an efficient recruitment of neutrophils to sites of infection. Th1 differentiation can be induced by IL-12 (34) and is characterized by the expression of the master transcription factor T-bet (35). Th2 cells differentiate in response to IL-4 (36, 37) and express the transcription factor GATA3 (38). TGF- β and IL-6 are necessary to induce Th17 differentiation and transcription factor retinoic orphan receptor γ t (ROR γ t) expression (30, 31, 39, 40). Notably, ROR γ t expression is dependent on the repression of Th1 and Treg-associated transcription factors by signal transducer and activator of transcription (STAT) 3 (41, 42). IL-23 may act on committed Th17 cells to maintain and expand the effector phenotype. Effector T-cell functions need to be regulated (43). Tregs produce suppressive cytokines (IL-10, TGF- β) and are identified by the expression of the transcription factor Foxp3 (44). They are grouped into natural CD4⁺ CD25⁺ Foxp3⁺ Tregs (nTregs) originating from the thymus and iTregs (45–47). iTreg generation is induced in the periphery and necessitates TGF- β and IL-2 besides TCR stimulation. The concept of terminal CD4⁺ T cell differentiation into effector phenotypes has been established

due to the identification of unique transcription factors and the description of crossregulatory networks. As an example, IFN- γ elevates Th1-cell proliferation but in parallel interferes with Th2-cell differentiation (26). In turn, IL-4 induces Th2 but inhibits Th1 differentiation. Recently, Aly *et al.* reported on JC virus-specific CD4⁺ T cells with a bifunctional Th1-2 phenotype (48). Possibly, effector CD4⁺ T cells retain certain plasticity and probably transdifferentiation has to be taken into account. Cytotoxic CD8⁺ T cells recognize antigens presented in the context of MHC class I by infected cells. They express the CD8 co-receptor, but not CD4. Upon activation they act on the target cell by releasing perforin, granzymes and granulysin to induce apoptosis. They can express Fas ligand (FasL) thereby inducing Fas-mediated apoptosis via the death-inducing signaling complex (DISC). B lymphocytes develop in the bone marrow. They specifically bind antigen by their B-cell receptors (BCRs) to allow subsequent presentation of processed antigen peptides in the context of MHC class II. The BCR is a heterodimeric complex of membrane-bound immunoglobulin (Ig) α and β . The formation of MHC class II:peptide complexes is facilitated by the BCRs which deliver endocytosed antigen to specialized compartments. These vesicles, class II peptide loading compartments, may be derived from late endosomes/early lysosomes and allow the efficient loading of MHC class II molecules. Naïve mature B cells express IgM and IgD on their surface but during antigen encounter B cells may undergo a class switch to produce IgG, IgA and IgE, a process that is influenced by Th cells. Notably, the antigen specificity remains conserved. B cells proliferate and differentiate into either antibody-producing plasma B cells or memory B cells.

1.1.3 Immunology of the central nervous system

The immune responses initiated by innate and adaptive immunity are convenient to antagonize infections and tissue damage. However, the mechanisms underlying inflammation are not of advantage for some specialized tissues, for instance the central nervous system (CNS). The recruitment of immune cells to inflamed tissue is facilitated by increased blood-vessel permeability, chemokine guidance and cell adhesion molecule upregulation on endothelial cells. As a result vasodilatation increases the local blood flow, fluid accumulates and swelling is observable. The brain (skull) and the spinal cord (spinal column) are enclosed by rigid bone. Moreover, the CNS is separated from the bone by durable meninges. The dura mater is closest to the bone, followed by the intermediate arachnoid mater and the pia mater enveloping the CNS. Thus, in the case of the CNS this inflammatory swelling will elevate the pressure on the tissue, suppress arterial blood supply and lead to ischemic damage. Adult CNS neurons display a tightly regulated cell cycle resulting in a “post-mitotic” state and they are restricted in their regeneration. Therefore, neuronal damage will be mostly irreversible. To still allow immune surveillance the CNS

necessitates the unique immune responses of an immunologically privileged site. In normal CNS tissue MHC class II expression is absent and limited to activated microglia during inflammation. Physiologically, the CNS lacks the lymphatic vessels that drain tissues of the periphery. However, distinct efferent and afferent pathways connect CNS and periphery (49). Additionally, the pia mater is percolated with blood vessels to supply the CNS. These pathways are controlled by the meninges, the blood-brain barrier (BBB) and the blood-cerebrospinal fluid (CSF)-barrier (50). The BBB is a barrier between cerebral blood vessels and the parenchyma composed of endothelial cells, pericytes, basement membrane and nearby astrocytes. The blood-CSF-barrier separates the choroid plexus blood vessels from the CSF, which is synthesized at the choroid plexus, and restricts passage of molecules by epithelial cells connected by apical tight junctions. In order to allow immunological control molecules from the CNS parenchyma are transported to cervical lymph nodes (51) and leukocytes transmigrate from the blood capillaries into the CSF-filled subarachnoid cavity or perivascular parenchyma (52).

1.2 Multiple Sclerosis

MS was first systematically described as a clinical entity by Jean-Martin Charcot in 1868 as “sclérose en plaque disséminée” (53) in an attempt to differentiate a condition of younger patients from the paralysis agitans introduced 1817 by James Parkinson (54). He attributed to MS a pattern of tremor, paralysis and, at autopsy, grey patches (plaques) scattered throughout the brain, brain stem and the spinal cord. The concept of MS as an autoimmune disease developed following transfer experiments of spinal cord and brain homogenates into healthy primates, which then showed a disease similar to MS (55, 56).

Clinically, the majority of MS patients presents with a relapsing-remitting course of MS with recurrent disease bouts. In contrast, the primary-progressive course of MS, characterized by a steady progression of disability, is much more infrequent. MS affects women twice as often as men. Hallmarks of MS pathology are inflammatory lesions within the CNS, de- and remyelination of axons, axonal loss and atrophy. Since its initial description MS was studied in order to identify the natural cause of MS. This question is addressed also with the help of animal models, which can be induced to develop MS-like disease. Animal and human studies point to a central role for autoreactive CD4+ T cells in MS pathology. These cells are part of CNS- and CSF-infiltrating cells in MS. Further, albeit indirect evidence for their role stems from the observation that a large fraction of the genetic risk of MS is conferred by the HLA class II molecules HLA-DR and –DQ.

Therefore, MS is considered to be a CD4+ Th cell-mediated demyelinating autoimmune disease of the CNS. Both the immune system and the CNS may determine the disease

process and the clinical course (57). Research and therapy of MS have focused primarily on the immunological part of MS. Neurodegenerative aspects, neuronal damage and repair have recently gained more interest, and it will be important in the near future to develop treatments addressing these aspects as well as advancing our understanding on the etiology and pathogenesis even further.

1.2.1 Epidemiology and etiology of MS

MS affects predominantly young people between 20 and 40 years of age (58, 59). There are 250,000 to 350,000 people affected by MS in the USA (60). In Europe, the estimated prevalence rate is 83 per 100,000 (61). In average, 60 to 200 people per 100,000 are diagnosed with MS in Northern Europe and North America compared to 6 to 20 per 100,000 in areas of low risk, e.g. Japan (57). The north-to-south gradient in MS prevalence on the northern hemisphere as well as the opposite situation on the southern hemisphere underline the influence of the environment on MS etiology. A genetic contribution to MS development was implied by studies of family members of MS patients (62–64). First-degree relatives of MS patients show a 20- to 50-fold higher risk (2 to 5%) to develop MS, and the concordance rate in monozygotic twins is at circa 25%. Studies on adoptees in MS families underline a higher contribution of the genetic risk to MS susceptibility compared to environmental influences (65). To identify responsible susceptibility genes large genomic screens have been performed pointing to a prominent role for gene sections on chromosome 6p21 (66). Interestingly, these sections are part of the MHC that is suspected of mediating 10 to 60% of the genetic risk in MS thereby linking MS to the immune system (67–69). In MS risk is conferred by HLA-DR and –DQ. In Caucasians MS is strongly associated with the DR15 haplotype, which contains DRB1*15:01, DRB5*01:01, DQA1*01:02 and DQB1*06:02 (70). By far most of the risk stems, however, from the two DR alleles themselves. Variations in the two cytokine receptors IL-7RA and IL-2RA and in numerous other genes have been described as additional risk alleles for MS (71–74). A recently published very large genome-wide association study shows 52 single nucleotide polymorphisms besides HLA-DR as risk alleles for MS (69), and interestingly, almost all of these are involved in T-cell activation and function. Furthermore, three environmental risk factors (Epstein-Barr virus (EBV) infection (75–77), low vitamin D levels (78–80) and smoking (81)) have now been firmly established. Viral infections are proposed to induce the expansion of autoreactive T cells, either by molecular mimicry or by bystander activation (82). The fact that women are affected by MS circa twice as often as men (1.6 to 2.0:1.0) implies differential hormone levels as additional risk factors in MS. Although the current understanding of MS etiology is not complete the following concept may apply: the disease may preferentially occur in genetically predisposed

people after encounter of environmental triggers that in succession lead to the activation of self-reactive T cells which may have escaped negative selection.

1.2.2 Pathogenesis

The central role of CD4⁺ T cells in MS pathogenesis is underlined by multiple lines of evidence. CD4⁺ T cells are present in CNS and CSF cellular infiltrates in both MS and EAE (83, 84), a model disease for MS that can be induced in animals. HLA class II molecules are the strongest genetic risk factors for MS. Their biological function is the presentation of antigens. EAE is induced actively with CNS homogenate or, more precisely, also by injection of myelin components into healthy, susceptible animals to trigger a CD4⁺ T cell-mediated MS-like disease (85–87). The importance of CD4⁺ T cells is highlighted by adoptive transfer experiments of EAE-induced animal-derived, *in vitro* reactivated myelin peptide-specific CD4⁺ T cells into naïve animals (passive induction) (86, 88). EAE cannot be induced by antibody transfer. Transgenic mice expressing myelin-specific murine TCRs restricted to MHC class II develop EAE (89, 90). EAE-derived findings were linked to MS by humanized mouse models transgenic for HLA-DR or -DQ molecules (91–93). Mice were susceptible to EAE, and mice that expressed both MS-linked DR molecules together with the myelin basic protein (MBP)-specific TCR derived from an MS patient were shown to develop spontaneous or induced EAE (94, 95). Furthermore, the therapeutic approach to treat MS patients with an altered peptide ligand of MBP₍₈₃₋₉₉₎ activated cross-reactive CD4⁺ T cells with Th1 phenotype. Notably, the trial led to MS exacerbations (96, 97). MBP, myelin oligodendrocyte glycoprotein (MOG) and the most abundant CNS-myelin protein proteolipid protein (PLP) are potential targets for autoreactive CD4⁺ T cells. These proteins are constituents of the myelin sheath wrapped around axons of neurons. Non-myelin candidates for autoantigens are the small heat shock protein α B-C (α -B crystalline) (98, 99), transaldolase-H (100), neurofilament M (101), neuron-specific enolase and arrestin (102).

CD4⁺ autoreactive Th1 cells are considered an important subset in MS and EAE pathogenesis. Myelin-specific Th1 cells produce large amounts of proinflammatory IFN- γ and TNF- α (103–105). The involvement of IFN- γ in MS is emphasized by disease exacerbations after administration of IFN- γ (106). Like Th1 also Th17 cells can induce adoptive transfer EAE but differences in the pathological presentation were reported (107). IL-17 production by human Th17 cells in the CNS of MS patients may reflect active disease (108, 109). Thus, both Th1 and Th17 cells are involved in MS pathology, although the data is overall much weaker for an involvement of Th17 cells.

Mechanistically, (auto)antigens are presented to autoreactive/crossreactive CD4⁺ T cells in the periphery. T-cell priming and activation is induced by APCs, e.g. DCs, in lymph nodes. Myelin-derived autoantigens from the CNS reach the peripheral lymphoid organs as soluble

molecules via the blood and the lymph. Alternatively, they are phagocytosed by CNS-resident APCs, e.g. microglia, which present antigen to CD4+ T cells after migration to lymph nodes. In succession, CD4+ T cells upregulate surface-adhesion molecules (CD2, VLA-4, LFA-1) and leave the lymph nodes via the blood, probably guided by a number of cues including adhesion molecules on endothelial cells, chemokines and cytokines. The interactions of adhesion molecules on T cells and endothelial cells of the BBB (LFA-3, VCAM-1, ICAM-1) allow transmigration of CD4+ T cells across the BBB and the blood-CSF-barrier (110–112). Subsequent guidance of T-cell infiltration within the parenchyma is again mediated along chemokine and cytokine gradients established by endothelial cells, infiltrated leukocytes and/or CNS-resident cells, e.g. microglia. Next, T cells become reactivated by APCs of the CNS (113) thereby producing additional proinflammatory chemokines/cytokines. Reactivation occurs either in the subarachnoid space or the perivascular parenchyma. This first subtle wave of infiltrating cells is considered to be followed by an even more pronounced second wave of recruited cells of the innate (neutrophils, macrophages, DCs, NK cells) and adaptive (CD4+ and CD8+ T cells, B cells) immune system (114–116). These immune cells create inflammatory lesions in interaction with the CNS (117). CD4+ T cells damage the myelin sheath by cytokine secretion, for instance, and induce the production of specific antibodies by B cells as well as the phagocytosis of myelin debris by macrophages (118, 119). Cytotoxic CD8+ T cells can lyse oligodendrocytes and axons (57, 120) which have been compromised in their function by cytokines (121, 122). The demyelination and loss of oligodendrocytes results in damaged myelin sheaths of axons. In this situation impulse conduction is impaired due to the redistribution of ion channels along the axons, mitochondrial dysfunction and energy failure. Improper exchange of Na⁺ and Ca²⁺ results in axonal degeneration (123). Additionally, glutamate, which is released by activated immune cells or raised by compromised astrocyte function, induces neuronal excitotoxicity (124, 125). Axonal degeneration correlates with clinical deficits of MS patients (126). These deficits may resolve, at least during the early stages of MS or in patients with benign disease course (127). The inflammation may last from a few days to two weeks. The lesions resolve as myelin is phagocytosed by macrophages, astrocytes proliferate and provide support for CNS tissue and both CNS cells and T cells may produce anti-inflammatory cytokines (IL-10, TGF-β) and growth factors (brain-derived neurotrophic factor (BDNF), platelet-derived growth factor, fibroblast growth factor) (128–132). CNS-resident oligodendrocyte precursors and surviving oligodendrocytes become activated and start to remyelinate demyelinated axonal segments between nodes of Ranvier. Notably, the former myelin thickness cannot be established again (133) and thus impulse-conduction velocity is reduced. However, pathogenesis varies inter-individually and MS lesions can be grouped into four patterns (134, 135). Pattern I is defined by T cells and macrophages predominating in

lesions, whereas pattern II is characterized by additional antibody and complement deposition. In pattern III, lesions show a loss of myelin-associated glycoprotein (MAG) and oligodendroglial pathology. Patients suffering from primary-progressive (PP)-MS possess a pattern IV of nonapoptotic degeneration of oligodendrocytes.

Many studies support this concept of antigen-induced, T cell-centered inflammation resulting in axonal demyelination, neuronal damage and atrophy. Nevertheless, the MS-initiating factor(s) remain elusive. Findings on MS etiology need to be deepened. Observations of primary oligodendrocyte apoptosis and cortical demyelination without apparent leukocyte infiltration await confirmation or refusal (136–138). Is MS initiated by autoreactive T cells which have escaped their sorting during development? Or is MS rather caused by neurodegenerative processes predisposing compromised CNS constituents to an immunological reaction? While the latter questions are not completely resolved, most of the current evidence, particularly the abovementioned, recent genome-wide association study (69) point at a primary disturbance in the immune system and in T cells.

1.2.3 Clinical course

When a patient suffers from a first clinical sign or symptom which would be consistent with MS, but the diagnosis cannot be made formally yet, it is referred to as clinically isolated syndrome (CIS). The diagnosis of MS is made according to standardized diagnostic criteria. Originally, it was based clinically on the occurrence of two separate bouts of the disease (dissemination in time), and these had to affect two different CNS systems, e.g. vision and sensation (dissemination in space) (139, 140). If these occurred, a clinical diagnosis of relapsing-remitting MS could be made without ancillary measures. While this basic concept regarding inflammatory lesions which are disseminated in time and space has remained, the newest diagnostic criteria are based on magnetic resonance imaging (MRI) findings, and a diagnosis of MS can today already often be made at the stage of first presentation (141, 142).

MRI scans are the main paraclinical tool (143) to define dissemination in time. CNS white matter lesions are present in more than 95% of patients. Using contrast-enhancing agents, e.g. gadolinium, areas in the initial stage of lesion development are examined (144). Dissemination in space describes the occurrence of symptoms which reflect the impairment of discrete CNS areas. Tests are MRI, electrophoresis (detection of oligoclonal bands of immunoglobulins with restricted specificity isolated from the CSF (145)) and evoked potentials. Visual, somatosensory and brainstem auditory evoked potentials correlate with the effect of demyelination on saltatory conduction, e.g. a prolonged latency.

In most MS-diagnosed patients the clinical manifestation involves motor, sensory, visual and autonomic systems. CIS symptoms and neurological deficits during RR-MS, but also in the

course of progressive MS may vary greatly depending on the affected CNS site. Impairment of the optic nerve can lead to reduced visual acuity and color vision. Brainstem lesions result in impaired swallowing, emotional lability and/or vertigo. Lesions within the spinal cord may lead to weakness, spasticity and dysfunction of the bladder. MS frequently leads to cognitive impairment and motor neuron dysfunction (paresis, limb weakness, gait ataxia, tremor). Clinical signs may improve or resolve spontaneously or in response to treatment. MS leads only to a minor or no shortening of the life-span (58, 59), and reduced life expectancy may be due to a secondary risk of infections, particularly of the skin, chest and the bladder (146).

Two major clinical manifestations of MS exist that differ in their course as well as their frequency (57). Whereas a minor fraction of patients (10-15%) shows a steady progression of disability (PP-MS) (147, 148), 85-90% of MS patients suffer from relapsing-remitting MS (RR-MS) (149). Remission phases may last for months to years and are clinically inconspicuous. As disease progresses and disability accumulates the majority of RR-MS patients (around 65%) develop secondary-progressive MS (SP-MS) at an age around 40 (150–152). At this stage, people suffer from progressive neurological deficits and rarely interspersed acute MS bouts. The least common presentation is progressive-relapsing MS (PR-MS) with progressive disease from onset with acute relapses. Once disability has become irreversible the temporal acquisition of progressive invalidity is similar in PP-MS and SP-MS groups (153). In line with these clinical presentations remyelination of axons may occur during the remission phases of disease but also to a lesser extent during progressive MS periods (127, 154). In contrast to other courses of MS which affect women twice as often as men PP-MS shows equal gender distributions (155).

1.2.4 Therapy

Prevailing treatment options in MS target inflammation and act as immunosuppressants/immunomodulators. For instance, glucocorticoids (steroids) are applied during acute clinical exacerbations. Glucocorticoids, e.g. cortisone, prednisone or prednisolone, are used also in asthma or allergy therapy and broadly suppress (auto)immunity. They may act by generally modulating IL-1, IL-2, IL-4, IL-6, IFN- γ and TNF- α (57), by induction of apoptosis in T cells (156) and/or by interfering with leukocyte migration across the BBB (157). Their main effect is probably the latter, i.e. closing the BBB. For MS, five drugs are currently approved. Glatiramer acetate (GA), IFN- β compounds and fingolimod are used as first-line treatments. Mitoxantrone and natalizumab are applied in escalation therapies.

GA (Copaxone) is a random copolymer with variable length made of alanine, lysine, glutamic acid and tyrosine at fixed molar ratios. Interestingly, it was developed to mimic MBP for EAE induction but disease was blocked (158). Possibly, GA acts by polyclonal T-cell stimulation,

Th2 activation (159), induction of Tregs (160), interference with DC differentiation and BDNF induction (161). GA shows an efficacy comparable to IFN- β therapy.

IFN- β formulations are the most frequently used treatment option for RR-MS. As other approved drugs IFN- β is applied by intraperitoneal (i.p.) injection. Its immunomodulatory activities comprise the upregulation and increased shedding of adhesion molecules (reduction of cell adhesion to the BBB), induction of IL-10 and neurotrophic factors and blocking of BBB opening by inhibition of matrix metalloproteinases (MMPs). Four IFN- β formulations are currently available: IFNB1a (Avonex and Rebif) and IFNB1b (Betaferon and Extavia). Clinical trials revealed an approximately 30% reduction in frequency and severity of exacerbations, although only moderately (162). Active lesions were reduced as well as the total lesion load (163, 164). Unresolved questions on IFN- β treatment are the dose, frequency and route of administration but also the long-term effects of the treatment. The mechanism of action is not completely understood and also the occurrence and relevance of neutralizing antibodies in patient subgroups is a matter of debate. The modest impact on MS progression, the frequency of subcutaneous (s.c.) injections, flu-like symptoms, expensive recombinant production and the existence of IFN- β non-responders even after initial responsiveness (antibody producers) are drawbacks of IFN- β therapy.

The synthetic sphingosine 1-phosphate receptor 1 (S1P₁) agonist fingolimod (FTY720, Gilenya) is the first approved, orally available immunosuppressant for MS (165). S1P₁ is expressed on lymphocytes and activated by lymphatic endothelial cell-produced S1P. Receptor-binding overrides C-C chemokine receptor (CCR) type 7-mediated lymphocyte retention in the lymph node. Fingolimod inhibits the egress of lymphocytes from lymph nodes thereby precluding the systemic trafficking of self-reactive T cells and their CNS invasion (166). After phosphorylation and S1P₁-binding fingolimod induces receptor internalization which reduces the egress signal in T cells in favor of the CCR7-mediated retention signal (167). In clinical trials in the context of RR-MS fingolimod was found to improve the time to first relapse, relapse rate and lesion load. However, no impact on EDSS change was shown (168, 169). Obviously, FTY720-mediated retention of lymphocytes obviates the immune system to function properly, e.g. in the clearance of infections. Fingolimod is now the first approved oral therapy for RR-MS.

Whilst glucocorticoids, GA and IFN- β formulations are widely used as first-line therapies treatment can be escalated as MS exacerbates and/or patients do not respond to those drugs. A multiplicity of chemotherapeutics with broad activities are available which are allocated with long-term immunosuppression. These are prevalently applied at the transition from RR-MS to SP-MS or if a patient shows aggressive disease bouts and no response to other treatment options. Among these immunosuppressants are mitoxantrone, cyclophosphamide, methotrexate, azathioprine and mycophenolate. Notably, chemotherapy

carries an elevated risk of severe side effects by eradication of immune cell subsets. For instance, the powerful immunosuppressive agent mitoxantrone is a DNA topoisomerase II inhibitor that induces immunodepletion. It is approved for treatment of worsening relapsing and secondary progressive MS. This treatment is associated with the risk of inducing therapy-related acute leukemia and cardiotoxicity, as well as secondary infections in addition to cough, diarrhea, hair loss, loss of menstrual period, fever or vomiting.

The second approved drug, which is used in active RR-MS patients to escalate the treatment intensity, is the humanized monoclonal antibody natalizumab (Tysabri). It recognizes the α 4-integrin of VLA-4 on activated leukocytes. In this way it interferes with the binding to vascular VCAM-1 on CNS endothelial cells thereby blocking transmigration into the parenchyma. In MS patients relapse rate and brain inflammation were reduced upon therapy. Drawbacks are increasing numbers of progressive multifocal leukoencephalopathy (PML) cases, the costly recombinant production in mammalian cell lines and hints from EAE experiments which imply the VLA-4-independent brain-parenchyma immigration of Th17 cells (170).

Besides these approved treatments, additional drugs are currently studied in the context of MS. Oral fumarate (BG00012) has already been tested in a phase II trial (171) and in two phase III trials (publications pending). In RR-MS patients, fumarate reduced the annual relapse rate by 32%. Observed side effects were abdominal pain, flushing, headache and fatigue. Laquinimod is another oral immunomodulatory drug. Phase II trials showed a reduction of gadolinium-enhancing lesions by 40%, and the drug was well tolerated (172). The third oral MS disease-modifying drug teriflunomide has anti-proliferative/anti-inflammatory properties. It acts as a pyrimidine-synthesis inhibitor. A phase II trial in RR-MS has shown that CNS lesions were reduced (173). The drug was well tolerated at all doses tested. However, nausea, diarrhea and neutropenia were observed. These three oral disease-modifying drugs are currently undergoing or have completed phase III evaluation.

Additionally, the MS intervention by therapeutic monoclonal antibodies is currently advanced in clinical trials. Examples are daclizumab and rituximab. Preferential perivascular and meningeal accumulation of autoreactive CD4+ T cells is a characteristic in demyelinating MS lesions. The recognition of (auto)antigens results in CD4+ T cell clonal activation, expansion and a Th1/Th17 proinflammatory response. However, in active MS lesions CD8+ T cells are more abundant than CD4+ T cells (174). Those cells show increased reactivity to myelin antigens and secrete cytokines, e.g. IL-2. IL-2 is an important cytokine and growth factor for activated T lymphocytes. It stimulates their clonal expansion and maturation. The humanized monoclonal antibody daclizumab is directed against the IL-2 receptor- α chain (CD25) which is expressed at high levels in activated T cells. This antibody-mediated block leads to an impaired proliferation and expansion of activated T cells *in vitro*. *In vivo*, the mode of action

of daclizumab is probably primarily mediated by an indirect effect, the expansion of CD56+ NK cells (175). A phase II clinical trial with RR-MS and SP-MS patients revealed that treated patients had a 78% reduction in brain inflammatory activity compared to baseline as well as a stabilization of clinical disease progression (176, 177). Daclizumab is considered to be safe and well tolerated, but the incidence of infections increased and mild-to-moderate cutaneous adverse events were observed.

For MS patients showing the type II pathological pattern, plasmapheresis has been shown to improve disease relapses, e.g. severe optic neuritis (178). B cells are also considered to be an attractive pharmaceutical target as they are able to act as APCs as well as to produce cytokines. Thus B cells may play a role in T-cell and macrophage activation. Rituximab is a chimeric murine-human IgG1 κ monoclonal antibody against CD20+ pre-B cells and mature B cells. Memory B cells also express CD20, but to a lower level than naïve B cells. Recent studies suggested that rituximab treatment may lead to circulating B-cell depletion by induction of apoptosis, complement-induced cytolysis and antibody-dependent cell-mediated cytotoxicity (115, 179–181). It is still unclear to which extent it affects different immune cell populations. Rituximab has been found to be highly effective in RR-MS patients in a phase II trial (115). But in a phase II/III trial with PP-MS subjects rituximab failed to delay the time of disease progression (182). The complication of PML has also been reported during rituximab use, but in most cases patients have also been under additional immunosuppression.

To reestablish tolerance is a further experimental concept in MS therapy. In one approach antigen-specific T cells are targeted to achieve anergy or AICD (183). A second approach uses immunization with autoantigenic peptides or altered peptide ligands. High dose altered peptide ligands were shown to exacerbate disease (96).

A cell therapy that has been used in MS to reestablish tolerance is the transplantation of autologous hematopoietic stem cells (AHSCs) after intense chemotherapy. Most if not all T cells are eradicated by this procedure followed by reconstitution of the immune system after successful engraftment of transplanted AHSCs (184, 185). This high-risk procedure was reported to halt inflammatory activity (186) but clinical disability progression was not reduced (187). Transplant-related complications are frequent, including allergy, bacteremia and transitory deterioration in neurological conditions (188).

Recently, the transplantation of multipotent mesenchymal stromal/stem cells (MSCs) has been suggested as a therapeutic option providing not only immunomodulatory but also reparative functions. So far, no adverse effects of autologous MSC transplantations were reported. Long-term safety data is necessary to approve cell therapies for MS (189–191).

Available treatments focus on the inflammatory facet of MS. There is no treatment for progressive MS (SP-MS, PP-MS). At these stages neuronal damage and axonal loss accumulate as the predominant pathologic feature. In addition to immunomodulatory and

-suppressive approaches, research and treatment development intensified efforts for neuroprotective therapies during the last years. Conceivable targets are ion channels (123, 192–196), excitotoxicity (197, 198), the induction of growth factors (199, 200) or the modulation of inhibitory signals, e.g. Nogo (201, 202).

The heterogeneity of MS, e.g. inter- and intra-individual fluctuations in the disease courses as well as distinct brain-pathology patterns, renders drug development challenging. MS as a complex disease cannot be entirely recapitulated by *in vivo* (EAE) and *in vitro* models. In summary, available treatments of MS target inflammatory events. They are hampered by only partial knowledge about their mode of action, the existence of non-responders, considerable side effects and high manufacturing costs. Except for FTY720 pharmaceuticals necessitate recurrent s.c., intramuscular (i.m.) or intravenous (i.v.) injections. A substantial number of MS patients refuse existing injectable treatment *per se* or during therapy due to needle phobia. Additional treatment options, especially for oral application, are required. Up to now pharmaceutical drugs are only able to meet part of MS patients needs.

1.3 Experimental autoimmune encephalomyelitis

Research on human autoimmune diseases is hampered by a limited, but increasing understanding of human immunology, the (genetic) diversity of humans and the inaccessibility of autoimmune lesion, e.g. brain tissue in MS. Nevertheless, strong data exists for human T-cell responses against some myelin components (MBP, MOG, PLP). The role for these autoantigens has often been examined in the EAE model first, and data from these studies in animal models is overall stronger than those obtained from MS patients.

First observations of neurological impairments in animals originate from Louis Pasteur in 1885: “neuroparalytic incidents” were reported after the vaccination with spinal cord from rabies-infected rabbits. Acute demyelination was induced by contaminating spinal cord constituents (55, 56). The actively induced, paralytic disease was later on termed EAE. EAE can also be induced in susceptible rodents, i.e. mice (203), rats (204), and guinea pigs (205), marmosets (206) and non-human primates (55). Immunization can be achieved by injecting spinal cord homogenate, myelin proteins or peptides reflecting the research progress to delineate causative antigens. For immunization, those are emulsified in complete Freund’s adjuvant (CFA) (207). CFA consists of paraffin oil, the emulsifier mannite monooleate and heat-inactivated *Mycobacterium tuberculosis* to evoke the activation of the immune system. Immunization leads to clinical and neuropathological phenotypes with some similarity to MS. Especially in inbred rodent strains EAE susceptibility and the phenotype depend on the genetic background and the injected antigen. Disease courses can be acute monophasic chronic progressive, RR or chronic relapsing (CR). Chronic progressive EAE is induced in

C57BL/6 mice (MHC restriction: H-2^b) by immunization with MOG₍₃₅₋₅₅₎, whereas RR-EAE in SJL mice (MHC restriction H-2^s) follows the injection of PLP (summarized by Miller *et al.* (208)). CR-EAE is induced by immunization of Lewis rats and Biozzi AB/H mice with total guinea pig spinal-cord tissue (209) and MOG (210), respectively. Lewis rats are also used to study monophasic EAE after immunization with MBP (211). MOG-induced EAE is most frequently applied in research, and transgenic mouse strains are commonly backcrossed to the C57BL/6 genetic background. The onset of clinical symptoms/deficits in actively immunized C57BL/6 and SJL mice is between 9 to 12 days after immunization. During the following days mice develop a maximal severe disease bout (acute phase). In C57BL/6 mice subsequent remission is only partial and mice retain a moderate, chronic deficit. A progressive deterioration may occur. The remission phase of EAE-induced SJL mice is marked by a profound amelioration up to absence of symptoms. Around day 25 after immunization mice face an EAE relapse that is followed by a second remission. The clinical deficit (motor function, gait) is assessed on a 5-point scale. Typically, myelin-specific CD4⁺ Th1 but also Th17 cells are considered to mediate EAE initiation. They can be isolated, cloned and transferred into naïve animals (87). The adoptive transfer of CD4⁺ T cells, which were isolated from EAE-induced mice and expanded *ex vivo* by incubation with the disease-specific antigen, into healthy animals is referred to as passive immunization. The clinical course is accelerated and exacerbated compared to actively induced EAE (86). Notably, both the active and the passive immunization induce an artificial disease with a myelin-specific immune response. This constraint may obscure key pathogenic mechanisms in MS.

The limitations of EAE models hamper the translation of findings to MS. EAE is induced with the help of *Mycobacterium tuberculosis*, an inducer of CD4⁺ Th1/Th17 responses by TLR activation (212). EAE induction elicits a comparatively homogenous clinical presentation within each model. Findings may be reproducible but do not reflect the heterogeneity of MS. In humans, MS manifests spontaneously at the age of 20 to 40 and patients suffer over years to decades. In contrast, it takes only days to induce EAE in mice. Long-term outcomes and adverse treatment effects at late disease stages are hardly predictable in EAE. A further drawback is the genetic restriction especially in inbred mice in comparison to humans, which represent an “outbred” species. Additionally, controlled housing conditions of animals contrast with environmental influences in humans. Pathological hallmarks, e.g. CD4⁺ T-cell infiltration of the CNS, axonal loss and neuronal damage, are shared by MS and EAE. In contrast to EAE, demyelination is more pronounced in MS. With regard to B cells, pattern II lesions of MS patients are identified, amongst others, by the involvement of antibody and complement. Additionally, B cells, antibodies and complement may become more important in the chronic disease phase of MS. This complexity, until now, could not be reflected in EAE models.

Differences between MS and EAE also became evident in the translation of therapeutic approaches. Only a small percentage of therapeutic concepts that were efficient in EAE were also successful in MS (213). In fact, some new approaches even worsened disease or caused severe side effects. One example for successful translation from EAE to MS is GA (214), whereas altered peptide ligand therapy was not found to be beneficial in MS thus far (96). Correlations of EAE models with MS need to be improved. "Humanized" mouse models have been created to mimic human disease by the transfer of genes from MS patients into mice. For instance, interactions of MS-associated HLA molecules with human TCRs specific for myelin peptides can be studied (94, 95, 215, 216). These transgenic mice may develop spontaneous EAE which is also seen in transgenic mice that express myelin-specific murine TCRs or BCRs (89, 90, 217–220). It is this spontaneous disease occurrence that may pave the way from an active, artificial disease induction to a more natural-like triggered disease. These models resemble human disease more closely regarding clinical (spontaneous) and histological (B-cell involvement) presentations and may thus contribute to an improved correlation.

In conclusion, EAE is a valuable tool to study principles of autoimmunity associated with inflammation and injury of the CNS. Concepts for therapeutic interventions can be studied and validated. The results need to be reviewed in experiments with human material *ex vivo* and/or in human clinical trials *in vivo*.

1.4 Apoptosis

Cell death is an elementary cellular response. It is essential during the development of organisms and regulates tissue homeostasis by eliminating unwanted cells, e.g. during T-cell development in the thymus. Thereby, vertebrates are able to regulate the development of potentially autoreactive T cells. Historically, cell death has been subdivided into regulated and unregulated mechanisms. In contrast to uncontrolled cell death (necrosis) and controlled, nonapoptotic cell death (autophagic cell death, necroptosis, poly (ADP-ribose) polymerase 1 (PARP1)-mediated cell death) apoptosis is defined mechanistically as a pathway for programmed cell death (PCD) by sequential activation of caspases. The pathways involving these Cys-proteases are positively and negatively controlled by B-cell lymphoma protein-2 (BCL2) family members. The BCL2 family consists of anti-apoptotic, multidomain pro-apoptotic and BH3-only members. Apoptosis was first described in *C. elegans* (221). Morphologically, apoptosis of cells is characterized by nuclear fragmentation, membrane blebbing and formation of apoptotic bodies. Generally, milder insults are considered to induce apoptosis whereas more intense insults cause necrosis (222).

A cell may sense severe stress in consequence of pathogenic infection, DNA damage, defective cell-cycle progression, detachment from the extracellular matrix, hypoxia or loss of cell-survival factors. Stress-inducible intrinsic molecules are c-Jun NH₂-terminal kinase (JNK), mitogen-activated protein kinase (MAPK)/extracellular signal-regulated protein kinase (ERK), nuclear factor kappa B (NF- κ B) or ceramide (223–228). They can transmit the apoptotic signal. In mammalian cells, the intrinsic apoptosis pathway can be initiated by pro-apoptotic BCL2-family members but also by BH3-only, pro-apoptotic BCL2-family members. The latter can also directly inhibit anti-apoptotic members of the BCL2-family. These BCL2-members protect cells from apoptosis primarily by preserving the integrity of mitochondria rather than directly inhibiting caspase activation at the level of adaptor molecules, e.g. apoptotic protease-activating factor-1 (APAF1) or p53-induced protein with a death domain (PIDD). Anti-apoptotic BCL2-family members reside at the outer mitochondrial membrane. They prevent the pro-apoptotic multidomain BCL2-family members BAX and BAK from causing mitochondrial damage (229). BH3-only proteins override this inhibition. BAX and BAK form an oligomeric channel leading to mitochondrial damage and subsequent cytochrome c release. Mitochondrial damage may also be induced by BAX/BAK-independent mechanisms, e.g. intra-mitochondrial K⁺ influx or protease-independent caspase-2 activity. After damage the release of mitochondrial proteins amplifies the apoptotic signaling. Released cytochrome c induces the formation of the “apoptosome” megacomplex, a heptamer composed of APAF1 and caspase-9. In succession, caspase-9 changes its conformation and thus becomes activated. Activated caspase-9 cleaves and activates downstream caspases, e.g. caspase-3, -6 and -7 thereby triggering the execution phase of apoptosis. This intrinsic pathway to induce apoptosis resembles PCD in *C. elegans*.

Additionally, mammalian cells can undergo apoptosis by an extrinsic pathway. This PCD is induced by pro-apoptotic and proinflammatory cytokines, e.g. FasL, TNF-related apoptosis-inducing ligand (TRAIL) and TNF- α , respectively. They are ligands for the death-receptor family (230). After binding to death-domain receptors, FasL, TRAIL and TNF- α induce the intracellular formation of specific DISCs (231, 232). DISCs deliver a pro-apoptotic signal through the recruitment of the adaptor protein Fas-associated protein with death domain (FADD) to engaged receptors and subsequent recruitment and activation of upstream caspases, e.g. caspase-8. In turn, caspase-8 cleaves downstream caspases (caspase-3 and -7) to execute cell death. Moreover, activated caspase-8 is able to cleave BID, a BH3-only pro-apoptotic protein. As a result the cell-death signal is amplified due to mitochondrial damage. Cytokine-mediated apoptosis in higher multicellular organisms enables the coordinated regulation of cell numbers in response to environmental stimuli. Different apoptosis regulators respond to different pro-apoptotic signals: FasL binds to the Fas receptor (Fas)/CD95, TRAIL binds TRAIL receptor 1/2 and TNF- α activates TNF receptor 1.

Further specification is provided by evolutionary gene duplications. Mammals possess a family of caspases with distinct functions according to their subcellular distribution and protein-protein interactions. Substrate specificities contribute only to a minor degree to this diversity. Basically, three classes of caspases do exist. Activator caspases, e.g. caspase-2, -4, -8, -9, -10 and -12, initiate the caspase cascade. They fulfill distinct roles which depend on the activation complex to which they are recruited to. The downstream execution steps are implemented by executioner caspases-3, -6 and -7. As a third group inflammatory caspases, namely caspase-1, -5 and -11, mediate cell death and inflammatory responses. Humans possess eleven caspases and the substrate is cleaved after aspartic acid residues. Caspases are activated by proteolytic cleavage of zymogens, removal of the prodomain, and the separation of large and small catalytic subunits or allosteric changes of the conformation. The diversification of caspases provides the equipment to allow multicellular organisms to sense and differentially respond to distinct stimuli.

Mitochondrial outer membrane permeabilization (MOMP) leads to the activation of caspases and apoptosis via the intrinsic pathway. Cells can additionally undergo caspase-independent cell death (CICD) after MOMP. This pathway is triggered by the progressive decline of mitochondrial function, e.g. ATP production, followed by the release of apoptosis-inducing factor (AIF) (233). Upon death induction AIF translocates from the mitochondrial intermembrane space to the nucleus to cause chromatin condensation and DNA fragmentation. Mitochondria-associated and other controlled CICD mechanisms necessitate further examination. If cells respond by apoptosis the early process is accompanied by cell shrinkage and pyknosis, the irreversible chromatin condensation. Additionally, extensive plasma-membrane blebbing can be seen. The nucleus is fragmented and cell fragments separate into apoptotic bodies ("budding"). These contain cytoplasm, intact organelles and possibly nuclear fragments enclosed by an intact plasma membrane. However, some changes occur at the plasma membrane that can be used to detect apoptosis in experimental approaches. Early apoptotic cells externalize phosphatidylserine (PS) residues on the outer plasma membrane. Binding of fluorescently labeled Annexin V to PS can be visualized by microscopy or flow cytometry. Notably, necrotic cells are labeled as well. Membrane integrity of PS/Annexin V-positive cells can be shown by co-staining with dyes like propidium iodide (PI) which are excluded by intact membranes. Necrotic cells will stain positive due to the loss of membrane integrity. Under physiological conditions macrophages, parenchymal or neoplastic cells quickly phagocytose the apoptotic bodies which are then subjected to degradation in phagolysosomes. As these processes may not be recapitulated *in vitro*, cells probably show secondary necrosis and will stain PI+ here. Essentially no inflammation is associated with apoptosis or the removal of apoptotic bodies.

The understanding of apoptosis inspired the development of specific cell death-targeting therapies. For instance, agents like BCL2 or “inhibitor of apoptosis” proteins have been invented to target apoptosis in cancer cells (234). Drugs for the interference with pathological tissue damage and functional decline as a result of cell death are also explored. However, the success of apoptosis-targeting therapies is limited, probably because the cell-death regulation is complex in mammals. Due to possible signaling crosstalks a therapy may require a combinational treatment. In addition, targeted pathways may also be active and treatment-affected in other physiologically important cell types besides the targeted cell subset. Disorder-tailored therapies need to be established for the efficient interference with human diseases that result from adverse, unbalanced cell-death regulation, e.g. stroke, myocardial infarction, CNS traumata, chronic neurodegenerations, inflammatory diseases and diabetes.

1.5 Edelfosine

In the 1960s, Herbert Fischer and Paul Gerhard Munder reported that macrophages upregulated the production of 2-lysophosphatidylcholine (lysolecithin, LPC) during phagocytosis of silicogenic quartz particles. LPC formation is catalyzed by phospholipase A₂. They made comparable observations upon addition of adjuvant substances, e.g. CFA and its components, *Corynebacterium parvum*, endotoxin and vitamin A. The phagocytic activity of macrophages could be enhanced *in vivo* and *in vitro* by the addition of exogenous LPC as adjuvant (235–238). At that time macrophages were considered to be the immune cell subset that is central to the induction of the inflammatory response since DCs were not discovered yet. The increased formation of LPC in macrophages upon encounter of adjuvants/pathogens was discussed as an endogenous mechanism of the organism to produce its own adjuvant, directly at the site of inflammation. The water-soluble LPCs might diffuse via the blood and/or lymph to activate other immune cells. The findings suggested an immunomodulatory function for LPCs in the defense mechanism of the immune system. To allow strong regulation of immune responses LPCs like other naturally occurring modulators could be rapidly metabolized. For example, acyltransferases convert LPCs to phosphatidylcholine (PC) and lysophospholipases synthesize glycerophosphocholine from LPCs.

To achieve sustained immunomodulation synthetic LPC analogues with longer *in vitro* and *in vivo* half-lives were generated (Figure 1). By replacing ester bonds for ether linkages at position C1 and C2 of the glycerol backbone these LPC analogues were unable to be metabolized by acyltransferases and lysophospholipases. Interestingly, some of those synthetic ether lipids were endowed with rather selective and strong antitumor activities *in*

vitro and *in vivo* (239–243). Edelfosine (1-O-octadecyl-2-O-methyl-*rac*-glycero-3-phosphocholine, ET-18-OCH₃) was the most effective synthetic anticancer alkylphospholipid (APL) analogue tested. It was synthesized in 1969 (244). Crystal x-ray structures of D-edelfosine monohydrate indicated that molecules arranged in a bilayer structure, in which the hydrocarbon chains were interdigitated and tilted (245).

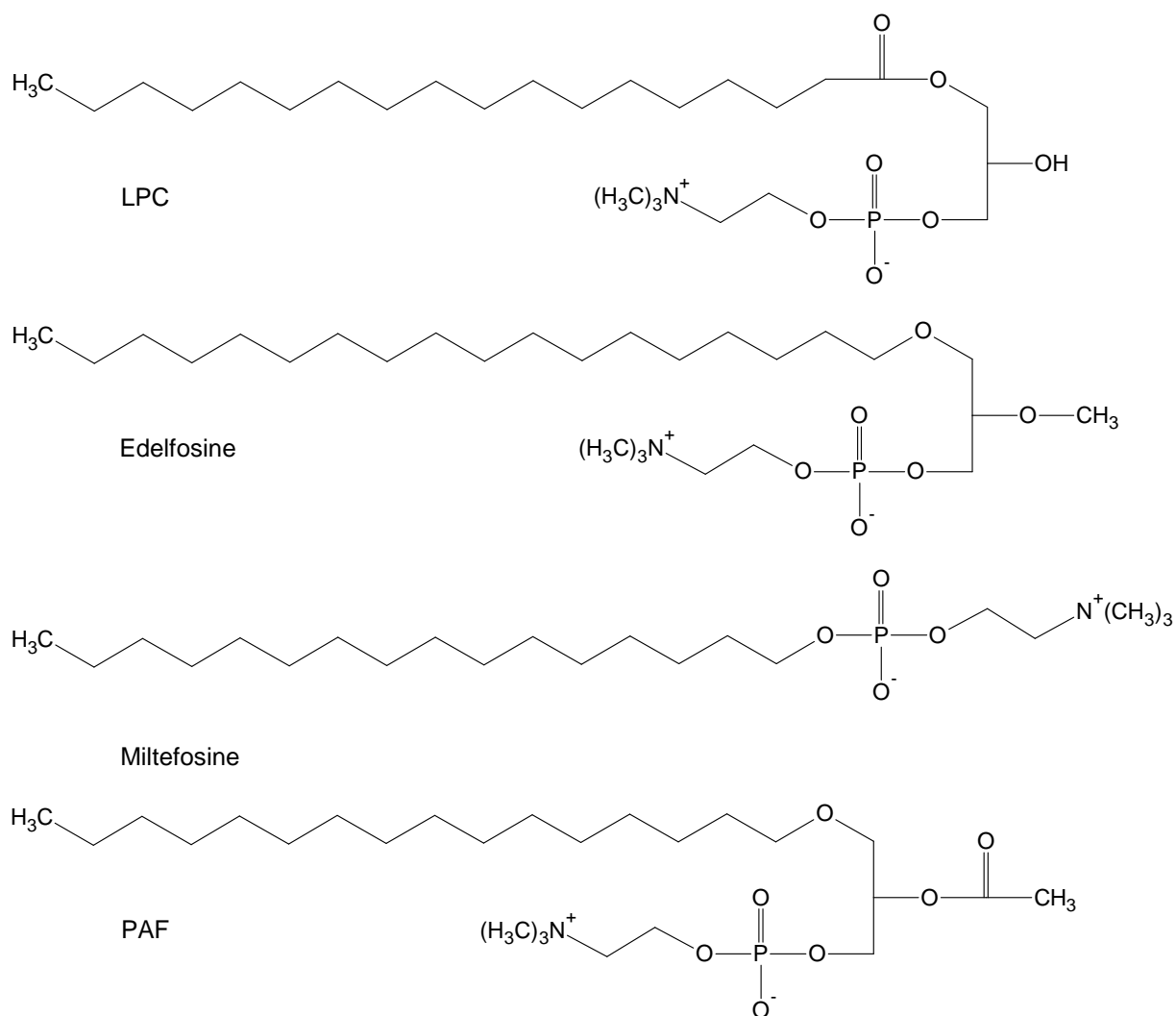


Figure 1. Chemical structure of the natural LPC from which the synthetic APL edelfosine is derived by the introduction of an ether bond for an ester linkage. Miltefosine represents a member of another, second ATL subgroup besides ALPs, the alkylphosphocholines. PAF is a natural phospholipid with substantial structural homology compared to edelfosine.

Edelfosine has been studied in phase I and II clinical trials for its effectiveness for purging bone marrow of acute leukemia patients (246, 247). Edelfosine possesses the advantage to selectively induce death in leukemic cells while normal bone marrow cells are spared (239, 248). The minimal structural requirement for the antitumor activity of APLs was identified in 1990: miltefosine (hexadecylphosphocholine) was lacking the glycerol backbone (249). Generally, antitumor lipids (ATLs) are classified into two categories. Alkyl ether phospholipids (AEPs) like the prototypic edelfosine, also referred to as alkyllysophospholipids (ALPs),

contain ether bonds in the glycerol backbone. In contrast, the alkylphosphocholines lack the glycerol backbone and are just formed by an esterified long-chain alcohol (e.g. miltefosine). Key findings on the mode of ATL action were reported in 1993 as edelfosine was found to induce selective apoptosis in leukemic cells (250, 251). In contrast to other cytotoxic drugs ATLs do not target the DNA. They do not directly interfere with the formation and function of the cellular replication machinery. ATLs, as lipid drugs, trigger directly the apoptotic machinery, e.g. in tumor cells (252, 253). Notably, normal cells are selectively spared. Edelfosine, for instance, is implicated in binding to Fas/CD95 in a lipid raft-mediated process thereby exerting its cytotoxic activity (252, 254, 255). This constitutes a novel mechanism in antitumor therapy. Importantly, lipid drugs are prone to promote unspecific events when used at high concentrations (cell lysis). It is therefore important to investigate ATLs at concentrations that do not prevent or divert examinations from the specific and relevant actions.

The amount of edelfosine that is incorporated into the cell is critical for the execution of the cytotoxic effects. A strong correlation exists between the cellular uptake of edelfosine and cytotoxicity. The cell membrane represents a barrier for edelfosine in normal, resting cells. Normal, resting cells are not able to take up significant amounts of ALPs even in long-term incubations for more than 72 h (252). By microinjection experiments it was shown that incorporation of edelfosine into the cell is required to induce DNA fragmentation and apoptosis. Data indicated a dose-response pattern with a threshold for intracellular ALP concentrations to trigger apoptotic cell death. Thus, cytotoxicity is determined by the number of drug molecules per cell, the cell density in *in vitro* experiments as well as in a specific organ and the cell type (256). Different mechanisms for the incorporation of edelfosine have been proposed ranging from direct adsorption to the plasma membrane and subsequent passive diffusion, endocytosis, lipid flip-flop to specific receptor-mediated transport (253, 257). Generally, transporters are pivotal for the maintenance of transbilayer lipid asymmetry of cell membranes.

ALPs as phospholipids readily incorporate into cellular membranes (258–260). In tumor-cell membranes incorporated edelfosine accounted for up to 17% of membrane phospholipids (261). Whereas association with the plasma membrane may be independent of the resistant or sensitive nature of the cell, internalization processes seem to be active in sensitive cells to mediate cellular uptake (262). The putative edelfosine-uptake mechanism may involve two steps. First, edelfosine binds in an unspecific way to the outer layer of the plasma membrane. Subsequently, the ether lipid is flipped across the membrane into the cytoplasmic leaflet. Potential transporters/flippases are not identified yet (263–265).

Edelfosine may not only induce apoptosis by intracellular binding to Fas/CD95. Edelfosine may accumulate in lipid rafts within the plasma membrane followed by endocytosis and

translocation to the intracellular location of the CTP:phosphocholine cytidyltransferase (CCT), the endoplasmic reticulum (ER) (255, 266, 267). Cytosolic CCT translocates to the ER to become activated. Here, edelfosine may inhibit the biosynthesis of PC leading to mitotic arrest and apoptosis (268, 269). Interestingly, the natural edelfosine analogue LPC is not preferentially located into lipid rafts. This emphasizes the importance of introduced ether linkages for the incorporation into these sphingolipid- and cholesterol-rich membrane microdomains. In this regard, edelfosine may induce the clustering of small rafts to larger conglomerates. The mechanism of edelfosine uptake may thus be through raft-dependent endocytosis and/or a specific transporter. The relative contribution of each mechanism may depend on the cell type. The degree of cellular edelfosine uptake and thus apoptosis correlates with the proliferative activity and the associated metabolic lipid turnover in the cell (253, 262, 270, 271). Therefore, not only tumor cells but also normal cells are sensitive to ALPs provided a proliferative state, as seen in activated T cells in the context of autoimmune diseases.

According to the mechanisms which have been implicated in the action of edelfosine the drug may activate components of the extrinsic (Fas/CD95) and/or the intrinsic (raft endocytosis) apoptosis pathways. Both pathways converge and activate caspase-3. Detailed mechanistic reports claim that edelfosine-treated Jurkat leukemic T cells undergo apoptosis by the recruitment of DISCs into lipid rafts (272). Under normal conditions Fas is located at the plasma membrane, but not in lipid rafts. Edelfosine accumulates in the inner leaflet of the plasma membrane in lipid rafts which in turn may induce the clustering of rafts and the recruitment of Fas into rafts. Due to this concentration of Fas, FADD and caspase-8 are translocated into rafts forming DISCs. In this way clusters of lipid rafts may act as supramolecular scaffolds for the concentration of DISCs allowing the activation of caspase-8 to induce apoptosis in the absence of FasL. The second proposed mechanism for edelfosine-mediated apoptosis is by endocytosis. Enabled by their one long apolar hydrocarbon chain APLs insert into the plasma membrane, become endocytosed and are proposed to interfere with phospholipid biosynthesis, turnover as well as lipid-based signal-transduction pathways. These targets are critical for the maintenance of membrane integrity and the assembly of lipid second messengers, e.g. diacylglycerol (DAG), phosphatidic acid (PA) and phosphoinositides from precursors. These molecules are important for cell functioning, survival and proliferation (273). If the lipid-dependent metabolic pathways are disturbed cellular stress is the result which may induce apoptosis. PC is the most abundant phospholipid in eukaryotic cell membranes, and the inhibition of PC biosynthesis is a major ALP-induced effect. In this way edelfosine imposes stress on cells (255, 267, 269, 274–278). Proliferating cells, that require high amounts of PC for membrane formation, may enter apoptosis. In the ER, ALPs inhibit the *de novo* PC synthesis by CCT. This effect was found in

all exponentially growing cells, normal quiescent cells were not affected (270, 279). The addition of exogenous LPC for PC synthesis prevents apoptosis induction by edelfosine and underlines the central role for PC-synthesis inhibition by edelfosine. Under physiological conditions PC is synthesized according to the Kennedy pathway including CCT and constitutes the precursor for DAG, PA and sphingomyelin (SM). The block of PC production may interfere with the downstream synthesis of DAG and SM by sphingomyelin synthase (SMS) in the trans-Golgi network. Ceramide as the second SMS substrate may accumulate and induce apoptosis (280, 281). Additionally, PC-synthesis inhibition in the ER may elicit apoptosis by causing ER stress (279, 282) and oxidative stress (283–285). PC depletion was reported to induce the ER stress related pro-apoptotic transcription factor CHOP/GADD153 that can activate BAX, BAK and BIM (282, 286) as well as ROS. Edelfosine also activates the stress-activated protein kinase (SAPK)/JNK pathway (287–291). This pathway is induced by Fas stimulation and environmental stress factors, e.g. heat shock, ROS and ER stress (292–294). Activated SAPK/JNK translocates to mitochondria to activate the apoptotic machinery (295, 296). APLs can also inhibit PC breakdown to PA and subsequently to DAG (297–299). PA and DAG act as second messengers of the MAPK pathway, for instance the Ras/Raf/MEK/ERK pathway of cell proliferation. Thus, APLs like edelfosine may affect a multiplicity of cellular processes, probably with cell type-dependent emphasis but with the joint outcome of apoptosis induction (Figure 2).

One outstanding advantage of edelfosine in contrast to other chemotherapeutic drugs lies in its oral administration. However, in clinical trials edelfosine has also been administered i.v. ELL-12, a liposome-based formulation of edelfosine, has been tested in a phase I trial in patients with solid tumors. It showed an excellent safety profile with low side effects in the absence of myelosuppression and hemolysis. Effectivity of edelfosine in the treatment of non-small cell lung carcinoma could not be shown in a phase II trial (300). Additionally, edelfosine, which is able to cross the BBB, was used in a phase II study to treat patients suffering from astrocytoma/glioblastoma brain tumors that previously did not respond to radiotherapy and/or chemotherapy (301). After two month, 56% of treated patients presented with a cessation of tumor growth. In fact, 50% of cancer patients are treated by radiotherapy. Edelfosine may increase the sensitivity of cancer cells to radiation. Conventional radiosensitizers act on DNA. The therapeutic effect of APLs as radiosensitizers is tested in a clinical phase I trial (302). Another application of edelfosine is MS and autoimmune diseases. In a pilot MS study edelfosine treatment improved clinical symptoms (303). A subsequent small phase I trial pointed to improved neurological symptoms after edelfosine treatment (304). Patents also describe the use of edelfosine to treat ulcerative colitis, viral infections and psoriasis. Edelfosine was also reported to be cytotoxic and beneficial in the treatment of *Leishmania* infections (305).

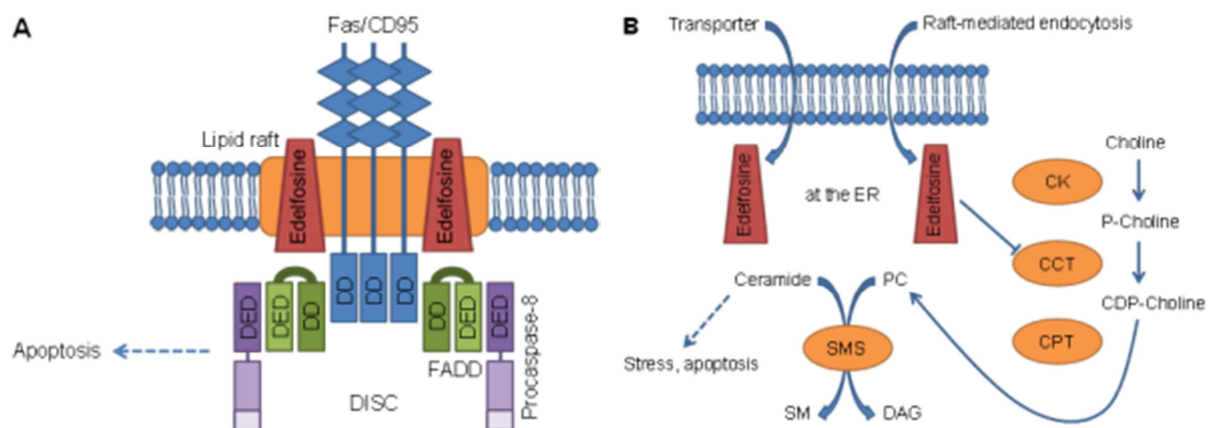


Figure 2. Schematic model for edelfosine-induced apoptosis. **(A)** DISCs are recruited to lipid rafts within the plasma membrane. Initially, edelfosine accumulates in lipid rafts. Rafts may cluster and recruit Fas/CD95. The concentration of Fas/CD95 induces the subsequent recruitment of FADD and procaspase-8 to form DISC (DD: death domain, DED: death-effector domain). Activation of caspase-8 may lead to apoptosis. **(B)** Edelfosine also targets signaling pathways of lipid metabolism. Edelfosine is endocytosed upon lipid-raft internalization and/or translocated by a transporter in the plasma membrane. At the ER edelfosine inhibits CCT and PC biosynthesis as well as the synthesis of DAG and SM. The shortage of PC and the accumulation of ceramide causes cellular stress which may ultimately induce apoptosis (CK: choline kinase, CPT: cholinephosphotransferase, P-Choline: phosphocholine, CDP-Choline: cytidine diphosphate-choline). The multiplicity of edelfosine-induced cellular processes is reviewed by Mollinedo *et al.* and van Blitterswijk *et al.* (272, 306–308).

2 Aims

The cytotoxic drug edelfosine is a synthetic analog of LPC. Edelfosine is incorporated by highly proliferating cells, e.g. activated immune cells. It acts on cellular membranes by selectively activating the cell-death receptor Fas. Edelfosine also interferes with PC synthesis catalyzed by CCT thereby inducing apoptosis, e.g. by oxidative stress and the accumulation of ceramide. Within this study, the effect of edelfosine on the immune system was investigated in the context of EAE, but also in human T cells.

As an established animal model of MS, EAE is frequently used to identify pathogenic mechanisms of autoimmune T-cell responses in the CNS. It is also applied to develop new treatment approaches for MS. In the course of EAE CD4⁺ T-cell and mononuclear cell inflammation is followed by axonal and neuronal damage in the CNS. The anti-inflammatory properties of edelfosine were studied in the RR-EAE model in SJL mice. Mechanisms of edelfosine action identified in the murine system were verified by the use of human T cells. The translational confirmation is indispensable for the potential application of edelfosine in MS. First, the edelfosine interference with human T-cell proliferation was characterized. These studies were extended to the genomic level. Specific questions were as follows:

1. Which is the effective edelfosine dose to induce clinical amelioration of the EAE-disease course in mice? The clinically effective edelfosine concentration, which was apparently devoid of side effects, was established in the SJL mouse model.
2. Can treatment effects be assigned to a distinct edelfosine mechanism or to a more general, possibly immunoablative action of the drug? Peripheral lymphoid organs were prepared from EAE-induced, edelfosine-treated SJL mice to clarify the impact of edelfosine treatment on immune cell compositions and T-cell functions.
3. Is edelfosine interfering with the immune cell infiltration into the CNS during the acute EAE phase? Immune cell infiltrates were determined and correlated with the neuronal damage in order to explain the potential mechanistic basis for clinical amelioration.
4. Which edelfosine concentrations interfere with the viability and/or functionality of stimulated or unstimulated human T cells? Edelfosine was examined for its dose-dependent impact on cell death and T-cell proliferation.
5. Which changes of gene expression are induced by edelfosine in human CD4⁺ T cells? This approach aimed at confirming proposed mechanisms of edelfosine action, but also at the detection of new edelfosine-induced pathways in human T cells.

3 Materials and Methods

3.1 Materials

3.1.1 Reagents

Reagents for animal experiments	Company	Cat. No.
Adjuvant, Incomplete (Freund)	BD Difco	263910
Aqua ad injectabilia	Braun	8445A-191
Edelfosine	R&D pharmaceuticals	AP-121
Ketanest [®] S (25 mg/ml)	Pfizer	647028001E
M. Tuberculosis H37 Ra	BD Difco	231141
Pertussis toxin, <i>Bordetella pertussis</i>	Calbiochem	516560
Rompun [®] 2%	Bayer Vital	01250847
Peptides:		
MOG35-55, rat	NeoMPS	
H-MEVGWYRSPFSRVVHLYRNGK-OH	Lot: W249B // 287040-15(27-2R2)	
PLP139-151	NeoMPS	
H-HSLGKWLGHDPDKF-OH	Lot: X20D // 346019-02(22-36)	
Reagents for cell culture		
AIM V serum free medium	Invitrogen	12055-091
Brefeldin A solution (1000x)	BioLegend	420601
DMEM	Gibco	31885
DMEM+GlutaMAX	Gibco	31966
RPMI1640	Gibco	61870
Serum, fetal bovine (lot: A10408-1568, A10409-1608)	PAA Laboratories	A15-104
Serum, human type AB (lot: C02106-1878)	PAA Laboratories	C15-021
Trypan Blue solution	Sigma Aldrich	T8154
Türk's solution	Merck	1092770100
X-Vivo 15	Lonza	BE04-418F
β-mercaptoethanol	Gibco	31350-010

Reagents for cell stimulation	Company	Cat. No.
Anti-CD3	eBioscience	16-0031
Anti-HLA-DR (L243) blocking antibody		
Anti-MHC class I (W6/32) blocking antibody		
Concanavalin A from <i>Canavalia ensiformis</i>	Sigma Aldrich	C0412
Ionomycin calcium salt from <i>Streptomyces conglobatus</i>	Sigma Aldrich	I0634
PHA, lectin from <i>Phaseolus vulgaris</i>	Sigma Aldrich	L9017
PMA	Sigma Aldrich	P1585
Reagents for histology	Company	Cat. No.
Acetic acid	Sigma Aldrich	27225
D(+)-sucrose	Carl Roth	4621.2
Eosin	Merck	1.15935.0100
Ethanol absolute (1% methyl ethyl ketone)	Th. Geyer	8100020144
H33258	Sigma Aldrich	B2883
Hematoxylin Harris	Merck	109243
Hydrochloric acid	Merck	1.09057.1000
Na ₂ HPO ₄	Applichem	A3599,1000
NaH ₂ PO ₄	Merck	1.06346.1000
Normal donkey serum (NDS)	Chemicon	S30-100ML
Paraformaldehyd	AppliChem	A3813,1000
XEM-200	Vogel	ND-HS-200
xylene	SDS	0750021
Reagents for flow cytometry	Company	Cat. No.
4-(2-hydroxyethyl)-1-piperazineethanesulfonic acid (HEPES)	Carl Roth	9105.3
Calcium chloride (CaCl ₂)	Fluka Chemika	21085
FACS Clean Solution	BD FACS	340345
FACSFlow Sheath Fluid, 20 l	BD FACSFlow	342003
FACS Rinse Solution	BD FACS	340346
FITC Annexin V	BD Pharmingen	556419
Fixation/Permeabilization Concentrate	eBioscience	00-5123
Fixation/Permeabilization Diluent	eBioscience	00-5223
IC Fixation Buffer	eBioscience	00-8222
Permeabilization buffer (10x)	eBioscience	00-8333

Propidium iodide	Sigma Aldrich	P4170-25MG
Sodium azide (NaN ₃)	Carl Roth	K305.1
Sodium chloride (NaCl)	Carl Roth	3957.2

Reagents for RNA isolation, cDNA synthesis

	Company	Cat. No.
Chloroform	Fluka Chemika	25690
DEPC-treated water	Ambion	AM9920
Ethanol	Carl Roth	9065.3
Isopropyl alcohol	Carl Roth	6752.4
Pellet Paint [®] Co-Precipitant	Merck	69049-3
Triton X 100	Carl Roth	3051.2
TRIzol [®] Reagent	Invitrogen	15596-026

Other reagents

	Company	Cat. No.
[Methyl- ³ H]-thymidine, 1.0 mCi/ml	Hartmann Analytic	MT6038
10x PBS	PAA	H15-011
1x PBS	PAA	H15-002
Ammonium chloride (NH ₄ Cl)	AppliChem	A3661,1000
Betaplate Scint	Perkin-Elmer	1205-440
BSA	PAA	K45-001
Collagenase I	Roche	11088793001
ddH ₂ O		
DNase I	Roche	11284932001
EDTA	AppliChem	A4892,0100
Ethylenediaminetetraacetic acid disodium salt (Na ₂ EDTA)	Carl Roth	8043.2
HBSS	Gibco	14170
LSM 1077 Lymphocyte Separation Medium	PAA	J15-004
Percoll	GE Healthcare	17-0891-01
Potassium bicarbonate (KHCO ₃)	Carl Roth	P748.2
Sodium bicarbonate (NaHCO ₃)	Merck	1.06329.1000
Sodium carbonate (Na ₂ CO ₃)	Carl Roth	8563.1
Sulfuric acid (H ₂ SO ₄)	Merck	1.00716.1000
TMB Single Solution	Invitrogen	00-2023
Tween-20	Sigma	P1379
Vybrant [®] CFDA SE Cell Tracer Kit	Invitrogen	V12883

3.1.2 Kits

Label	Company	Cat. No.
Bielschowsky for neurofibrils	Bio-Optica	04-040805
CD4 T Lymphocyte Enrichment Set - DM	BD IMag	557939
GeneChip Hybridization, Wash, and Stain Kit	Affymetrix	900720
GeneChip WT Terminal Labeling Kit	Affymetrix	900671
Human Th1/Th2/Th9/Th17/Th22 13plex FlowCytomix	eBioscience	BMS817FF
LIVE/DEAD [®] Fixable Aqua Dead Cell Stain Kit	Invitrogen	L34957
MACS T cell activation / expansion kit	Miltenyi	130-091-441
RNA 6000 Nano Kit	Agilent	5067-1511
RNeasy MinElute Cleanup Kit	Qiagen	74204
WT Expression Kit	Ambion	4411973

3.1.3 ELISA

Label	Company	Cat. No.
Human IFN- γ ELISA MAX [™] Standard	BioLegend	430102
VeriKine [™] Human Interferon-Alpha ELISA Kit	PBL Laboratories	PBL41100-1
VeriKine [™] Human Interferon-Beta ELISA Kit	PBL Laboratories	PBL41410-1

3.1.4 Software

Label	Company
2100 expert (Eukaryote Total RNA Nano)	Agilent
AxioVision AxioVs40 V 4.6.3.0	Zeiss
CellSens Entry 1.4.1	Olympus
TIGR MeV 4.6.1	TM4 Development Group
NanoDrop ND-1000 V3.5.2	Thermo Scientific
FlowJo 7.6.2	Tree Star
Expression Console 1.1	Affymetrix
FlowCytomix Pro 2.4	eBioscience
GeneChip Command Console 3.0	Affymetrix
FACSDiva 5.0.3	BD
Prism 5.02	GraphPad Software
R statistical platform 2.12, gplots 2.8.0	

3.1.5 Laboratory animals

Strain	Company
C57BL/6J	The Jackson Laboratory*
SJL/JCrI	Charles River Laboratories
SJL/JHanHsd	Harlan Laboratories

*mice were imported and bred by the animal facility of the University Medical Center Hamburg-Eppendorf

3.1.6 Equipment

Label	Company	Cat. No.
μQuant™ microplate spectrophotometer	Biotek Instruments	
2100 Bioanalyzer	Agilent	G2938A
accu-jet® pro	Brand	26300
AxioCam HRm	Zeiss	426511-9901-000
Axiovert 40	Zeiss	
CKX41	Olympus	
CMV-min rotator	CMV	79029
Cryo 1°C Freezing Container	Nalgene	5100-0001
CX21	Olympus	
Ebq100 isolated	Leica Microsystems	
Feeding Needle	Fine Science Tools	18060-20
Filtermat A, GF/C	Perkin Elmer	1450-421
Filtermat cassettes	Perkin-Elmer	1450-101
freezer	Sanyo	
fridges	Bosch, Liebherr	
Harvester 96 Mach III M	TOMTEC	96-3M-FM
Heat Sealer 1295-012 Bag Sealer	LKB Wallac	
HERAcell® 240	Thermo Scientific	
LABS-40K nitrogen tank	Taylor-Wharton	
LSRII flow cytometer	BD	
MiniSpin®	Eppendorf	5452 000.018
Multifuge 3S-R	Heraeus	75004371

NanoDrop Spectrophotometer ND1000	Thermo Scientific	
Neubauer Counting Chamber	Marienfeld	0640110
RAININ Pipet-Lite LTS™ 8-channel	Mettler Toledo	L8-200
RC-5C Plus	Sorvall	
REGLO Analog MS-4/8	ISMATEC	ISM 827
Research Cryostat Leica CM3050 S	Leica	
RNA Nano Chips	Agilent	5067-1511
Sample Bag, for MicroBeta® Trilux	Perkin Elmer	1450-432
Shaking water bath	GFL	1083
Single channel pipettes	Gilson, eppendorf	
SS-34 rotor	Thermo Scientific	28020
Swinging Bucket Rotor	Sorvall	75006445
SZX16	Olympus	
Vortex Mixer	VWR International	444-1372
Wallac Trilux 1450 MicroBeta® Counter	Wallac	

3.1.7 Consumables

Label	Company	Cat. No.
96-well flat-bottom microplate	Corning	9018
96-well round-bottom microplate	Greiner Bio-One	650180
Absolute Counting Tubes	BD Trucount	340334
Cell culture dish	Greiner Bio-One	632171
Cell culture dish	Greiner Bio-One	628160
Cell culture flask, 175 cm ²	Greiner Bio-One	660160
Cell strainer 40 µm	BD Falcon	352340
Combidyn® adapter, Luer-Lock	B. Braun Melsungen	5206634
Cover slips, square	Carl Roth	1871
Cutoffix® scalpel	B. Braun Melsungen	5518059
FACS tubes	Sarstedt	55.1579
Fluoromount G	SouthernBiotech	0100-01
GeneChip Human Gene 1.0 ST Array	Affymetrix	901087
Injekt® Solo syringe	B. Braun Melsungen	4606027V
Micro tubes, 1.2 ml	Henze Laboratory Equipment	11622
Omnifix®-F syringe	B. Braun Melsungen	9161406V
Pipette 10 ml	Greiner Bio-One	607180
Pipette 1ml	Greiner Bio-One	604181

Pipette 2 ml	Greiner Bio-One	710180
Pipette 25 ml	Greiner Bio-One	760160
Pipette 5 ml	Greiner Bio-One	606180
Pipette tips	Mettler-Toledo	GPS-L250
Pipette tips, 10 µl	Sarstedt	
Pipette tips, 1000 µl	Sarstedt	70.762
Pipette tips, 200 µl	Sarstedt	70.760.002
Round-Bottom Tube	BD Falcon	352054
S-Monovette® 9 ml, K-EDTA	Sarstedt	02.1066.001
Sterican® G 24 x 1	B. Braun Melsungen	4657675
Sterican® G 26 x 1	B. Braun Melsungen	4657683
Sterican® G 30 x 1/2	B. Braun Melsungen	4656300
Stericup-GP Express PLUS, 0.22 µm	Millipore	SCGPU05RE
Superfrost/Plus	Karl Hecht	2409/1
Tissue Freezing Medium	Jung	020108926
Tube 15 ml	Greiner Bio-One	188271
Tube 50 ml	Greiner Bio-One	227261

3.1.8 Cell culture media

Complete mouse medium	50 µM β-mercaptoethanol 10% FCS in RPMI1640+GlutaMAX
Complete TCL medium	L-glutamine P/S gentamycin 10% human serum in RPMI

3.1.9 Buffers and solutions

0.1 M phosphate buffer	57 ml NaH ₂ PO ₄ 243 ml Na ₂ HPO ₄ in 1 l ddH ₂ O pH 7.4
4% PFA	40 g/l PFA

	in 0.1 M phosphate buffer
	heat 0.1M phosphate buffer, stir and add PFA
Annexin binding buffer	10 mM HEPES
	140 mM NaCl
	2.5 mM CaCl ₂
	in ddH ₂ O
	pH 7.4
Assay diluent for IFN-γ-ELISA	1% BSA
	in PBS
Blocking solution	0.1% Triton X 100
	10% NDS
	in PBS
Coating buffer for IFN-γ-ELISA	8.4 g/l NaHCO ₃
	3.56 g/l Na ₂ CO ₃
	in ddH ₂ O
	pH 9.5
Digestion solution	1 mg/ml collagenase I
	0.1 mg/ml DNase I
	in DMEM
Eosin solution	50 ml eosin solution (stock)
	2 ml acetic acid
	390 ml 96% ethanol
Eosin solution (stock)	10 g/l eosin in ddH ₂ O
FACS buffer	0.02% NaN ₃
	0.1% BSA
	in 1x PBS
MACS buffer	1% human serum
	2mM EDTA
	in PBS
Percoll 90%	10% 10x PBS
	in Percoll
Percoll A	78% Percoll 90%
	in PBS
Percoll B	30% Percoll 90%
	in HBSS
Phosphate buffer component A	0.2 M NaH ₂ PO ₄
	in ddH ₂ O

Phosphate buffer component B	0.2 M Na ₂ HPO ₄ in ddH ₂ O
PI solution	10% PI solution (stock) in FACS buffer
PI solution (stock)	10 mg/ml PI in ddH ₂ O
Red blood cell lysis buffer	0.15 M NH ₄ Cl 10 mM KHCO ₃ 0.1 mM Na ₂ EDTA in ddH ₂ O pH 7.4
Stop Solution for IFN- γ -ELISA	1.8 N H ₂ SO ₄
Wash buffer for IFN- γ -ELISA	0.05 % Tween-20 in PBS

3.1.10 Antibodies

Antibody	Clone	Company	Cat. No.
<i>Anti-mouse</i>			
Anti-B220-PE-Cy5.5	RA3-6B2	eBioscience	35-0452-82
Anti-caspase-3-PE	C92-605	BD Pharmingen	550821
Anti-CD3-PB	500A2	BD Pharmingen	558214
Anti-CD3-PerCP-Cy5.5	145-2C11	BioLegend	100328
Anti-CD4-APC-eFluor 780	RM4-5	eBioscience	47-0042-82
Anti-CD4-eFluor 450	RM4-5	eBioscience	48-0042-82
Anti-CD4-FITC	GK1.5	BioLegend	100406
Anti-CD4-PE	GK1.5	eBioscience	12-0041-82
Anti-CD8a-eFluor 450	53-6.7	eBioscience	48-0081-82
Anti-CD8a-PE-Cy7	53-6.7	BioLegend	100721
Anti-CD11b-APC	M1/70	eBioscience	17-0112-83
Anti-CD11b-FITC	M1/70	eBioscience	11-0112-82
Anti-CD11c-APC	N418	eBioscience	17-0114-82
Anti-CD11c-PE-Cy7	N418	eBioscience	25-0114-82
Anti-CD16/CD32	93	eBioscience	16-0161-82
Anti-CD25-APC	PC61.5	eBioscience	17-0251-82

Anti-CD44-APC	IM7	eBioscience	17-0441-81
Anti-CD45-APC-Cy7	30-F11	BioLegend	103116
Anti-CD45-PE-Cy7	30-F11	eBioscience	25-0451-82
Anti-CD62L-PE-Cy7	MEL-14	eBioscience	25-0621-81
Anti-CD69-FITC	H1.2F3	eBioscience	11-0691-82
Anti-IFN- γ -PE	XMG1.2	eBioscience	12-7311-81
Anti-IL-17A-Alexa647	17B7	eBioscience	51-7177-82
Anti-Ly-6G (Gr1)-FITC	RB6-8C5	eBioscience	11-5931-82
Anti-Ly-6G (Gr1)-PE	RB6-8C5	eBioscience	12-5931-82
Anti-NK1.1-PE	PK136	eBioscience	12-5941-81
Anti-NK1.1-PE-Cy7	PK136	BD Pharmingen	552878

Anti-human

Anti-CD3-PE-Cy7	UCHT1	eBioscience	25-0038-42
Anti-CD45RA-PE-Cy5.5	MEM-56	Invitrogen	MHCD45RA18
Anti-CD4-APC	RPA-T4	eBioscience	17-0049-42
Anti-CD4-APC-Alexa Fluor 750 (1:20)	RPA-T4	eBioscience	27-0049-73
Anti-CD4-APC-Cy7 (1:3)	SK3	BD Pharmingen	341115
Anti-CD5-PerCP-Cy5.5	L17F12	BD Pharmingen	341109
Anti-CD8-PB	DN25	Dako	PB984
Anti-CD19-V450	HIB19	BD Pharmingen	560353
Anti-CD27-APC-Alexa Fluor 750	CLB-27/1	Invitrogen	MHCD2727
Anti-CD38-APC	HIT2	BD Pharmingen	555462
Anti-CD69-PE	FN50	eBioscience	12-0699-73
Anti-HLA-DR/DP/DQ-FITC	TÜ39	BD Pharmingen	555558
Anti-IgD-PE	IA6-2	BD Pharmingen	555779
Anti-IgG	polyclonal	Jackson IR	009-000-003
Mouse IgG _{2a} , κ -FITC	G155-178	BD Pharmingen	553456

Antibodies for IHC

Clone

Company

Cat. No.

Primary antibodies

Anti-CD3	145-2C11	eBioscience	14-0031
Anti-CD45	30-F11	BD Pharmingen	550539
Anti-NeuN	A60	Millipore	MAB377

Secondary antibodies

Anti-hamster Cy2	Jackson IR	127-225-160
Anti-mouse Cy3	Jackson IR	115-165-062
Anti-mouse DyLight488	Jackson IR	715-486-150
Anti-rat Cy3	Jackson IR	712-166-150

3.2 Methods**3.2.1 Preparation of edelfosine**

For *in vitro* experiments dilutions of dissolved edelfosine in dest. H₂O were prepared and stored at -20°C until use. For *in vivo* applications of edelfosine, 20 mg and 5 mg edelfosine were dissolved in 1 ml aqua ad injectabilia, respectively. To achieve the final concentrations of 1 mg/ml edelfosine and 0.1 mg/ml edelfosine, 60 µl and 24 µl of the respective predilutions were diluted with 1140 µl and 1176 µl PBS. The diluted edelfosine was stored in 1.5 ml reaction tubes at -20°C and thawed on the day of application. Based on the injection volume of 200 µl per mouse and the assumed weight of 0.02 kg per mouse the injected edelfosine dose per mouse was 1 mg/kg, 10 mg/kg, 15 mg/kg and 25 mg/kg edelfosine. Edelfosine was applied by intraperitoneal injection or by gavage.

3.2.2 Active induction of EAE

For EAE experiments C57BL/6J mice, SJL/JCrI or SJL/JHanHsd mice were housed in “individually ventilated cages (IVC)”-racks at least one week prior to the active induction of EAE. On the day of immunization mice were injected subcutaneously at two sites of the flanks with 200 µg of MOG₍₃₅₋₅₅₎ or 75 µg/ml of PLP₍₁₃₉₋₁₅₁₎ peptide in incomplete Freund’s adjuvant (IFA) supplemented with 4 mg/ml *Mycobacterium tuberculosis* H37A. C57BL/6J mice were injected intravenously with 300 ng of Pertussis toxin on the day of immunization and 48 h later. SJL/JCrI and SJL/JHanHsd mice received a single dose of 200 ng Pertussis toxin on the day of immunization. Body weight and clinical score were monitored on a 0 to 5 scale with classifications of disease severity: 0 = healthy, 1 = limp tail, 2 = ataxia and/or paresis of hind limbs, 3 = paraplegia, 4 = paraplegia with forelimb weakness, 5 = moribund or dead. In the following chapters, C57BL/6J and SJL/J mice are referred to as C57BL/6 and SJL, respectively. Animal experiments were performed in accordance with the guidelines of the local authorities (approved animal license: 22/08).

3.2.3 Organ preparation and cell isolation from mice

Preparation of cells from secondary lymphoid organs

Mice were sacrificed at day 9 after immunization. Lymph nodes and spleens were prepared, respectively. A single cell suspension was prepared by mincing the tissue and pushing it through a 40 µm cell sieve. The sieve was rinsed with cold PBS + 1% FCS. Cells were centrifuged at 250xg for 7 min at 4°C. Cells derived from the spleen were resuspended in 5 ml red blood cell lysis buffer and incubated on ice for 7 min. After addition of 30 ml PBS + 1% FCS the cell suspension was subjected to the next centrifugation step at 250xg for 7 min at 4°C. Cells derived from either lymph nodes or spleen were washed with PBS + 1% FCS and centrifuged again. Cells were resuspended in FACS buffer or PBS + 1% FCS if the preparation was followed by recall experiments.

Preparation of cells from the CNS of mice

Mice were sacrificed by general anesthesia (20% O₂ + 80% CO₂ followed by pure CO₂). Using a peristaltic pump mice were perfused with PBS + 1% FCS for 5 min at 10 ml/min. Brain and spinal cord were prepared and processed. Dissected tissue was digested for 60 min at 37°C by addition of 1 mg/ml collagenase I and 0.1 mg/ml DNase I in D-MEM. The cell suspension was passed through a 40 µm cell strainer and centrifuged (250xg, 10 min, 4°C). Cells were then washed with PBS + 1% FCS, centrifuged (250xg, 10 min, 4°C) and separated from myelin and neurons by Percoll-gradient centrifugation. In brief, cells were resuspended in 2 ml 30% Percoll. Carefully, the cell suspension was underlain with 3 ml 78% Percoll. After centrifugation (250xg, 30 min, 4°C) the CNS-infiltrating cells and microglia were collected from the interface of the gradient. Cells were resuspended in FACS buffer, centrifuged (550xg, 10 min, 4°C) and washed two additional times (250xg, 10 min, 4°C).

Preparation of the CNS for histology

Mice were anesthetized by intraperitoneal injection of 120 mg ketamine (Ketanest[®] S) and 16 mg xylazine (Rompun[®] 2%) per kg body weight. Mice were transcatheterially perfused at 5 ml/min with 5 ml cold PBS followed by 25 ml 4% cold PFA in phosphate buffer. The CNS was prepared as described below.

Processing of CNS for cryosections

Preparation of brain, spinal cord and optic nerves was followed by post-fixation of the tissue in 4% PFA in phosphate buffer (30 min, 4°C). The tissue was impregnated 2-3 days in 30% sucrose in PBS for cryoprotection. Cervical, thoracic and lumbar spinal cord as well as cerebellum and forebrain were separated. The tissue was embedded in Tissue Freezing Medium and frozen in isopentane cooled on dry ice. Tissue was stored at -80°C. 12-14 µm slices were generated using a cryostat, mounted on glass microslides, stored at -80°C and used for immunohistochemical analysis.

Preparation of the CNS for paraffin sections

Brain, optic nerves and the spinal cord contained within the spinal column were prepared and incubated o.n. at 4°C in 4% PFA in 0.1 M phosphate buffer. The spinal column was then transferred into EDTA buffer for 14 days in which EDTA acted as a chelator for osseous calcium. Paraffin-embedding as well as hematoxylin-eosin (HE) staining and Bielschowsky-silver impregnation was performed at the Department of Neuropathology at the University Medical Center Hamburg-Eppendorf. In brief, paraffin-embedded tissue was cut to yield 2-4 µm thin sections and slices were mounted on glass microslides. For histological stainings paraffin was removed by incubating the tissue sections repeatedly in xylene for 5 min. Subsequently, sections were watered by successive transfer into anticlimactic ethanol dilutions. First, tissue slices were washed 2x in 100% ethanol, 2x in 96% ethanol and in 90% ethanol for 60 s, respectively. Afterwards, sections were washed in 80%, 70% and 50% ethanol and rinsed 2x with ddH₂O.

3.2.4 Histological analysis

Immunohistochemical analysis

Cryoslices mounted on glass microslides were rinsed 3x with PBS for 5 min. Slides were incubated with blocking solution for 2 h at RT. The respective primary antibody was diluted in PBS as indicated and 100 µl of the dilution were transferred per slide. Tissue slices were incubated o.n. at 4°C and then washed 3x with PBS for 5 min. The secondary antibody was diluted in PBS as indicated and 100 µl per slide were applied. After 2.5 h of incubation at RT the tissue was rinsed 3x in PBS for 5 min. Finally, glass coverslips were mounted on Fluoromount G-coated tissue. Images were acquired using a Zeiss Axiovert 40 inverted microscope and analyzed with AxioVision AxioVs40 V 4.6.3.0 software.

Quantification of neuronal cell bodies

For quantification of NeuN-positive neuronal cells within the cervical spinal cord 14 μm cryosections were prepared. The primary anti-NeuN antibody was diluted 1:100 in PBS, the secondary antibody was diluted 1:400 in PBS. For each mouse, six cervical spinal cord sections were selected and two adjacent photographs per ventral horn were made. Photographs were taken with 20x magnification. NeuN+ cells were counted and the average number of neurons per section was calculated.

Detection of CNS-infiltrating leukocytes and T cells

For the immunohistochemical investigation of infiltrating leukocytes into CNS tissue 12 μm cryosections were prepared. The primary anti-CD45 antibody was diluted 1:50 in PBS and the secondary antibody was used 1:400 diluted in PBS. To detect infiltrating T cells a primary antibody against CD3 was diluted 1:100 in PBS. The corresponding secondary antibody was diluted 1:200 in PBS. One representative mouse per treatment condition was selected and photographs of the anterior fissure were taken using 20x magnification.

Hematoxylin-eosin staining

Paraffin-embedded tissue was processed as described before. Subsequently, sections were incubated for 5 min in filtered hematoxylin Harris. Slices were rinsed with ddH₂O and differentiated in 0.2% hydrochloric acid. To allow blueing of stains sections were rinsed with alkaline tap water for 5 min. After incubation in 70% ethanol for 3 min sections were transferred into eosin solution for circa 3 min. Unbound eosin was removed by washing the sections 3x in 100% ethanol and xylene, respectively. Finally, glass coverslips were mounted on Fluoromount G-coated tissue. Images were acquired using an Olympus SZX16 research stereomicroscope and analyzed by Olympus CellSens Entry 1.4.1 software.

Bielschowsky-silver staining

To visualize nerve fibers, axons and tangles of neurofibrils, paraffin-embedded tissue sections were treated as mentioned before. Generally, tissues were incubated in silver nitrate solution. The addition of ammonia produces ammonium nitrate as well as oxidized, precipitated silver. In brief, after incubation in H₂O sections were placed in wet chambers, 10 drops of reagent A were added and the slides were incubated for 5 min at 40°C. After repeated washing in ddH₂O and application of 10 drops of reagent B the sections were

incubated again in wet chambers (20 min, 40°C). Immediately afterwards, sections were transferred into reduction solution, incubated for 2 min, washed 2x with ddH₂O and incubated with 10 drops of reagent G for 3 min. Finally, tissue was washed twice with ddH₂O, dehydrated in successive ascending ethanol dilutions and xylol. Tissue was coated with Fluoromount G and covered with glass coverslips. Microscopy was done using an Olympus SZX16 research stereomicroscope and analyzed by Olympus CellSens Entry 1.4.1 software.

3.2.5 Flow cytometry

Cell-surface staining

For Fc-receptor blocking cells were incubated at 10x10⁶ cells per ml in FACS buffer supplemented with 1:1000 anti-mouse CD16/CD32 antibody and with 1:20 anti-human IgG, respectively (10 min, 4°C). After addition of antibodies for cell-surface staining the cells were incubated for another 30 min at 4°C. Cells were washed with FACS buffer and centrifuged (350xg, 5 min, RT). Data was acquired on an LSRII flow cytometer and analyzed using FACSDiva and FlowJo software.

Quantification of CNS-infiltrating cells

Cells prepared from the CNS of mice were resuspended in 500 µl PBS + 1% FCS. 50 µl of the cell suspension were transferred into Absolute Counting Tubes followed by addition of 50 µl FACS buffer containing 1:50 anti-mouse CD16/32 antibody and anti-CD45-APC-Cy7 antibody. During this sample preparation a lyophilized pellet of a known number of fluorescent beads was released by the tubes. After incubation (20 min, 4°C) 300 µl FACS buffer were added and data was acquired by flow cytometry. The absolute number of CNS-infiltrating cells was calculated by appropriate gating on CD45+ events as well as bead events:

$$\frac{events_{cells}}{events_{beads}} \cdot \frac{beads / test}{volume_{test}} = count_{cells}$$

Intracellular cytokine staining

Cells were incubated for 4 h in complete mouse medium supplemented with 100 ng/ml PMA and 1 µg/ml ionomycin. After 1 h 10 µg/ml Brefeldin A was added to inhibit the intracellular protein transport thereby inducing the accumulation of proteins within the ER. If cells were prepared from the CNS of mice, cells were additionally washed 2x with PBS and centrifuged

(350xg, 5 min, RT). Subsequently, cells were incubated for 30 min at 4°C in PBS supplemented with Component A of the LIVE/DEAD Fixable Dead Cell Stain Kit according to the manufacturer's instructions. Cells were washed 2x in PBS (350xg, 5 min, RT).

Cells were resuspended in fixation buffer and incubated for 20 min at RT. The cells were washed in PBS and additionally 2x in permeabilization buffer to allow detection of intra-cellular proteins. For cell-surface staining cells were blocked with 1:1000 anti-mouse CD16/CD32 antibody in permeabilization buffer and incubated for 10 min at 4°C. Permeabilization buffer was added and cells were centrifuged (350xg, 5 min, RT). Cells were resuspended in permeabilization buffer containing antibodies for cell-surface staining and incubated for 30 min at 4°C. Cells were washed with permeabilization buffer and centrifuged (350xg, 5 min, RT). For intracellular cytokine staining cells were resuspended in permeabilization buffer supplemented with antibodies against IFN- γ and IL-17A. After incubation for 30 min at RT permeabilization buffer was added and cells were centrifuged (350xg, 5 min, RT). After repeated washing in permeabilization buffer cells were resuspended in FACS buffer for data acquisition.

Staining for the nuclear transcription factor Foxp3

Cell surface staining was performed according to the cell-surface staining protocol. Afterwards cells were washed in FACS buffer (350xg, 5 min, RT) and Foxp3 Fixation/Permeabilization Concentrate and Diluent were applied according to the manufacturer's instructions. After 1 h of incubation at 4°C cells were washed repeatedly in permeabilization buffer. Cells were resuspended in permeabilization buffer supplemented with antibody against Foxp3 and incubated for 1 h at 4°C. Again, cells were washed repeatedly in permeabilization buffer. Finally, cells were resuspended in FACS buffer and analyzed.

Staining for active caspase-3

Cell-surface staining was performed according to the cell-surface staining protocol. Afterwards cells were washed in FACS buffer (350xg, 5 min, RT), incubated in fixation buffer (20 min, RT) and washed in permeabilization buffer (350xg, 5 min, RT). Subsequently, the cells were incubated in permeabilization buffer that contained anti-activated caspase-3 antibody (60 min, RT). Finally, cells were washed repeatedly in permeabilization buffer. For data acquisition cells were resuspended in FACS buffer.

Strategy for immunophenotyping of cells isolated from immunized mice

To investigate the impact of edelfosine treatment on immune cell subsets, organs from EAE-affected mice were prepared as mentioned above. Several combinations of antibodies and fluorophores were applied. Table 1 summarizes the antibodies utilized for analysis of lymph node- and spleen-derived cells.

Table 1: Immunophenotyping of cells prepared from peripheral lymphoid organs. Cells were isolated as described in 2.2.3. Antibodies were applied according to the *cell-surface staining* protocol except for antibodies against cytokines IFN- γ and IL-17A (refer to: *intracellular cytokine staining*), Foxp3 (refer to: *Staining for the nuclear transcription factor Foxp3*) as well as antibodies against activated caspase-3 (refer to: *Staining for active caspase-3*).

	APC / Alexa647	APC-Cy7 / APC-eFluor780	FITC	Pacific Blue	PE	PE-Cy7	PE-Cy5.5 / PerCP-Cy5.5
Cell types	CD11b	CD45	Ly-6G (Gr1)	CD3	NK1.1	CD11c	CD45R (B220)
Naive and memory T cells	CD44			CD8a	CD4	CD62L	CD3
T cell activation and Tregs	CD25	CD4	CD69	CD8a	Foxp3		CD3
Apoptosis	CD25	CD4	CD69	CD8a	Caspase-3		CD3
T cell differentiation	IL-17A	CD4	CD11b	CD8a	IFN- γ	CD45	CD3

For analysis of CNS-infiltrating immune cells antibodies were used as mentioned in Table 2. Here, in all cases the LIVE/DEAD[®] Fixable Aqua Dead Cell Stain Kit was integrated which possessed an approximate fluorescence-emission maximum at 526 nm.

Table 2: Immunophenotyping of CNS-infiltrating cells. After preparation and isolation of cells from brains and spinal cords according to 2.2.3 antibodies were used for cell-surface staining. Antibodies against IFN- γ , IL-17A, Foxp3 as well as activated caspase-3 were applied as mentioned in the respective protocols.

	APC / Alexa647	APC-Cy7 / APC-eFluor780	FITC	Pacific Blue / V450	PE	PE-Cy7	PE-Cy5.5 / PerCP-Cy5.5
Cell types	CD11c	CD45	CD11b	CD3	Ly-6G (Gr-1)	NK1.1	CD45R (B220)
T cell activation	CD25		CD69	CD4	Foxp3	CD8a	CD3

and Tregs							
Apoptosis	CD25	CD4	CD69	CD8a	Caspase-3		CD3
T cell differentiation	IL-17A		CD4	CD8a	IFN- γ		CD3

3.2.6 Isolation of human cells from blood

Isolation of human PBMCs

Buffy Coats were diluted with PBS and PBMCs were separated by Ficoll gradient centrifugation (650xg, 30 min, RT). Mononuclear cells which accumulated at the interphase were resuspended in ice-cold PBS and centrifuged (550xg, 10 min, 4°C). Cells were washed in ice-cold PBS and spun down (350xg, 5 min, 4°C). The cell number was determined by staining of cells with Türks Blue.

Enrichment of human CD4+ T cells

To achieve enrichment of CD4+ T cells PBMCs were resuspended in Biotin-containing enrichment cocktail, washed with MACS buffer and incubated with streptavidin particles for 30 min at RT. Negative selection of CD4+ T cells was performed according to the manufacturer's instructions (CD4 T Lymphocyte Enrichment Set). Briefly, the cell suspension was exposed to a magnetic field for 8 min. The enrichment of CD4+ T cells was repeated and cells were resuspended in MACS buffer. The cell number was determined by staining with Türks Blue-solution. 2×10^5 cells were employed to determine CD4+ T cell purity by flow cytometry using anti-CD3 and anti-CD4 antibodies. A purity of more than 90% was achieved.

3.2.7 *In vitro* cell-culture experiments

Staining for Annexin V-positive cells after in vitro culture with edelfosine

The impact of edelfosine on activated murine T cells was investigated by preparation of draining lymph node cells from 6 weeks-old female C57BL/6 mice. Cells were seeded at 2×10^5 cells per well of a 96-well plate in complete mouse medium. For T-cell activation 5 μ g/ml Concanavalin A (Con A) and 1 μ g/ml anti-CD3 antibody were added, respectively. After 48 h of incubation edelfosine was added. Cells were analyzed after 96 h. To study the impact of edelfosine on T-cell activation as well as activated T cells, PBMCs were isolated and seeded in triplicate at 2×10^5 cells per well in 96-well plates in 200 μ l X-Vivo 15. Cells

were stimulated with 2.5 µg/ml PHA in presence of edelfosine ranging from 1 µg/ml to 33.3 µg/ml. After 24 h or 3 days of incubation, triplicates of each approach were pooled for analysis. Alternatively, edelfosine was added after 2 days and cells were pooled after 3 days. For analysis cells were washed in FACS buffer and blocking of Fc-receptors was performed as described above. After washing with FACS buffer (350xg, 5 min, RT) cells were resuspended in binding buffer containing antibodies for cell surface staining as well as Annexin V. For murine lymph node cells the incubation with antibodies (15 min, RT) was followed by addition of 1 µl PI-solution 5 min prior to flow cytometry. For PBMCs, each approach was split into equal volumes after incubation for 15 min at RT in binding buffer. One part was used to discriminate between viable cells, cells that were in early apoptosis and cells that were in late apoptosis or already dead. Therefore, 1 mg/ml of the vital dye PI was added 5 min prior to cell acquisition by flow cytometry. The second part was washed in FACS buffer (350xg, 5 min, RT) and stained with anti-activated caspase-3 antibody as described before. Data was acquired on an LSRII flow cytometer and analyzed using FACSDiva and FlowJo software.

Generation of human antigen-specific T-cell lines (TCLs)

T cells specific for MBP₍₈₃₋₉₉₎ were prepared from PBMCs of an MS-affected individual that was proven to carry the HLA-DR15-haplotype. In brief, 2×10^5 PBMCs per well were seeded in 96-well plates in complete TCL medium supplemented with 10 µg/ml MBP₍₈₃₋₉₉₎ peptide. At day 7 after seeding 20 IU/ml IL-2 were added to the cells. Subsequently, at day 12 after seeding proliferating cells were counted and plated at 2×10^5 cells per well in 96-well plates in RPMI complete medium supplemented with 10 µg/ml MBP₍₈₃₋₉₉₎ peptide, 20 IU/ml IL-2 on 1×10^5 autologous feeder cells irradiated at 60 Gray. Cells were incubated for another 12 days and the addition of IL-2 was repeated every 3-4 days.

[³H-methyl]thymidine-incorporation assay

T cells were derived from lymph nodes and spleens of SJL mice that were immunized as previously described. Human PBMCs and TCLs were obtained as mentioned before. Cells were seeded in 96-well plates at 2×10^5 cells/well or 2×10^4 cells/well in the case of TCLs. Murine cells were cultured in 200 µl of complete mouse medium supplemented with the disease relevant peptide PLP₍₁₃₉₋₁₅₁₎, a polyclonal anti-CD3e antibody or mitogenic Concanavalin A. Human cells were incubated in X-Vivo 15 medium supplemented with a polyclonal stimulus (particles coated with antibodies against CD2, CD3 and CD28), mitogenic PHA or with the relevant peptide MBP₍₈₃₋₉₉₎ plus 5-fold autologous irradiated feeder

cells. Only in the case of the homeostatic proliferation experiment for up to seven days were human PBMCs cultured in AIM V serum free medium including blocking antibodies against HLA-DR and MHC class I, both at 30 µg/ml. Edelfosine was added as indicated. T-cell proliferation was determined by the incorporation of [³H-methyl]thymidine after 72 h of incubation. Precisely, 37x10⁶ Bq [³H-methyl]thymidine was added to each well 16 h before harvesting the cells. For quantification of beta particle emission the cells were harvested, washed and analyzed by using a beta counter. The stimulation index (SI) is calculated by dividing the mean counts per minute (cpm) of stimulated cells by cpm of respective unstimulated controls.

Characterization of edelfosine impact on T-cell proliferation by CFSE

Cells were prepared from draining lymph nodes of 6 week-old female C57BL/6 and SJL mice. Cells were labeled by incubation with 0.5 µM CFSE in PBS (10 min, RT) and blocked by addition of an equal volume of RPMI1640 + 15% FCS. Afterwards, cells were incubated again (10 min, RT) and washed repeatedly with RPMI1640 + 10% FCS (350xg, 5 min, RT). Finally, cells were seeded at 2x10⁵ cells per well of a 96-well plate in complete mouse medium. Cells were stimulated by addition of 5 µg/ml Concanavalin A or 1 µg/ml anti-CD3 antibody. Edelfosine was added at 1 µg/ml, 3 µg/ml, 5µg/ml and 10 µg/ml, respectively. After 4 days of incubation cells were washed in FACS buffer (350xg, 5 min, RT), blocked and stained as described before. Cells were washed in FACS buffer and 5 min prior to analysis by flow cytometry 1 mg/ml PI was added.

Culture of enriched human CD4+ T cells for gene-expression analysis

Enriched CD4+ T cells obtained from Buffy Coats were prediluted in the respective cell-culture medium to meet the planned culture conditions. Cells were resuspended in X-Vivo 15, X-Vivo 15 supplemented with 3.3 µg/ml edelfosine, 10 µg/ml edelfosine, bead particles coated with antibodies against CD2, CD3 and CD28, or 3.3 µg/ml edelfosine in combination with bead particles coated with antibodies against CD2, CD3 and CD28, respectively. Bead particles were loaded and used according to the manufacturer's instructions at a ratio of 1:2 of loaded beads per cell. The CD4+ T cells were seeded at 2x10⁵ cells per well of a 96-well plate in 200 µl of the respective cell-culture medium. Cells were incubated for 30 h. 100 µl of the cell-culture supernatant per well were saved and stored at -20°C prior to subjecting cells to RNA isolation.

Analysis of MHC class II expression of CD4⁺ T cells by flow cytometry

PBMCs were isolated as described before. Cells were seeded at 2×10^6 cells in sterile 5 ml round bottom tubes. Cells were cultured in 500 μ l X-Vivo supplemented with 3.3 μ g/ml or 10 μ g/ml edelfosine as well as particles coated with antibodies against CD2, CD3 and CD28 as indicated for 24 h. First, cells were washed twice with FACS buffer (350xg, 5 min, RT) and stained for viability by using the LIVE/DEAD Fixable Dead Cell Stain Kit as recommended. Cells were washed with PBS (350xg, 5 min, RT), blocked and stained for cell-surface antigen expression as described before. Data was acquired on an LSRII flow cytometer and analyzed with FACSDiva and FlowJo software.

3.2.8 RNA isolation, cDNA synthesis and microarray analysis

Isolation of RNA from CD4⁺ T cells

After 30 h of incubation CD4⁺ T cells of each approach were pooled and counted. The cell pellets were resuspended in 1 ml TRIzol reagent, respectively. By using 0.6 mm and 0.45 mm needles and syringes the cells were mixed and 1 μ l Pellet Paint[®] Co-Precipitant as well as 200 μ l chloroform were added. After mixing, cells were incubated for 2 min at RT followed by centrifugation (12,000xg, 15 min, 4°C). The upper phases were transferred to a new 1.5 ml reaction tube and 500 μ l isopropanol were added. Cells were mixed and after 10 min of incubation at RT the suspensions were centrifuged (12,000xg, 10 min, 4°C). Subsequently, cells were washed in 1 ml 75% ice-cold ethanol, centrifuged (12,000xg, 5 min, 4°C) and the dried cell pellets were resuspended in 100 μ l DEPC-treated water.

For RNA concentration and purification the RNeasy MinElute Cleanup Kit was used as recommended by the manufacturer. In brief, RNA samples were mixed in 350 μ l buffer RLT and 250 μ l 100% ethanol were added. The sample volumes were transferred into spin columns and centrifuged (6,600xg, 30 s, RT). The columns were eluted by addition of 500 μ l buffer RPE and centrifugation (6,600xg, 30 s, RT). The wash step was followed by the addition of 500 μ l 80% ethanol and centrifugation (6,600xg, 2 min, RT). The elution of purified RNA was achieved by the addition of 14 μ l RNase-free water and a final centrifugation step (12,000xg, 1 min, RT).

Determination of RNA concentration and purity

To define the RNA concentration 1 μ l per purified RNA sample was transferred on a NanoDrop spectrophotometer ND-1000 and analyzed by using the program "ND-1000

V3.5.2". To determine the quality of the prepared RNA the Agilent RNA 6000 Nano Kit was used according to the manufacturer's instructions. RNA samples were heated at 70°C for 2 min prior to use. Subsequently, Agilent Nano Chips were loaded and analyzed by using the Agilent 2100 Bioanalyzer and the program "*Eukaryote Total RNA Nano*".

Gene-expression analysis by microarray technology

Reverse transcription of RNA to synthesize cDNA was done by using the Ambion WT Expression Kit. cDNA fragmentation and labeling was performed by applying the Affymetrix GeneChip WT Terminal Labeling Kit. Subsequently, probes were prepared using the Affymetrix GeneChip Hybridization, Wash, and Stain Kit and analyzed by microarray technology (Affymetrix GeneChip Human Gene 1.0 ST Array). The approach simultaneously allows to measure the expression levels of about 28,869 genes (whole-transcript coverage). Genes are represented by 26 probes, respectively, which are distributed across the full length of a gene thereby quantifying all transcripts from the same gene. The gene-expression scan was performed with the Affymetrix GeneChip Command Console 3.0 Software. The robust multi-array average (RMA) algorithm was applied for background correction, using the Affymetrix Expression Console 1.1 Software. The samples were quantile normalized, followed by mean signal summarization. Hierarchical clustering, t-test and significance analysis of microarrays (SAM) were performed using the TIGR (the institute for genomic research) multi experiment viewer (MeV) 4.6.1 Software.

3.2.9 ELISA

Enriched CD4+ T cells were cultured as mentioned before. Stored cell-culture supernatants were thawed, 12 wells per approach were selected and pooled. For ELISA analysis of IFN- α and - β according to the manufacturer's instructions, 100 μ l of mixed supernatant were transferred into microplate strips and incubated for 1 h at RT. Wells were rinsed with wash buffer and 100 μ l of antibody solution was added. After incubation (1 h, RT) wells were washed 3x with wash buffer. 100 μ l of horseradish peroxidase (HRP) solution was added to the wells and incubation (1 h, RT) was followed by four additional washing steps with wash buffer. Finally, 100 μ l of TMB Substrate Solution was added, wells were incubated for 15 min at RT and 100 μ l Stop Solution was added. Cytokines were quantified by using a microplate reader to determine the absorbance at 450 nm within 5 min after the addition of the Stop Solution.

For detection of IFN- γ , wells of a 96-well plate were coated with Capture Antibody in Coating Buffer according to the instructions of the manufacturer. In brief, the coated wells were

incubated at 4°C o.n. and washed 4x with 300 µl Wash Buffer per well. 200 µl Assay Diluent were added per well to block non-specific binding. The sealed plate was incubated (1 h, RT) on a plate shaker (200 rpm). After washing in Wash Buffer (4x) 100 µl of pooled supernatant were transferred into respective wells and sealed samples were incubated for 2 h at RT on a plate shaker (200 rpm). Wells were washed 4x with Wash Buffer. 100 µl diluted Detection Antibody solution was added per well and sealed wells were incubated with shaking (1 h, RT). Again, wells were washed 4x with Wash Buffer. 100 µl of Avidin-HRP solution were added per well. Sealed wells were incubated for 30 min at RT with shaking. Wells were washed 5x with Wash Buffer for 1 min. Finally, 100 µl of TMB Substrate Solution were added per well followed by incubation for 15-30 min to allow color development. The reaction was stopped by addition of 100 µl Stop Solution per well. Within 30 min the absorbance at 450 nm was acquired using a microplate reader.

3.2.10 Analysis of cytokine production by flow cytometry

Enriched CD4⁺ T cells were cultured as mentioned before. Saved cell-culture supernatants were thawed, 10 wells per approach were selected and 20 µl per well were pooled. Cytokines secreted by CD4⁺ T cells were determined by applying the Human Th1/Th2/Th9/Th17/Th22 13plex Kit FlowCytomix according to the manufacturer's instructions. Briefly, 25 µl of mixed supernatants were incubated for 2 h at RT with an equal volume of Bead Mixture and 50 µl Biotin-Conjugate Mixture. Cells were washed repeatedly with Assay Buffer (200xg, 5 min). Afterwards, cells were resuspended in 100 µl Assay Buffer and 50 µl Streptavidin-PE Solution and incubated for 1 h at RT. Again, cells were washed repeatedly in Assay Buffer (200xg, 5 min). For analysis with FACSDiva and FlowCytomix Pro 2.4 software, cells were resuspended in Assay Buffer and acquired using an LSRII flow cytometer.

3.2.11 Statistical analysis

EAE-disease courses and the homeostatic proliferation experiment were analyzed by two-way ANOVA and Bonferroni multiple testing correction (post-hoc analysis) using GraphPad Prism 5.02 software. In graphs representing the EAE-disease courses treatment effects were indicated by asterisks. Significant differences between groups were described in respective figure legends after Bonferroni post-hoc analysis. Cumulative disease scores and neuronal quantification by immunohistochemistry were analyzed by 1-way ANOVA followed by Bonferroni post-hoc test with asterisks indicative of significant differences between

groups. Moreover, data generated by flow cytometry for leukocyte subsets derived from EAE-induced mice were evaluated by Bonferroni post-hoc analysis after 1-way ANOVA. With regard to lymph nodes and spleen-derived subsets, frequencies were normalized and expressed as fold-changes in order to allow merging of two independent experiments. *Ex vivo* proliferation assays of murine lymph node cells were analyzed by 1-way ANOVA and Bonferroni post-hoc analysis, whereas results of proliferation assays of spleen-derived cells were tested by non-parametric Kruskal-Wallis test followed by Dunns post-hoc analysis. For analysis of human PBMC proliferation, proliferation of MBP₍₈₃₋₉₉₎-specific TCLs as well as expression of HLA by human B and T cells Bonferroni post-hoc tests succeeded repeated measures ANOVA. Data generated by ELISA and 13plex FlowCytomix kit were evaluated by paired t-tests, microarray data was examined by t-test analysis (adjusted P-value for significant genes: $P < 0.01$).

4 Results

4.1 Reduced proliferation of T lymphocytes in vitro in the presence of edelfosine

The proliferative capacity of T lymphocytes isolated from lymph nodes of naïve C57BL/6 and SJL mice was assessed in CFSE-proliferation assays. Cells were labeled with CFSE and stimulated with anti-CD3 antibody. After four days of culture, cells were stained for the expression of CD4 and CD8 and with PI to exclude dead cells. The gradual loss of CFSE-fluorescence intensity allowed to display the impact of edelfosine on T-cell proliferation. CD4+ as well as CD8+ T cells from both strains showed an edelfosine dose-dependent reduction of the proliferative response over eight generations (Figure 3).

In C57BL/6 lymphocytes, the addition of 5 µg/ml edelfosine reduced CD4+ T-cell frequencies below 1% in generation 3 or higher. 76.2% of the cells were found in generation 0 representing cells that underwent no cell division. However, most C57BL/6 CD4+ T cells were found in generation 1 and 2 in the absence of edelfosine. For CD8+ T cells, 5 µg/ml edelfosine decreased the proliferation with equal frequencies appearing in generations 2 and 3. Frequencies in higher generations were reduced. In comparison, the highest frequency of CFSE+ CD8+ T cells could be assigned to generation 4 (28.8%) in absence of edelfosine (generation 0: only 0.9% of all cells). This proliferative pattern is reflected by the corresponding analysis of progenitor frequencies.

For SJL-derived CD4+ T cells, 10 µg/ml edelfosine led to a distribution of frequencies which was comparable to the distribution for unstimulated cells. The addition of 1 µg/ml and 3 µg/ml edelfosine resulted in a dose-dependent reduction of CD4+ T cells which proliferated in accordance to increasing frequencies in generation 0. Regardless of being cultured with or without edelfosine, the major fraction of SJL mouse-derived CD4+ T cells did not proliferate. With regard to SJL-derived CD8+ T-cell frequencies, the largest fraction of cells was detected in generation 3 (26.2%) in the absence of edelfosine (C57BL/6-derived CD8+ T cells: generation 4). Upon presence of edelfosine largest fractions of SJL-derived CD8+ T cells accumulated in generation 0 in a dose-dependent manner. Focusing on SJL-derived CD4+ as well as CD8+ T cell progenitor distributions, largest fractions were found in generation 0. Progenitor frequencies reflected an edelfosine dose-dependent increase of cells which did not proliferate upon stimulation.

Progenitor frequencies of CD4+ T cells from C57BL/6 and SJL mice appeared to be directly dependent on edelfosine concentrations. CD8+ T cells from either mouse strains also demonstrated an edelfosine dose-dependent proliferative response. Generally, CD8+ T cells displayed an accelerated proliferative response compared to CD4+ T cells.

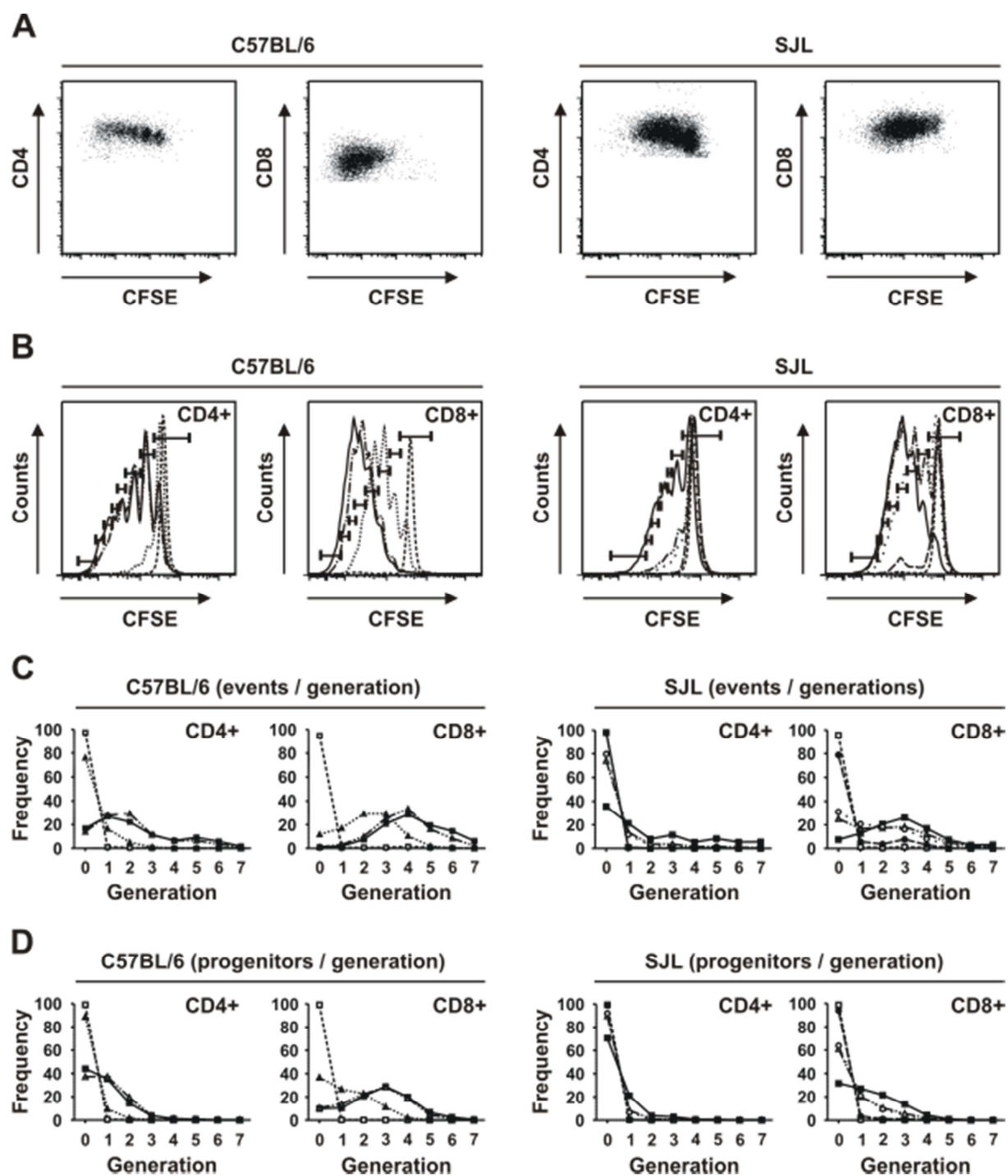


Figure 3. Edelfosine reduced the proliferation of lymphocytes derived from C57BL/6 as well as SJL mice ($n=1$ for each strain). **(A)** In CFSE proliferation assays CD4⁺ and CD8⁺ lymphocytes proliferated upon stimulation with anti-CD3 antibody as shown by flow cytometry. **(B)** The addition of edelfosine decreased CD4⁺ and CD8⁺ T cell proliferation in a dose-dependent manner. Bars indicate generations based on corresponding approaches of stimulated cells in absence of edelfosine. **(C)** Determination of lymphocyte frequencies in each generation revealed that CD8⁺ T cells of either strain origin possessed a higher proliferation rate in comparison to CD4⁺ T cells. The presence of edelfosine revealed a dose-dependent shift in frequency distributions over generations. **(D)** Frequency distributions of lymphocyte progenitors (parental cells of proliferated progeny) over generations were also shifted back to low generation numbers in dependency on the edelfosine concentration added (—■— no edelfosine, —△— 1 $\mu\text{g/ml}$ edelfosine, --○-- 3 $\mu\text{g/ml}$ edelfosine, ----▲---- 5 $\mu\text{g/ml}$ edelfosine, -●- 10 $\mu\text{g/ml}$ edelfosine, ---□--- unstimulated, no edelfosine).

4.2 Edelfosine treatment influences clinical symptoms in the EAE-mouse model

4.2.1 Preventive oral edelfosine administration reveals dose-dependent treatment effects in EAE-induced C57BL/6 mice (dose finding)

C57BL/6 mice were immunized using the MOG₍₃₅₋₅₅₎ peptide to develop chronic-progressive EAE. Five days prior to immunization mice received PBS by gavage on a daily basis to allow adaption to treatment procedure. After induction of EAE at day 0 mice were administered with equal volumes of PBS or edelfosine every day until day 31 (Figure 4 A). The PBS-treated control cohort developed first signs of EAE at day 12 after immunization reaching maximum EAE score at day 18 (2.83 ± 0.17). This acute phase of disease was shifted if mice were treated with edelfosine. Moreover, mice revealed concentration-dependent side effects at certain edelfosine concentrations. Mice treated with 25 mg/kg edelfosine had a maximum disease score of 1.5 ± 0 . But edelfosine treatment had to be stopped at day 19 after immunization as mice developed severe side effects like tremor, inactivity, slowed motion as well as whistling and squealing. Cessation allowed amelioration of impairments. Although much milder, the latter problems were also observed when mice were treated with 15 mg/kg edelfosine. This cohort showed a delayed EAE onset with the maximum EAE score (2.5 ± 0.25) at day 23. Interestingly, the treatment of mice with 10 mg/kg edelfosine was not only found to delay the maximum disease score of 1.17 ± 0.67 to day 27 in comparison with PBS-treated controls, but it also did not lead to apparent side effects. Administration of edelfosine led to a significant overall treatment effect with significant differences between PBS-treated controls and mice treated with 10 mg/kg edelfosine (day 14 to day 26, day 29 after immunization). The analysis of cumulative disease scores underscored the treatment effect with significant differences when mice were treated with 10 mg/kg edelfosine (cumulative disease score: 3.25 ± 0.58) compared to PBS control cohorts (cumulative disease score: 43.75 ± 3.84) (Figure 5 A). Taking into account the edelfosine-treatment effects as well as the observed side effects 10 mg/kg edelfosine appeared to be the effective concentration of edelfosine to ameliorate EAE-disease course while causing no detectable side effects.

4.2.2 Preventive treatment of EAE in SJL mice with edelfosine every other day has no influence on disease course

After having demonstrated the effectiveness of oral application of 10 mg/kg edelfosine on a daily basis edelfosine was examined in a subsequent preventive approach that aimed at proving amelioration of RR-EAE disease course by edelfosine in SJL mice. Additionally, this approach aimed to clarify further options for reducing edelfosine doses by reducing both

dose and dosing interval. SJL mice were immunized with the PLP₍₁₃₉₋₁₅₁₎ peptide (day 0). From day 5 after immunization mice were treated with PBS, 1 mg/kg edelfosine or 10 mg/kg edelfosine every other day by i.p. injection which was the more convenient way of drug application compared to gavage. Progression of disease course was followed until day 35 (Figure 4 B). No significant differences were detected between cohorts regarding treatment effects in the course of EAE and regarding cumulative disease scores (Figure 5 B) despite implicated ameliorations.

4.2.3 Preventive treatment of EAE in SJL mice with edelfosine on a daily basis ameliorates disease course

SJL mice were immunized with PLP₍₁₃₉₋₁₅₁₎. Immediately, PBS, 1 mg/kg edelfosine or 10 mg/kg edelfosine was administered and repeated on a daily basis by i.p. injection. The progression of disease course was monitored until day 40 (Figure 4 C). A significant treatment effect was found in this preventive setting, with significant differences between EAE scores of mice treated with PBS and mice that were treated with 10 mg/kg edelfosine. Interestingly, those differences emerged at the first disease bout from day 12 to 14 as well as at the first EAE relapse from day 28 to 33. A significant treatment effect was also detected when the cumulative disease scores of the three cohorts were analyzed (Figure 5 C). Significant differences in post-hoc analysis were found for the comparison of PBS-treated controls (cumulative disease score: 53.39 ± 9.53) to 10 mg/kg edelfosine-treated mice (cumulative disease score: 17.79 ± 7.61).

4.2.4 Investigation of the therapeutic effectiveness of edelfosine on EAE in SJL mice

After immunization of SJL mice the disease scores were monitored and mice showed first distinct and evenly distributed signs of EAE across groups at day 11. At this phase of disease onset the administration of PBS, 1 mg/kg edelfosine or 10 mg/kg edelfosine was started and continued until day 45 after immunization (Figure 4 D). The comparison of disease progression implied a reduction of clinical scores upon edelfosine treatment. However, a treatment effect could not be confirmed by statistical analysis, which was in concordance with the analysis of cumulative disease scores (Figure 5 D). Despite the observed tendency towards reduced cumulative disease scores in edelfosine-treated cohorts (treated with 1 mg/kg edelfosine: 32.5 ± 17.87 , treated with 10 mg/kg edelfosine: 23.75 ± 11.81) compared to PBS-treated mice (cumulative disease score: 63.08 ± 18.89) the differences were not statistically significant. This fact might be ascribed to enhanced variations of EAE scores especially in the phase of remission after the first relapse.

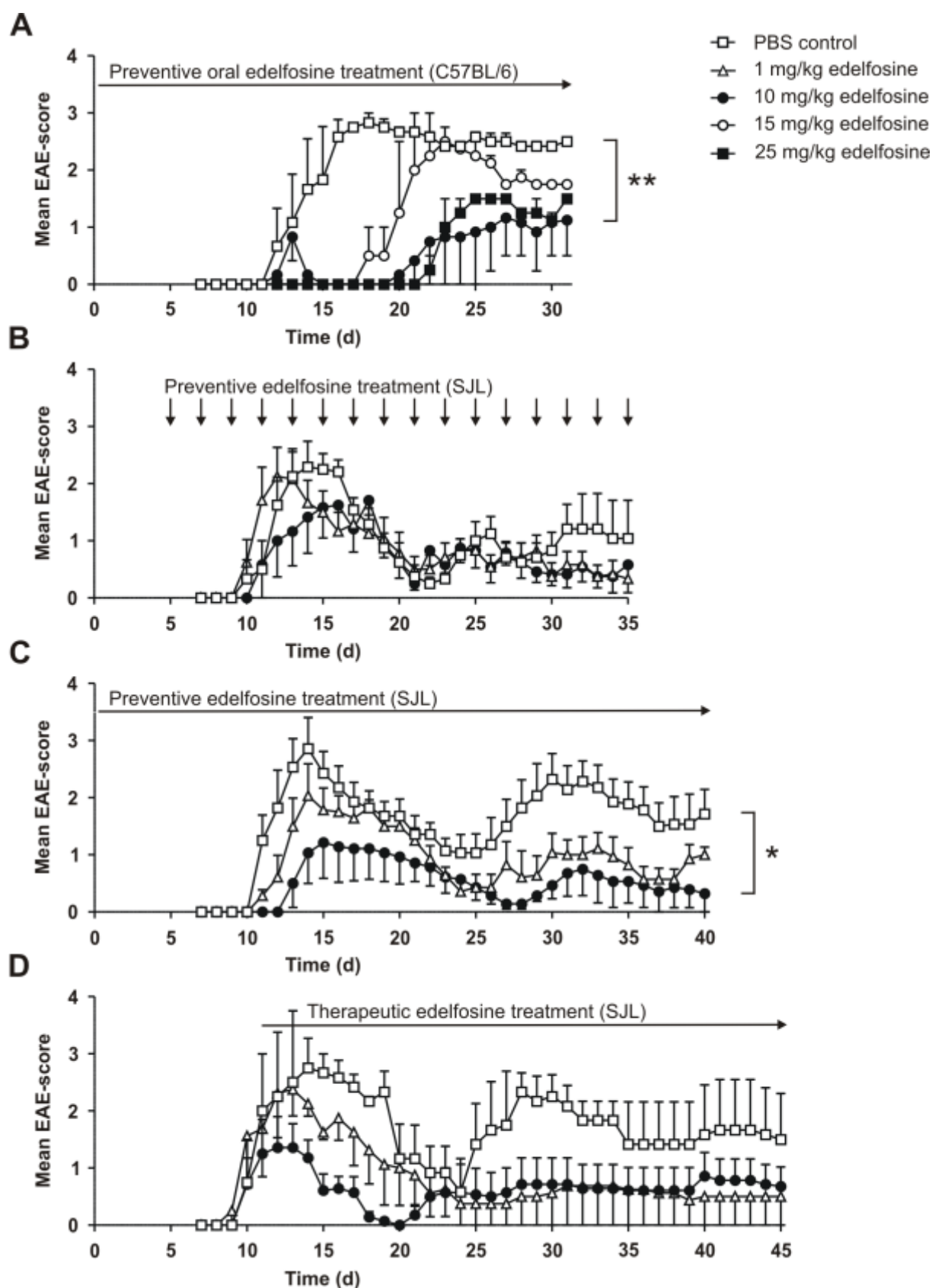


Figure 4. Preventive edelfosine treatment influenced EAE in C57BL/6 and SJL mice. **(A)** Whereas PBS-treated C57BL/6 mice developed the classical chronic-progressive EAE course, mice treated with edelfosine appeared to be impacted in their EAE development but also in their physical presentation due to side effects at concentrations higher than 10 mg/kg edelfosine. Clinical scores for groups of PBS-treated (n=3), 10 mg/kg edelfosine treated (n=3), 15 mg/kg edelfosine treated (n=2) and 25 mg/kg edelfosine treated (n=2) EAE mice. Note that the

treatment of mice with 25 mg/kg and 15 mg/kg edelfosine led to drug-related side effects which possibly had an impact on EAE development in immunized mice that remained clinically inconspicuous **(B)** The preventive administration of edelfosine every other day had no significant effect on RR-EAE clinical scores in immunized SJL mice. Depicted groups: PBS-treated (n=6), 1 mg/kg edelfosine treated (n=6) and 10 mg/kg edelfosine treated (n=6) EAE mice. **(C)** In contrast, the preventive treatment of EAE-induced SJL mice with 10 mg/kg edelfosine on a daily basis ameliorated the disease course: depiction of clinical scores for groups of PBS-treated (n=7), 1 mg/kg edelfosine treated (n=7) and 10 mg/kg edelfosine treated (n=7) EAE mice. **(D)** Clinical scores for groups of PBS-treated (n=3), 1 mg/kg edelfosine treated (n=4) and 10 mg/kg edelfosine treated (n=7) EAE mice with administration starting at disease onset (day 11). A treatment effect could not be proved. EAE experiments are shown as mean values \pm SEM; *P<0.05, **P<0.01 after 2-way ANOVA.

4.3 Analysis of preventive edelfosine-treatment effects in RR-EAE

For a detailed analysis of the impact of edelfosine on different immunological parameters SJL mice were immunized with the PLP₍₁₃₉₋₁₅₁₎ peptide. The administration of PBS and 1 mg/kg edelfosine or 10 mg/kg edelfosine by i.p. injection was started at this day of immunization (day 0) and continued on a daily basis. Schematically, the disease-relevant peptide PLP₍₁₃₉₋₁₅₁₎ is presented to antigen-specific T cells by APCs after immunization. These T cells are activated in lymph nodes and migrate into the blood and into the spleen, subsequently pursuing their way into the CNS. A comparable exemplary, migratory pattern has been identified in passively immunized rats by the transfer of MBP-specific T cells that have been retrovirally transduced to express GFP (113). The infiltration of immune cells, of which T cells constitute a prominent fraction, into the CNS coincides with the onset of clinical symptoms of EAE. Accordingly, spleens and lymph nodes were prepared from SJL mice at day 9, a phase when EAE is not yet clinically apparent. Flow cytometry and *ex vivo* proliferation assays were used to analyze the effect of edelfosine treatment on immune cell composition and function. Flow cytometry, histology and immunohistochemistry were applied in the acute phase of EAE to study the effects of edelfosine treatment on immune cell infiltration into the CNS.

4.3.1 Preventive edelfosine treatment increases activated caspase-3 expression in the preclinical phase of RR-EAE

At day 9 after immunization of SJL mice, spleens as well as draining lymph nodes were prepared from PBS-treated, 1 mg/kg edelfosine-treated and 10 mg/kg edelfosine-treated mice. Single cell suspensions were made to determine absolute cell numbers followed by flow cytometry analysis (gating strategy for cell types: Figure 6). With regard to the absolute cell number in spleens and lymph nodes, the preventive treatment of SJL mice with PBS, 1 mg/kg edelfosine or 10 mg/kg edelfosine until day 9 was found not to induce differences when comparing these three groups. In detail, absolute cell numbers are depicted in Table 3.

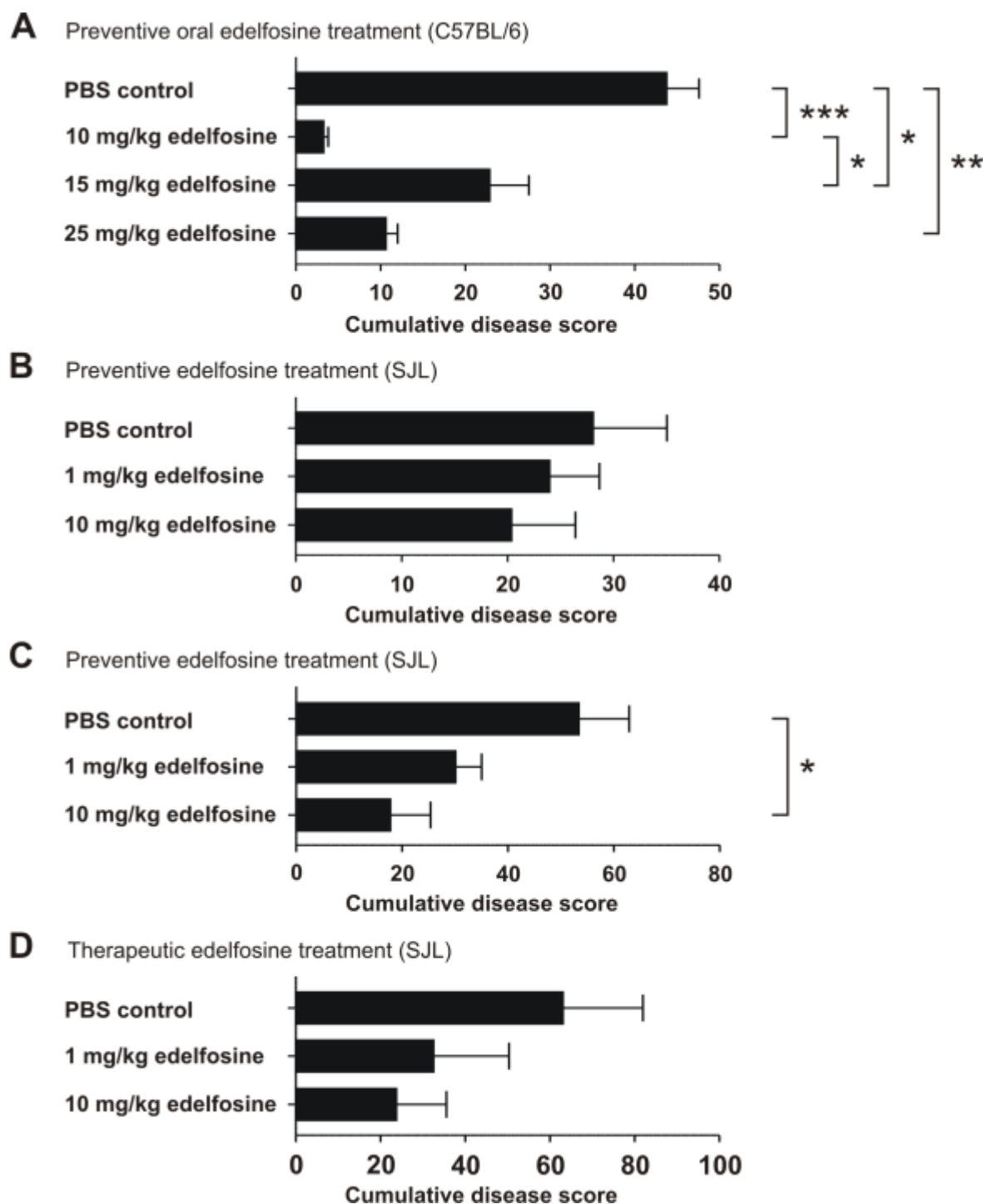


Figure 5. Cumulative disease scores were reduced upon preventive edelfosine treatment of EAE-induced C57BL/6 and SJL mice. **(A)** C57BL/6 mice were treated daily with PBS ($n=3$), 10 mg/kg edelfosine ($n=3$), 15 mg/kg edelfosine ($n=2$) and 25 mg/kg edelfosine ($n=2$), respectively. Application of 10 mg/kg edelfosine led to a significant reduction of the cumulative disease score when compared with PBS-treated controls. **(B)** No significant reduction in cumulative disease scores was determined for groups of immunized SJL mice that were treated every other day beginning at day 5 with 1 mg/kg edelfosine ($n=6$) or 10 mg/kg edelfosine ($n=6$) compared to PBS-treated mice ($n=6$). **(C)** Instead, the daily administration of 10 mg/kg edelfosine to EAE-induced SJL mice ($n=7$), but not the administration of 1 mg/kg edelfosine ($n=7$), reduced the cumulative disease score compared to PBS-treated controls ($n=7$). **(D)** The therapeutic treatment of EAE-induced SJL mice starting at disease onset (day 11) yielded cumulative disease scores that implied an edelfosine dose-dependent reduction compared to PBS-treated controls. However, significance could not be proved. The data that is based on EAE experiments whose corresponding disease courses are depicted in Figure 4, are shown as mean values \pm SEM; * $P<0.05$, ** $P<0.01$, *** $P<0.001$ after post-hoc analysis.

Table 3. Summary of absolute cell counts derived from spleens and lymph nodes of EAE-induced mice at day 9 after immunization. Values are expressed as mean \pm SEM.

Treatment	Spleen	Lymph nodes
PBS	$6.63 \times 10^7 \pm 6.23 \times 10^6$	$2.31 \times 10^7 \pm 6.25 \times 10^6$
1 mg/kg edelfosine	$5.39 \times 10^7 \pm 1.91 \times 10^7$	$2.25 \times 10^7 \pm 9.06 \times 10^5$
10 mg/kg edelfosine	$6.32 \times 10^7 \pm 1.86 \times 10^7$	$2.08 \times 10^7 \pm 2.27 \times 10^6$

Furthermore, neither immune cell-type subset of cells derived from spleens nor subsets derived from lymph nodes displayed any edelfosine treatment-associated changes in frequencies compared to PBS-treated controls (Figure 7). In general, frequencies were calculated by relating gated subset events to gated parental events that corresponded to 100 percent. T cells were identified by expression of CD3. As expected, comparatively higher fractions of CD3⁺ T cells were found in lymph nodes of the animals compared to spleens (Table 4).

Table 4. Frequency of CD3⁺ T cells from spleens and lymph nodes of EAE-induced SJL mice at day 9 after immunization. Data is expressed as mean \pm SEM.

Treatment	Spleen	Lymph nodes
PBS	$40.11 \pm 3.36 \%$	$84.32 \pm 1.43 \%$
1 mg/kg edelfosine	$36.65 \pm 2.19 \%$	$82.85 \pm 3.94 \%$
10 mg/kg edelfosine	$31.48 \pm 2.80 \%$	$81.09 \pm 1.74 \%$

Despite the fact that EAE is considered as a T cell-mediated disease model, it was of interest to determine if edelfosine treatment induces changes in other immune cell subsets. B cells are essential in mediating the humoral part of the adaptive immune response, and they were also found to act as APCs. However, by edelfosine treatment frequencies of B220⁺ B cells did not appear to be affected in spleens or lymph nodes (Table 5).

Table 5. Frequency of B220⁺ B cells from spleens and lymph nodes of EAE-induced SJL mice at day 9 after immunization. Data is expressed as mean \pm SEM.

Treatment	Spleen	Lymph nodes
PBS	$20.65 \pm 1.25 \%$	$8.03 \pm 1.09 \%$
1 mg/kg edelfosine	$24.43 \pm 0.51 \%$	$8.45 \pm 2.47 \%$
10 mg/kg edelfosine	$21.23 \pm 2.37 \%$	$10.40 \pm 1.36 \%$

Macrophages, which are part of the innate immune system, link to the adaptive immune system by acting as APCs and by secretory activation of T cells. Analysis of CD11b⁺ CD11c⁻ macrophages in spleens and lymph nodes of mice that received PBS or edelfosine resulted in equal frequency distributions across cohorts (Table 6).

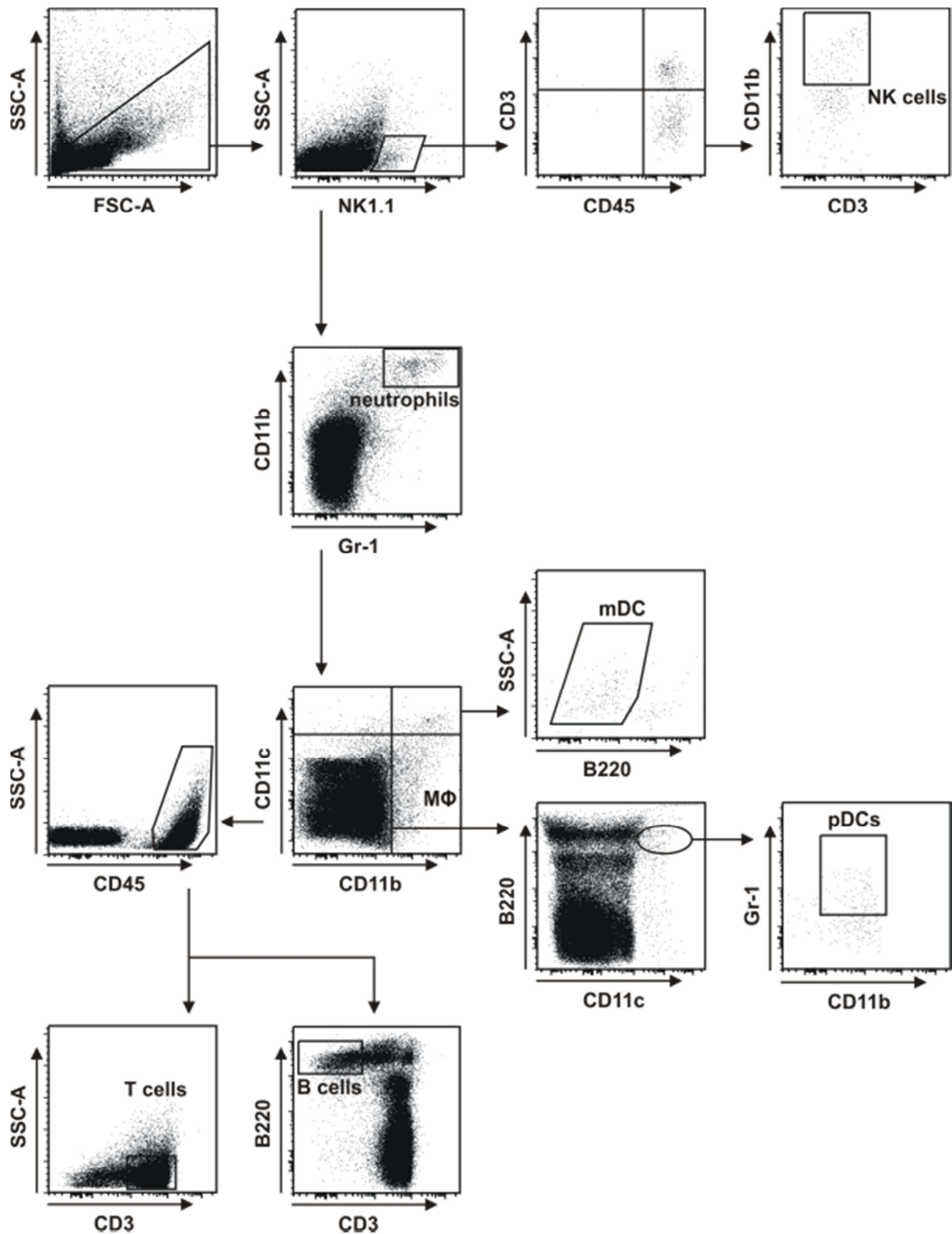


Figure 6. Analysis of leukocyte-subset frequencies. The specific expression of cell-surface markers allowed discrimination between cell types as exemplified by this gating strategy depicting lymph node cells from an EAE-induced, 10 mg/kg edelfosine-treated mouse. Frequencies were determined by relating the detected number of events within the respective gate to the measured number of CD45+ events.

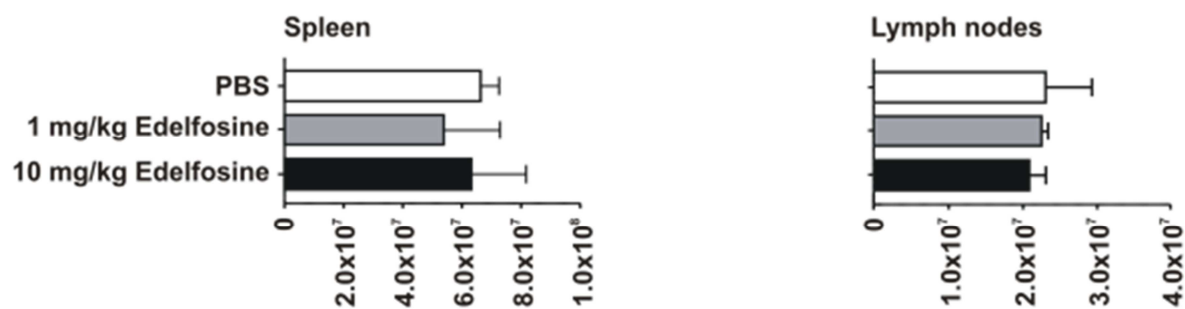
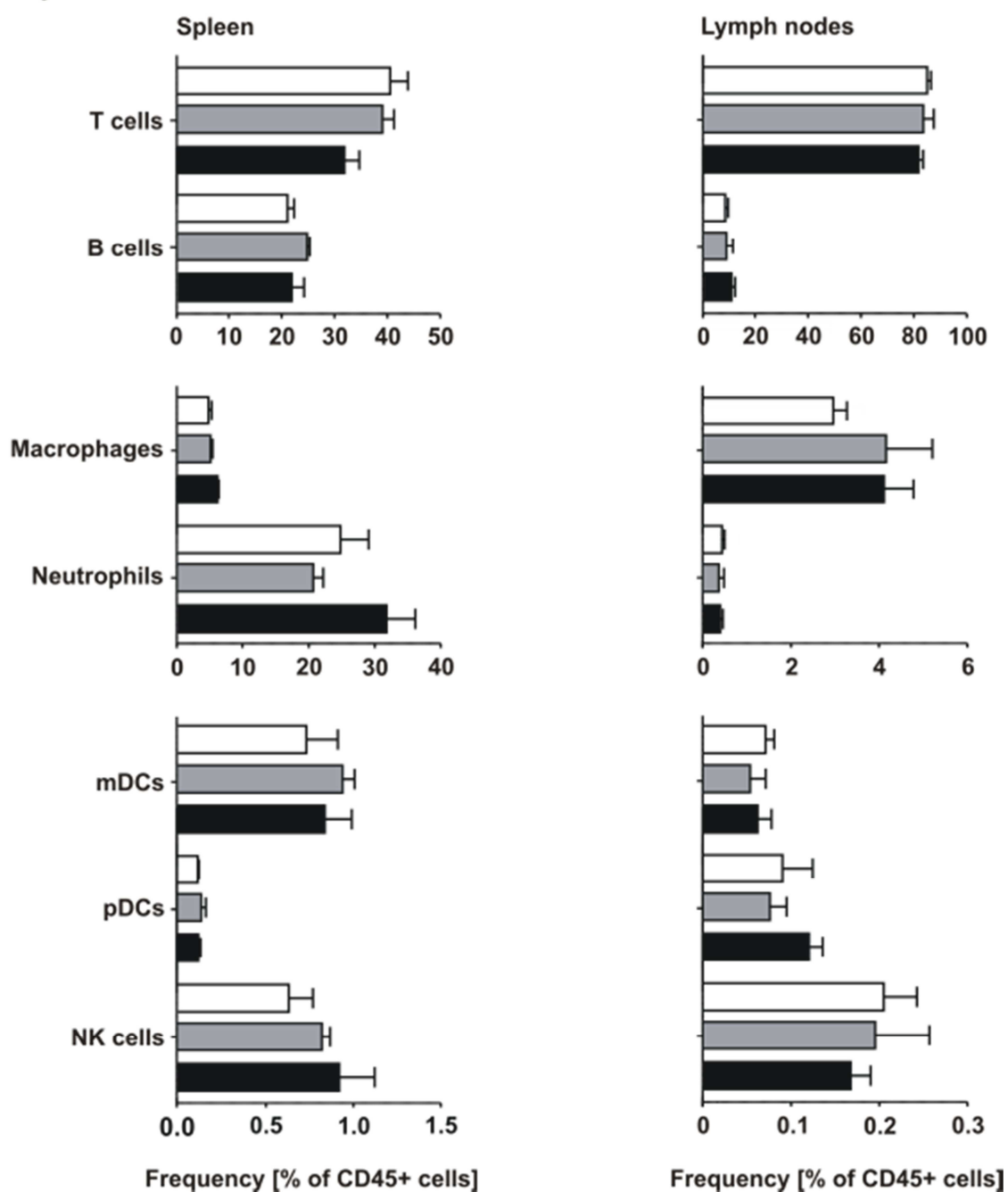
A Absolute cell counts**B** Leukocyte subset distribution

Figure 7. Preventive daily treatment of EAE-induced SJL mice with PBS or edelfosine until day 9. **(A)** Cells were prepared from spleens and lymph nodes for quantification. **(B)** For analysis of possible edelfosine-induced changes in immune cell frequencies within peripheral lymphoid organs, the number of recorded events was

always related to all recorded CD45+ events. Absolute cell counts and frequencies for groups of PBS-treated (n=3), 1 mg/kg edelfosine treated (n=3) and 10 mg/kg edelfosine treated (n=3) EAE mice. Data from one representative of two independent EAE experiments are shown as mean values \pm SEM (□ PBS, ■ 1 mg/kg edelfosine, ■ 10 mg/kg edelfosine).

Table 6. Frequency of CD11b+ CD11c- macrophages from spleens and lymph nodes of EAE-induced SJL mice at day 9 after immunization. Data is expressed as mean \pm SEM.

Treatment	Spleen	Lymph nodes
PBS	4.63 \pm 0.49 %	2.94 \pm 0.31 %
1 mg/kg edelfosine	4.94 \pm 0.31 %	4.14 \pm 1.05 %
10 mg/kg edelfosine	6.00 \pm 0.20 %	4.09 \pm 0.67 %

In lymph nodes of either PBS or edelfosine-treated mice a much lower frequency of GR-1+ CD11b+ neutrophils was detected compared to spleens. However, the frequencies were not changed in both compartments across treatment groups (Table 7).

Table 7. Frequency of Gr-1+ CD11b+ neutrophils from spleens and lymph nodes of EAE-induced SJL mice at day 9 after immunization. Data is expressed as mean \pm SEM.

Treatment	Spleen	Lymph nodes
PBS	24.57 \pm 4.26 %	0.42 \pm 0.06 %
1 mg/kg edelfosine	20.46 \pm 1.51 %	0.34 \pm 0.12 %
10 mg/kg edelfosine	31.55 \pm 4.32 %	0.35 \pm 0.07 %

No differences in conventional CD11c+ CD11b- B220- mDC frequencies were identified in spleens. Additionally, frequencies in lymph nodes stayed at a low but constant level, even after edelfosine treatment (Table 8).

Table 8. Frequency of CD11c+ CD11b- B220- mDCs from spleens and lymph nodes of EAE-induced SJL mice at day 9 after immunization. Data is expressed as mean \pm SEM.

Treatment	Spleen	Lymph nodes
PBS	0.73 \pm 0.18 %	0.07 \pm 0.01 %
1 mg/kg edelfosine	0.93 \pm 0.07 %	0.05 \pm 0.02 %
10 mg/kg edelfosine	0.83 \pm 0.15 %	0.06 \pm 0.02 %

The second major DC subset are CD11c^{low} CD11b- B220+ Gr-1^{low} pDCs (309). In spleens and lymph nodes of EAE-induced mice frequencies of pDCs were low and no differences were detected across treatment groups (Table 9).

Table 9. Frequency of CD11c^{low} CD11b- B220+ Gr-1^{low} pDCs from spleens and lymph nodes of EAE-induced SJL mice at day 9 after immunization. Data is expressed as mean \pm SEM.

Treatment	Spleen	Lymph nodes
PBS	0.11 \pm 0.01 %	0.09 \pm 0.03 %
1 mg/kg edelfosine	0.13 \pm 0.03 %	0.08 \pm 0.02 %
10 mg/kg edelfosine	0.12 \pm 0.01 %	0.12 \pm 0.02 %

NK cells constitute members of innate immunity that are also effective in immune responses against intracellular pathogens and viruses. NK cells were identified by gating on NK1.1+ CD45+ CD11b+ CD3- cells. No differences in frequencies were detected (Table 10).

Table 10. Frequency of NK1.1+ CD45+ CD11b+ CD3- NK cells from spleens and lymph nodes of EAE-induced SJL mice at day 9 after immunization. Data is expressed as mean \pm SEM.

Treatment	Spleen	Lymph nodes
PBS	0.63 \pm 0.14 %	0.20 \pm 0.04 %
1 mg/kg edelfosine	0.82 \pm 0.05 %	0.19 \pm 0.06 %
10 mg/kg edelfosine	0.92 \pm 0.20 %	0.17 \pm 0.02 %

These frequency values were representative from one of two independent EAE experiments. Apparent reproducible treatment effects were assessed by using fold-changes. Each group of mice comprised three animals in each experiment. Focusing now on T-cell subsets no differences were found regarding CD4+ and CD8+ T-cell frequencies upon edelfosine treatment compared to spleens and lymph nodes from PBS-treated controls (Table 11).

Table 11. Frequency of CD4+ and CD8+ T cells from spleens and lymph nodes of EAE-induced SJL mice at day 9 after immunization. Data is expressed as mean \pm SEM.

Treatment	Spleen	Lymph nodes
<u>CD4+</u>		
PBS	24.46 \pm 2.74 %	53.98 \pm 0.89 %
1 mg/kg edelfosine	25.75 \pm 1.85 %	56.08 \pm 1.54 %
10 mg/kg edelfosine	19.93 \pm 2.25 %	53.19 \pm 1.40 %
<u>CD8+</u>		
PBS	10.90 \pm 0.45 %	23.83 \pm 1.56 %
1 mg/kg edelfosine	9.99 \pm 0.83 %	24.30 \pm 1.92 %
10 mg/kg edelfosine	9.58 \pm 0.88 %	24.26 \pm 0.62 %

Interestingly, a significant increase in T-cell frequencies showing a naïve CD4+ CD62L^{high} CD44^{low} phenotype was observed in lymph nodes upon edelfosine treatment: whereas 47.71 \pm 3.11 % CD4+ T cells with a naïve phenotype could be isolated from PBS-treated mice, 53.99 \pm 3.37 % and 55.41 \pm 3.09 % were found in mice treated with 1 mg/kg and 10 mg/kg edelfosine, respectively. Results from two individual experiments were expressed and merged as fold-changes to allow statistical analysis (Figure 8). The treatment of EAE-induced mice with 10 mg/kg edelfosine led to a significant, 1.22-fold increase in naïve CD4+ T-cell frequencies in lymph nodes compared to PBS-treated, immunized mice. No significant changes were observed for naïve CD8+ T cells from lymph nodes and CD4+ or CD8+ T lymphocytes isolated from spleens. Moreover, frequencies of CD62L^{low} CD44^{high} memory CD4+ or CD8+ T cells were analyzed. However, no treatment-dependent differences were found in spleens or lymph nodes of EAE-induced SJL mice.

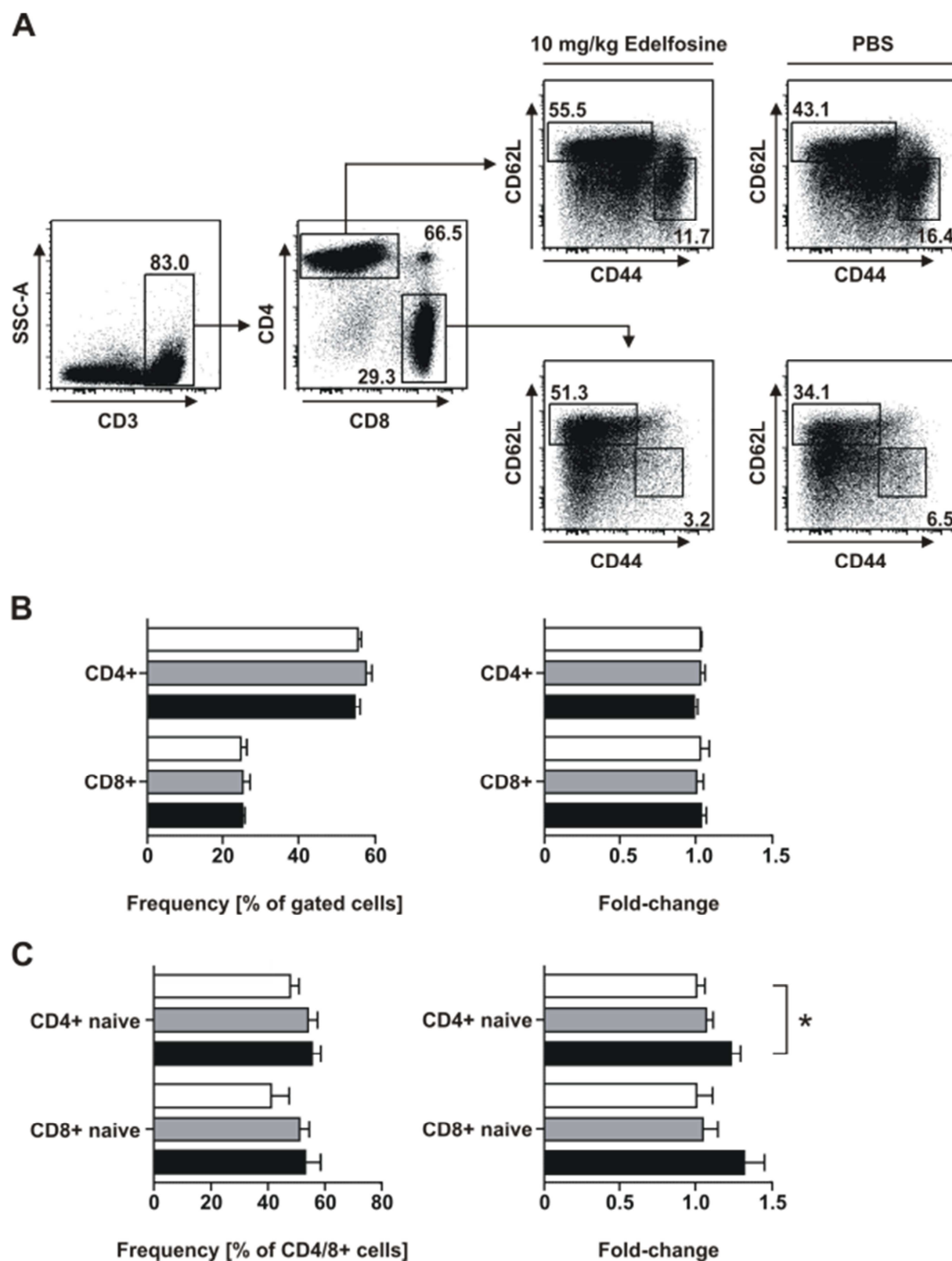


Figure 8. Increased frequency of naïve CD4⁺ T cells after treatment with 10 mg/kg edelfosine. **(A)** Lymph node T cells of EAE-induced PBS- or edelfosine-treated SJL mice were analyzed for frequencies of CD4⁺ and CD8⁺ T-cell subsets, but also for their expression of CD62L and CD44 on the cell surface. **(B)** CD4⁺ and CD8⁺ T-cell frequencies remained unchanged irrespective of the treatment. **(C)** Increased frequencies of CD62L⁺ CD44⁻ naïve CD4⁺ T cells were detected in lymph nodes of mice that received 10 mg/kg edelfosine. Frequencies from one representative of two independent EAE experiments (n=3 for each group in each experiment), fold-changes merged from two independent EAE experiments are shown as mean values \pm SEM (□ PBS, ▒ 1 mg/kg edelfosine, ■ 10 mg/kg edelfosine); *P<0.05 after post-hoc analysis.

To study the possible influence of edelfosine treatment on T-lymphocyte activation in EAE-induced mice, the expression of the early, transiently expressed activation marker CD69 and CD25, the IL-2 receptor α chain, was analyzed. No differences were seen between frequencies of CD4⁺ CD69⁺ or CD4⁺ CD25⁺ T cells isolated from spleens and lymph nodes of either PBS- or edelfosine-treated groups (Figure 9). The same holds true for the respective CD8⁺ T-cell populations. Thus, edelfosine treatment was found not to influence strong activation signals on T cells in the periphery. For instance, after treatment of immunized mice with PBS 4.90 \pm 0.65 % CD69⁺, activated CD4⁺ T cells related to CD4⁺ T cells were determined in lymph nodes. Upon treatment with 1 mg/kg or 10 mg/kg edelfosine 6.00 \pm 1.08 % or 4.96 \pm 0.59 % CD69⁺ CD4⁺ T cells were found in the CD4⁺ T-cell pool from lymph nodes, respectively. Interestingly, CD25⁺ and CD69⁺ CD4⁺ T cells in lymph nodes appeared to be slightly more frequent upon 1 mg/kg edelfosine treatment.

As an additional CD4⁺ T-cell subset CD4⁺ CD25⁺ Foxp3⁺ nTregs were identified in spleens and lymph nodes of EAE-induced mice by gating on CD4⁺ CD25⁺ populations excluding CD69⁺ events (Figure 9) (310). In lymph nodes, nTreg frequencies of CD4⁺ T cells were determined to be 5.95 \pm 0.22 % (PBS-treated mice), 5.75 \pm 0.25 % (1 mg/kg edelfosine-treated mice) and 5.88 \pm 1.21 % (10 mg/kg edelfosine-treated mice). The comparison of nTreg frequencies from PBS-treated and edelfosine-treated cohorts in either spleens or lymph nodes did not indicate treatment-dependent changes.

Two T-cell populations considered to be important in EAE are the immunopathogenic Th1 and Th17 effector T cells. These populations can be identified by their characteristic production of the cytokines IFN- γ and IL-17A (in the following: IL-17), respectively. In detail, cells were gated by their expression of CD45, CD3 and CD4 and the intracellular production of the relevant cytokines, IFN- γ and IL-17, in the absence of CD11b⁻ and CD8⁻ expression. To sum up, the treatment of EAE-induced mice with edelfosine was not found to have an impact on IFN- γ or IL-17-producing CD4⁺ (Table 12) as well as CD8⁺ lymphocyte-subset frequencies in the spleen or lymph nodes compared to PBS-treated control mice.

Table 12. Frequencies of lymph node-derived CD4⁺ IFN- γ ⁺ and CD4⁺ IL-17⁺ T cells. Data is related to CD4⁺ T-cell frequencies and shown as mean \pm SEM.

Treatment	CD4 ⁺ IFN- γ ⁺	CD4 ⁺ IL-17 ⁺
PBS	0.33 \pm 0.004 %	0.44 \pm 0.03 %
1 mg/kg edelfosine	0.32 \pm 0.07 %	0.52 \pm 0.14 %
10 mg/kg edelfosine	0.34 \pm 0.06 %	0.60 \pm 0.09 %

In previous reports it has been suggested that apoptosis may be involved in eliminating T lymphocytes from inflammatory brain lesions in EAE-affected Lewis rats (311). In the present study EAE-induced mice were treated with edelfosine which is considered to act on cells by apoptosis induction (253, 312).

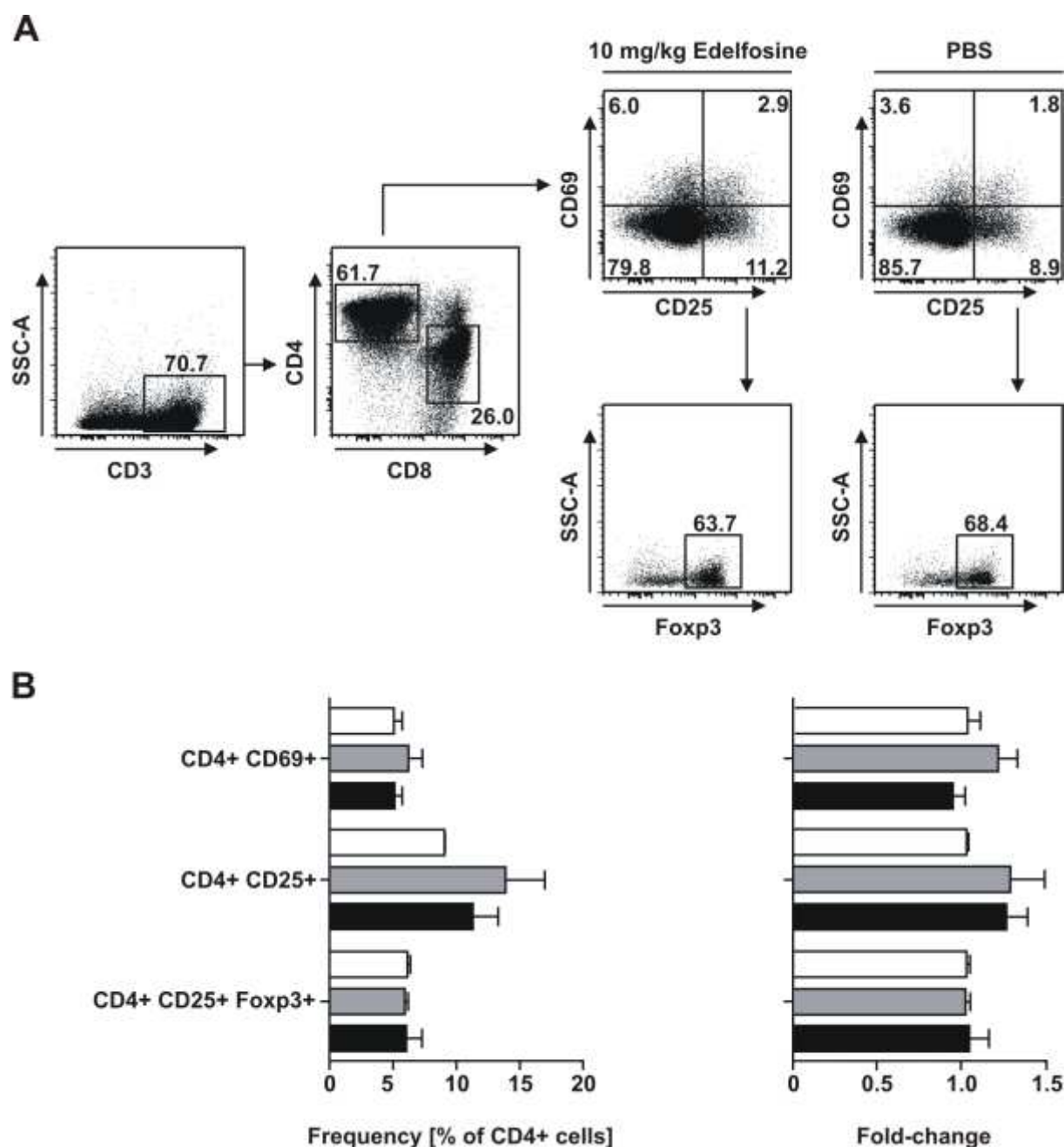
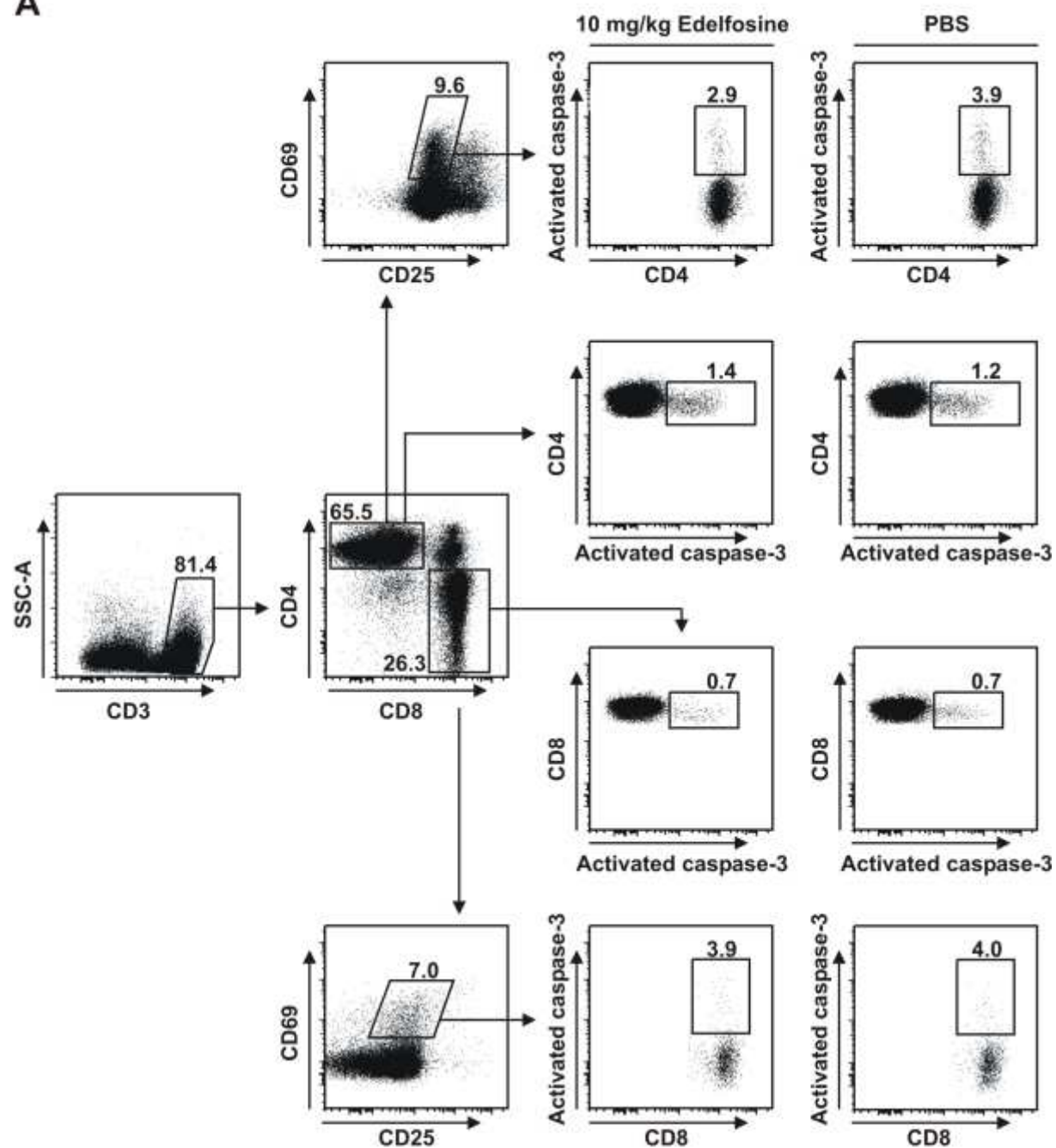


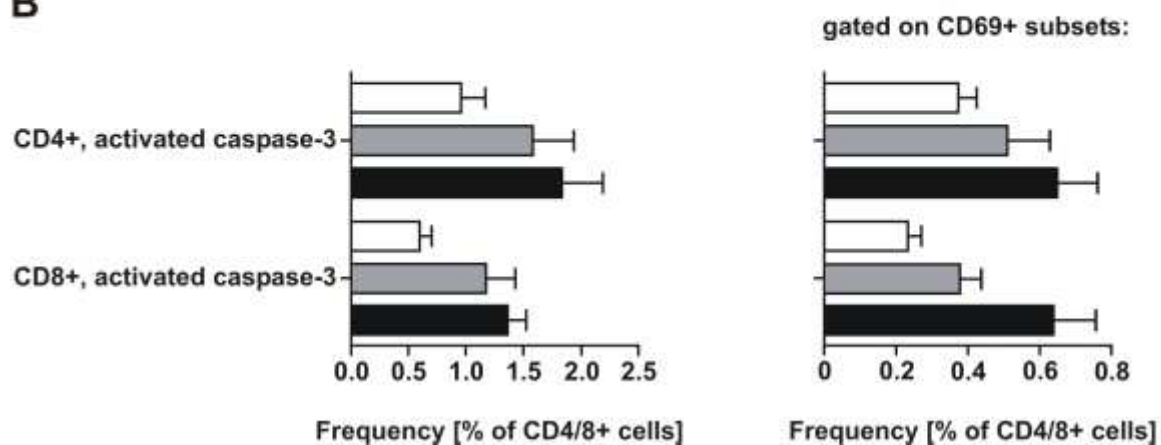
Figure 9. No changes in T-cell activation and regulatory T-cell frequencies upon edelfosine treatment. **(A)** Activated T-cell subsets were determined by activation markers CD69 and CD25. **(B)** Edelfosine treatment was not found to induce changes in frequencies of CD69+ or CD25+ CD4 T cells. Equal frequencies were also found for CD4+ CD25+ Foxp3+ natural Tregs across treatment groups. Frequencies of lymph node-derived cells from one representative of two independent EAE experiments ($n=3$ for each group in each experiment), fold-changes merged from two independent EAE experiments are shown as mean values \pm SEM (□ PBS, ▒ 1 mg/kg edelfosine, ■ 10 mg/kg edelfosine).

To determine the induction of apoptotic processes by edelfosine treatment, expression of caspase-3 was analyzed. Caspase-3 is known to be activated during the early events of apoptosis. Therefore, CD4+ and CD8+ T cells prepared from spleen and lymph nodes of EAE-induced mice that were treated with PBS, 1 mg/kg edelfosine or 10 mg/kg edelfosine were stained for caspase-3 activation. As edelfosine is described as acting primarily on proliferating cells, CD69 was used to specifically determine activated T cells.

A



B



C

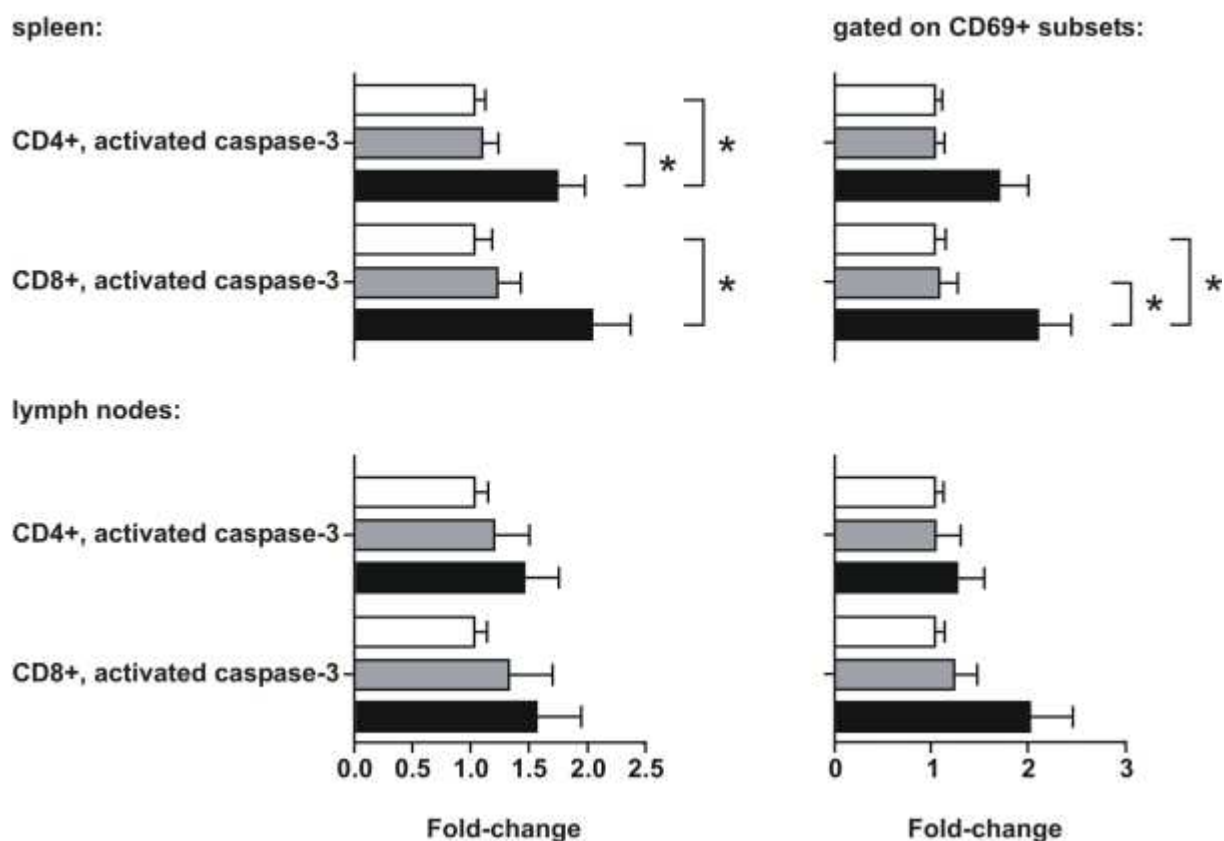


Figure 10. Edelfosine treatment induced the upregulation of activated caspase-3. **(A)** Gating strategy for activated caspase-3 in CD4+ and CD8+ T cells as well as their activated, CD69+ descendants. **(B)** Representative frequencies of CD4+ and CD8+ T cells as well as activated CD4+ and CD8+ T cells with activated caspase-3. Here, cells were prepared from lymph nodes. **(C)** Treatment of EAE-induced mice with 10 mg/kg edelfosine resulted in a significant increase in CD4+ and CD8+ T-cell frequencies with activated caspase-3 which was also found for CD8+ CD69+ T cells (spleens). Frequencies from one representative of two independent EAE experiments ($n=3$ for each group in each experiment), fold-changes merged from two independent EAE experiments are shown as mean values \pm SEM (□ PBS, ▒ 1 mg/kg edelfosine, ■ 10 mg/kg edelfosine); * $P<0.05$ after post-hoc analysis.

CD69, as an activation antigen, is expressed on the surface of activated proliferating T cells. For this reason the activation of caspase-3 was also determined in activated T cells in order to detect a treatment-dependent edelfosine effect. Cells from both spleens and lymph nodes were analyzed (Figure 10). In lymph nodes 0.93 ± 0.21 % of CD4+ T cells expressed activated caspase-3 in PBS-treated mice, compared to 1.54 ± 0.35 % of CD4+ T cells that showed caspase-3 activation after treatment with 1 mg/kg edelfosine and 1.79 ± 0.35 % after treatment with 10 mg/kg edelfosine. By analyzing lymph node-derived T cells from PBS-treated mice 0.36 ± 0.05 % of CD4+ T cells expressed CD69+ and showed activation of caspase-3. Upon treatment with 1 mg/kg edelfosine 0.50 ± 0.12 % of CD4+ T cells were found to be CD69+ with activated caspase-3. Frequencies were further increased in mice treated with 10 mg/kg edelfosine: on that condition 0.63 ± 0.11 % of CD4+ T cells expressed CD69 and were stained positive for activated caspase-3. Results from two individual experiments were expressed and merged as fold-changes to allow statistical analysis. In

spleens the treatment of EAE-induced mice with 10 mg/kg edelfosine led to a significant increase in frequencies of CD4⁺ (1.70-fold) and CD8⁺ (1.99-fold) T cells with activated caspase-3 compared to PBS-treated, immunized mice. In view of spleen-derived CD4⁺ T cells with activated caspase-3 the treatment with 10 mg/kg edelfosine also resulted in a significant, 1.59-fold increase in frequencies compared to frequencies of respective cells derived from mice treated with 1 mg/kg edelfosine. With regard to activated CD69⁺ CD8⁺ T cells which showed activated caspase-3, significant higher frequencies were also detected in spleens of mice that were treated with 10 mg/kg edelfosine compared to PBS-treated (2.04-fold) and 1 mg/kg edelfosine-treated mice (1.95-fold).

4.3.2 The proliferative capacity of T cells is not compromised after preventive edelfosine treatment in RR-EAE

To examine the influence of edelfosine on proliferation of antigen-specific cells in the periphery, lymph nodes and spleens from SJL mice were prepared for thymidine-proliferation assays 9 days after immunization. Mice were treated with PBS, 1 mg/kg edelfosine or 10 mg/kg edelfosine from the day of immunization on a daily basis. Cells were restimulated *ex vivo* by addition of a mitogenic (Concanavalin A (Con A)), polyclonal (anti-CD3) or disease-relevant antigen PLP₍₁₃₉₋₁₅₁₎. Lymph node and spleen cells of edelfosine-treated mice retained their proliferative function (Figure 11). The reactivation of cells with PLP₍₁₃₉₋₁₅₁₎ implied an edelfosine dose-dependent proliferation. Notably, antigen-induced proliferation appeared to be accompanied by a treatment-dependent background proliferation in unstimulated control approaches. Therefore an increased SI was found upon edelfosine treatment.

4.3.3 CNS-infiltrating T cells appear at lower frequencies and show a higher expression of activated caspase-3 upon preventive edelfosine treatment

The acute phase of EAE is clinically apparent in affected mice through maximal impairment of motor function. Pathologically, this period is characterized by a marked infiltration of immune cells from the periphery into the CNS (Figure 12). In the case of the EAE model in SJL mice prominent infiltrates are detectable in the cervical spinal cord region. In this set of experiments SJL mice were immunized with PLP₍₁₃₉₋₁₅₁₎ to induce EAE. Mice were either treated with PBS, 1 mg/kg edelfosine or 10 mg/kg edelfosine from the day of immunization on a daily basis. PBS-treated control mice displayed a maximum mean EAE score of 2.67 ± 0.51 at day 14 after immunization. By contrast, mice treated with 1 mg/kg edelfosine or 10 mg/kg edelfosine showed a considerably lower clinical score (1.63 ± 0.42 and 0.13 ± 0.13 , respectively).

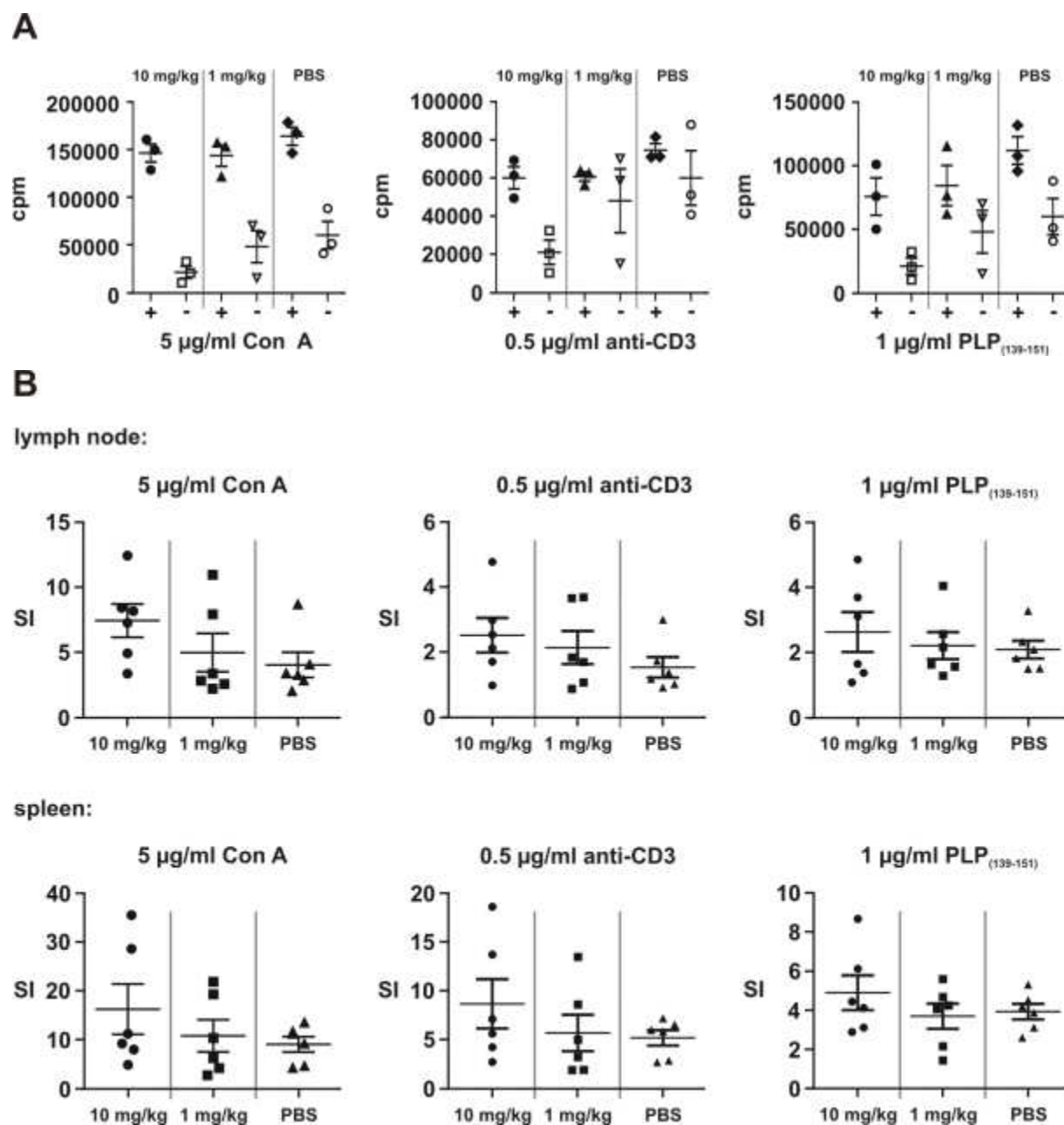


Figure 11. Edelfosine treatment of EAE-induced mice did not compromise proliferation capacity of lymph node- or spleen-derived cells. **(A)** After daily treatment of EAE-induced mice with either PBS or edelfosine, lymph node cells and spleen cells (not shown) were prepared, restimulated *ex vivo* with Con A, anti-CD3 antibody or PLP₍₁₃₉₋₁₅₁₎ and cultured for 72 h (+ stimulus added, - controls, absence of stimulus). Each symbol represents the mean value of triplicate approaches. Results from one representative of two independent EAE experiments ($n=3$ for each group in each experiment). **(B)** The relative proliferative response of cells within each condition expressed as SI. Lymph node- as well as spleen-derived cells showed no significant differences comparing the SIs of cells that were prepared from mice that received PBS, 1 mg/kg edelfosine or 10 mg/kg edelfosine and challenged with the same stimulus. Graphs display merged results from two independent experiments ($n=6$).

At day 15 spinal cords and brains were prepared to analyze cellular infiltration of the CNS by flow cytometry (Figure 13). Determination of absolute cell numbers was performed by using BD Trucount tubes which contained a defined amount of fluorescent beads. Thus, cells from a sample could be quantified by relating gated CD45+ events to the number of gated BD Trucount bead events. No significant differences of absolute cell numbers in the CNS were

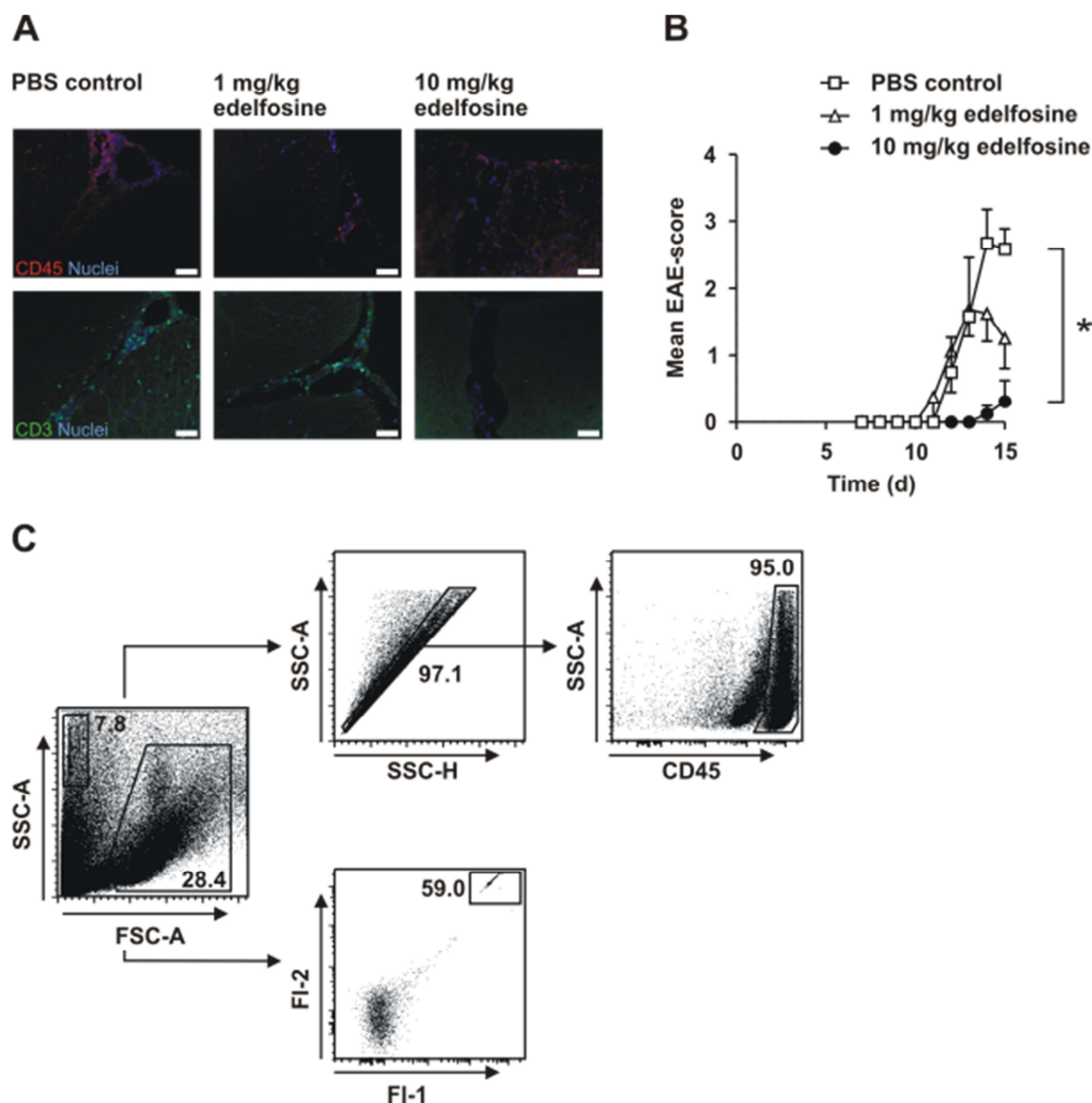


Figure 12. Quantification of immune cell infiltration at the acute phase of EAE. **(A)** Maximal EAE scores in PLP₍₁₃₉₋₁₅₁₎-immunized SJL mice were indicative of cellular CNS infiltration, for instance of CD45⁺ and CD3⁺ cells. Immunohistochemical stainings of cervical spinal cord sections of representative mice from either PBS, 1 mg/kg or 10 mg/kg edelfosine-treated groups indicate an edelfosine treatment-based effect on leukocyte and CD3⁺ T-cell infiltrates. **(B)** The acute phase of EAE was accompanied by a maximal clinical impairment of mouse movement. PBS-treated mice showed the expected development of EAE whereas the treatment of mice with 1 mg/kg edelfosine or 10 mg/kg edelfosine resulted in milder clinical EAE scores. In detail, a significant treatment effect was found with significant differences between PBS-treated and 1 mg/kg edelfosine-treated groups (day 14, 15) as well as between PBS-treated and 10 mg/kg edelfosine-treated groups (day 13 to 15). **(C)** Quantification of CNS-infiltrating CD45⁺ leukocytes was performed by flow cytometry using BD Trucount tubes according to the displayed gating strategy. CD45⁺ events were related to detected bead events in the FI-1/FI-2-defined gate and the absolute number of infiltrating cells was calculated using the absolute bead number.

detected when comparing mice that had been treated with PBS, 1 mg/kg edelfosine or 10 mg/kg edelfosine (Table 13). Single cell preparations of cells from the CNS were also used to determine frequencies of immune cell subtypes within the tissue in order to identify edelfosine treatment-related effects (Figure 14, Table 14).

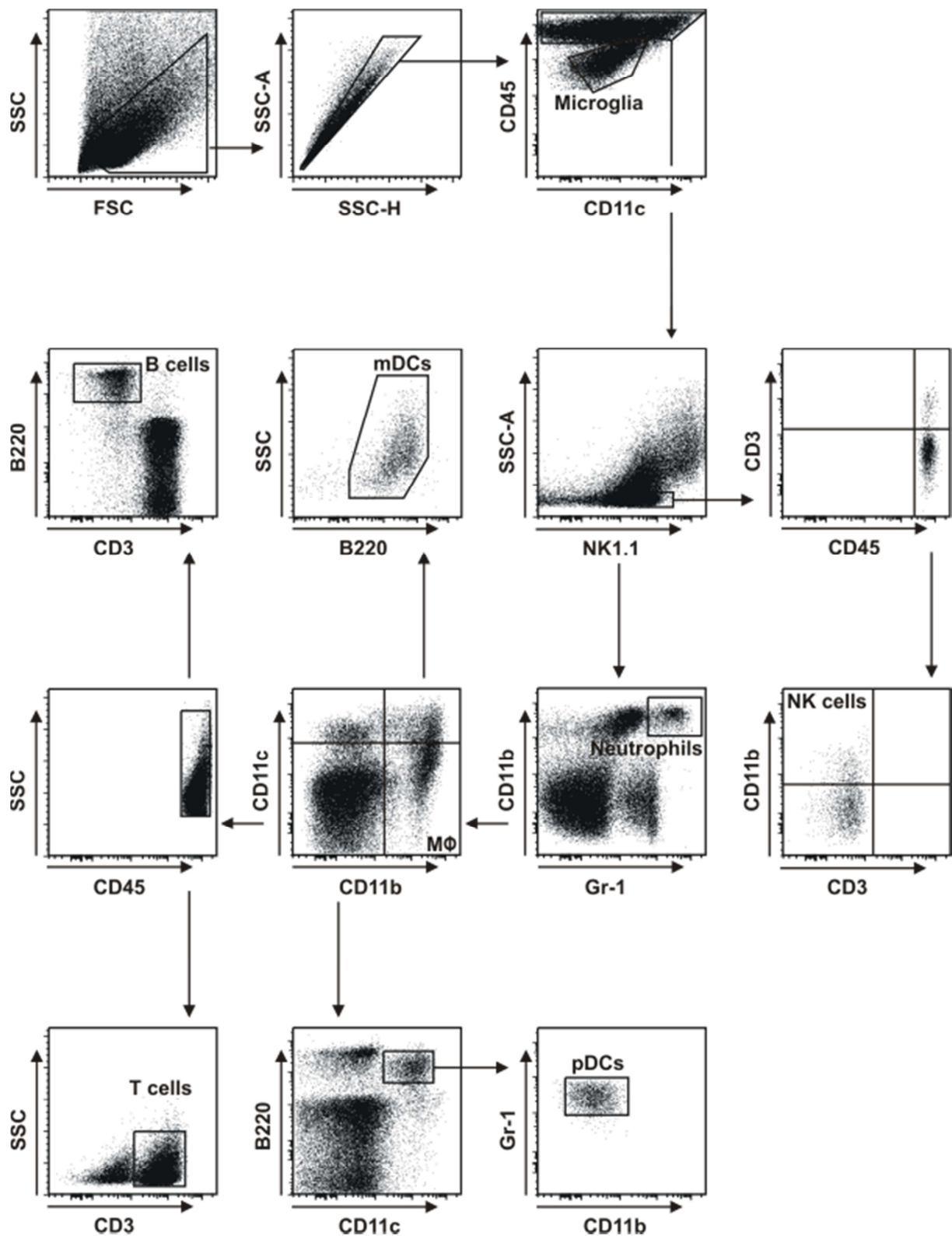


Figure 13. Identification of infiltrating cells into the CNS of EAE-induced SJL mice in the acute phase due to the expression of characteristic surface-marker molecules. After the separation of CD45^{int} CNS-residing microglia from CD45^{high} infiltrating leukocytes, the latter population was further specified (leukocyte subsets) as exemplified by this gating strategy depicting cells from an EAE-induced, 10 mg/kg edelfosine-treated mouse.

Table 13. Absolute numbers of CD45+ cells infiltrating into the CNS of EAE-affected SJL mice in the acute disease phase. Data is expressed as mean \pm SEM (n=4 for each group, except PBS-treated group: n=3).

Treatment	CNS-infiltrating CD45+ cells
PBS	$1.98 \times 10^6 \pm 1.27 \times 10^5$
1 mg/kg edelfosine	$1.90 \times 10^6 \pm 3.94 \times 10^5$
10 mg/kg edelfosine	$1.04 \times 10^6 \pm 6.18 \times 10^5$

The treatment of EAE-induced mice with 10 mg/kg edelfosine resulted in significantly reduced frequencies (-1.71-fold) of CD3+ T cells in the CNS. A reduction was also discovered with regard to CD11c^{low} CD11b- B220+ Gr-1^{low} pDCs in which case 10 mg/kg edelfosine additionally led to a significant reduction of frequencies compared to the treatment of mice with 1 mg/kg edelfosine. In more detail, for mice treated with 10 mg/kg edelfosine the reduction of pDC frequencies was -3.09-fold compared to PBS-treated and -4.52-fold compared to 1 mg/kg edelfosine-treated mice. Interestingly, this characteristically increased frequency upon application of 1 mg/kg edelfosine was also detected for CD11c+ CD11b- B220- mDCs as well as B220+ B cells, in which cases no differences in frequencies were found comparing PBS-treated cohorts to 10 mg/kg edelfosine-treated mice. With regard to mDCs detected frequencies in 1 mg/kg edelfosine-treated mice reflected a significantly elevated fraction compared to 10 mg/kg edelfosine-treated mice. After treatment of mice with 1 mg/kg edelfosine 5.77 \pm 0.72 % of CD45+ cells within the CNS were identified as B220+ B cells. This frequency appeared not only to have significantly increased in comparison with 10 mg/kg edelfosine-treated mice but also compared to PBS-treated control mice. Significantly increased frequencies of neutrophils were found in the CNS of mice that received 10 mg/kg edelfosine compared to mice which were treated with either PBS or 1 mg/kg edelfosine. In detail, a 6.46-fold increase in neutrophil frequencies was seen upon 10 mg/kg edelfosine treatment compared to PBS-controls. No differences in frequencies of CD11b+ CD11c- macrophages and NK1.1+ CD11b+ CD3- NK cells were found.

Table 14. Frequencies of cell types of all CD45+ cells that infiltrated into the CNS of EAE-affected mice. Mice were treated with PBS, 1mg/kg edelfosine or 10 mg/kg edelfosine from the day of immunization. Data is shown as mean \pm SEM (n=4 for each group, except PBS-treated group: n=3).

Cell type	PBS	1 mg/kg edelfosine	10 mg/kg edelfosine
T cells	44.32 \pm 2.95 %	40.08 \pm 2.19 %	25.94 \pm 5.74 %
B cells	4.03 \pm 0.21 %	5.77 \pm 0.72 %	1.79 \pm 0.20 %
Macrophages	17.95 \pm 2.28 %	15.64 \pm 2.59 %	17.33 \pm 1.07 %
NK cells	0.99 \pm 0.20 %	1.19 \pm 0.23 %	2.21 \pm 0.60 %
pDCs	3.75 \pm 0.56 %	5.49 \pm 0.42 %	1.21 \pm 0.67 %
mDCs	9.64 \pm 1.42 %	11.40 \pm 1.09 %	4.50 \pm 1.74 %
Neutrophils	5.64 \pm 0.66 %	4.42 \pm 0.58 %	36.41 \pm 7.26 %

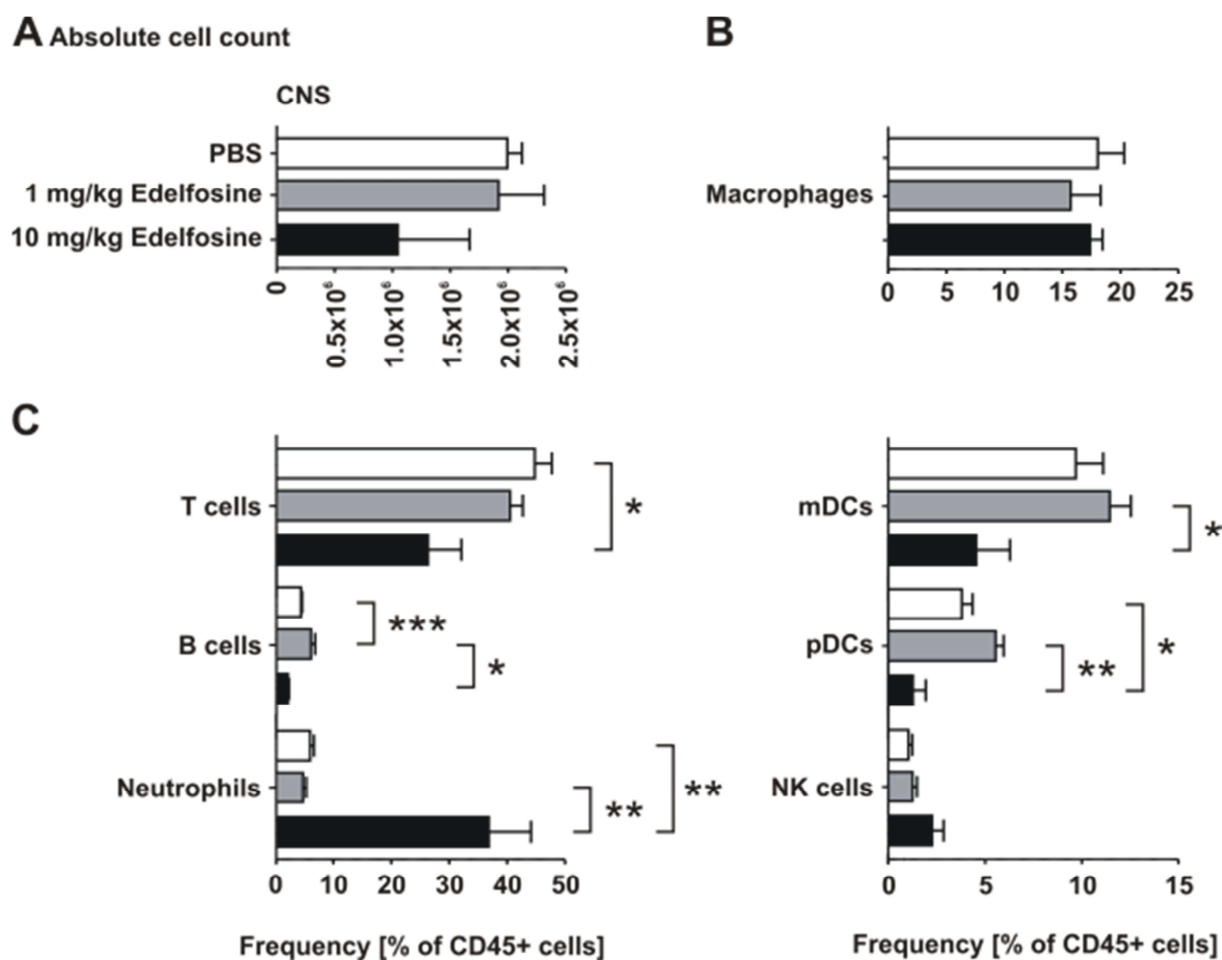


Figure 14. Edelfosine treatment-induced changes in infiltrating immune cell frequencies in the acute EAE phase. **(A)** Infiltrating CD45⁺ immune cells into brains and spinal cords were prepared and quantified by flow cytometry. **(B)** No changes in macrophage frequencies were identified upon edelfosine treatment compared to PBS-treated control mice. **(C)** The treatment of immunized mice with edelfosine was found to modulate frequencies of various immune cell subsets that infiltrated into the CNS. For instance, the treatment with 10 mg/kg edelfosine led to a significant reduction in T-cell frequencies compared to PBS treatment. Frequencies from one EAE experiment (n=4 for each group, except PBS-treated group: n=3), frequencies are shown as mean values \pm SEM (\square PBS, \blacksquare 1 mg/kg edelfosine, \blacksquare 10 mg/kg edelfosine); *P<0.05, **P<0.01, ***P<0.001 after post-hoc analysis.

Regarding T helper cell subsets the treatment of EAE-induced mice with 10 mg/kg edelfosine was found to induce a significant reduction in CD4⁺ T-cell frequencies in comparison to 1 mg/kg edelfosine or PBS in the CNS during the acute disease phase (Figure 15). In spinal cords and brains of PBS-treated mice 81.60 ± 0.59 % of CD3⁺ T cells expressed CD4 in comparison to 81.91 ± 1.41 % upon treatment with 1 mg/kg edelfosine. Interestingly, the treatment of mice with 10 mg/kg edelfosine resulted in only 69.85 ± 2.95 % of CD3⁺ T cells that co-expressed CD4 on their surface. This related to a -1.17-fold decrease of CD4⁺ T-cell frequencies due to 10 mg/kg edelfosine treatment compared to PBS-treated controls. In contrast, no differences were determined for CD8⁺ T cells (5.63 ± 0.83 % after PBS treatment, 6.16 ± 0.70 % after treatment with 1 mg/kg edelfosine, 8.36 ± 0.76 % after 10 mg/kg edelfosine treatment).

Interestingly, the treatment of mice with 1 mg/kg edelfosine resulted in significantly increased frequencies of CD4⁺ CD25⁺ Foxp3⁺ nTregs. No differences in frequencies were seen on comparing PBS-treated controls to edelfosine-treated mice. Instead a significant difference was determined between 1 mg/kg edelfosine-treated mice and mice which were treated with 10 mg/kg edelfosine (9.70 ± 1.31 % after PBS treatment, 13.39 ± 1.42 % after treatment with 1 mg/kg edelfosine and 5.25 ± 2.55 % after treatment with 10 mg/kg edelfosine (nTregs of CD4⁺ T cells).

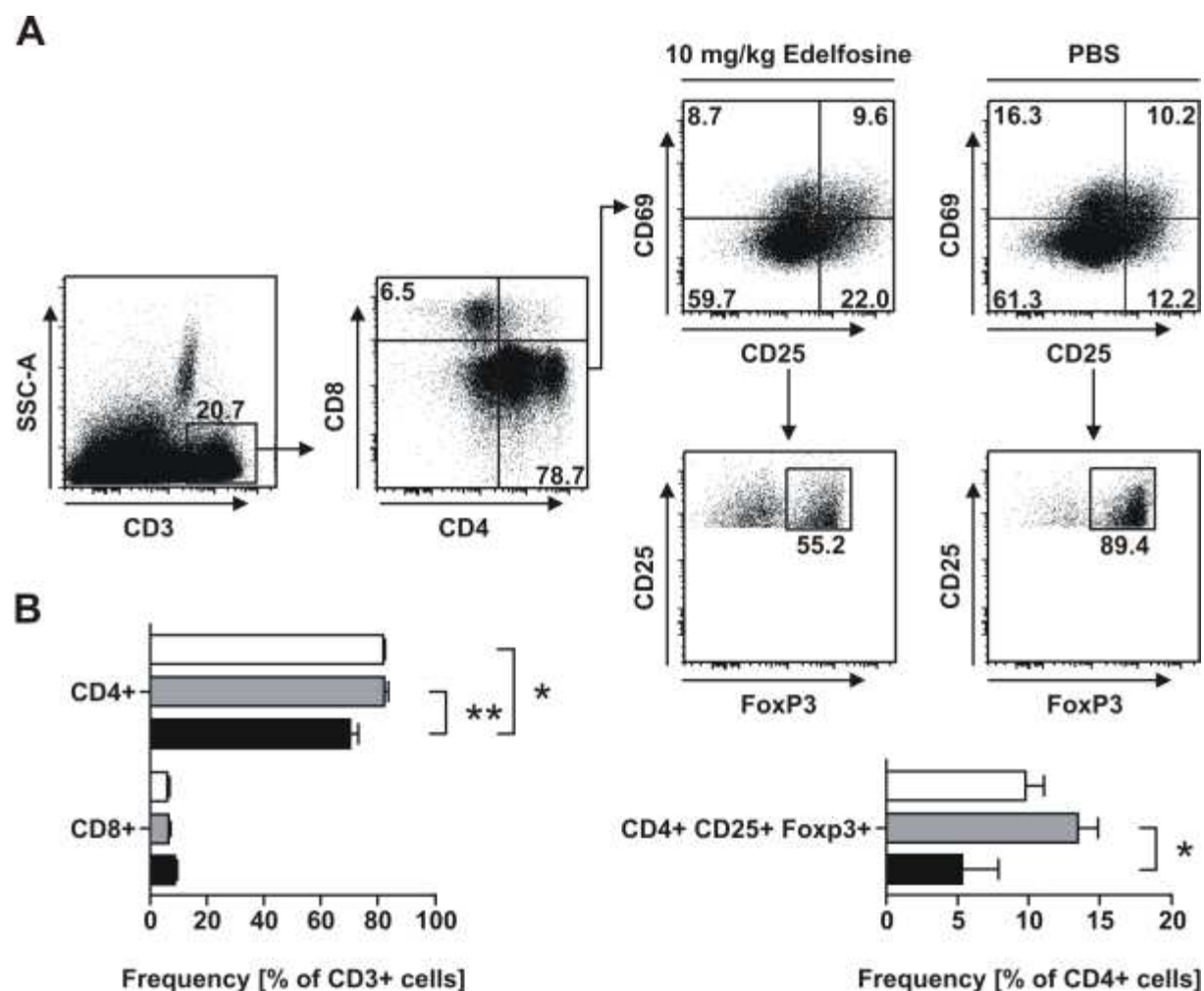


Figure 15. Analysis of edelfosine-treatment outcome on T-cell subsets. **(A)** The gating strategy allows to examine CD4⁺ and CD8⁺ T-cell frequencies as well as CD4⁺ CD25⁺ Foxp3⁺ nTregs. Treatment of mice with 10 mg/kg edelfosine resulted in a reduced frequency of CD4⁺ T cells in the CNS in the acute phase of EAE compared to treatment with PBS or 1 mg/kg edelfosine. **(B)** Flow cytometry also revealed an increased frequency of nTregs in CNS of 1 mg/kg edelfosine-treated mice in comparison to 10 mg/kg edelfosine-treated mice. Frequencies from one EAE experiment (n=4 for each group, except PBS-treated group: n=3), frequencies are shown as mean values ± SEM (□ PBS, ▒ 1 mg/kg edelfosine, ■ 10 mg/kg edelfosine); *P<0.05, **P<0.01, after post-hoc analysis.

Moreover, the daily treatment of immunized mice with edelfosine led to a significant treatment effect by decreasing frequencies of IL-17-producing CD4⁺ T cells in the CNS at acute disease phase in comparison to PBS treatment (Figure 16). No differences could be

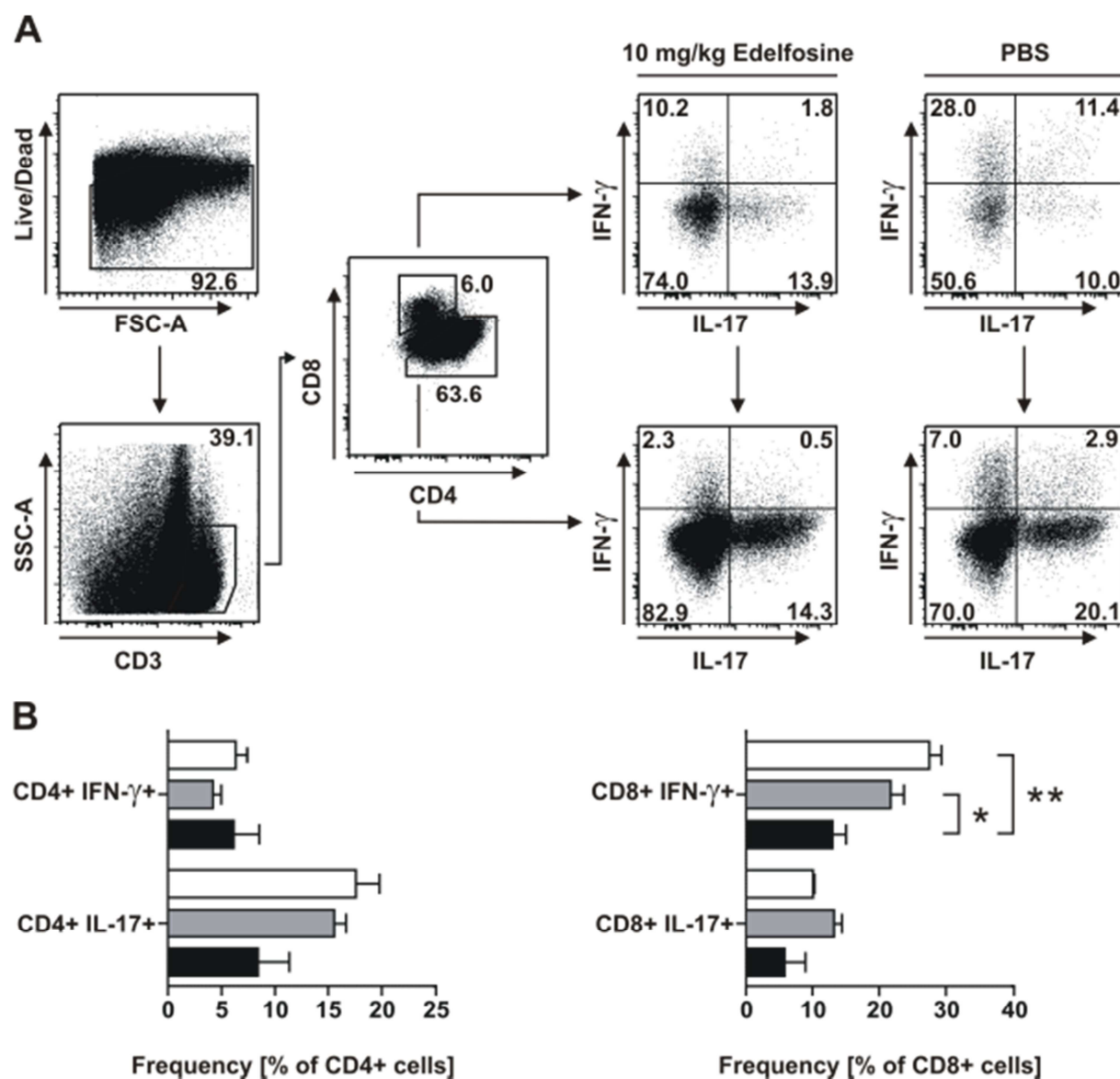


Figure 16. Edelfosine treatment affected cytokine production of T lymphocytes. **(A)** The production of IFN- γ and IL-17 by CD4+ or CD8+ T cells was analyzed after intracellular cytokine staining. Dead cells were excluded. **(B)** The treatment of mice with 10 mg/kg edelfosine led to a decrease in frequencies of IFN- γ -producing CD8+ T cells compared to PBS-treated and 1 mg/kg edelfosine-treated mice. For CD4+ IL-17+ cells the P-value was 0.0463, but no differences between groups were found in post-hoc analysis. Frequencies from one EAE experiment ($n=4$ for each group, except PBS-treated group: $n=3$), frequencies are shown as mean values \pm SEM (\square PBS, \blacksquare 1 mg/kg edelfosine, \blacksquare 10 mg/kg edelfosine); * $P<0.05$, ** $P<0.01$, after post-hoc analysis.

Table 15. Frequencies of IFN- γ and IL-17-producing T cells in the CNS related to CD4+ or CD8+ T cells. Results are expressed as mean \pm SEM.

Phenotype	PBS	1 mg/kg edelfosine	10 mg/kg edelfosine
CD4+ IFN- γ +	6.25 \pm 1.08 %	4.15 \pm 0.78 %	6.10 \pm 2.38 %
CD4+ IL-17+	17.51 \pm 2.21 %	15.46 \pm 1.12 %	8.34 \pm 2.93 %
CD8+ IFN- γ +	27.28 \pm 1.83 %	21.49 \pm 2.01 %	12.82 \pm 2.01 %
CD8+ IL-17+	9.88 \pm 0.23 %	13.04 \pm 1.19 %	5.66 \pm 3.11 %

detected between groups after post-hoc analysis. No treatment effect could be detected with regard to IFN- γ -producing CD4⁺ T cells. Interestingly, the treatment of mice with 10 mg/kg edelfosine was found to reduce frequencies of IFN- γ -producing CD8⁺ T cells compared to mice that received PBS or 1 mg/kg edelfosine. However, IL-17-producing CD8⁺ T cells displayed no differences in frequencies related to all CD8⁺ T cells after application of PBS, 1 mg/kg edelfosine or 10 mg/kg edelfosine (Table 15).

Elevated population frequencies upon 1 mg/kg edelfosine treatment, which have already been described for nTregs, were also found for activated T cells. By gating on activated CD69⁺ T cells of both CD4-positive and CD8-positive phenotype, significantly higher frequencies were detected in the CNS of 1 mg/kg edelfosine-treated mice compared to mice that received 10 mg/kg edelfosine (Table 16).

Table 16. By gating on CD69⁺ T cells of the CD4⁺ and CD8⁺ T-cell fraction, frequencies of activated cells which infiltrated into brains and spinal cords of EAE-induced mice were identified. Data is expressed as mean \pm SEM.

Phenotype	PBS	1 mg/kg edelfosine	10 mg/kg edelfosine
CD4 ⁺ CD69 ⁺	28.34 \pm 5.50 %	32.86 \pm 1.80 %	14.06 \pm 4.12 %
CD8 ⁺ CD69 ⁺	22.45 \pm 3.88 %	34.20 \pm 5.56 %	9.10 \pm 2.84 %

Finally, the impact of edelfosine treatment on apoptosis induction in CNS-infiltrating T-lymphocyte subsets was investigated. In addition to the analysis performed at the preclinical phase of EAE, activation of caspase-3 upon edelfosine treatment was also determined at the acute phase (Figure 17).

With respect to CD4⁺ T cells from the CNS a significant, 4.63-fold increase was detected if mice were treated with 10 mg/kg edelfosine compared to PBS-treated controls. No differences were detected for caspase-3 activation in CD8⁺ T cells in general and in activated CD69⁺ CD8⁺ T cells (Table 17).

Table 17. Frequencies of CD4⁺ or CD8⁺ T cells as well as their respective CD69⁺ subsets with activated caspase-3 of infiltrating CD4⁺ and CD8⁺ T cells. Data is shown as mean \pm SEM.

Phenotype	PBS	1 mg/kg edelfosine	10 mg/kg edelfosine
CD4 ⁺ , activated caspase-3	1.93 \pm 0.23 %	3.05 \pm 0.27 %	8.91 \pm 2.36 %
CD4 ⁺ CD69 ⁺ , activated caspase-3	0.53 \pm 0.08 %	0.91 \pm 0.11 %	0.87 \pm 0.11 %
CD8 ⁺ , activated caspase-3	2.08 \pm 0.29 %	2.07 \pm 0.22 %	1.89 \pm 0.66 %
CD8 ⁺ CD69 ⁺ , activated caspase-3	0.99 \pm 0.19 %	0.97 \pm 0.13 %	1.20 \pm 0.66 %

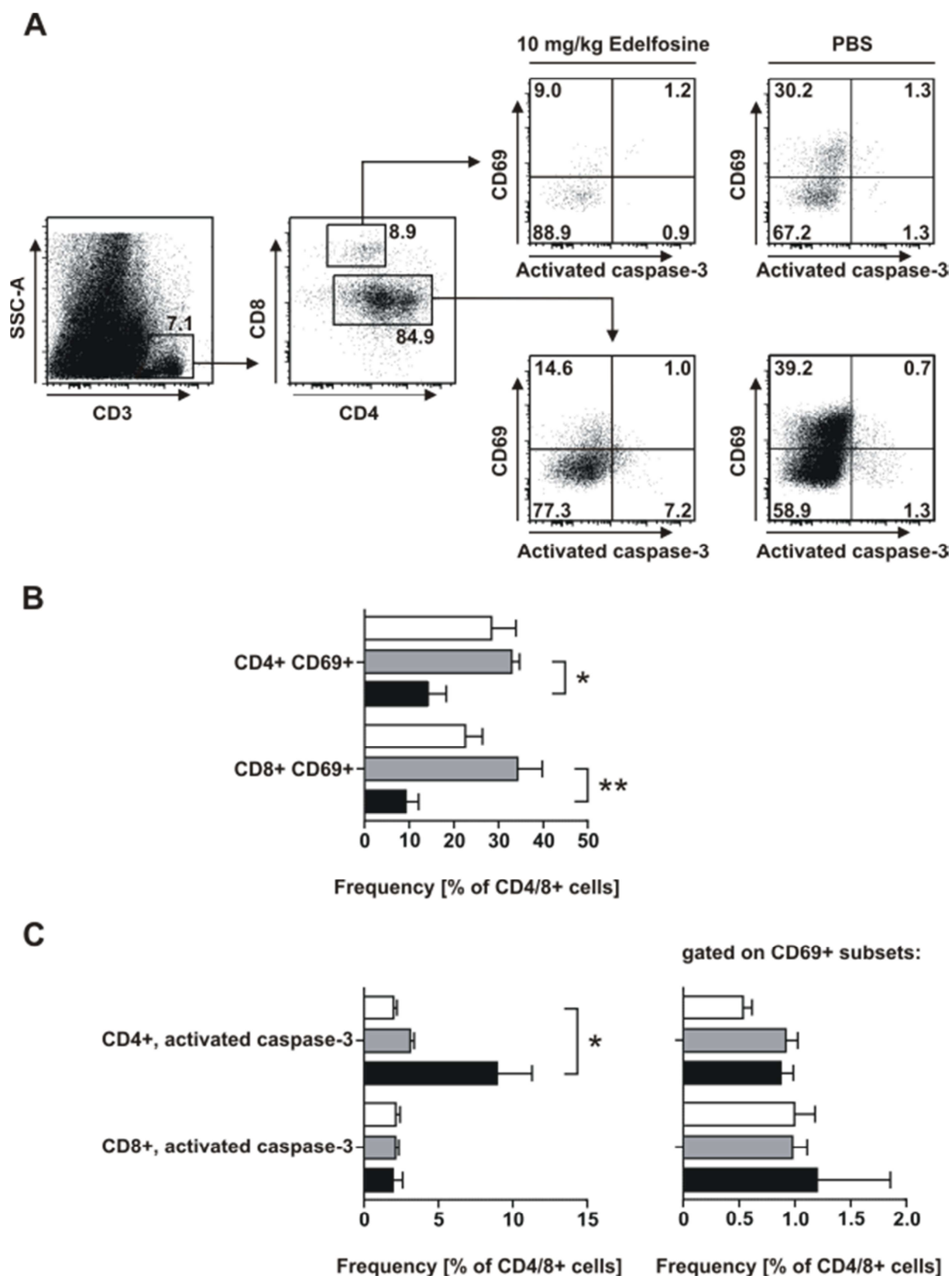


Figure 17. Increased caspase-3 activation upon application of edelfosine. **(A)** CD4, CD8 and CD69 allowed the investigation of caspase-3 activation induced by edelfosine treatment. **(B)** Frequencies of activated CD4+ but also CD8+ T cells were upregulated in the CNS of mice that received 1 mg/kg edelfosine compared to 10 mg/kg. **(C)** CD4+ T cells with activated caspase-3 showed that treatment with 10 mg/kg edelfosine increased the frequency of this apoptosis-indicative population compared to respective cells from PBS-treated mice. Frequencies from one EAE experiment (n=4 for each group, except PBS-treated group: n=3), frequencies are shown as mean values \pm SEM (\square PBS, \blacksquare 1 mg/kg edelfosine, \blacksquare 10 mg/kg edelfosine); *P<0.05, **P<0.01, after post-hoc analysis.

4.3.4 The preventive edelfosine treatment prohibits neuronal loss in acute RR-EAE

To investigate and model MS, EAE in mice is not only suitable for the study of the inflammatory facets of this disease but it is suitable for the examination of autoimmunity-driven damage of CNS tissue and cells. To detect and quantify the damage of neurons within the cervical spinal cord of EAE-affected SJL mice during the acute disease phase, tissue sections were prepared for immunohistochemistry. Sections were stained with antibodies against the neuron-specific nuclear protein called Neuronal Nuclei (NeuN). Cervical spinal cord sections from age-matched, non-immunized SJL control mice were used to rank EAE-induced neuronal loss and edelfosine-mediated treatment effects. Quantification was carried out by detection of NeuN+ neurons within the ventral horn including the lower motor neurons. Compared to non-immunized controls a significant decrease in NeuN+ neurons was detected in EAE-induced, PBS-treated mice (Figure 18). Mice which were treated with 1 mg/kg or 10 mg/kg edelfosine did not reveal a significant neuronal loss. Furthermore, tissue sections were used to display mononuclear cell infiltrations into the cervical spinal cord by histology (HE-staining). Cells could be readily identified at the anterior side of the spinal cord including the anterior median fissure. Neuronal damage within cervical spinal cord sections was assessed by Bielschowsky silver impregnation. Reduced silver visualized nerve fibers and neurofibrils. Since the anterior and lateral corticospinal tracts comprise mostly motor axons and are thus fundamentally important for voluntary movements those regions were of special interest in the context of EAE and its impairment with locomotive functioning. Light-colored stainings in the white matter of spinal cord sections indicated axonal damage.

4.4 Edelfosine interferes with human T-cell proliferation and modulates distinct signaling pathways

4.4.1 Edelfosine induces cell death in a concentration-dependent manner in CD4+ and CD8+ T cells

To delineate the impact of various edelfosine concentrations on human T cells and to determine a possible damaging range of concentrations, PBMCs were isolated from human blood. Cells were seeded in triplicates, incubated for 24 h in the absence of a stimulus, pooled for each respective condition and analyzed by flow cytometry. After gating on CD4+ and CD8+ populations apoptotic cells and dead cells were analyzed by gating on annexin V+ and/or PI+ cell populations (Figure 19). Apoptosis is characterized by the translocation and exposure of the phospholipid phosphatidylserine from the inner to the outer leaflet of the plasma membrane (313). This translocation can be detected by staining with Annexin V.

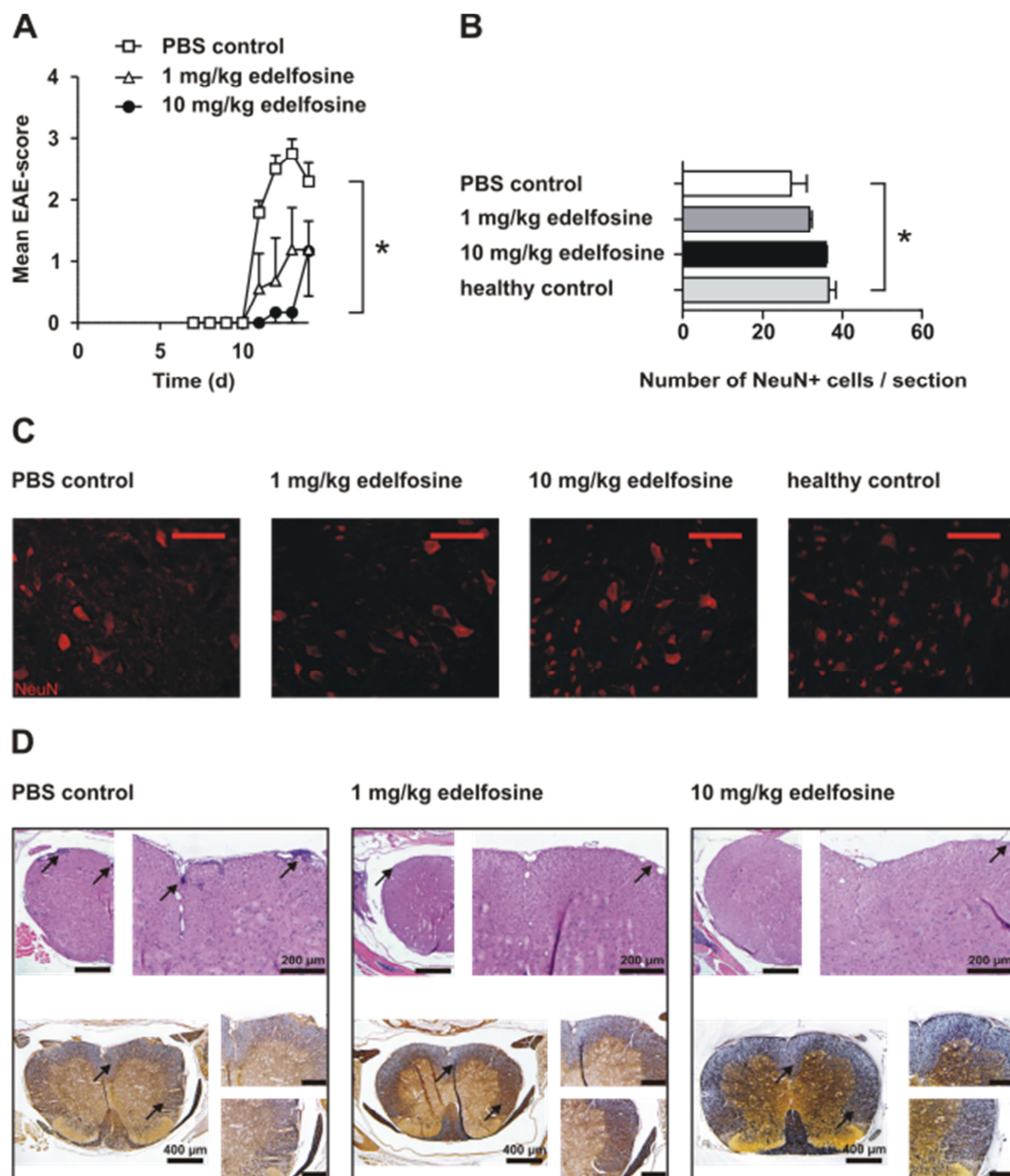


Figure 18. Reduction of NeuN+ neurons in the acute phase was prevented by edelfosine. **(A)** Immunized SJL mice were treated daily with PBS or edelfosine. CNS was prepared at day 14. The EAE course revealed a significant treatment effect with differences between PBS-treated mice and mice that received either 1 mg/kg or 10 mg/kg edelfosine (day 11 to 13). **(B)** For each mouse, six sections of the cervical spinal cord were stained using an anti-NeuN antibody. Per section two photographs were evaluated for each of the two ventral horns. NeuN+ neurons were counted to determine means. Compared to non-immunized, age-matched SJL mice PBS-treated mice showed a reduced number of NeuN+ neurons. This reduction could be prevented by treatment with either 1 mg/kg or 10 mg/kg edelfosine. **(C)** Representative photographs of cervical spinal cord sections stained for NeuN+ neurons after treatment with either PBS, 1 mg/kg or 10 mg/kg edelfosine (scale bar represents 100 μ m, magnification: 20x). **(D)** Upper panel: Histological depiction of mononuclear cell infiltration of the cervical spinal cord by HE-staining (scale bar represents 200 μ m as indicated with 10x magnification, otherwise scale bars represent 400 μ m, magnification: 4x). Lower panel: Bielschowsky silver impregnation for neuronal damage depicted as overview with close-ups of the anterior and lateral spinal tracts. Arrows denote areas of axon damage/loss (scale bar represents 400 μ m (magnification: 4x) or otherwise 200 μ m with 10x magnification).

Viable cells with intact membranes exclude PI. Thus, viable cells are annexin V- PI-, cells in early apoptosis are annexin V+ PI- and cells in late apoptosis or dead cells are annexin V+ PI+. Notably, this assay does not discriminate between cells that died by apoptosis and those that died by necrosis.

The incubation of PBMCs with 10 µg/ml edelfosine led to a decrease of the annexin V- PI- frequencies in CD4+ T cells compared to frequencies in approaches without edelfosine, with 1 µg/ml or 3.3 µg/ml edelfosine. The incubation in the presence of 33.3 µg/ml edelfosine resulted in only 2.4 % annexin V- PI- CD4+ T cells. Correspondingly, the frequencies of annexin V+ PI+ CD4+ T cells increased reaching a maximum after culture in the presence of 33.3 µg/ml edelfosine. Here, the frequencies of annexin V+ PI- CD4+ T cells showed only a mild increase with increasing edelfosine concentrations (Table 18).

Table 18. Frequencies of CD4+ T cells to determine edelfosine-mediated induction of apoptosis or cell death.

Treatment	Annexin V- PI-	Annexin V+ PI-	Annexin V+ PI+
No edelfosine	94.9 %	3.1 %	1.9 %
1 µg/ml edelfosine	94.1%	4.3 %	1.6 %
3.3 µg/ml edelfosine	94.3 %	4.3 %	1.4 %
10 µg/ml edelfosine	58.3 %	9.9 %	31.0 %
33.3 µg/ml edelfosine	2.4 %	11.4 %	86.1 %

Notably, annexin V+ PI- and annexin V+ PI+ CD8+ populations displayed a comparable increase in frequencies if cultured in the presence of 33.3 µg/ml edelfosine. Frequencies appeared to be rather constant upon culture without edelfosine and also with 1 µg/ml, 3.3 µg/ml or 10 µg/ml edelfosine. With regard to annexin V- PI- CD8+ T cells 33.3 µg/ml edelfosine appeared to interfere massively with cell viability. The addition of 10 µg/ml edelfosine still made it possible to identify 75.7 % annexin V- PI- cells (Table 19). By affecting cellular viability in unstimulated T cells, edelfosine may also interfere with the cells' functional capacity to respond to antigen and to proliferate.

Table 19. Frequencies of CD8+ T cells to determine edelfosine-mediated induction of apoptosis or cell death.

Treatment	Annexin V- PI-	Annexin V+ PI-	Annexin V+ PI+
No edelfosine	76.3 %	19.1 %	4.7 %
1 µg/ml edelfosine	81.5 %	15.8 %	2.7 %
3.3 µg/ml edelfosine	82.1 %	15.8 %	2.0 %
10 µg/ml edelfosine	75.7 %	13.5 %	10.0 %
33.3 µg/ml edelfosine	6.5 %	45.2 %	48.2 %

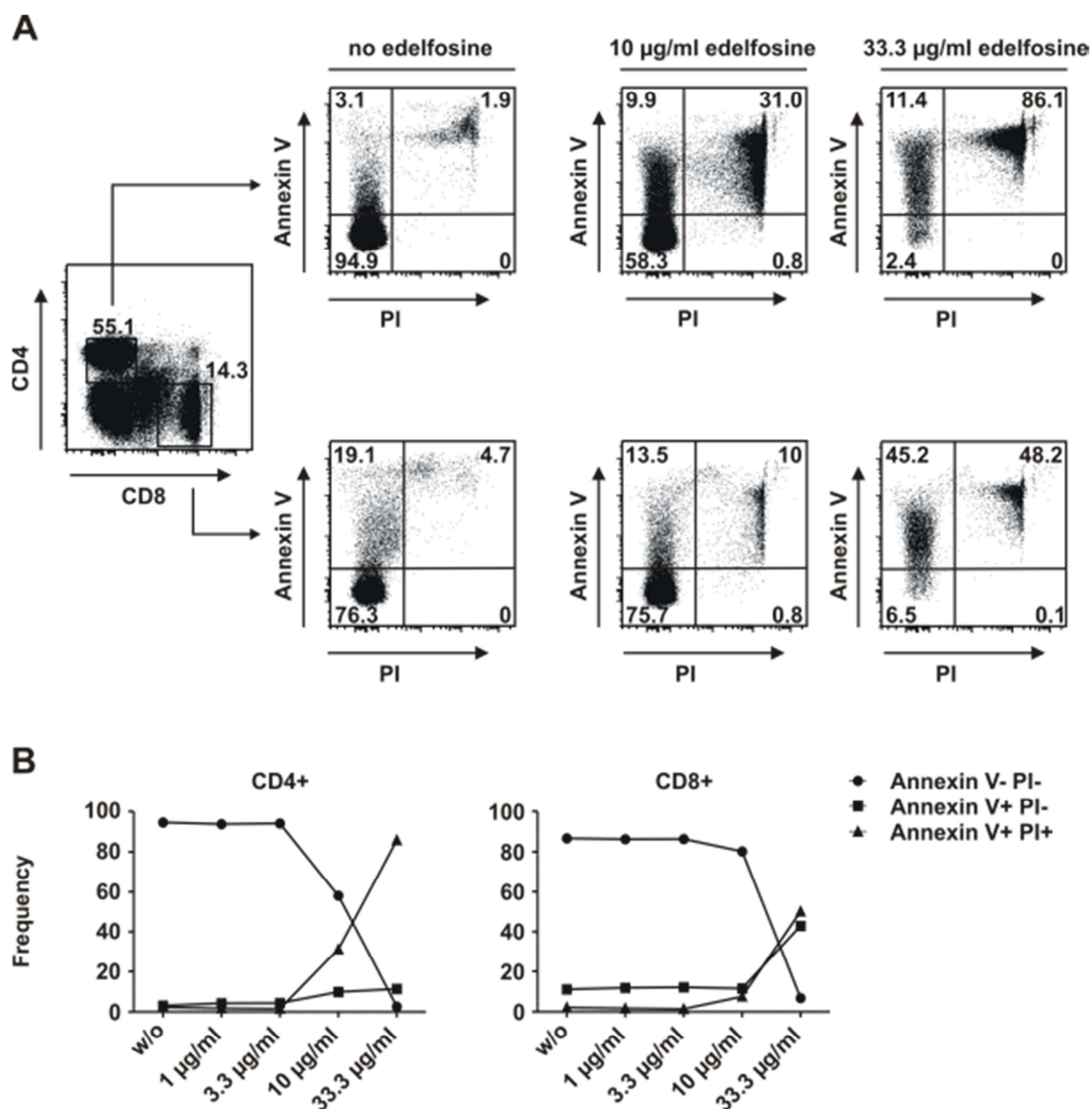


Figure 19. Edelfosine impact on T-cell viability. **(A)** Gating strategy to determine frequencies of annexin V+ and/or PI+ CD4+ as well as CD8+ T cells. Dot plots for annexin V- and PI-gating of approaches in absence of edelfosine, with 10 µg/ml edelfosine or 33.3 µg/ml edelfosine. **(B)** With regard to CD4+ T cells just 10 µg/ml edelfosine led to a decrease in annexin V- PI- frequencies accompanied by a remarkable increase in annexin V+ PI+ CD4+ T-cell frequencies. In the case of CD8+ T cells a marked decrease in annexin V- PI- cells was only observed with 33.3 µg/ml edelfosine which resulted in comparable frequencies of annexin V+ PI- as well as annexin V+ PI+ cells.

4.4.2 Edelfosine interferes with proliferation of human PBMCs after mitogenic activation, but also with proliferation of antigen-specific T-cell lines

In order to characterize the influence of edelfosine on the proliferation of human T cells, PBMCs were first stimulated with a mitogenic stimulus, PHA. Proliferation was analyzed after three days of culture. First, the impact of edelfosine on T-cell activation and proliferation was investigated by adding edelfosine immediately as the cells were seeded. Cells were

incubated without or in the presence of PHA. A reduction in proliferation was already detectable upon addition of 1.0 µg/ml edelfosine and also found in the case of higher concentrations (Figure 20 A). Interestingly, unstimulated controls also showed a reduction in cellular proliferation in presence of 10 µg/ml edelfosine or higher concentrations. Here, the half maximal inhibitory concentration (IC_{50}) was determined by nonlinear regression. For stimulated cells the IC_{50} was 0.64 ± 0.10 µg/ml edelfosine. In the absence of PHA the IC_{50} was 0.44 ± 0.05 µg/ml edelfosine.

The second approach aimed at characterizing the edelfosine influence on already proliferating cells. For that reason cells were activated with PHA, and edelfosine was added two days later. Here, concentrations of 3.3 µg/ml edelfosine or higher resulted in an efficient reduction of proliferation (Figure 20 B). In comparison, 33.3 µg/ml edelfosine was found to significantly reduce the proliferation in unstimulated controls.

In chapter 4.4.1 the question was raised if edelfosine, which was found to affect viability of unstimulated cells, may also compromise the capacity of T cells to proliferate upon stimulation. To address this question PBMCs were incubated with or without edelfosine for 24 h in the absence of stimulation. Cells were washed extensively to remove edelfosine followed by further culturing for three days. In control approaches cells were incubated without PHA. Cells were found to retain their proliferative function after incubation with edelfosine at concentrations of up to 1 µg/ml (Figure 20 C). 3.3 µg/ml edelfosine or higher interfered with the cellular capacity to proliferate upon stimulation with PHA. With regard to unstimulated cells, no significant reductions of proliferation were identified.

To further investigate the influence of edelfosine on T-cell proliferation in the context of antigen-specific stimulation, T-cell lines (TCLs) specific for MBP₍₈₃₋₉₉₎ were used. Edelfosine was added immediately after seeding of cells. After three days of culture 1.0 µg/ml edelfosine was already detected to profoundly reduce T-cell proliferation in stimulated as well as unstimulated conditions (Figure 20 D).

In an additional approach PBMCs were incubated for up to seven days without the addition of a stimulus. Cells were cultured in medium alone, in presence of anti-HLA-DR- and anti-MHC class I-blocking antibody or with 3.3 µg/ml edelfosine. Both the addition of the antibody and edelfosine resulted in considerably lower proliferations. In the case of edelfosine the proliferation was reduced to non-detectable levels (Figure 20 E). These results implied an effect of edelfosine on cellular proliferation even if cells were not activated by adding a defined stimulus, i.e. in the unstimulated condition.

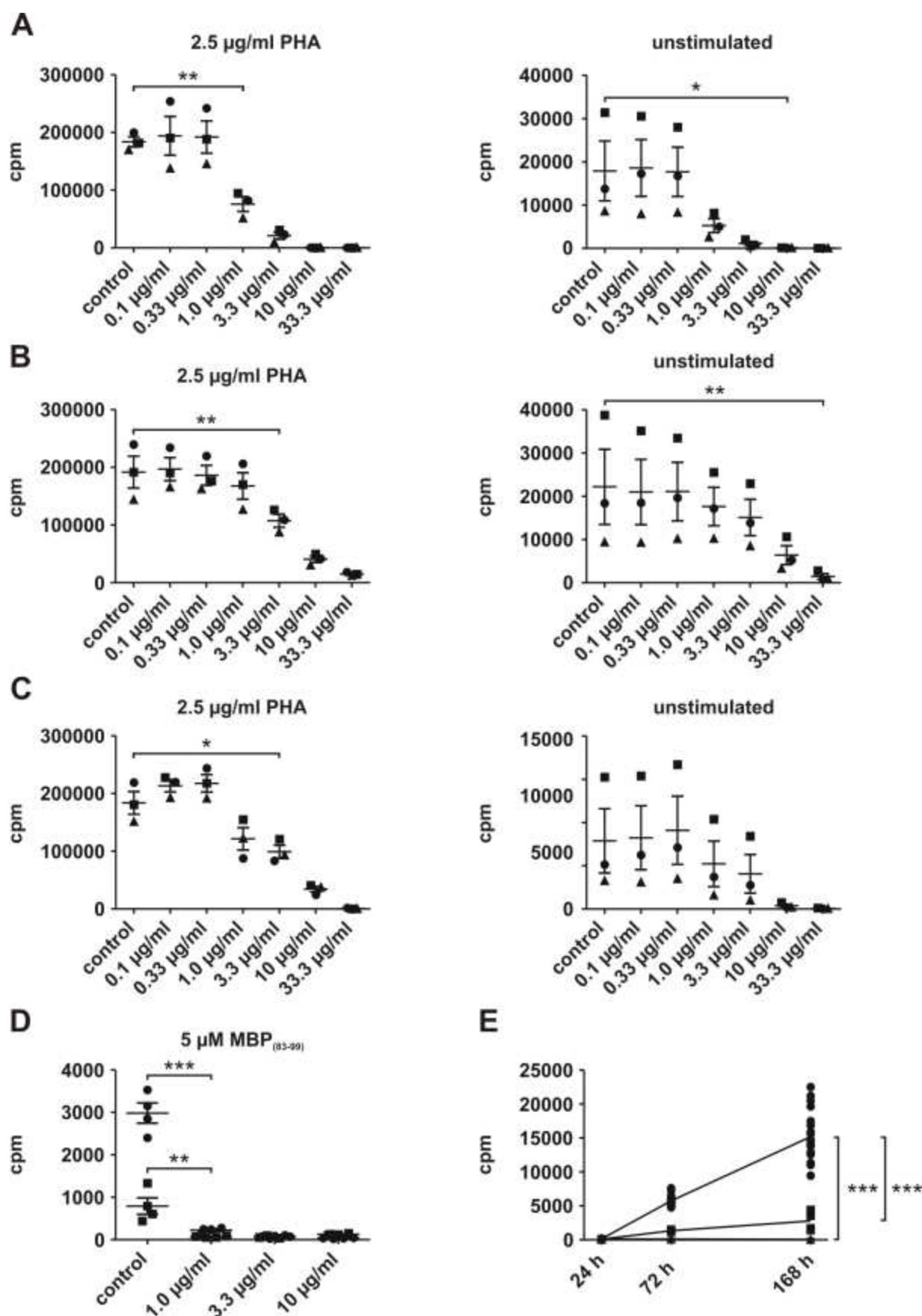


Figure 20. Human T-cell proliferation was affected by edelfosine. **(A)** Reduced PBMC proliferation upon addition of edelfosine on cell seeding was independent of the addition of PHA. Notably, PHA-activated cells appeared to be susceptible to edelfosine at 10-fold lower concentrations. **(B)** The inhibitory effect of edelfosine was also observed if the drug was added to already activated, proliferating T cells. Here, a significant reduction of

proliferation in unstimulated cells was only detectable with 33.3 µg/ml edelfosine. **(C)** Preincubation of PBMCs with at least 3.3 µg/ml edelfosine interfered with the cells' capacity to proliferate upon PHA stimulation. No effect was detected in preconditioned, but unstimulated cells (experiments A-C: sample size n=3 donors, each approach was seeded in triplicates). **(D)** 1 µg/ml edelfosine or higher concentrations profoundly diminished proliferation in MBP₍₈₃₋₉₉₎-specific TCLs. One representative TCL of two is shown. Cells were incubated in quadruplicates. **(E)** PBMCs were cultured without addition of stimulus. Proliferation was detectable after seven days. The presence of anti-HLA-DR- and anti-MHC class I-blocking antibodies or 3.3 µg/ml edelfosine inhibited cellular proliferation. Bars represent mean values ± SEM, *P<0.05, **P<0.01 and ***P<0.001 after post-hoc analysis.

4.4.3 Whole genome expression analysis of CD4+ T cells reveals impact of edelfosine on a distinct set of signaling pathways

Enriched CD4+ T cells from PBMCs of two age-matched female as well as two age-matched male donors were incubated for 30 h without edelfosine, in presence of 3.3 µg/ml edelfosine and 10 µg/ml edelfosine, respectively. In parallel approaches, cells were incubated with beads coated with antibodies against CD2, CD3 and CD28 or with coated beads and 3.3 µg/ml edelfosine. Cell-culture supernatant was saved and cells were subjected to RNA isolation, cDNA synthesis and microarray analysis for gene expression. Comparative gene-expression analysis was performed according to Table 20.

Table 20. Modulated gene expression in CD4+ T cells upon culture with edelfosine. A signal log ratio (SLR) ≥ 0.8 for upregulated genes or ≤ -0.8 for downmodulated genes was set as a cut-off to determine genes whose expressions were significantly modulated after t-test analysis.

Pairwise comparison	SLR ≤ -0.8	SLR ≥ 0.8
<i>Unstimulated</i>		
3.3 µg/ml edelfosine vs. no edelfosine	21	0
10 µg/ml edelfosine vs. no edelfosine	60	11
<i>Stimulated</i>		
3.3 µg/ml edelfosine vs. no edelfosine	665	287

In general, edelfosine modulated the gene expression of human CD4+ T cells in the case of stimulation but also if no exogenous stimulus was added, although to a limited extent. Except for the transcription factor 4 (TCF4) gene, every significantly downregulated gene in cells cultured with 3.3 µg/ml edelfosine could also be identified in cells cultured with 10 µg/ml edelfosine. Moreover, the latter condition yielded 11 upregulated genes (SLR ≥ 0.8) and additional downregulated genes (SLR ≤ -0.8). Therefore, further analysis of the unstimulated cells focused on the 10 µg/ml edelfosine approach. Next, the database for annotation, visualization and integrated discovery (DAVID)-bioinformatics database was used to annotate the differentially expressed genes to functional themes/groups and assign to them so-called gene-ontology (GO) terms for specific pathways of cellular function (314). The GO project is an effort to consistently describe gene products in databases. DAVID, as a tool, is designed to allow systematical mapping of large numbers of genes in lists associated with biological annotations (e.g. GO terms). Three structured controlled vocabularies (ontologies)

have been developed to describe gene products in a species-independent manner: the associated biological process (BP), cellular components and molecular functions. The GOTERM_BP_FAT set which has been specifically designed by the DAVID consortium was selected to filter the broadest terms in order to prevent overshadowing of more specific terms. Table 21 summarizes the top-3 GO-terms which were selected due to their highest GO P-values. As expected from its originally identified activities, the addition of 10 µg/ml edelfosine was leading to an upregulation of genes associated with apoptosis and cell death in the unstimulated setting, a knowledge-based finding that was in accordance with the previously described analysis for annexin V and PI after edelfosine incubation.

Table 21. Gene-expression analysis allowed clustering of up- or downregulated genes to determine biological pathways affected by edelfosine in human CD4+ T cells. **(A)** The incubation of unstimulated cells with 10 µg/ml edelfosine for 30 h resulted in the upregulation of apoptosis- and cell death-associated genes. Genes involved in immune response and antigen processing and presentation were downregulated. **(B)** In the case of stimulated cells which were cultured in presence of 3.3 µg/ml edelfosine the downmodulation of cell-cycle progression-related genes was found. Additionally, the incubation with edelfosine resulted in the upregulation of genes assigned to immune response- and virus response-pathways characterized by type I interferon-regulated genes.

A Setting: unstimulated + 10 µg/ml edelfosine vs. unstimulated

Up (ID)	Gene Examples	GO P-value
Apoptosis (GO:0006915)	JUN, RHOB, KRAS	1.8×10^{-2}
Programmed cell death (GO:0012501)	JUN, RHOB, KRAS	1.9×10^{-2}
Learning (GO:0007612)	JUN, KRAS	2.2×10^{-2}

Down (ID)	Gene Examples	GO P-value
Immune response (GO:0006955)	CD74, CD79A, IGJ, IRF8, CCL22	3.9×10^{-14}
Antigen processing and presentation of peptide or polysaccharide antigen via MHC class II (GO:0002504)	CD74, IFI30, HLA-DMA, HLA-DPA1	2.2×10^{-11}
Antigen processing and presentation (GO:0019882)	CD74, IFI30, HLA-DMB, HLA-DRA	1.3×10^{-8}

B Setting: stimulated + 3.3 µg/ml edelfosine vs. stimulated

Up (ID)	Gene Examples	GO P-value
Immune response (GO:0006955)	IFIH1, IFI6, IFI44L, TNFSF10, CXCR4	2.6×10^{-10}
Response to virus (GO:0009615)	IRF7, ISG20, IFI44, MX1, MX2, RSAD2	7.5×10^{-10}
Regulation of apoptosis (GO:0042981)	CASP10, CARD16, DDIT3, HSPA1A	1.0×10^{-8}

Down (ID)	Gene Examples	GO P-value
Cell cycle (GO:0007049)	BARD1, CKS1B, E2F1, CDCA2, CCNF	3.4×10^{-81}
Cell cycle phase (GO:0022403)	CKS2, DMC1, E2F1, RAD51, CCNA2	2.6×10^{-80}
M phase (GO:0000279)	FBXO43, MAD2L1, MKI67, CENPV	3.0×10^{-77}

A second novel and interesting finding was the downmodulation of MHC class II-associated genes, if cells were cultured in presence of 10 µg/ml edelfosine without stimulus. Here, genes were clustered by the GO-terms immune response, antigen processing and presentation of peptide or polysaccharide antigen via MHC class II, or antigen processing and presentation. In stimulated CD4+ T cells edelfosine interfered with the cell-cycle progression by downmodulation of cell cycle-associated genes. Strikingly, besides the upregulation of genes associated with the regulation of apoptosis, the incubation of stimulated cells with 3.3 µg/ml edelfosine was leading to the upregulation of genes that were allocated to GO-terms like immune response and response to virus. Most of these genes were found to be type I interferon-associated genes. Gene lists were created to focus

Table 22. Gene-list summary of antigen processing and presentation (MHC class II)- as well as immune response (type I interferon)-associated genes. **(A)** Unstimulated human CD4+ T cells were cultured with 10 µg/ml edelfosine. 25 downregulated genes were assigned to biological pathways for antigen processing and presentation (SLR ≤ -0.8). **(B)** Stimulated, 3.3 µg/ml edelfosine-treated CD4+ T cells demonstrated upregulation of genes involved in biological processes of immune response and response to virus (SLR ≥ 0.6).

A unstimulated + 10 µg/ml edelfosine vs. unstimulated: HLA class II-associated genes

Gene ID	Description	Signal Log Ratio
HLA-DRA	major histocompatibility complex, class II, DR alpha	-2.7
IGJ	immunoglobulin J polypeptide, linker protein for immunoglobulin alpha and mu polypeptides	-2.7
LYN	tyrosine-protein kinase Lyn	-1.8
IGHM	immunoglobulin heavy constant mu	-1.7
IGHD	immunoglobulin heavy constant delta	-1.7
MEF2C	myocyte enhancer factor 2C	-1.6
IGKC	immunoglobulin kappa constant	-1.6
HLA-DMB	major histocompatibility complex, class II, DM beta	-1.5
IGLJ3	immunoglobulin lambda joining 3	-1.5
IRF8	interferon regulatory factor 8	-1.4
HLA-DPA1	major histocompatibility complex, class II, DP alpha 1	-1.4
IGK@	immunoglobulin kappa locus	-1.4
VSIG6	V-set and immunoglobulin domain containing 6	-1.4
IGKC	immunoglobulin kappa constant	-1.3
HLA-DQA2	major histocompatibility complex, class II, DQ alpha 2	-1.2
IGHA1	immunoglobulin heavy constant alpha 1	-1.2
FCRL3	Fc receptor-like 3	-1.2
IL13RA1	interleukin 13 receptor, alpha 1	-1.1
CD79A	B-cell antigen receptor complex-associated protein alpha chain	-1.1
IFI30	interferon, gamma-inducible protein 30	-1.0
CD74	HLA class II histocompatibility antigen gamma chain	-1.0
BLNK	B-cell linker	-0.9
HLA-DMA	major histocompatibility complex, class II, DM alpha	-0.9
IGHV4-31	immunoglobulin heavy variable 4-31	-0.9
BTK	Bruton agammaglobulinemia tyrosine kinase	-0.8

B stimulated + 3.3 µg/ml edelfosine vs. stimulated: type I interferon-regulated genes

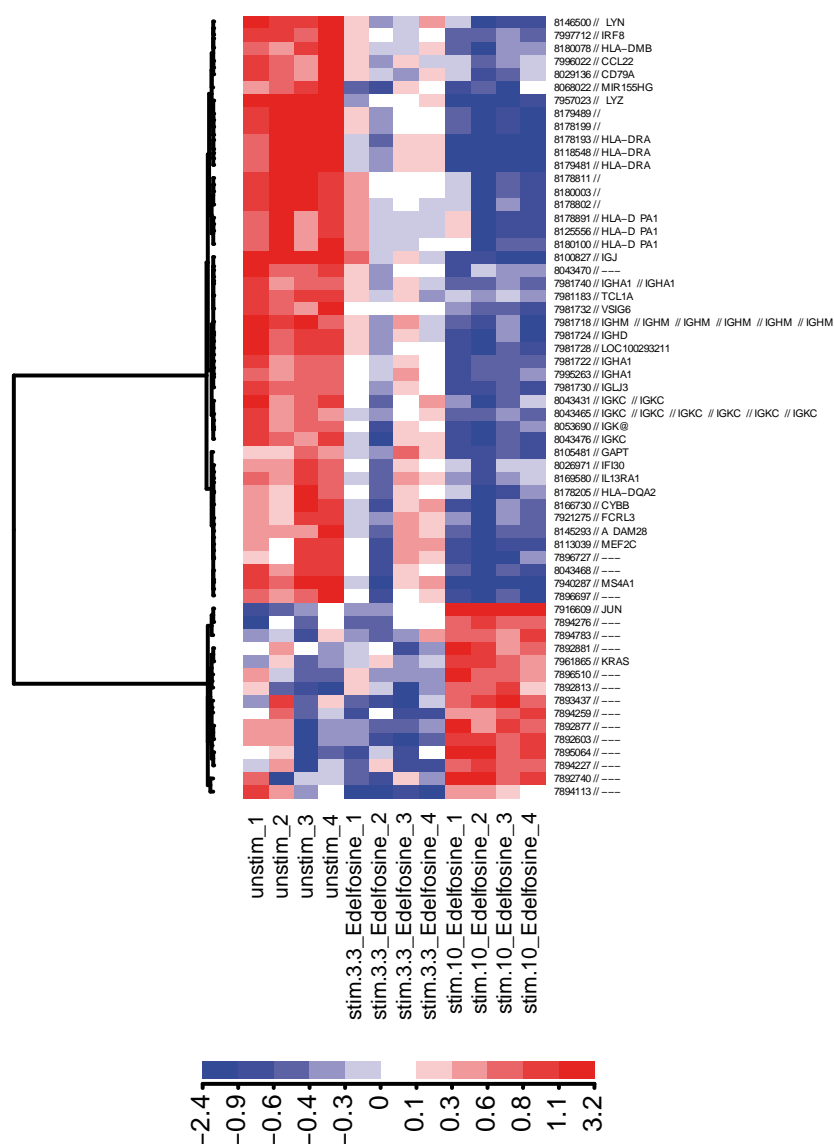
Gene ID	Description	Signal Log Ratio
IFIT2	interferon-induced protein with tetratricopeptide repeats 2	4.1
IFI44	interferon-induced protein 44	3.4
RSAD2	radical S-adenosyl methionine domain containing 2	3.4
IF44L	interferon-induced protein 44-like	3.3
IFIT1	interferon-induced protein with tetratricopeptide repeats 1	3.3
IFIT3	interferon-induced protein with tetratricopeptide repeats 3	3.3
DDX60	DEAD (Asp-Glu-Ala-Asp) box polypeptide 60	2.8
DDX60L	DEAD (Asp-Glu-Ala-Asp) box polypeptide 60-like	2.8
MX1	interferon-induced GTP-binding protein Mx1	2.6
OAS1	2',5'-oligoadenylate synthetase 1, 40/46kDa	2.6
XAF1	XIAP associated factor 1	2.5
IFI6	interferon, alpha-inducible protein 6	2.3
OAS3	2'-5'-oligoadenylate synthetase 3, 100kDa	2.0
MX2	interferon-induced GTP-binding protein Mx2	1.9
OASL	2'-5'-oligoadenylate synthetase-like	1.8
RGS1	regulator of G-protein signaling 1	1.8
IFIH1	interferon induced with helicase C domain 1	1.6
TNFSF13B	tumor necrosis factor (ligand) superfamily, member 13b	1.3
ISG20	interferon stimulated exonuclease gene 20kDa	1.4
IRF7	interferon regulatory factor 7	1.0
EIF2AK2	interferon-induced, double-stranded RNA-activated protein kinase	0.9
TNFSF10	TNF-related apoptosis inducing ligand TRAIL	0.8
IL-8	interleukin 8	0.6
ISG15	interferon-stimulated protein, 15 kDa	0.6

especially on the prominent, novel identified biological pathways that appeared to be modulated upon edelfosine treatment of human CD4+ T cells (Table 22).

In the case of unstimulated cells that were incubated with 10 µg/ml edelfosine, the list of downmodulated genes summarizes genes with SLR \leq -0.8 which could be allocated to the GO terms immune response and antigen processing and presentation. These genes were largely assignable to MHC class II- and immunoglobulin-regulation. The second gene list collects genes that appeared to be upregulated in human stimulated CD4+ T cells if cultured with 3.3 µg/ml edelfosine. This list contains not only genes allocated to type I interferon-associated immune responses with SLR \geq 0.8 but also type I interferon-associated genes with SLR = 0.6 that were previously detected in a longitudinal gene-expression study of PBMCs derived from interferon beta-treated MS patients (315). Probably, the performed microarray analysis of our study underestimated the strength of regulation of those genes. Theoretically, a group of weakly regulated genes may have a profound cumulative biological effect comparable to the potential effect of some genes which appear to be strongly regulated. In order to determine and to visualize patterns of gene expression consecutive

comparisons were performed by generating heatmaps (Figure 21). The first sequence for downregulated, antigen processing- and presentation-related genes was as follows: approach “unstimulated” in comparison to approaches “unstimulated with 3.3 $\mu\text{g/ml}$ edelfosine” and “unstimulated with 10 $\mu\text{g/ml}$ edelfosine”. The heatmap indicates the consecutive downregulation of genes with increasing edelfosine concentration. Only those genes were considered that presented with at least one $\text{SLR} \leq -0.8$ in all three possible pairwise comparisons. Thus, in absence of edelfosine the highest expression levels were determined for these genes that may be involved in antigen-processing and presentation. The second sequence comprised upregulated, immune and virus response-allocated genes by comparing the “unstimulated” condition to the approaches “stimulated” and “stimulated with 3.3 $\mu\text{g/ml}$ edelfosine”. Here, only those genes were considered that presented with at least two $\text{SLR} \geq 0.8$ in all three possible pairwise comparisons.

A Edelfosine-induced downregulation of expression of genes for antigen processing.



B Edelfosine-mediated increased expression of type I interferon-associated genes.

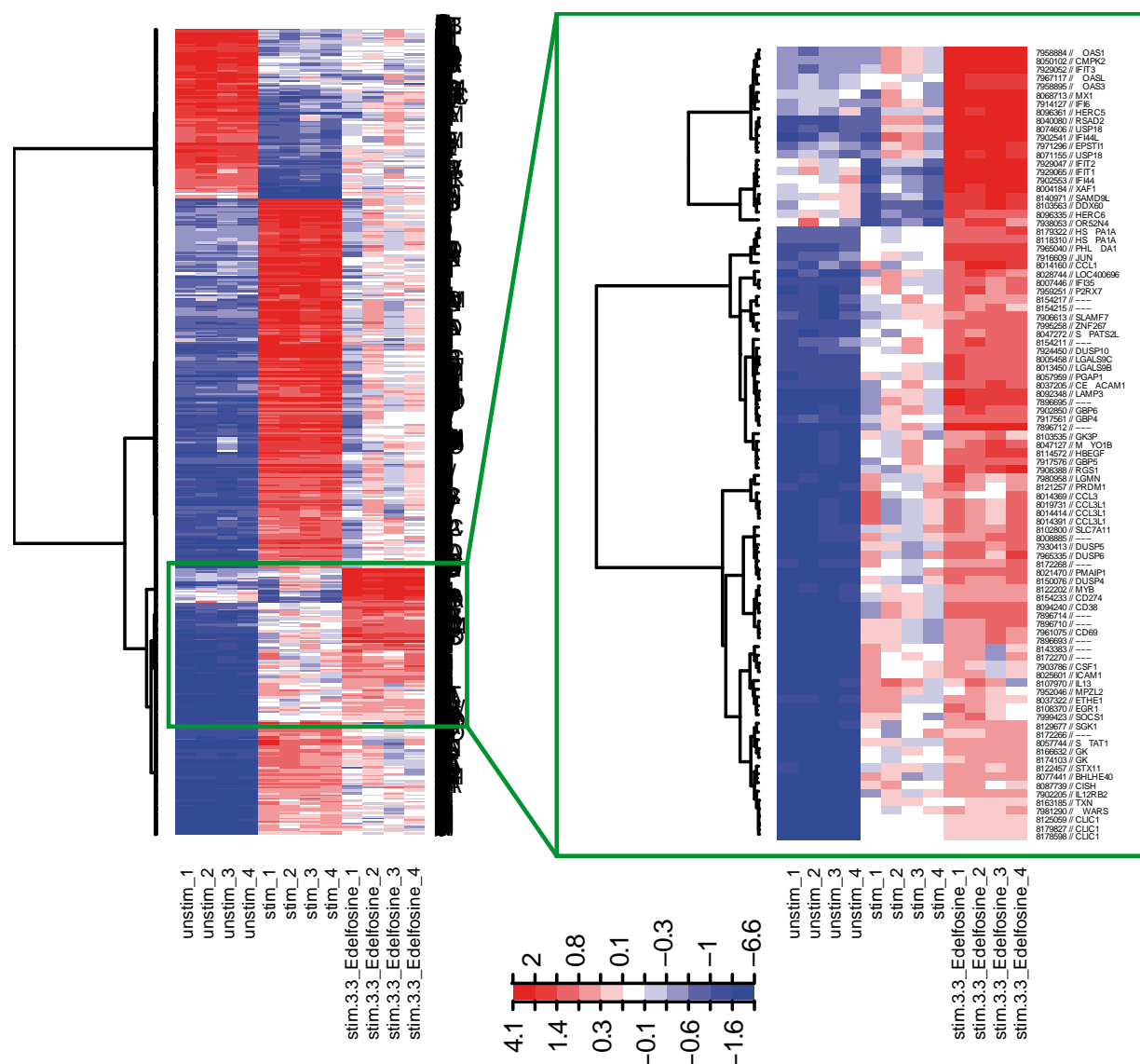


Figure 21. Modulation of gene expression in human CD4⁺ T cells mediated by stimulation and edelfosine addition. **(A)** The incubation of cells in absence of a stimulus resulted in an edelfosine concentration-dependent downregulation of antigen processing- and presentation-associated genes. **(B)** The activation of cells with beads coated with antibodies against CD2, CD3 and CD28 in presence of 3.3 µg/ml edelfosine resulted in a consistent upregulation of immune and virus response-associated genes. The values of differential gene-expression changes correspond to the SLR (red for upregulation, blue for downregulation). Genes are clustered hierarchically in the dendrogram over the expression matrix. The height of the branches is inversely proportional to the degree of neighborhood between clusters (images generated with R statistical platform 2.12, gplots package 2.8.0).

The constructed heatmap emphasized the consistent upregulation of immune and virus response-associated, type I interferon-related genes upon stimulation in presence of 3.3 µg/ml edelfosine. Provided that cells were incubated without edelfosine, the absence and presence of a stimulus for CD4⁺ T cells resulted in the clustering of immune- and virus-associated genes into two subgroups. These groups were either characterized by a subtle upregulation of genes if cells were stimulated or downregulation in case of stimulation. Despite these detected differences in gene expression between the two clusters, they could

not be discriminated by divergent induction: genes in both clusters are interferon-inducible. Regardless of this clustering of genes in the absence of edelfosine, the addition of 3.3 µg/ml edelfosine induced a consistent and profound upregulation of expression of these genes.

4.4.4 Edelfosine-induced downmodulation of MHC class II-surface expression of B-cell subsets

The RNA microarray of CD4⁺ T cells revealed that under non-stimulating conditions in presence of edelfosine, cells downregulated the expression of genes associated with MHC class II antigen presentation. Therefore, HLA-DR/DP/DQ expression in CD4⁺ and CD8⁺ T cells and additionally in B cells as classical APCs was investigated. The knowledge of MHC class II expression on human CD4⁺ T cells is rather limited, and the impact of edelfosine may shed new light on this aspect for the function of CD4⁺ T cells. After PBMC isolation from three donors cells were incubated for 24 h without edelfosine, in presence of 3.3 µg/ml edelfosine and with 10 µg/ml edelfosine, respectively. The median fluorescence intensities (MedFIs) for HLA-DR/DP/DQ expression on B-cell subsets and T-cell subsets were determined by flow cytometry. After excluding dead cells CD19⁺ B cells were selected. CD19 is expressed on B cells during all stages of development, but expression is lost on the surface of terminally differentiated plasma cells. The further subdivision by the surface markers IgD and CD27, a tumor necrosis factor receptor family member, allowed to define the impact of edelfosine on MHC class II expression of distinct B-cell populations. Adult peripheral blood B lymphocytes can be divided by these markers into discrete subsets: IgD⁺ CD27⁻, IgD⁺ CD27⁺ and IgD⁻ CD27⁺ B cells. Whereas IgD⁺ CD27⁺ B cells produce mainly IgM, IgD⁻ CD27⁺ B cells produce IgG, IgM and IgA. The function of CD27 in B cells is the interaction with CD70 to promote the differentiation of CD27⁺ memory B cells towards plasma cells (316, 317). CD27 is not expressed on naïve B cells. Surface IgD is expressed on the surface of mature B cells. With regard to CD19⁺ B cells en bloc, but also for IgD⁺ CD27⁻ and IgD⁺ CD27⁺ B-cell subsets the culture of PBMCs with 3.3 µg/ml edelfosine and 10 µg/ml edelfosine resulted in a concentration-dependent downregulation of HLA-DR/DP/DQ expression on the cell surface (Figure 22). In comparison the expression levels appeared to be rather low on IgD⁻ CD27⁺ B cells. In the latter population no differences in HLA-DR/DP/DQ expression levels were found. Since edelfosine was initially found to affect MHC class II-related genes in CD4⁺ T cells flow cytometry was also used to assess the impact of 3.3 µg/ml edelfosine and 10 µg/ml edelfosine on HLA-DR/DP/DQ expression on the surface of T cells. After PBMC isolation followed by incubation for 24 h, cells were stained with antibodies to gate on CD4⁺ and CD8⁺ T cells preceded by the exclusion of dead cells. Antibodies directed against CD27 and CD45RA were included. In detail, CD27 is expressed by naïve as well as memory T cells.

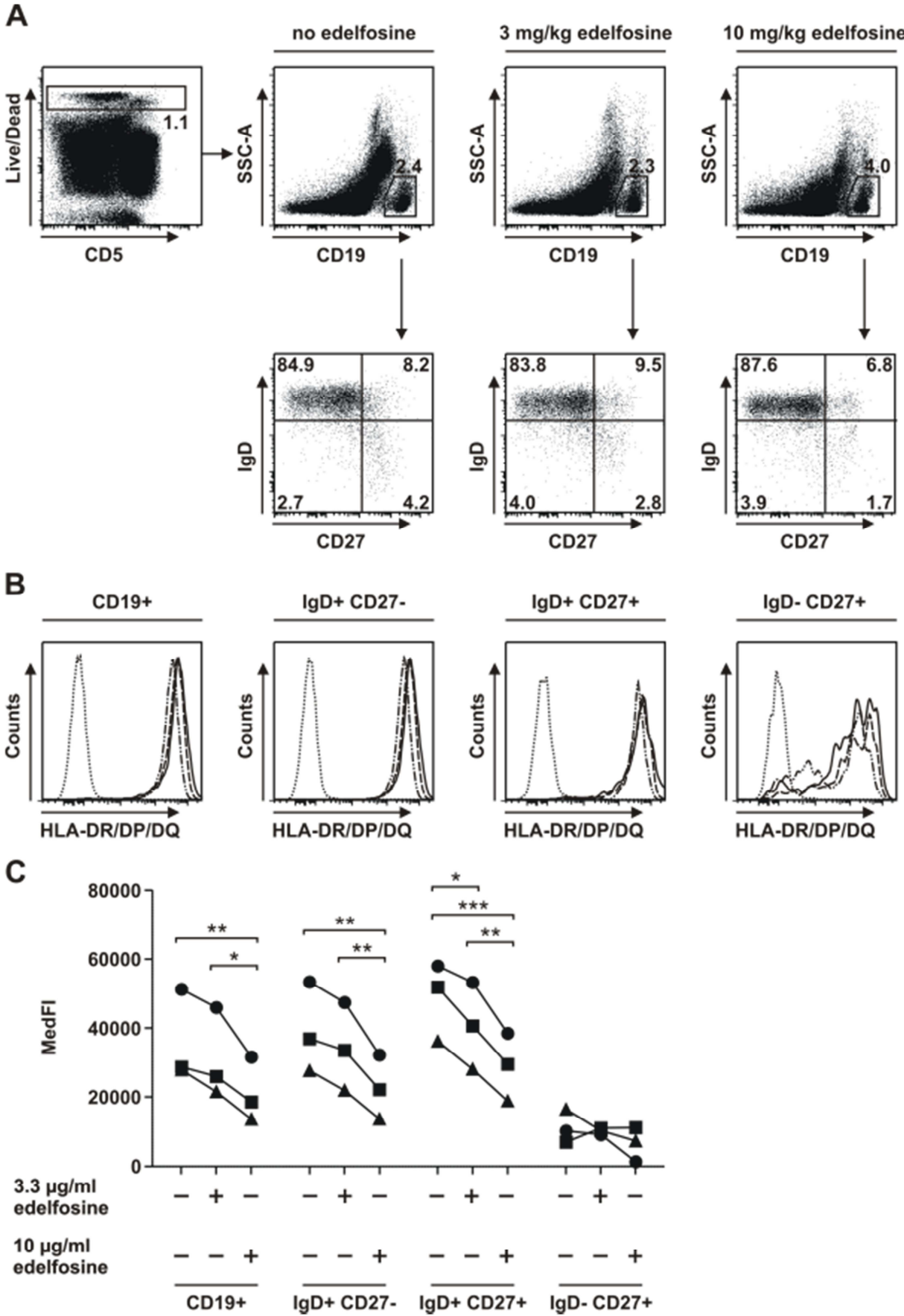


Figure 22. Edelfosine-mediated downmodulation of HLA-DR/DP/DQ expression on human B cells. **(A)** Gating strategy to identify viable CD19+ B cells and their IgD+ CD27-, IGD+ CD27+ and IgD- CD27+ subsets after the incubation of PBMCs for 24 h in the absence of edelfosine or in the presence of 3.3 µg/ml and 10 µg/ml

edelfosine, respectively. **(B)** Histograms display the edelfosine-induced downmodulation of HLA-DR/DP/DQ on the previously described B-cell subsets in comparison to the respective unstained control approach (— no edelfosine, ---- 3.3 µg/ml edelfosine, -·-·-· 10 µg/ml edelfosine, ····· isotype control). **(C)** Summary of MedFl values determined for each treatment within each B-cell subset (n=3 donors, + edelfosine added as indicated, - no edelfosine added). For CD19+, IgD+ CD27- and IgD+ CD27+ populations significant reductions of HLA-DR/DP/DQ expression were observed (*P<0.05, **P<0.01 after post-hoc analysis).

CD45RA, a transmembrane tyrosine phosphatase also known as the 220 kDa isoform of the leukocyte common antigen (LCA), is expressed on naïve CD4+ and CD8+ T cells. The MedFls for HLA-DR/DP/DQ expression on naïve and memory CD4+ and CD8+ T cells were determined. Although an edelfosine-induced downmodulation of HLA-DR/DP/DQ expression could not be proven on CD4+ and CD8+ T cells, at least memory T cells, which showed an approximately 2-fold higher HLA-DR/DP/DQ expression compared to naïve T cells, pointed to a comparable tendency as found in B cells (Figure 23). Potentially, the very low expression levels of HLA-DR/DP/DQ interfered with the detection of the edelfosine-treatment effect in T cells. More importantly, in the case of B cells as classical HLA-DR/DP/DQ-expressing antigen-presenting cells the impact of edelfosine on MHC class II expression previously identified by whole genome expression analysis was verified.

4.4.5 Edelfosine reduces IFN-γ secretion of stimulated CD4+ T cells

The whole genome expression analysis of CD4+ T cells activated with stimulatory beads coated with antibodies against CD2, CD3 and CD28 in presence of 3.3 µg/ml edelfosine indicated the upregulation of genes with close association to immune response and response to virus. Table 22 B summarizes upregulated genes that are assignable to type I interferon-mediated signaling pathways. To exclude that the upregulation of type I interferon-associated genes in stimulated, edelfosine-treated CD4+ T cells reported from the gene-expression analysis was due to the presence of IFN-α or -β in the cell-culture medium, cell-culture supernatants were analyzed by ELISA to determine the concentrations of IFN-α and IFN-β, but also IFN-γ. In the case of detection of type I interferons T cells themselves or accidentally transferred pDCs may be the potential producers of these cytokines and may explain the observed gene induction. Interestingly, IFN-α as well as IFN-β were virtually undetectable by ELISA in supernatants of stimulated CD4+ T cells after 30 h of incubation in both absence or presence of 3.3 µg/ml edelfosine. Instead, supernatants of cells cultured without edelfosine contained $3,606.09 \pm 525.12$ pg/ml IFN-γ (Figure 24 A). Interestingly, the presence of 3.3 µg/ml edelfosine allowed the detection of only 940.78 ± 81.23 pg/ml IFN-γ which is equivalent to a -3.83-fold reduction. The downmodulation of IFN-γ was verified by using the flow cytometry-based human Th1/Th2/Th9/Th17/Th22 13plex Kit FlowCytomix (Figure 24 B). The presence of 3.3 µg/ml edelfosine led to an IFN-γ-reduction from $1,462.76 \pm 282.26$ pg/ml to 552.93 ± 86.61 pg/ml (-2.65-fold less). Moreover, the Th1-related cytokines IL-2 and TNF-α were also reduced if incubated with 3.3 µg/ml edelfosine in comparison to their respective

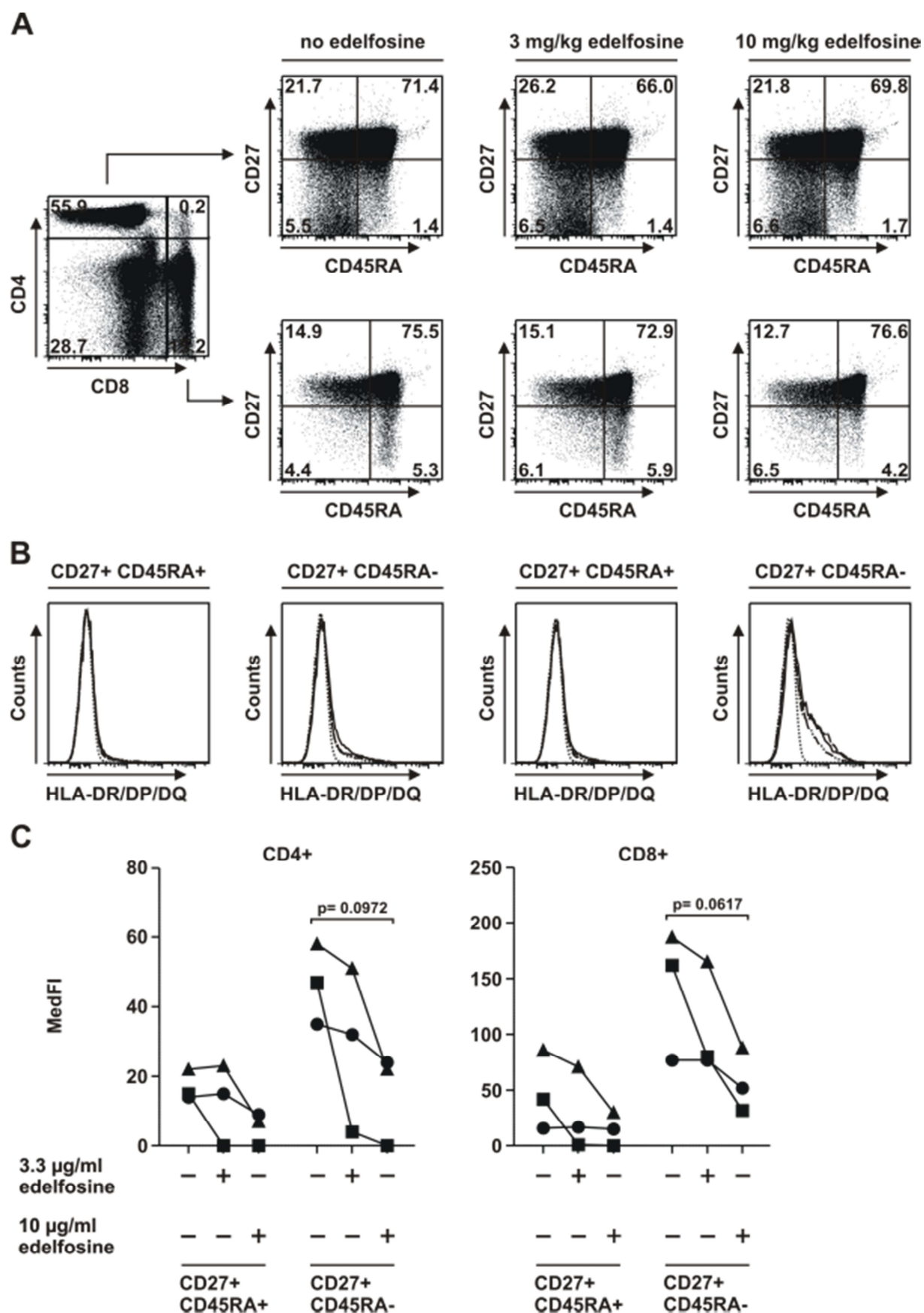


Figure 23. Edelfosine impact on HLA-DR/DP/DQ expression on human T cells. **(A)** Gating strategy to identify viable CD4+ and CD8+ T cells and their naïve (CD27+ CD45RA+) and memory (CD27+ CD45RA-) subsets after the incubation of PBMCs for 24 h in the absence of edelfosine or in the presence of 3.3 µg/ml and 10 µg/ml edelfosine, respectively. **(B)** Histograms display the considerably low expression of HLA-DR/DP/DQ on the

previously described T-cell subsets in comparison to the respective unstained control approach (— no edelfosine, ---- 3.3 µg/ml edelfosine, - - - - 10 µg/ml edelfosine, isotype control). **(C)** Summary of MedFl values determined for each treatment within each T-cell subset (n=3 donors, + edelfosine added as indicated, - no edelfosine added). For CD27+ CD45RA+ and CD27+ CD45RA- populations of CD4+ and CD8+ T cells no significant reduction of HLA-DR/DP/DQ expression was observed after post-hoc analysis (depicted P-value: as determined by repeated measures ANOVA).

control approaches in absence of edelfosine. Concentrations of IL-2 were reduced to $3,632.17 \pm 355.19$ pg/ml compared to 8015.25 ± 624.31 pg/ml. Concentrations of TNF-α were reduced to $1,993.94 \pm 349.69$ pg/ml compared to $4,332.94 \pm 853.58$ pg/ml.

With regard to the secretion of Th17-associated cytokines, IL-17A, IL-22 as well as IL-6 revealed an edelfosine-dependent downregulation. The concentration of IL-17A was 282.88 ± 50.76 pg/ml in absence of edelfosine compared to 243.92 ± 41.13 pg/ml in presence of 3.3 µg/ml edelfosine. In case of IL-22, $3,038.11 \pm 470.69$ pg/ml (no edelfosine) and $1,507.88 \pm 205.23$ pg/ml (3.3 µg/ml edelfosine) were found. Concentrations of IL-6 were 315.44 ± 78.44 pg/ml (no edelfosine) and 41.28 ± 9.99 pg/ml (3.3 µg/ml edelfosine).

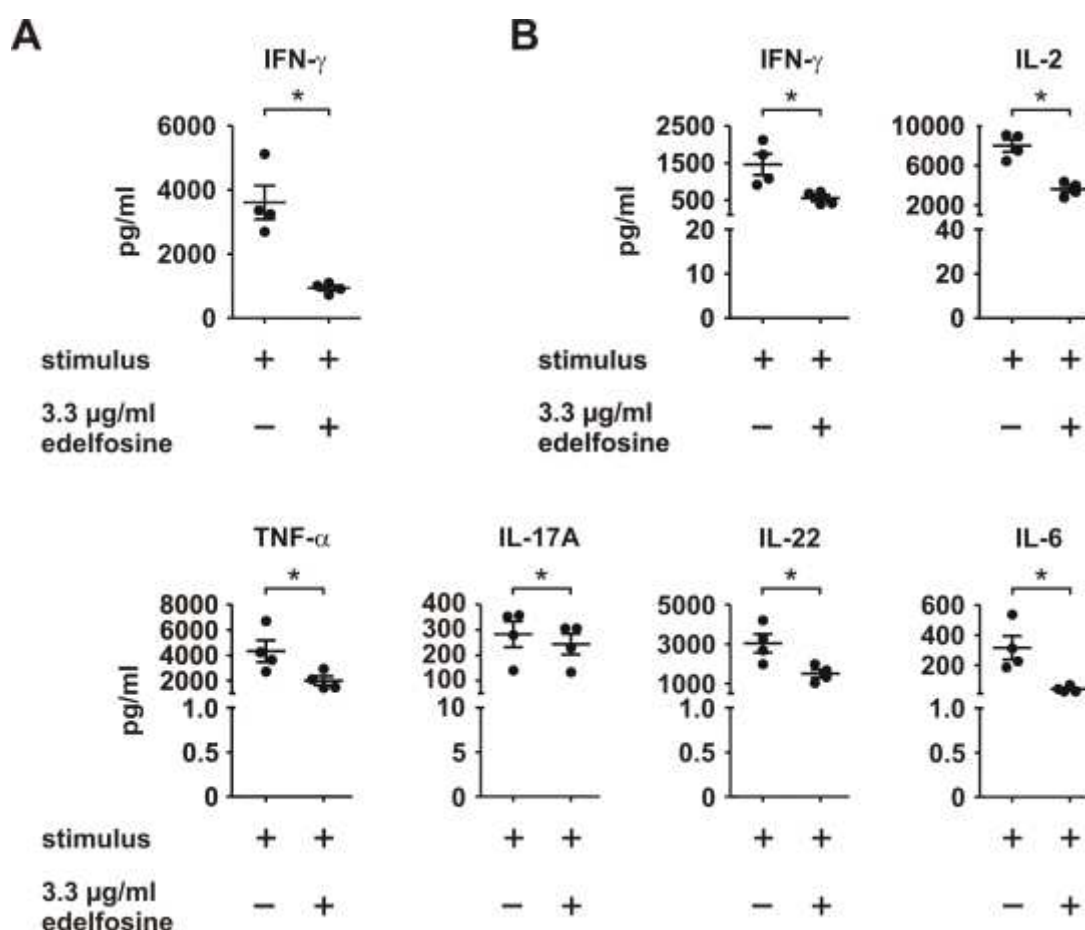


Figure 24. Cytokine secretion was modulated in activated CD4+ T cells by edelfosine. **(A)** A significant reduction of IFN-γ-secretion was monitored upon edelfosine treatment. **(B)** This result was confirmed by a human 13plex kit which allowed the detection of not only reduced concentrations of IFN-γ in supernatants of edelfosine-treated cells, but also reduced concentrations of the Th1-associated cytokines IL-2 and TNF-α as well as the Th17-associated cytokines IL-17A, IL-22 and IL-6. Cells of 4 individuals were used, error bars indicate SEM of respective means (*P<0.05, **P<0.01 after post-hoc analysis).

5 Discussion

In 1979 Andreessen *et al.* already reported that edelfosine selectively induced cell death in mitogen-activated human peripheral blood lymphocytes (PBLs) *in vitro*, whereas the viability of resting PBLs was not impaired (318). The demonstration of these immunomodulatory properties led to further investigation of edelfosine and its applicability as a treatment in autoimmune diseases, for instance MS. In a pilot study MS patients at different disease stages were treated with edelfosine, and improved clinical symptoms were reported (303). Due to these immunomodulatory as well as the antitumoral activities ALPs were already used in 1992 in a phase I trial to treat two patients that suffered from both cancer and MS (304). Not only was a tumor response detected, but also neurological symptoms were improved. These exploratory clinical investigations were accompanied by a series of descriptive EAE studies, mostly with rats, but also with mice (304, 319–321). The above studies lack functional investigations to detect edelfosine-induced modifications of cellular responses to treatment. In 1999, Cabaner *et al.* pursued mechanistic research of immunomodulation by edelfosine (312). Their findings implied that apoptosis induction might not only be the mechanism leading to the drug's antitumor activity, but might also account for its immunomodulatory capacity. The data obtained within the present study shows that edelfosine not only interferes with T-cell proliferation *in vitro* by modulating distinct biological processes, but demonstrates further that edelfosine induces apoptosis in T cells of EAE-induced mice with ameliorated clinical disease outcome, and has additional, entirely unexpected effects.

Influence of edelfosine on murine T-cell proliferation

By labeling cells prepared from lymph nodes of C57BL/6 mice with CFSE, the proliferation of anti-CD3 antibody-stimulated CD4+ and CD8+ T cells was found to be inhibited by edelfosine in a concentration-dependent manner (Figure 3). With increasing concentrations of edelfosine not only the gated events, but also progenitor numbers were redistributed towards lower generation numbers. With regard to both T-cell subsets 1 µg/ml edelfosine only induced subtle reductions of T-cell proliferation whereas 5 µg/ml edelfosine potently interfered with proliferation. SJL mice-derived lymph node cells were used not only to prove edelfosine's dose-dependent effects on T-cell proliferation, but also to more precisely define the inhibitory effects of edelfosine within the concentration range between 1 µg/ml and 5 µg/ml (Figure 3). 1 µg/ml and 3 µg/ml edelfosine inhibited proliferation with only minor differences. Both concentrations induced a more than twofold increase in frequencies of non-proliferating cells compared to frequencies of cells cultured in absence of edelfosine.

10 µg/ml edelfosine induced an almost complete block of proliferation of CD4⁺ and CD8⁺ T cells. Moreover, with regard to progenitor frequencies of CD4⁺ and CD8⁺ T cells from SJL mice, a dose-dependent decrease of cells, which have left generation 0 and proliferated, was identified.

In summary, the results point to an edelfosine concentration-dependent inhibition of C57BL/6- or SJL-derived CD4⁺ and CD8⁺ T-cell proliferation. Moreover, a concentration of 10 µg/ml edelfosine prohibited a cellular proliferative response. Concentrations of 3 µg/ml and 5 µg/ml edelfosine were effective in impairing proliferation. To sum up the results for both T-cell subsets from the two mouse strains, 1 µg/ml edelfosine-mediated interference with T-cell proliferation appeared to be only comparably low, especially in C57BL/6 mouse-derived CD4⁺ T cells. These results are in accordance with earlier reports. The IL-2-dependent propagation of MBP-specific T-cell lines (TCLs) generated from lymph node cells of immunized Lewis rats was found to be suppressed in a dose-dependent manner by edelfosine (304). A dose of 5 µg/ml or higher resulted in an almost complete inhibition of T-cell proliferation. This effect was not seen with other phospholipids tested (natural 2-lysophosphatidylcholine, PAF and 1-octadecyl-2-glycero-3-phosphocholine). Upon restimulation of T cells using MBP or Con A the proliferation of T cells appeared to be inhibited at 10 µg/ml edelfosine. Additionally, edelfosine was identified to induce dose- and time-dependent apoptosis in human mitogen-activated T cells isolated from peripheral blood while sparing resting T cells (312). This apoptotic response was found to be even more profound in human leukemic TCLs. Notably, in these studies edelfosine was used at 10 µM, i.e. approximately 5.24 µg/ml. Compared to CD4⁺ T cells, CD8⁺ T cells of both mouse models displayed accelerated clonal expansion following contact with antigen, a functional difference that has been reported also in the context of anti-viral immune responses (322). In general, the speed and nature of a T-cell response is not only dependent on antigen concentration and the duration of antigen exposure, but also on the context of antigen recognition by T cells. Interactions between co-stimulatory molecules on APCs and their ligands expressed on the surface of T cells, for instance CD80:CD28, influence the level of T-cell activation (323, 324). Different requirements identified for co-stimulatory molecules in CD4⁺ and CD8⁺ T-cell responses point to distinct mechanisms to activate these cells (325). Furthermore, these findings indicate that different thresholds or activation requirements exist to develop effector CD4⁺ and CD8⁺ T cells (326, 327). One contributing factor might be the almost ubiquitous cellular MHC class I expression, whereas MHC class II molecules are expressed only on limited cell subsets (328).

Amelioration of EAE-disease course by edelfosine treatment

In 1992, the first reports on edelfosine-treatment effects in EAE, the experimental model for MS, were published. Klein-Franke and Munder induced EAE in female Lewis rats by injecting MBP from guinea pig CNS tissue (304). For immunization MBP was dissolved in PBS and emulsified in mineral oil supplemented with *M. tuberculosis* H37Ra. For daily treatment, edelfosine was dissolved in full fat milk and administered using an intragastric cannula. Rats received edelfosine doses of between 0.5 mg and 10 mg, which corresponded to 3 to 60 mg/kg. Doses of 3 mg/kg up to 15 mg/kg edelfosine per day reduced clinical symptoms and duration of disease without any side effects irrespective of initiation of treatment (day 0 and day 5 were compared). Higher doses were reported to suppress EAE symptoms but they were accompanied by severe side effects (dehydration, apathy, cachexia and high mortality). Therapy after EAE onset was found not to influence the disease course. In summary, 2.5 mg edelfosine (corresponding to circa 15 mg/kg) elicited a significant treatment effect, but a dose-dependency could not be established. In the same year, data on the effectiveness of a cyclic ether analogue of edelfosine, SRI 62-834, in the treatment of EAE in Lewis rats were published (319). For the induction of CR-EAE rats were immunized with total guinea pig spinal-cord tissue (209). The drug was dissolved in 20% ethanol and mixed with milk before administration for 16 days to immunized rats starting at day 15, the beginning of spontaneous remission. SRI 62-834 was given daily at 25 mg/kg by gavage. Half of the animals were found to be fully protected from relapse and mice with relapse showed only mild symptoms compared to controls. Interestingly, after cessation of treatment no rat exhibited a relapse pointing to a curative potential of SRI 62-834. These studies were extended in 1995 by using CR-EAE in immunized Lewis rats to study the therapeutic treatment with SRI 62-834 in comparison to edelfosine (320). Treatment started at day 16 after immunization and was commenced daily until day 31. Edelfosine, SRI 62-834 (racemate) and its R-(+)-enantiomer MLS 266-337 were dissolved in 5% ethanol, water and milk for oral application by gavage at 25 mg/kg. Whereas cyclosporine, for instance, only delayed disease relapse until discontinuation of treatment, all three lysolecithin derivatives tested (edelfosine, SRI 62-834, MLS 266-337) suppressed the manifestation of further relapses with curative effects upon treatment cessation. Regarding the examination of edelfosine by EAE in mice, Baker *et al.* have used Biozzi AB/H mice to induce chronic-relapsing EAE with autologous spinal cord homogenate (321). Mice were treated with 10 mg/kg or 50 mg/kg edelfosine dissolved in milk beginning on the day immunization (day 0). The treatment with 10 mg/kg edelfosine was found to delay EAE onset and to reduce clinical severity. Instead, 50 mg/kg edelfosine completely inhibited EAE onset and weight loss of the animals. 90% of mice treated with 25 mg/kg edelfosine did not develop EAE. Also when application was started prior to disease onset (day 9) or at EAE acute phase (day 12),

the treatment of mice with 50 mg/kg edelfosine led to reduced clinical scores compared to controls. The effect of edelfosine on the EAE relapse was additionally studied. Administration was started at day 27 (post-acute remission) and led to a reduction of incidences of relapsing disease (from 56% and 61% in controls to 33%, respectively). Significance in reduction of relapse incidences was only reached when applying 75 mg/kg edelfosine. Interestingly, in contrast to the first disease bout, no differences in relapse onset and severity of EAE were monitored during comparison of edelfosine-treated to control mice. Of note, the authors did not report any treatment-related side effects despite the comparably high edelfosine doses administered in some experiments. Based on these elementary findings the following EAE experiments were designed to refine and to characterize the treatment outcome of edelfosine in EAE-induced mice. In a first EAE experiment in MOG₍₃₅₋₅₅₎-immunized C57BL/6 mice the preventive treatment effect of 25 mg/kg, 15 mg/kg and 10 mg/kg edelfosine was examined (Figure 4 A). 10 mg/kg edelfosine was identified to be effective in ameliorating chronic-progressive EAE without causing any side effects after oral administration. Reduced EAE scores were also seen for the treatments with higher edelfosine concentrations. However, in contrast to previously reported EAE experiments in Lewis rats and in Biozzi AB/H mice, C57BL/6 mice revealed edelfosine-related side effects when receiving 15 mg/kg edelfosine or higher (tremor, inactivity, slowed motion). Additionally, EAE incidences were reduced upon edelfosine treatment (25 mg/kg: 2 (5), 15 mg/kg: 2 (5), 10 mg/kg: 3 (5)) compared to controls (PBS-treated mice: 3 (4)) reflecting an observation that has been also described in Biozzi AB/H mice. In accordance with previous EAE trials in Biozzi AB/H mice, 10 mg/kg edelfosine treatment resulted in a delayed onset of EAE. The beneficial effect of 10 mg/kg edelfosine was subsequently validated in EAE-induced SJL mice, which developed a relapsing-remitting clinical disease course after immunization with PLP₍₁₃₉₋₁₅₁₎. To evaluate the relative efficacy of 10 mg/kg edelfosine the following trials comprised also a cohort of 1 mg/kg edelfosine-treated mice. As experiments by Klein-Franke and Munder pointed to the effectiveness of treatment initiation from day 5 after immunization, EAE-induced SJL mice received 1 mg/kg or 10 mg/kg edelfosine from day 5. Additionally, dose rates were limited by edelfosine treatment only every other day in order to further reduce the risk of side effects. Clinical scores of 10 mg/kg edelfosine-treated mice pointed to an ameliorated disease course, a treatment-dependent delay of EAE onset and reduced cumulative disease scores compared to PBS-treated controls, but results were not significant (Figure 4 B). In 2003, Bhamra *et al.* presented data on pharmacokinetics and tissue distribution of a liposomal formulation of the edelfosine L-isomer (TLC ELL-12) in female Buffalo rats (329). Various tissues and blood samples were analyzed for L-edelfosine by high-performance liquid chromatography (HPLC) after administration of 12.5 mg/kg TLC ELL-12 by i.v. injection. A rapid distribution and uptake of the drug into the tissues was found as the time to reach highest concentrations

was 0.25 to 8 h in all organs examined except ovaries and uterus ($T_{\max}=24$ h). Interestingly, half-lives were determined to be 13.1 h in the blood as well as 14 h in spleens. Furthermore, Kötting *et al.* have demonstrated that circa 96% of edelfosine was absorbed in the first 24 hours after oral treatment of rats (330). After application of 10 mg/kg edelfosine to BALB/c mice, concentrations in blood plasma were found to decrease from 50.7 ± 28.1 $\mu\text{g/ml}$ to 2.5 ± 1.3 $\mu\text{g/ml}$ 24 h after i.v. injection and the half-life of elimination was 22.29 ± 14.02 h (331). Moreover, no saturation of the edelfosine-elimination process was detected with concentrations between 5 and 30 mg/kg after i.v. administration. These data indicate that edelfosine given every 48 h may not be suitable for maintaining a local concentration necessary to interfere with the priming of autoreactive immune cells in EAE and that intervals need to be reduced to antagonize clearance of edelfosine from peripheral lymphoid organs. Consequently, in the present study EAE-induced mice received 1 mg/kg or 10 mg/kg edelfosine on a daily basis from the day of immunization (day 0). A significant treatment effect with differences between PBS- and 10 mg/kg edelfosine-treated groups during acute disease phases emphasized the effectiveness of this dose in ameliorating EAE in a preventive setting (Figure 4 C). Daily treatment was adequate, probably by sustaining edelfosine concentrations in peripheral lymphoid organs which were effective to interfere with immune cell functions. Interestingly, in these *in vivo* EAE experiments an effective edelfosine-concentration range was identified that can be used to deviate a theoretically effective *in vitro* dose. Equivalence with applied edelfosine concentrations in *in vitro* experiments, for instance the introductory CFSE assays, would underline the *in vivo* relevance of the chosen *in vitro* concentrations of edelfosine. According to Bhamra *et al.* 12.5 $\mu\text{g/kg}$ edelfosine, formulated as TLC ELL-12, injected i.v. into Buffalo rats resulted in maximally 153.9 $\mu\text{g/ml}$ edelfosine after 8 h in spleens of treated rats (329). Theoretically, 10 mg/kg would result in 123,12 $\mu\text{g/ml}$ edelfosine. Taking into account the absolute number of splenocytes isolated from a SJL mouse (circa $3\text{-}10 \times 10^7$ cells) and the maximally possible cell number per 96-well in *in vitro* trials (2×10^5 cells) the inferred effective edelfosine concentration is 0.82 to 0.25 $\mu\text{g/ml}$ edelfosine. This order of magnitude is similar to the concentrations investigated in the already discussed CFSE-assay experiments, but also the edelfosine concentrations effective in inhibiting human T-cell proliferation (discussed later). Using this theoretical approach provides another interesting piece of information. On the basis of the rat data, 1 mg/kg edelfosine treatment would result in 12.31 $\mu\text{g/ml}$ edelfosine in the spleen. Considering the number of splenocytes of SJL mice the local concentration would be 0.41 to 0.12 $\mu\text{g/ml}$ edelfosine/ 1×10^6 splenocytes. Munder and Modolell reported that the incubation of spleen-derived macrophages with PC (lysolecithin) at low concentrations (2.5 $\mu\text{g/ml}$ and 1.0 $\mu\text{g/ml}$ PC per 1×10^7 cells, equivalent to 0.25 to 0.1 $\mu\text{g/ml}$ PC per 1×10^6 cells) *in vitro* increased the immune response/number of plaque-forming cells (238). This

observation of immune activation at low PC/edelfosine concentrations will be recurrently referred to in the course of the discussion.

In the present study the characterization of edelfosine has been conducted primarily in SJL mice. This model of RR-EAE allowed to study the impact of edelfosine treatment on the course of EAE during the first disease bout, but also during further remissions and relapses. In the subsequent EAE trial the therapeutic effect of edelfosine was tested. The administration was started during the clinical onset of EAE. In view of the human situation, MS is present in affected patients in two major forms. Whereas the primary-progressive disease course affects 10-15% of patients, 85-90% of individuals suffer from relapsing-remitting MS. Based on the clinical situation, in which a RR-MS patient is requesting medical advice when experiencing a disease bout, the subsequent EAE experiment was designed to investigate the therapeutic effect of edelfosine treatment.

Mice were treated daily with PBS, 1 mg/kg or 10 mg/kg edelfosine as soon as they manifested clinical symptoms. PBS-treated mice in the control group showed the characteristic RR-EAE disease course (Figure 4 D). Treatment with edelfosine appeared to reduce clinical severity in a dose-dependent manner during the first disease bout. During the course of the subsequent remission phase and first relapse, mean EAE scores of 1 mg/kg and 10 mg/kg edelfosine-treated mice appeared to be almost identical. The fact that no significant treatment effect and no differences between groups were detectable may be assigned to small sample sizes per treatment group as a result of comparably low EAE incidences (PBS-treated mice: 6 (8), 1 mg/kg edelfosine: 5 (8), 10 mg/kg edelfosine: 7 (8)) and concomitant drop-outs of mice that presented with EAE scores of 4 or mice that developed an irregular disease course. Here, 3 (3) PBS-treated mice experienced a relapse, whereas 10 mg/kg edelfosine-treated mice developed an EAE-relapse incidence of 3 (7) which equates to 57.14% of mice without disease progression upon treatment. In comparison, in Biozzi AB/H mice the initiation of oral treatment in the remission phase with 50 mg/kg edelfosine was reported to lead to absence of clinical disease in 66% of mice (321).

To sum up, results implied that edelfosine interfered with relapsing EAE in SJL mice. Significant differences between preventive PBS and 10 mg/kg edelfosine treatment were observed during the acute disease phases (a significant treatment effect with significant differences between PBS-treated and 10 mg/kg edelfosine-treated groups is also detectable by 2-way ANOVA after Bonferroni post-hoc analysis for the therapeutic treatment setting when EAE scores are analyzed until day 20). These results suggest that the major effect of edelfosine is not only the modulation of T-cell priming for EAE induction but also the induction of relapses. In the SJL mouse model EAE is actively induced by the injection of PLP₍₁₃₉₋₁₅₁₎, which is presented to and recognized by antigen-specific autoreactive T cells.

These cells migrate into the CNS to induce autoimmune inflammation in concert with other leukocyte subsets leading to demyelination of axons, neuronal damage and the induction of clinical symptoms. Subsequently after remission relapses occur due to intermolecular epitope spreading. This process is very well characterized in immunized SJL mice by the priming of T cells specific for PLP₍₁₇₈₋₁₉₁₎ (primary relapse) and MBP₍₈₄₋₁₀₄₎ (secondary relapse) (332, 333). These repeated priming processes may constitute ideal phases for intervention by edelfosine application.

Edelfosine treatment of EAE-induced SJL mice modulates caspase-3 activation of peripheral lymphocytes without constraining their proliferative capacity

MS but also EAE, as autoimmune inflammatory diseases, are mediated by brain-specific encephalitogenic T cells. Their progenitor T cells constitute normal, inconspicuous parts of the immune system. Upon activation by specific antigen, superantigens or crossreaction to microbial antigens autoreactive T cells are activated and become pathogenic. Their progeny migrate into the CNS after crossing the disrupted BBB, followed by the initiation of the disease (86, 87, 334, 335). Seminal studies in EAE have provided insights into this homing process by adoptive transfer of T cells specific for myelin constituents (88, 336, 337). By transferring GFP-expressing MBP-specific, *ex vivo* activated T cells from Lewis rats into naïve recipients the migratory pathways for encephalitogenic T cells have been shown (113). After transfer T cells were detected in parathymic lymph nodes (12-36 h), followed by emigration into the blood (60 h) and subsequently into the spleen. Only few transferred T cells were found in peripheral lymph nodes at this disease phase. T cells migrated into the CNS (60-80 h) whereas T cells in the spleen were depleted. With regard to actively immunized SJL mice injected with PLP₍₁₃₉₋₁₅₁₎, disease onset was seen much later (day 9-12) compared to adoptive transfer-based EAE with MBP-specific T cells (day 3-5 in the Lewis rat model (113), around day 7 in the SJL model (88)). As the daily preventive edelfosine treatment appeared to ameliorate clinical signs of EAE day 9 after immunization was chosen to determine treatment effects on encephalitogenic T-cell priming in secondary lymphoid tissues (spleen, lymph nodes). 2-lysophosphatidylcholine and its synthetic analogs were initially described to enhance the phagocytic activity of macrophages (235–237). Therefore they were assigned an immunomodulatory role in defense mechanisms of the immune system. Based on these prior data the investigation of edelfosine-treatment effects was not limited to T cells but extended to other constituents of the adaptive (B cells) and innate immune system (macrophages, neutrophils, mDCs, pDCs, NK cells). In addition, preventive treatment was used to elucidate the effect of edelfosine on CNS-infiltrating cells both of the adaptive and the innate immune system (discussed later).

Independent of the treatment with PBS, 1 mg/kg edelfosine or 10 mg/kg edelfosine, no differences in absolute cell numbers of spleens and lymph nodes were detectable (Table 3) indicating that edelfosine does not lead to major perturbations or loss of peripheral immune cells. Edelfosine does not act by eradicating total cell numbers in secondary lymphoid organs that are indispensable for priming and triggering antigen-specific immunity. Furthermore, the comparison of leukocyte subsets from spleens and lymph nodes also showed that edelfosine did not induce frequency changes relative to PBS controls (Table 4-10). Frequencies of Th-cell subsets (CD4+ T cells, CD8+ T cells) were not changed in either organ (Table 11). Interestingly, in lymph nodes of mice treated with 10 mg/kg edelfosine relative frequencies of naïve CD4+ T cells related to all CD4+ T cells were increased compared to controls, possibly reflecting an edelfosine-mediated interference with T-cell priming by APCs (Figure 8). Upon priming T cells are activated and develop from naïve to effector T cells. Changes in frequencies of activated T cells due to edelfosine treatment were analyzed by CD69, a marker for early cellular activation, and CD25, a general activation marker. Moreover, CD25 expression is considered a marker of CD4+ Foxp3+ nTregs. Despite the determination of increased naïve CD4+ T-cell frequencies in lymph nodes of 10 mg/kg edelfosine-treated mice, no changes were observed for frequencies of activated T cells (Figure 9). The data pointed at a trend that was also found in the case of frequency comparisons of other, notably CNS-infiltrating cell types: the treatment of mice with 1 mg/kg edelfosine was frequently seen to increase the frequencies of various cell types. Here, previous descriptions implied that small amounts of edelfosine enhanced the phagocytic activity of peritoneal macrophages *in vivo* and *in vitro* (235, 238), an effect of immunological activation that may also be considered for other cell types, e.g. T cells, and will be discussed at a later point. Importantly, the treatment with edelfosine did not induce the ablation of nTregs from peripheral lymphoid organs (Figure 9). Tregs are thought to be involved in preventing the development of autoimmune diseases since changes in number and function were identified in MS (338, 339) and EAE (340–342). The activation of the immune system needs to be regulated by distinct mechanisms in order to ensure tolerance to autoantigens. Among other mechanisms like AICD and apoptosis of immature self-reactive lymphocytes, Tregs were identified as important, active mediators of peripheral tolerance that control effector T cells (343). This immune tolerance is mediated by natural CD4+ CD25+ Foxp3+ nTregs originating from the thymus (47). However, also peripheral naïve CD4+ and CD8+ T cells were described to differentiate into IL-10 and/or TGF- β -producing iTregs during activation in presence of specific cytokines (e.g. TGF- β) (344, 345). Tregs actively participate in peripheral immune homeostasis and restriction of tissue injury during inflammation in draining lymph nodes and the target organs. Thus, invariant nTreg frequencies after recurring edelfosine treatment did not point to adverse side effects on nTreg-mediated peripheral tolerance mechanisms.

Activation by specific antigens presented by APCs in the context of MHC class II leads to the differentiation of CD4⁺ T cells into functionally distinct effector subtypes, which possess specific cytokine phenotypes. Th1 cells produce IFN- γ , Th2 cells produce IL-4 and, as a third subset, Th17 cells are defined by their production of IL-17A (IL-17). Th1 cells have been shown to possess pathogenic potential (336, 346), but also Th17 cells were found to induce autoimmunity (347–349). Therefore, both effector subsets are of special interest in the context of EAE. No differences were found for Th1- and Th17-frequencies in spleens or lymph nodes of either 1 mg/kg or 10 mg/kg edelfosine-treated immunized mice compared to PBS controls (Table 12). Edelfosine was thus not found to interfere with the differentiation of CD4⁺ or CD8⁺ T cells into IFN- γ - or IL-17-producing subsets within peripheral lymphoid organs.

To confirm the proposed mechanism of apoptosis induction by edelfosine the frequencies of caspase-3-activated CD4⁺ and CD8⁺ T cells were evaluated. For the first time the *ex vivo* analysis of peripheral T cells from edelfosine-treated, EAE-induced mice demonstrated increased frequencies of apoptosis-prone T cells (Figure 10). Significant differences were found for CD4⁺ and CD8⁺ T cells from spleens of 10 mg/kg edelfosine-treated mice compared to PBS-treated mice. The effectiveness of this edelfosine dose was emphasized by the significant difference compared to the 1 mg/kg edelfosine treatment, but also by the consistency of frequencies from 1 mg/kg edelfosine-treated and PBS-treated mice. Elevated levels of apoptosis-induced T cells were also detected in CD4⁺ and CD8⁺ T cells derived from lymph nodes, although no significance could be shown. As mentioned before, EAE is considered as a CD4⁺ T cell-mediated autoimmune disease. Interestingly, the active immunization of C57BL/6 mice with MOG₍₃₅₋₅₅₎ was also reported to generate CD8⁺ $\alpha\beta$ TCR⁺ encephalitogenic T cells (350). The subsequent enrichment of MOG-specific CD8⁺ T cells from lymph nodes and spleens allowed the adoptive transfer of EAE into naïve C57BL/6 recipient mice. These findings imply that apoptosis induction in CD8⁺ T cells of EAE-induced mice may constitute an additional beneficial edelfosine-treatment effect.

Prior data indicated that edelfosine induces apoptosis in activated peripheral blood T cells after stimulation with mitogen but not in resting ones (312). In contrast to these *in vitro* experiments, the initial T-cell priming and activation in EAE-induced animals occurs by presentation of the disease-relevant PLP₍₁₃₉₋₁₅₁₎ peptide in the context of MHC class II. Probably, the role of these encephalitogenic T cells as early immigrants is to drive and to initiate tissue damage. In contrast, their relevance in the effector phase may only be secondary. The initial infiltration of the CNS by autoreactive T cells and their restimulation by resident APCs results in elevated proinflammatory cytokine (IFN- γ , IL-23, TNF- α) and chemokine (RANTES, IP-10, IL-8) levels (57). CNS-persistent microglia and astrocytes become activated and immune cells (neutrophils, monocytes, CD4⁺ and CD8⁺ T cells,

B cells) infiltrate into the CNS constituting a second, effector wave manifesting inflammatory CNS lesions and the onset of clinical deficit (334, 351). Notably, the populations of CD4+ as well as CD8+ T cells in general, but also CD69+ activated T cells, with activated caspase-3 were considerably low. Therefore, the observed increase in frequencies of apoptotic T cells upon 10 mg/kg edelfosine treatment may be sufficient to interfere with processes necessary to mediate full-blown EAE, like the effective priming, transmigration and reactivation of encephalitogenic, early invading T cells.

To further delineate the influence of daily edelfosine treatment on the functional properties of spleen and lymph node-derived T cells, cells were used in *ex vivo* restimulation experiments. The repetitive edelfosine treatment of mice was not found to interfere with the capacity of lymphocytes to proliferate and to respond to inflammatory cues independent of the stimulus used (mitogenic, polyclonal or disease-relevant) (Figure 11). Within each stimulation/activation approach no significant changes in SIs were observed by daily edelfosine treatment of mice confirming that selected edelfosine doses did not act by prohibition of functional T-cell properties. These findings are of great practical and translational relevance. In contrast to edelfosine, the vast majority of immunosuppressant drugs, which are in clinical use nowadays to treat autoimmune diseases, e.g. mitoxantrone and cyclophosphamide, eradicate certain immune cells or broadly inhibit immune function. These therapies carry the risk of various side effects, among which the increase in susceptibility to infections due to immunosuppression/leukopenia is a major drawback.

EAE induction leads to T-cell activation *in vivo* that was possibly reflected by these recall experiments *in vitro*. This was indicated by readily detectable proliferation in control approaches, which lacked the addition of a recall stimulus. Interestingly, not only after restimulation but also after *ex vivo* culture in the absence of a recall stimulus the cells revealed a tendency towards edelfosine dose-dependent decline in proliferation. Since the SIs upon each recall stimulus appeared not to be of equal values but rather elevated with increasing edelfosine concentrations, these SI-skewings may reflect a more pronounced edelfosine-treatment effect *in vivo*.

These restimulation experiments did not provide more detailed information about the basis for that indicated SI-skewing. Further investigations of this SI-skewing and the underlying influence of edelfosine on T-cell proliferation *in vivo* have to be performed to clarify conceivable mechanisms. On the one hand edelfosine treatment of EAE-induced mice may interfere with the general proliferative capacity of T cells *in vivo*. Thus, *ex vivo* analysis of T cells may show a comparable frequency of proliferated cells as in PBS-treated control mice. However, reductions may be seen in numbers of generations. On the other hand the edelfosine treatment may block proliferation of a defined T-cell subset while others may not be affected. Here, one may expect a reduced frequency of proliferating cells compared with

PBS-treated mice. No reductions may be seen in generation numbers, whereas frequencies of T cells within each generation may be diminished. One way to approach this question may be the transfer of CFSE-labeled T cells into EAE-induced, PBS- or edelfosine-treated mice. Daily treatment of mice would continue as the T cells become activated after homing to lymphoid tissue. Labeled cells may be detected by flow cytometry after preparation from peripheral lymphoid organs and additional antibody staining, possibly including Ki-67 to detect proliferation.

To sum up, on day 9 after immunization spleens and lymph nodes of PBS- and edelfosine-treated mice showed equal absolute cell numbers, equal frequencies of immune cell subsets and comparable proliferative responses upon recall stimulations. Interestingly, differences were found in frequencies of naïve CD4⁺ T cells and frequencies of cells in early stages of apoptosis induction after 10 mg/kg edelfosine treatment compared with PBS controls. These findings may be related in EAE amelioration upon treatment with 10 mg/kg edelfosine.

Edelfosine treatment ameliorates clinical symptoms, reduces CNS-infiltrating T-cell frequencies and reduces neuronal damage

In MS and EAE, impairment of motor function is maximal during acute disease. This effector phase was characterized by significant differences in EAE scores between PBS- and edelfosine-treated mice. The cellular basis of these discrepancies in clinical outcomes was studied by analyzing absolute leukocyte numbers that infiltrated into the CNS. No differences in numbers of CNS-migrating cells were determined after daily PBS, 1 mg/kg or 10 mg/kg edelfosine application despite a tendency to reduced cell numbers with increased edelfosine concentrations (Table 13). 10 mg/kg edelfosine led to reduced T-cell and pDC frequencies compared to PBS controls (Figure 14, Table 14). Notably, the treatment with 1 mg/kg edelfosine increased frequencies of B cells, mDCs and pDCs compared with infiltrates from 10 mg/kg edelfosine treated mice. This effect might be explained by advancing the already introduced notion of enhanced phagocytic activity of macrophages at lower edelfosine concentrations (235, 238). Macrophages and PAF-activated platelets have been identified as the major sources of lysophosphatidic acid (LPA), a biologically active lysophospholipid. Moreover, platelets and mast cells are the major producers of a second lysophospholipid, S1P. LPA is synthesized extracellularly in microvesicles. Pathways for LPA synthesis as well as formation and membrane shedding of microvesicles are enhanced after immunological activation, probably by edelfosine, resulting in increased LPA release into extracellular fluids. LPA- and S1P₁-receptors expressed by lymphocytes are regulated by activation and play important roles in lymphocyte migration and distribution in lymphoid tissue. The development of the immunosuppressive S1P₁ agonist FTY720 has taken advantage of this function (352,

353). Additionally, it was shown that both LPA and S1P enhanced the production of proinflammatory IL-6 and IL-8 by human maturing DCs when LPS was added to *in vitro* generated, immature DCs (354). Interestingly, signaling via S1P₁ on mature classical myeloid CD8 α ⁺ DCs inhibits the expression of IL-12 which reduces differentiation of Th0-cells into IFN- γ -producing Th1 cells (355). It remains speculative if edelfosine acts on macrophages and, due to its structural similarity to PAF, on platelets thereby enhancing LPA- and S1P-release resulting in elevated DC activation and maturation. Since phagocytosis is also an intrinsic function of other cell types besides macrophages, low concentrations of edelfosine may also increase the phagocytic activity in the DC population. Potentially, the structural similarity of edelfosine to endogenous biologically active lysophospholipids like LPA and S1P allows a direct impact of the drug on activation of DCs and other leukocyte subsets. Thus, naïve DCs may be induced to mature, a process that has been shown to be accompanied by CCL19 expression. These initial CCL19-producing DCs may migrate into the CNS in response to RANTES. CCL19 is a chemokine that in concert with CCL21 acts on CCR7-expressing cell types. In this way CCL19 mediates homing of mature DCs (5, 356–358) and B cells (359, 360). Interestingly, it was shown that CCR7⁺ central memory T cells express lymph node homing factors in contrast to CCR7⁻ effector memory T cells that express receptors to invade inflamed tissue (361). Possibly, central memory T cells may home to the CNS in the case of 1 mg/kg edelfosine-treated, EAE-induced mice executing their function of DC activation to generate a profound wave of effector cells. In contrast, edelfosine treatment did not affect the recruitment of macrophages into the CNS, a process mainly guided along gradients of the complement component C5a produced by Kupffer cells.

A dramatic increase in frequencies of neutrophils was observed when mice received 10 mg/kg edelfosine compared to PBS- and 1 mg/kg edelfosine-treated mice. Previous reports confirmed comparably low detectable concentrations of edelfosine in brains of treated naïve rats (329) and mice (331). Due to the ability of edelfosine to cross the BBB (362), the effect of acute EAE (an opened BBB) on local drug concentrations in the CNS may be only secondary. However, achieved drug concentrations after 10 mg/kg edelfosine treatment may be sufficient to induce activation in neutrophils. Neutrophils can be readily activated *in vitro* by the addition of PAF (363). Interestingly, PAF is a natural analogue of edelfosine and is involved in inflammation processes, like neutrophil chemotaxis (364, 365). The two molecules differ in their structure on account of a methoxy group (edelfosine) replaced for an acetyl group (PAF) in the glycerol backbone at position *sn*-2. Mollinedo *et al.* have shown that HL-60 tumor cells lacking PAF-receptor (PAF-R) undergo edelfosine-induced apoptosis (253). These neutrophilic promyelocyte leukemia cell lines can be induced to undergo granulocytic differentiation by the addition of dimethylsulfoxid. During this process PAF-Rs develop and the cells become apoptosis-resistant indicating that apoptotic action of

edelfosine is not related to PAF-Rs. Also peripheral blood mature neutrophils were not susceptible to apoptosis. Moreover, human neutrophils showed an increased cytosolic free Ca^{2+} concentration mediated by edelfosine binding to PAF-R, but the affinity was 5000-fold lower compared to PAF (366). Thus, edelfosine may not be able to induce apoptosis but rather activates neutrophils due to molecular similarity with its physiological counterpart PAF. CD4- and CD8-expression was analyzed to examine T-cell subsets that contributed to the significantly reduced frequencies of T cells in the CNS in 10 mg/kg edelfosine treated mice compared to mice that received PBS. Whereas no impact of edelfosine on CD8+ T-cell frequencies could be proven, CD4+ T-cell frequencies were markedly reduced upon 10 mg/kg edelfosine treatment (Figure 15). EAE in PLP₍₁₃₉₋₁₅₁₎-immunized SJL mice is considered to be a CD4+ T cell-mediated disease (88). Therefore, the present results emphasize the effectiveness of edelfosine therapy to specifically affect the disease-relevant cell populations. With regard to previously observed shifts in disease onset upon 10 mg/kg edelfosine treatment for 1-3 days compared to PBS controls, one might argue for a delayed EAE onset and that maximal infiltration might occur 1-3 days later compared to controls. Instead, it has been shown in introductory experiments that a delayed onset upon edelfosine treatment is not accompanied by an equally acute, severe disease bout as seen in PBS-treated animals. Therefore, to investigate edelfosine-mediated changes in the CNS across groups as soon as scores of PBS-treated controls peak, appears to be an adequate procedure to generate reliable, stringent and reproducible data.

As already indicated for activated T cells in lymph nodes of 1 mg/kg edelfosine-treated mice the analysis of T-cell frequencies in CNS infiltrates confirmed the previous assumption. Whereas frequencies of CD69+ CD4+ and CD8+ T cells appeared to be diminished in the CNS of 10 mg/kg edelfosine-treated mice compared to PBS-treated controls, the application of 1 mg/kg edelfosine significantly elevated frequencies of CD69+ T cells compared to 10 mg/kg edelfosine-treated mice (Figure 17 B, Table 16). Naïve and effector T cells are (re)activated after their transmigration into the CNS by brain-resident APCs (microglia, astrocytes) along with DCs (113, 351, 367). Possibly, this process is more pronounced in the case of 1 mg/kg edelfosine treatment. Interestingly, Miller *et al.* have postulated a hierarchy for CNS-migrated APCs according to their potential in T-cell activation (367). mDCs were observed to be superior to both pDCs and CD8 α + CD11c+ DCs, which in turn were superior to macrophages in presenting PLP₍₁₃₉₋₁₅₁₎ peptide to naïve and effector T cells. Since infiltrate analyses showed enhanced frequencies of DCs after 1 mg/kg edelfosine treatment, this population may contribute to elevated T-cell restimulation and activation in the CNS. Along this line, nTreg recruitment to sites of antigen presentation may be enhanced, thus explaining the observed increased frequencies of CNS-infiltrating nTregs if mice were injected daily with 1 mg/kg edelfosine compared to 10 mg/kg edelfosine-treated mice (Figure 15). It has been

shown *in vitro* that nTregs are capable of suppressing activation and/or proliferation as well as cytokine formation of CD4⁺ and CD8⁺ T cells in the absence of APCs (368, 369). The induction of nTreg suppressive activity requires antigenic stimulation, for instance by means of activation signals provided through TCRs, whereas the suppression by activated nTregs is not antigen specific (370). Several modes of nTreg functioning have been postulated. Activation of suppressive function in nTregs may be conferred by APCs (e.g. pDCs, which show elevated frequencies upon 1 mg/kg edelfosine treatment) in a contact-dependent manner due to CTLA-4 (CD152) and LAG3 on Tregs interacting with co-stimulatory CD80 and CD86 expressed by APCs (371, 372). Interestingly, Fallarino *et al.* proposed that nTregs might directly mediate suppression via CTLA-4 (373). The interaction with CD80 and CD86 induces indoleamine 2,3-dioxygenase (IDO) in DCs, an enzyme catalyzing the depletion of tryptophan. Hereby, elevated nTreg frequencies in 1 mg/kg edelfosine-treated mice might interfere with proinflammatory actions of activated T cells in the CNS. To sum up, the increased frequencies of DC subsets in the CNS of 1 mg/kg edelfosine-treated mice may exert secondary effects on T-cell subsets.

EAE is primarily a CD4⁺ T cell-mediated disease (88) and specificity of autoreactive T cells for distinct myelin peptides has been studied in detail (374). Both CD4⁺ Th1 cells secreting IFN- γ and IL-17-producing CD4⁺ Th17 cells are involved in pathology with the latter especially important during disease onset. CD8⁺ T cells in EAE may have regulatory functions (375–377). However, these cells also readily produce IFN- γ potentially acting as an early source of IFN- γ driving Th1-cell differentiation (378). Notably, treatment with 10 mg/kg edelfosine led to reduced frequencies of IFN- γ -producing CD8⁺ T cells compared to PBS- or 1 mg/kg edelfosine-treated mice (Figure 16, Table 15). In contrast, no effect could be observed for either the edelfosine treatment or for the previously mentioned diminished CD8⁺ IFN- γ -producing T cells on CD4⁺ IFN- γ -producing T cells. The potential of noncytotoxic CD8⁺ T cells to be sources for IL-17 has been reported before (379).

As frequencies of apoptosis-prone T cells were observed to be elevated in spleens of 10 mg/kg edelfosine-treated mice, the frequencies of T cells with activated caspase-3 were also evaluated in lymphocyte infiltrates of the CNS. In this study increased frequencies of CD4⁺ T cells that expressed activated caspase-3 after daily treatment with 10 mg/kg edelfosine were found (Figure 17, Table 17). These data indicate that either edelfosine is able to induce apoptosis in T cells that have infiltrated the CNS of EAE-induced mice or that the treatment is sufficient to induce apoptosis in T cells in the periphery, an effect that may not inhibit those cells to infiltrate into the CNS but still lead to disease amelioration. Statistical analysis was performed by 1-way ANOVA as for all other subset analysis, but data is not normally distributed in this case. Conservative Kruskal–Wallis testing did not allow the detection of a significant treatment effect here pointing to the necessity of larger sample numbers.

CNS-infiltrating cells in the acute phase of EAE were characterized due to their expression of surface antigens, transcription factor Foxp3 and cytokines. The recruitment of encephalitogenic T cells acting in concert with other leukocytes and CNS-resident cells mediates the formation of inflammatory lesions. At this stage CNS damage is already observable which not only affects the myelin sheath and oligodendrocytes but also neuronal cell survival. Whereas NeuN+ neurons were reduced if EAE-induced mice were treated daily with PBS compared to healthy controls, edelfosine treatment prevented a significant neuronal loss (Figure 18 B). Results indicated unchanged numbers of neurons per section for 10 mg/kg edelfosine-treated mice compared to healthy controls and pointed to a gradual loss of neurons upon 1 mg/kg edelfosine treatment. Immunohistochemical data correlated with disease scores of the mice. NeuN+ cells were quantified in ventral horn regions of spinal cords which contain alpha motor neurons. These neurons are primarily involved in extrafusal muscle fiber innervation of skeletal muscles. In this way it is probable that their damage has a direct impact on clinical disease and treatment outcome. Qualitative evaluation of mononuclear cell infiltration by HE-staining pointed to an edelfosine dose-dependent treatment effect (Figure 18 D). Infiltrating cells readily accumulated at the anterior side of spinal cord sections of PBS-treated mice. In contrast, the tissue of 10 mg/kg edelfosine-treated mice hardly allowed detection of infiltrating cell accumulations. Notably, the depicted tissue sections were prepared from representative mice with EAE scores correlating with respective mean EAE scores of each treatment group. Bielschowsky silver impregnation of respective sections indicated reduced axonal densities if mice were treated with PBS in comparison to edelfosine-treated mice (Figure 18 D). Treatment-dependent EAE-course alterations correlated with the extent of neuronal damage reflected by light-colored areas in corticospinal tracts within the white matter. These anterior and lateral corticospinal tracts contain motor axons that synapse with second-order alpha motor neurons of the ventral horn within the grey matter. In this way reduced axonal densities may affect locomotive functions of EAE-induced mice.

Edelfosine interferes with human T-cell activation and proliferation

After having shown the effectiveness of edelfosine treatment in the murine system, it is necessary to translate these findings into the human setting. Therefore, experiments with human cells were performed. The culture of unstimulated human PBMCs in the presence of 10 µg/ml edelfosine or higher resulted in a marked reduction in viable CD4+ T-cell frequencies. Frequencies of cells that were in late apoptosis or dead were concomitantly increased (Figure 19, Table 18). Interestingly, frequencies of CD4+ T cells in early apoptosis were only increased moderately. In contrast, frequencies of both early and late

apoptotic/dead CD8+ T cells were equally increased if cultured with 10 µg/ml or 33.3 µg/ml edelfosine (Figure 19, Table 19). To sum up, CD4+ T cells appeared to be more susceptible to edelfosine-induced cell death. It remains speculative if apoptosis in CD4+ T cells progresses so fast that most apoptosis-prone cells have already entered late apoptosis/death after 24 h or if concentrations higher than 3.3 µg/ml directly induce cell death by necrosis. Due to its chemical structure including one apolar hydrocarbon chain edelfosine inserts easily into the lipid bilayer of plasma membranes. Thus, if present in high concentrations edelfosine may rather act as a detergent and lead to cell lysis and necrosis. In comparison, in CD8+ T cells apoptosis either progresses with slower kinetics, or CD8+ T cells are less susceptible to edelfosine-mediated toxicity. Edelfosine was shown to integrate into lipid rafts within the cellular membrane thereby recruiting Fas/CD95, FADD and caspase-8 (272). These DISC-raft clusters are implicated to elicit FasL-independent apoptosis. Probably, high concentrations of the drug induce membrane disruptions upon excessive lipid raft integration. Obviously, the amount of edelfosine incorporated into the cell determines its cytotoxicity. The number of drug molecules per cell, the cell density/dilution among cells and the prevailing cell types are important determinants of the drug's killing effect (256).

Additionally, edelfosine interfered with the activation and proliferation of mitogen-stimulated PBMCs in a dose-dependent manner. A profound, significant reduction in proliferative response was observed at concentrations of 1.0 µg/ml edelfosine or higher (Figure 20 A). 10 µg/ml edelfosine led to a significant reduction in proliferation in unstimulated controls. Interestingly, these findings indicate that *ex vivo* mitogen stimulation is not the only condition to study edelfosine effects on T-cell proliferation. Additionally, edelfosine was effective in reducing PHA-mediated T-cell proliferation when added 48 h after activation (Figure 20 B). In this case a significant reduction was only observed at 3.3 µg/ml edelfosine or higher. Moreover, the proliferation in unstimulated controls was significantly diminished at edelfosine concentrations higher than in the preceding approach for unstimulated cells. Results showed a greater effect of edelfosine-mediated inhibition when added coincidentally with activation. In addition, 3.3 µg/ml edelfosine induced a significant inhibition of T-cell proliferation if PBMCs were preincubated for 24 h with edelfosine in the absence of a mitogenic stimulus (Figure 20 C). Nevertheless, some proliferation was detectable even after preincubation with 10 µg/ml edelfosine, whereas 33.3 µg/ml edelfosine blocked T-cell proliferation completely. Unstimulated control approaches could not identify significant differences comparing the various edelfosine concentrations tested. Here, 33.3 µg/ml edelfosine also maximally ablated T-cell proliferation or otherwise affected T-cell function. These results are in agreement with the previously discussed data on apoptosis induction and cell death (Figure 19, Table 18-19) since the frequencies of viable CD4+ T cells were reduced after incubation with 10 µg/ml edelfosine. The incubation with 3.3 µg/ml did not affect viability in preincubation experiments.

However, it effectively interfered with T-cell proliferation after preincubation and also when added coincidentally with or 48 h after T-cell activation. When comparing the edelfosine-mediated reduction of proliferation in all three PHA-stimulated settings, an interaction was observed with significant differences between immediate addition and addition 48 h after activation, but also between immediate addition and preincubation if cells were treated with 3.3 µg/ml edelfosine. In this way 3.3 µg/ml edelfosine inhibited proliferation more effectively when added immediately compared to addition 48 h after activation or pretreatment. No such differences were found for comparisons of the three approaches at other edelfosine concentrations.

To test the drug's interference with a more physiological condition, i.e. antigen-specific T-cell proliferation, MBP₍₈₃₋₉₉₎-specific T-cell lines (TCLs) were incubated with edelfosine. These experiments not only showed the inhibition of proliferation of activated cells by edelfosine, but they also illustrated the impact of edelfosine on proliferation of cells, that have not been stimulated by the addition of MBP₍₈₃₋₉₉₎ (Figure 20 D). Obviously, edelfosine not only interferes with actively induced proliferation, namely the addition of a mitogenic or a disease-relevant, specific stimulus *in vitro*, but also with the "background"-proliferation in the unstimulated control conditions. This effect was already observed in *ex vivo* proliferation experiments with lymphocytes derived from EAE-induced SJL mice (chapter 4.3.2). In the case of lymphocyte preparations from peripheral blood or lymphatic organs, activated T cells as well as APCs may be concomitantly used for *ex vivo* proliferation assays. The APCs may provide stimulation for T cells albeit on a comparably lower level. Instead, the use of TCLs enabled the detection of proliferation, even without the addition of a stimulus in a setting devoid of APCs loaded with exogenous antigen. This proliferation may be assigned to a process named "homeostatic proliferation". Homeostatic proliferation depends on contact to self peptide-MHC ligands and cytokines (e.g. IL-7) provided by other cells, e.g. classical APCs and probably T cells, in order to prevent apoptosis of T cells that lack the encounter of their cognate antigen (380–384). Mouse models implied that the peptides involved in positive T-cell selection in the thymus also drive homeostatic proliferation (385, 386). Especially DCs were shown to act on MBP-specific T-cell clones *in vitro* in absence of nominal, exogenous antigen (387, 388). A distinct activation (induction of IL-12Rβ₂ and IFN-γ expression, Ca²⁺ currents) and long term survival of T cells were reported upon cell-cell contact. It is this homeostatic proliferation that plays a fundamental role in maintaining the T-cell pool during the lifetime of an individual. In fact, proliferation of PBMCs could be readily observed after seven days in the presented experiment (Figure 20 E). In order to block TCR:MHC interactions cells were also cultured with anti-HLA class I and II antibodies. Only minor antigen-independent proliferation was detectable indicating that proliferation was mediated to a large degree by MHC class I and/or class II interactions with TCRs. Here, the culture with

3.3 µg/ml edelfosine dramatically reduced proliferation to baseline levels interfering profoundly with homeostatic proliferation of T cells.

The presented findings allow to conclude that edelfosine is capable to inhibit the proliferation of T cells after mitogenic and antigen-specific activation, also at concentrations that were clearly shown not to be toxic/lytic. Moreover, edelfosine may exert its immunomodulatory effects by interference with proliferation that is not dependent on presentation of exogenous antigen.

Edelfosine modulates MHC class II- and type I interferon-associated signaling pathways of human CD4+ T cells

Edelfosine was shown to induce apoptosis in tumor cells and activated T cells (253, 312). Previous reports proposed Fas ligand-independent mechanisms to induce DISC-complex formation by edelfosine recruitment into lipid rafts (254, 272, 389). Moreover, edelfosine may also act by inhibiting the PC biosynthesis resulting in apoptosis in proliferating cells (255, 274, 275). Cell proliferation was also found to be interrupted by edelfosine inhibiting PC breakdown into lipid second messengers for the MAPK pathway (297, 299, 390). The goals of the present gene-expression analysis were to deepen the understanding of already known mechanisms of edelfosine action (apoptosis induction, cell-cycle arrest), but also to discover novel effects of edelfosine in the context of immune cells. The two main questions that were asked are: which pathways are induced *de novo* by edelfosine treatment of unstimulated cells? Which pathways are modulated in stimulated CD4+ T cells upon drug application?

Whole genome gene-expression analysis was performed using enriched human CD4+ T cells. Cells were incubated for 30 h in absence or presence of edelfosine. It has been previously shown that 3.3 µg/ml edelfosine do not induce reductions in frequencies of unstimulated, viable annexin V- PI- PBMCs (Figure 19 B). Thus, this concentration can be excluded to be toxic/lytic. However, 3.3 µg/ml edelfosine appeared to be potent in interfering with CD4+ T-cell proliferation after preincubation (Figure 20 C). Moreover, homeostatic T-cell proliferation was inhibited by 3.3 µg/ml edelfosine (Figure 20 E). Figure 19 B also implies that 10 µg/ml edelfosine differs from 3.3 µg/ml by inducing a profound increase in frequencies of unstimulated, late apoptotic/dead annexin V+ PI+ CD4+ T cells at the expense of viable T cells. 10 µg/ml edelfosine also significantly reduced the proliferation of PBMCs which were cultured for three days in absence of an exogenous stimulus (Figure 20 A). Based on these data, which reflect both differences with regard to CD4+ T-cell viability and a potential enhancement of interference with T-cell proliferation, gene-expression analysis was performed of unstimulated CD4+ T cells cultured with 3.3 µg/ml or 10 µg/ml edelfosine. To investigate the impact of edelfosine on the gene-expression profile of stimulated CD4+

T cells, cells were incubated with 3.3 µg/ml edelfosine. As mentioned previously, this concentration did not reduce frequencies of viable CD4+ T cells after 24 h of incubation without exogenous stimulus. However, it significantly reduced the proliferation of activated T cells (Figure 20 B) and T cells after 24 h of preincubation (Figure 20 C). The particular effectiveness of 3.3 µg/ml edelfosine when added immediately was not only emphasized by the significant reduction of T-cell proliferation (Figure 20 A). Performing a comparison between all three settings of PHA-mediated T-cell proliferation (immediate edelfosine addition, addition after 48 h, 24 h pretreatment followed by T-cell activation) 3.3 µg/ml edelfosine was found to be unique among all concentrations tested. Due to its profound impact on proliferation when added immediately significant differences were found compared to the addition after 48 h and the pretreatment condition.

Despite the mentioned differences induced by 3.3 µg/ml and 10 µg/ml edelfosine on unstimulated T cells both concentrations induced consistent changes of gene expression in CD4+ T cells (Table 20). The fact that all genes whose expression was modulated by 3.3 µg/ml edelfosine also appeared in lists of modulated genes after 10 µg/ml treatment (except TCF4) underlined the effect of enhancement of induced changes by increased edelfosine concentrations. Therefore, further in-depth analysis of the unstimulated setting was performed using the 10 µg/ml edelfosine approach. In contrast, the stimulated condition generated a large number of up- and downmodulated genes.

The clustering of differentially upregulated genes of unstimulated CD4+ T cells treated with 10 mg/kg edelfosine confirmed the well-described induction of apoptosis by edelfosine (Table 21 A). Notably, this confirmation was generated by analyzing cells cultured in absence of exogenous stimulation and previous reports attributed apoptosis induction specifically to activated cells. Here, one has to take into account that upregulations may have occurred in cells that have already been activated *in vivo* or cells that were activated *in vitro* by transferred APCs. This hypothesis is underlined by the comparably moderate presentation of apoptosis-associated pathways with 2×10^{-2} as the lowest GO P-value, the limited number of upregulated genes (11) and the comparatively high edelfosine concentration of 10 µg/ml edelfosine which was necessary to achieve upregulation in the unstimulated setting. The JUN proto-oncogene, also referred to as c-Jun, is activated by the JNK pathway. The induction of c-Jun has been reported in response to cellular stress (UV light, ionizing irradiation, hydrogen peroxide, TNF-α) leading to apoptosis (224, 227, 391, 392). Its role in apoptosis is not associated with its function in cell cycle progression and proliferation (393). Moreover, activated Ras can induce elevated transcription activity of c-Jun by phosphorylation of its transactivation domain (226, 394). Interestingly, both identified proto-oncogenes RhoB and KRAS are members of the Ras superfamily of GTPases, which are involved in regulation of the actin cytoskeleton, cell adhesion, motility, proliferation and

apoptosis. RhoB itself is an important mediator of antineoplastic and apoptotic functions of farnesyltransferase inhibitors for inhibiting malignant cell growth (395). The Ras signaling pathway itself can be induced by ceramide upon Fas-initiated apoptosis (228).

In contrast, 10 µg/ml edelfosine but also 3.3 µg/ml edelfosine readily downmodulated the expression of genes assigned to immune response and antigen processing and presentation via MHC class II (lowest GO P-value: 3.9×10^{-14}) (Table 21 A, Table 22 B). This interesting treatment outcome is even more remarkable in view of the cell type under investigation. In general, CD4⁺ T cells interact via their TCR with MHC class II on APCs (DCs, B cells, macrophages, thymic epithelial cells). On other cell types MHC class II expression can be induced by activation, for instance by proinflammatory cytokines like IFN-γ. In this way human T cells may express HLA class II as an activation marker, which is involved in antigen presentation and subsequent bystander activation of T cells (396–398). This is possibly pointing to a role in homeostatic proliferation. MHC class II on T cells was also reported to act as a signal-transducing receptor via its cytoplasmic tail into T cells thereby mediating protein kinase C (PKC) membrane translocation. CD3 and HLA class II triggering elevates CD3-mediated T-cell blast proliferation (399). The master regulator of MHC class II expression is the class II transactivator (CIITA). The CIITA promoter (P) III isoform, which is responsible for HLA-DR, -DP and -DQ cell-surface expression, is not transcribed in activated mouse T cells due to methylated CIITA-P III (400). In the present experiment CD4⁺ T cells were cultured without or with edelfosine in the absence of stimulation. IFN-γ concentrations were at baseline, undetectable levels in both conditions as found by 13plex Kit FlowCytomix analysis (not shown). A conceivable deprivation of IFN-γ upon edelfosine addition could not account for the observed downregulation of MHC class II-associated genes, which was reproducible in human B cells on protein level by flow cytometry (Figure 22). But possibly, again referring to the 13plex data, edelfosine is interfering with vesicular transport of cytokines (Figure 24) and HLA class II to the T-cell surface. In this regard, edelfosine may act as an immunomodulatory, chemotherapeutic drug, maybe by integration into the phospholipid bilayer of transport vesicles and/or endosomal compartments for MHC class II loading. To develop a better understanding, the molecular mechanisms how edelfosine affects molecules of the MHC class II processing/presentation pathways clearly merit further study.

If incubated with stimulated human CD4⁺ T cells, edelfosine induced the downregulation of genes assigned to cell-cycle progression (Table 21 B). This effect of edelfosine has been examined in previous reports. Interestingly, edelfosine inhibits cell division, but it does not interfere with cell nuclear division thereby multinucleated cells accumulate in G₂/M phase of cell cycle followed by apoptosis (276, 401–406). Pushkareva *et al.* observed tetra- and octaploid cells at the G₀/G₁ phase of the cell cycle (407). Of note, microtubule assembly

appears not to be compromised by edelfosine (408). Thus, edelfosine is able to directly induce apoptosis, e.g. by DISC-complex formation, and/or to exert a cytostatic effect by inhibiting cytokinesis of the same cell type. The relative contribution of each effect is considered to be dependent on the cell type as well as the drug dose (409). The inhibition of PC biosynthesis may constitute a mechanism mediating the edelfosine-induced inhibition of mitosis (241, 410). Comprising about 50 mol% of phospholipids, PC is the most abundant phospholipid in membranes of eukaryotic cells. Its unobstructed biosynthesis is therefore required to cope with the increased demand to generate cellular membranes during mitosis. Edelfosine inhibits CCT (274), the key enzyme controlling the rate-limiting step of the *de novo* PC biosynthesis (411–413), thereby inducing severe stress sufficient to impose apoptosis on proliferating cells. This cytotoxic effect can be abrogated by the addition of LPC as an exogenous source of phospholipid (274, 276) as well as by the overexpression of CCT (414). In this way edelfosine-treated cells can be prevented from accumulation in the G₂/M phase and subsequent apoptosis. Interestingly, the cytostatic G₀/G₁ block is not resolved and may be independent of the inhibition of PC synthesis. CCT α is a soluble enzyme of the nucleus, the Golgi apparatus, ER and transport vesicles that gets activated upon association with the nuclear membrane. It is not established if edelfosine directly interacts with CCT or by other indirect processes. One possibility to explain more precisely how the inhibition of PC synthesis is initiating apoptosis would be that reduced PC blocks the downstream synthesis of SM and DAG by SMS. Thus, a second SMS substrate may accumulate: ceramide, which has been associated with apoptosis (228). Besides interfering with the biosynthesis of PC, APLs can also interfere with PC breakdown into PA by phospholipase D and its subsequent degradation to DAG (297, 299, 390). PA and DAG act as lipid second messengers on the MAPK pathway, for instance the Ras/Raf/MEK/ERK pathway of cell proliferation. Edelfosine also diminishes formation of DAG and concomitant inositol 1,4,5-trisphosphate (IP3) by phospholipase C, an enzyme that conducts the breakdown of PI-4,5 bisphosphate (PIP2) (415, 416). In this regard, the biosynthesis and turnover of phospholipids is not only important for the maintenance of membrane integrity. They are also the stock for precursors of lipid second messengers that mediate cellular function, survival and proliferation. As some reports on tumor cells described dissociations between apoptosis induction and detectable changes in PC metabolism it has to be elucidated if the interference with lipid biosynthesis is the general cause for cell-cycle arrest and the cytotoxic action of edelfosine (417–419).

A further finding of high interest was the prominent upregulation of type I interferon-associated genes upon incubating stimulated CD4⁺ T cells with 3.3 μ g/ml edelfosine. Physiologically, the expression of type I interferons is induced by viral components, e.g. ss/dsRNA, DNA and viral glycolipids, but also by bacterial components (DNA, LPS). In the majority of triggers, responding cells are macrophages, mDCs and/or pDCs (420). The

present finding may be a side effect mediated by type I interferons binding to the ubiquitously expressed heterodimeric type I interferon receptor, which is composed of IFNAR1 and IFNAR2 subunits. In subsequent downstream signaling events, STAT1/STAT2 get phosphorylated and this heterodimer translocates into the nucleus to initiate transcription of IFN- α/β -inducible genes. Interestingly, IFN- α/β activates also other pathways. For instance, the formation of STAT1 homodimers can induce the transcription of genes that contain the IFN- γ -activated sequence (GAS). Of note, cross-talks by feedback circuits have been reported for IFN- α/β and the type II interferon IFN- γ . IFN- α/β signaling pathways were found to upregulate IFN- γ production by DCs but also by T cells which leads to the induction and maintenance of Th1 cells (421–423). Together with signaling via the TCR, IFN- α and - β were found to induce IFN- γ production by STAT4 activation. IFN- γ was also identified to have an impact on IFN- α/β . The enhancement of IFN- α signaling by IFN- γ was found to be dependent on the tyrosine kinase Syk (424). Therefore, type I and II interferons may influence each other in terms of signaling and production. The findings of gene-expression analysis would argue in favor of the expectation of elevated IFN concentrations taking into account previously described crosstalks of IFN pathways. Interestingly, type I interferons were absent in supernatants of CD4⁺ T cells used for gene-expression analysis thereby contradicting theoretical autocrine or paracrine type I interferon-induced gene expression. ELISA- and 13plex-data results indicate that, upon treatment with 3.3 $\mu\text{g/ml}$ edelfosine, viable CD4⁺ T cells are inhibited to express and/or secrete IFN- γ . The decrease in IFN- γ concentration may be the consequence of edelfosine interfering with cellular activation, proliferation and type II interferon production. This downmodulation occurs despite the induced expression of type I IFN-associated genes in stimulated, edelfosine-treated cells. In future experiments one could reduce the possibility of IFN- γ crosstalk *a priori* by enriching naïve CD4⁺ T cells after PBMC isolation. In this way the culture of already *in vivo* activated T cells, e.g. Th1, as sources of IFN- γ could be avoided. However, no apparent downregulations of IFN- γ -associated genes were found by microarray analysis. Nevertheless, reduced IFN- γ concentrations could have been the result of edelfosine interfering with T-cell activation and/or vesicle transport to the cell membrane. Interestingly, this inhibitory effect of edelfosine appeared not only to affect secretion of IFN- γ but also of other cytokines as a more general effect.

To sum up, the detected upregulation of type I interferon-associated genes in stimulated, edelfosine-treated CD4⁺ T cells cannot be deduced from the presence of either IFN- α or - β in the cell culture supernatant. Moreover, even the concentration of IFN- γ was reduced in edelfosine-containing approaches compared to approaches without edelfosine. This finding excludes the additional possibility of induction of type I interferon-associated genes due to feedback cross-talk by type II interferon and emphasizes the role of edelfosine.

Serrano-Fernandez *et al.* have performed a longitudinal analysis on IFNB1b treatment of MS patients (315). Subjecting isolated PBMCs to microarray analysis over one year, 14 significantly upregulated genes were identified at all three timepoints. Those biomarkers have also previously been shown to be differentially expressed in the case of IFNB1a- (IFI44L, ISG15) (425, 426), IFNB1b therapy (IFIT3, SN/SIGLEC1) (427) or both (EI2AK2, IFI6, IFI44, IFIH1, IFIT1, IFIT2, MX1, OASL, RSAD2 and XAF1) (425–429). Postulated biomarkers like IL-8 were identified only directly after onset of IFNB1b therapy. These IFN-regulated transcripts may constitute early biomarkers for long term IFNB activity. The authors identified IFI44L, IFIT1 and RSAD2 to show the greatest fold-change (>1.3). By incubating stimulated human CD4+ T cells with edelfosine, these candidates were also found to be highly upregulated (fold-changes of SLR: 3.3 to 3.4), thereby seconded only by IFI44 (3.4) and IFIT2 (4.1). In principle, except for SN all 14 upregulated transcripts were also identified as upregulated genes in the case of edelfosine-incubated stimulated CD4+ T cells. Additionally, further type I interferon-regulated genes were identified (Table 22 B). Functionally, transcripts can be grouped according to their role in immune response and/or response to virus (Table 21 B). IFN- β -inducible XAF1 may act as an intermediate regulator for TRAIL-induced apoptosis (430).

Stürzebecher *et al.* compared the differential gene expression of responders, initial responders, who produced neutralizing antibodies in the course of treatment, and non-responders to identify unique responder-expression profiles (431). Responders were found to upregulate nine genes comprising OAS but also TRAIL, potentially linking IFNB treatment to elevated apoptosis. Probably, the induction of genes associated with the activation of the immune response by interferon therapy may exhaust components of cellular (auto)immunity in the periphery. In this way, the inflammatory response in the CNS of MS-affected individuals may be diminished. Type I interferons also possess anti-proliferative properties by directly inducing apoptosis (432), possibly by amplifying FasL/Fas-induced apoptosis (433, 434) and induction of p53 (435, 436). For instance, apoptosis mediated by IFN- β in melanoma cell lines was dependent on the cleavage and activation of caspase-3, -8 and -9, cytochrome c release from mitochondria and DNA fragmentation. Moreover, the expression of TRAIL was induced (437). Considering the IFNB treatment-induced change of MS-patient subsets from responders to antibody-producing non-responders, the *a priori* existence of non-responders as well as the high costs of recombinant IFNB production reliable approaches are necessary to classify patients before deciding on a course of treatment. One meaningful *a priori* approach may be the identification of responsible single nucleotide polymorphisms (438).

As expected, genes attributed to the regulation of apoptosis were also upregulated (Table 21 B). Among these genes were the previously mentioned c-Jun and KRAS, but also

the GTPase GIMAP1 and the Rho guanine nucleotide exchange factor (GEF) 3, which accelerates the activity of GTPases by catalyzing the release of bound GDP. SMAD3, an intracellular signal transducer that can associate to form SMAD3/SMAD4/JUN/FOS complexes, was also upregulated. As mentioned, TNF- α was described earlier to induce apoptosis. Stimulated, edelfosine-treated CD4⁺ T cells showed a significant upregulation of TRAIL and tumor necrosis factor (ligand) superfamily, member 13 (APRIL). The binding of TRAIL to its receptor can activate MAPK8/JNK, caspase-8 and -3 (439, 440). Like caspase-8, upregulated caspase-10 acts as an initiator caspase independently of caspase-8 to mediate apoptosis by Fas and TNF (441). In this way edelfosine may induce DISC-complex formation and subsequent apoptosis in T cells in the absence of FasL (272). The novel identification of increased expression of type I interferon-regulated genes in activated, edelfosine-treated human CD4⁺ T cells may point to edelfosine as a potent apoptosis-inducing, immunomodulating, cost-effective and orally available treatment in the context of MS.

6 Summary

Edelfosine was tested in EAE-mouse models to define effective concentrations which ameliorate the clinical course in the absence of side effects. Consequently, 10 mg/kg edelfosine were used to treat EAE in SJL mice in a preventive as well as in a therapeutic setting. 1 mg/kg edelfosine was used as a reference regimen. Trials additionally included a PBS-treated control cohort. To link the detected amelioration of EAE to mechanistic changes upon edelfosine treatment, secondary lymphoid organs (lymph nodes, spleens) were investigated at day 9 after immunization by flow cytometry (start of treatment: day of immunization). A significant higher frequency of T cells which showed signs of activated caspase-3 was found in lymphoid organs of mice that were treated with 10 mg/kg edelfosine. Here, also significantly more naïve T cells were detected.

At day 9 after immunization, the proliferative capacity of lymph node cells as well as splenocytes was tested in *ex vivo* thymidine-incorporation assays. Upon edelfosine treatment in EAE mice, lymphocytes retained their proliferative capacity irrespective of the recall stimulus (mitogenic, polyclonal or disease-relevant).

Flow cytometry was used to investigate treatment-dependent changes in the composition of immune cells infiltrating into the CNS of immunized mice in the acute phase of EAE. The treatment with 10 mg/kg edelfosine led to a significantly reduced frequency of infiltrating CD4⁺ T cells. Within the CD4⁺ T-cell population the frequency of T cells with activated caspase-3 was significantly increased. The immunohistochemical evaluation of NeuN⁺ neurons in the acute phase of EAE using cervical spinal cord sections revealed a significant loss of neurons if mice were treated with PBS compared to non-immunized control mice. In comparison, no significant loss was found when comparing non-immunized mice to mice that were treated with 10 mg/kg edelfosine.

The treatment of human CD4⁺ T cells with edelfosine led to an edelfosine dose-dependent decrease of the proliferative response in thymidine-incorporation assays. Subsequently, CD4⁺ T cells were used to perform gene-expression analysis. Here, an edelfosine-induced decrease of MHC class II molecules and molecules involved in MHC class II-associated processing and presentation was found in unstimulated CD4⁺ T cells. Furthermore, type I interferon-associated genes were found to be upregulated if cells were stimulated in the presence of edelfosine. Interestingly, those genes were also identified to be upregulated in a published longitudinal study of gene-expression profiles, in which PBMCs from MS patients under IFN- β treatment were investigated. Both observations are novel and might offer the opportunity to develop edelfosine further for clinical use. Since the drug is orally available and well tolerated, this remains an important and interesting goal.

7 Abbreviations

(c)DNA	(complementary) deoxyribonucleic acid
(S1P) ₁	(sphingosine 1-phosphate) receptor 1
AEP	alkyl ether phospholipids
AHSC	autologous hematopoietic stem cell
AICD	activation-induced cell death
AIF	apoptosis-inducing factor
ALP	alkyllysophospholipid
ANOVA	analysis of variance
APAF1	apoptotic protease-activating factor-1
APC	antigen-presenting cell, allophycocyanin
APL	alkylphospholipid
APRIL	tumor necrosis factor (ligand) superfamily, member 13
ATL	antitumor lipid
BBB	blood brain barrier
BCL2	B-cell lymphoma protein-2
BCR	B-cell receptor
BDNF	brain-derived neurotrophic factor
BP	biological process
BSA	bovine serum albumin
CCL	CC chemokine ligand
CCR	C-C chemokine receptor
CCT	CTP:phosphocholine cytidyltransferase
CD	cluster of differentiation
CFA	complete Freund's adjuvant
CFSE	carboxyfluorescein diacetate, succinimidyl ester
CICD	caspase-independent cell death
CIITA	class II transactivator
CIS	clinically isolated syndrome
Con A	Concanavalin A
cpm	counts per minute
CSF	cerebrospinal fluid
CTLA-4	cytotoxic T-lymphocyte antigen 4
Cy	cyanine
DAG	diacylglycerol
DC	dendritic cell
ddH ₂ O	deionized-distilled water
DISC	death-inducing signaling complex
ds	double-stranded
EAE	experimental autoimmune encephalomyelitis
EBV	Epstein-Barr virus
EDSS	expanded disability status score
ELISA	enzyme-linked immunosorbent assay
ER	endoplasmic reticulum
ERK	extracellular signal-regulated protein kinase

FADD	Fas-associated protein with death domain
FasL	Fas ligand
Fas	Fas receptor
FITC	fluorescein isothiocyanate
Foxp3	forkhead box protein 3
GA	glatiramer acetate
GAS	IFN- γ -activated sequence
GEF	Rho guanine nucleotide exchange factor
GM-CSF	granulocyte-macrophage colony stimulating factor
GO	gene ontology
HE	hematoxylin-eosin
HLA	human leukocyte antigen
HSC	hematopoietic stem cell
i.m.	intramuscular
i.v.	intravenous
IC	inhibitory concentration
ICAM	intercellular adhesion molecule
ID	identity document
IDO	indoleamine 2,3-dioxygenase
IFN	Interferon
Ig	Immunoglobulin
IHC	Immunohistochemistry
IL	interleukin
IP3	inositol 1,4,5-trisphosphate
iTreg	induced regulatory T cell
JNK	c-Jun N-terminal kinase
KIR	killer cell Ig-like receptors
LCA	leukocyte common antigen
LFA	lymphocyte function-associated antigen
LPA	lysophosphatidic acid
LPC	2-lysophosphatidylcholine
LPS	lipopolysaccharide
MAG	myelin-associated glycoprotein
MAPK	mitogen-activated protein kinase
MBP	myelin basic protein
MCP-1	monocyte chemotactic protein-1
M-CSF	macrophage colony-stimulating factor
mDC	myeloid DC
MedFI	median fluorescence intensity
MHC	major histocompatibility complex
MMP	matrix metalloproteinase
MOG	myelin oligodendrocyte glycoprotein
MOMP	mitochondrial outer membrane permeabilization
MRI	magnet resonance imaging
MS	multiple sclerosis
MSC	mesenchymal stromal/stem cell
NeuN	neuronal nuclei

NF-κB	nuclear factor kappa B
NK	natural killer
nTreg	natural regulatory T cell
PA	phosphatidic acid
PAF	platelet activating factor
PARP1	poly (ADP-ribose) polymerase 1
PBL	peripheral blood lymphocyte
PBMC	peripheral blood mononuclear cell
PBS	phosphate buffered saline
PC	phosphatidylcholine
PCD	programmed cell death
pDC	plasmacytoid DC
PE	phycoerythrin
PHA	phytohemagglutinin
PI	propidium iodide
PIDD	p53-induced protein with a death domain
PIP2	PI-4,5 bisphosphate
PKC	protein kinase C
PLP	proteolipid protein
PMA	phorbol myristate acetate
PML	progressive multifocal leukoencephalopathy
PP	primary-progressive
PR	progressive-relapsing
PS	phosphatidylserine
RANTES	regulated upon activation, normal T cell expressed, and secreted
ROR γ t	retinoic orphan receptor γ t
ROS	reactive oxygen species
RR	relapsing-remitting
s.c.	subcutaneous
SAPK	stress-activated protein kinase
SI	stimulation index
SLR	signal log ratio
SM	sphingomyelin
SMS	sphingomyelin synthase
SP	secondary-progressive
ss	single-stranded
STAT	signal transducer and activator of transcription
TCL	T-cell line
TCR	T-cell receptor
TGF	tumor growth factor
Th	T helper
TLR	toll like receptor
TNF	tumor necrosis factor
TRAIL	TNF-related apoptosis-inducing ligand
UV	ultraviolet
VCAM-1	vascular-cell adhesion molecule-1
VLA-4	very late antigen 4

8 References

1. F. P. Gay, Immunology: a medical science developed through animal experimentation, *Journal of the American Medical Association* **56**, 578-83 (1911).
2. P. Ehrlich, On immunity with special reference to cell life, *Proceedings of the Royal Society of London* **66** (1900).
3. D. W. Talmage, Presidential address to the sixty-sixth annual meeting of the American Association of Immunologists in Dallas, April 8, 1979, in honor of its first president, Dr. Gerald B. Webb. Beyond cellular immunology., *Journal of Immunology* **123**, 1-5 (1979).
4. N. Romani et al., Proliferating dendritic cell progenitors in human blood., *The Journal of Experimental Medicine* **180**, 83-93 (1994).
5. B. F. Sallusto, A. Lanzavecchia, Efficient presentation of soluble antigen by cultured human dendritic cells is maintained by granulocyte/macrophage colony-stimulating factor plus interleukin 4 and downregulated by tumor necrosis factor alpha., *Journal of Experimental Medicine* **179**, 1109-111 (1994).
6. L. J. Zhou, T. F. Tedder, CD14+ blood monocytes can differentiate into functionally mature CD83+ dendritic cells., *Proceedings of the National Academy of Sciences of the United States of America* **93**, 2588-92 (1996).
7. S. Becker, M. K. Warren, S. Haskill, Colony-stimulating factor-induced monocyte survival and differentiation into macrophages in serum-free cultures., *Journal of Immunology* **139**, 3703-9 (1987).
8. B. Beutler, A. Cerami, Cachectin: more than a tumor necrosis factor., *The New England Journal of Medicine* **316**, 379-85 (1987).
9. E. A. Carswell et al., An endotoxin-induced serum factor that causes necrosis of tumors., *Proceedings of the National Academy of Sciences of the United States of America* **72**, 3666-70 (1975).
10. R. Essner, K. Rhoades, W. H. McBride, D. L. Morton, J. S. Economou, IL-4 down-regulates IL-1 and TNF gene expression in human monocytes., *Journal of Immunology* **142**, 3857-61 (1989).
11. D. F. Bainton, J. L. Ulliyot, M. G. Farquhar, The development of neutrophilic polymorphonuclear leukocytes in human bone marrow., *The Journal of Experimental Medicine* **134**, 907-34 (1971).
12. K. Steinbach, R. Martin, Role of autoimmune inflammation and impaired neuroregeneration in the pathogenesis of experimental autoimmune encephalomyelitis, *Dissertation* (2011).
13. D. E. Doherty, G. P. Downey, G. S. Worthen, C. Haslett, P. M. Henson, Monocyte retention and migration in pulmonary inflammation. Requirement for neutrophils., *Laboratory Investigation* **59**, 200-13 (1988).
14. M. Naegele et al., Neutrophils in multiple sclerosis are characterized by a primed phenotype., *Journal of Neuroimmunology* (2011), doi:10.1016/j.jneuroim.2011.11.009.

15. P. Kalinski, E. Wieckowski, R. Muthuswamy, E. de Jong, S. H. Naik, Ed. Generation of stable Th1/CTL-, Th2-, and Th17-inducing human dendritic cells., *Methods in Molecular Biology* **595**, 117-33 (2010).
16. P. Kaliński, C. M. Hilkens, A. Snijders, F. G. Snijdewint, M. L. Kapsenberg, Dendritic cells, obtained from peripheral blood precursors in the presence of PGE₂, promote Th2 responses., *Advances in Experimental Medicine and Biology* **417**, 363-7 (1997).
17. C. Buelens et al., Human dendritic cell responses to lipopolysaccharide and CD40 ligation are differentially regulated by interleukin-10., *European Journal of Immunology* **27**, 1848-52 (1997).
18. A. Boonstra et al., Macrophages and myeloid dendritic cells, but not plasmacytoid dendritic cells, produce IL-10 in response to MyD88- and TRIF-dependent TLR signals, and TLR-independent signals., *Journal of Immunology* **177**, 7551-8 (2006).
19. L. L. Lanier, NK cell recognition., *Annual Review of Immunology* **23**, 225-74 (2005).
20. V. M. Braud et al., HLA-E binds to natural killer cell receptors CD94/NKG2A, B and C., *Nature* **391**, 795-9 (1998).
21. R. E. Vance, J. R. Kraft, J. D. Altman, P. E. Jensen, D. H. Raulet, Mouse CD94/NKG2A is a natural killer cell receptor for the nonclassical major histocompatibility complex (MHC) class I molecule Qa-1(b)., *The Journal of Experimental Medicine* **188**, 1841-8 (1998).
22. A. Moretta et al., Identification of four subsets of human CD3-CD16+ natural killer (NK) cells by the expression of clonally distributed functional surface molecules: correlation between subset assignment of NK clones and ability to mediate specific alloantigen recognition., *The Journal of Experimental Medicine* **172**, 1589-98 (1990).
23. M. Colonna, J. Samaridis, Cloning of immunoglobulin-superfamily members associated with HLA-C and HLA-B recognition by human natural killer cells., *Science* **268**, 405-8 (1995).
24. F. M. Karlhofer, R. K. Ribaldo, W. M. Yokoyama, MHC class I alloantigen specificity of Ly-49+ IL-2-activated natural killer cells., *Nature* **358**, 66-70 (1992).
25. M. D. Cooper, R. D. Peterson, R. A. Good, Delineation of the thymic and bursal lymphoid systems in the chicken., *Nature* **205**, 143-6 (1965).
26. T. R. Mosmann, R. L. Coffman, TH1 and TH2 cells: different patterns of lymphokine secretion lead to different functional properties., *Annual Review of Immunology* **7**, 145-73 (1989).
27. S. Diehl, M. Rincón, The two faces of IL-6 on Th1/Th2 differentiation., *Molecular Immunology* **39**, 531-6 (2002).
28. R. K. Gershon, K. Kondo, Infectious immunological tolerance., *Immunology* **21**, 903-14 (1971).
29. S. Vigouroux, E. Yvon, E. Biagi, M. K. Brenner, Antigen-induced regulatory T cells., *Blood* **104**, 26-33 (2004).
30. E. Bettelli et al., Reciprocal developmental pathways for the generation of pathogenic effector TH17 and regulatory T cells., *Nature* **441**, 235-8 (2006).

31. M. Veldhoen, R. J. Hocking, C. J. Atkins, R. M. Locksley, B. Stockinger, TGFbeta in the context of an inflammatory cytokine milieu supports de novo differentiation of IL-17-producing T cells., *Immunity* **24**, 179-89 (2006).
32. L. E. Harrington et al., Interleukin 17-producing CD4+ effector T cells develop via a lineage distinct from the T helper type 1 and 2 lineages., *Nature Immunology* **6**, 1123-32 (2005).
33. H. Park et al., A distinct lineage of CD4 T cells regulates tissue inflammation by producing interleukin 17., *Nature Immunology* **6**, 1133-41 (2005).
34. C. S. Hsieh et al., Development of TH1 CD4+ T cells through IL-12 produced by Listeria-induced macrophages., *Science* **260**, 547-9 (1993).
35. S. J. Szabo et al., A novel transcription factor, T-bet, directs Th1 lineage commitment., *Cell* **100**, 655-69 (2000).
36. C. S. Hsieh, A. B. Heimberger, J. S. Gold, A. O'Garra, K. M. Murphy, Differential regulation of T helper phenotype development by interleukins 4 and 10 in an alpha beta T-cell-receptor transgenic system., *Proceedings of the National Academy of Sciences of the United States of America* **89**, 6065-9 (1992).
37. R. A. Seder, W. E. Paul, M. M. Davis, B. Fazekas de St Groth, The presence of interleukin 4 during in vitro priming determines the lymphokine-producing potential of CD4+ T cells from T cell receptor transgenic mice., *The Journal of Experimental Medicine* **176**, 1091-8 (1992).
38. W. Zheng, R. A. Flavell, The transcription factor GATA-3 is necessary and sufficient for Th2 cytokine gene expression in CD4 T cells., *Cell* **89**, 587-96 (1997).
39. I. I. Ivanov et al., The orphan nuclear receptor RORgammat directs the differentiation program of proinflammatory IL-17+ T helper cells., *Cell* **126**, 1121-33 (2006).
40. P. R. Mangan et al., Transforming growth factor-beta induces development of the T(H)17 lineage., *Nature* **441**, 231-4 (2006).
41. X. O. Yang et al., STAT3 regulates cytokine-mediated generation of inflammatory helper T cells., *The Journal of biological chemistry* **282**, 9358-63 (2007).
42. A. Laurence et al., Interleukin-2 signaling via STAT5 constrains T helper 17 cell generation., *Immunity* **26**, 371-81 (2007).
43. E. M. Shevach, Mechanisms of foxp3+ T regulatory cell-mediated suppression., *Immunity* **30**, 636-45 (2009).
44. S. Hori, T. Nomura, S. Sakaguchi, Control of regulatory T cell development by the transcription factor Foxp3., *Science* **299**, 1057-61 (2003).
45. M. A. Curotto de Lafaille, J. J. Lafaille, Natural and adaptive foxp3+ regulatory T cells: more of the same or a division of labor?, *Immunity* **30**, 626-35 (2009).
46. S. Z. Josefowicz, A. Rudensky, Control of regulatory T cell lineage commitment and maintenance., *Immunity* **30**, 616-25 (2009).

47. S. Sakaguchi, N. Sakaguchi, M. Asano, M. Itoh, M. Toda, Immunologic self-tolerance maintained by activated T cells expressing IL-2 receptor alpha-chains (CD25). Breakdown of a single mechanism of self-tolerance causes various autoimmune diseases., *Journal of Immunology* **155**, 1151-64 (1995).
48. L. Aly et al., Central role of JC virus-specific CD4+ lymphocytes in progressive multi-focal leucoencephalopathy-immune reconstitution inflammatory syndrome., *Brain* **134**, 2687-702 (2011).
49. B. Engelhardt, R. M. Ransohoff, The ins and outs of T-lymphocyte trafficking to the CNS: anatomical sites and molecular mechanisms., *Trends in Immunology* **26**, 485-95 (2005).
50. M. J. Cipolla, The Cerebral Circulation, *Colloquium Series on Integrated Systems Physiology: From Molecule to Function* **1**, 1-59 (2009).
51. H. F. Cserr, C. J. Harling-Berg, P. M. Knopf, Drainage of brain extracellular fluid into blood and deep cervical lymph and its immunological significance., *Brain Pathology* **2**, 269-76 (1992).
52. R. M. Ransohoff, P. Kivisäkk, G. Kidd, Three or more routes for leukocyte migration into the central nervous system., *Nature Reviews Immunology* **3**, 569-81 (2003).
53. J. M. Charcot, Histologie de la sclerose en plaque., *Gazette des Hopitaux* **41**, 554–66 (1868).
54. T. J. Murray, *Multiple sclerosis: The history of a disease* (Demos Medical Publishing, New York, 2005).
55. T. M. Rivers, D. H. Sprunt, G. P. Berry, Observations on attempts to produce acute disseminated encephalomyelitis in monkeys., *The Journal of Experimental Medicine* **58**, 39-53 (1933).
56. B. H. Waksman, Allergic encephalomyelitis in rats and rabbits pretreated with nervous tissue., *Journal of Neuropathology and Experimental Neurology* **18**, 397-417 (1959).
57. M. Sospedra, R. Martin, Immunology of multiple sclerosis., *Annual Review of Immunology* **23**, 683-747 (2005).
58. D. E. McFarlin, H. F. McFarland, Multiple sclerosis (first of two parts)., *The New England Journal of Medicine* **307**, 1183-8 (1982).
59. D. E. McFarlin, H. F. McFarland, Multiple sclerosis (second of two parts)., *The New England Journal of Medicine* **307**, 1246-51 (1982).
60. D. W. Anderson et al., Revised estimate of the prevalence of multiple sclerosis in the United States., *Annals of Neurology* **31**, 333-6 (1992).
61. M. Pugliatti et al., The epidemiology of multiple sclerosis in Europe., *European Journal of Neurology* **13**, 700-22 (2006).
62. D. A. Dyment, G. C. Ebers, A. D. Sadovnick, Genetics of multiple sclerosis., *Lancet Neurology* **3**, 104-10 (2004).

63. S. E. Baranzini et al., Genome, epigenome and RNA sequences of monozygotic twins discordant for multiple sclerosis., *Nature* **464**, 1351-6 (2010).
64. T. Hansen et al., Risk for multiple sclerosis in dizygotic and monozygotic twins., *Multiple Sclerosis* **11**, 500-3 (2005).
65. G. C. Ebers, A. D. Sadovnick, N. J. Risch, A genetic basis for familial aggregation in multiple sclerosis. Canadian Collaborative Study Group., *Nature* **377**, 150-1 (1995).
66. GAMES, A meta-analysis of whole genome linkage screens in multiple sclerosis., *Journal of Neuroimmunology* **143**, 39-46 (2003).
67. J. Hillert, O. Olerup, Multiple sclerosis is associated with genes within or close to the HLA-DR-DQ subregion on a normal DR15,DQ6,Dw2 haplotype., *Neurology* **43**, 163-8 (1993).
68. J. L. Haines et al., Linkage of the MHC to familial multiple sclerosis suggests genetic heterogeneity. The Multiple Sclerosis Genetics Group., *Human Molecular Genetics* **7**, 1229-34 (1998).
69. T. I. M. S. G. C. & T. W. T. C. C. Consortium, Genetic risk and a primary role for cell-mediated immune mechanisms in multiple sclerosis., *Nature* **476**, 214-9 (2011).
70. J. Hillert, O. Olerup, HLA and MS., *Neurology* **43**, 2426-7 (1993).
71. F. Lundmark et al., Variation in interleukin 7 receptor alpha chain (IL7R) influences risk of multiple sclerosis., *Nature Genetics* **39**, 1108-13 (2007).
72. J. P. McElroy, J. R. Oksenberg, Multiple sclerosis genetics., *Current Topics in Microbiology and Immunology* **318**, 45-72 (2008).
73. D. A. Hafler et al., Risk alleles for multiple sclerosis identified by a genomewide study., *The New England Journal of Medicine* **357**, 851-62 (2007).
74. S. G. Gregory et al., Interleukin 7 receptor alpha chain (IL7R) shows allelic and functional association with multiple sclerosis., *Nature Genetics* **39**, 1083-91 (2007).
75. E. L. Thacker, F. Mirzaei, A. Ascherio, Infectious mononucleosis and risk for multiple sclerosis: a meta-analysis., *Annals of Neurology* **59**, 499-503 (2006).
76. J. D. Lünemann et al., Increased frequency and broadened specificity of latent EBV nuclear antigen-1-specific T cells in multiple sclerosis., *Brain* **129**, 1493-506 (2006).
77. J. D. Lünemann et al., EBNA1-specific T cells from patients with multiple sclerosis cross react with myelin antigens and co-produce IFN-gamma and IL-2., *The Journal of Experimental Medicine* **205**, 1763-73 (2008).
78. K. L. Munger et al., Vitamin D intake and incidence of multiple sclerosis., *Neurology* **62**, 60-5 (2004).
79. K. L. Munger, L. I. Levin, B. W. Hollis, N. S. Howard, A. Ascherio, Serum 25-hydroxyvitamin D levels and risk of multiple sclerosis., *JAMA* **296**, 2832-8 (2006).

80. J. M. Lemire, D. C. Archer, 1,25-dihydroxyvitamin D3 prevents the in vivo induction of murine experimental autoimmune encephalomyelitis., *The Journal of Clinical Investigation* **87**, 1103-7 (1991).
81. T. Riise, M. W. Nortvedt, A. Ascherio, Smoking is a risk factor for multiple sclerosis., *Neurology* **61**, 1122-4 (2003).
82. R. S. Fujinami, M. G. von Herrath, U. Christen, J. L. Whitton, Molecular mimicry, bystander activation, or viral persistence: infections and autoimmune disease., *Clinical Microbiology Reviews* **19**, 80-94 (2006).
83. M. Pette et al., Myelin basic protein-specific T lymphocyte lines from MS patients and healthy individuals., *Neurology* **40**, 1770-6 (1990).
84. J. R. Richert, D. E. McFarlin, J. W. Rose, H. F. McFarland, J. I. Greenstein, Expansion of antigen-specific T cells from cerebrospinal fluid of patients with multiple sclerosis., *Journal of Neuroimmunology* **5**, 317-24 (1983).
85. C. B. Pettinelli, R. B. Fritz, C. H. Chou, D. E. McFarlin, Encephalitogenic activity of guinea pig myelin basic protein in the SJL mouse., *Journal of Immunology* **129**, 1209-11 (1982).
86. R. Martin, H. F. McFarland, D. E. McFarlin, Immunological aspects of demyelinating diseases., *Annual Review of Immunology* **10**, 153-87 (1992).
87. S. S. Zamvil, L. Steinman, The T lymphocyte in experimental allergic encephalomyelitis., *Annual Review of Immunology* **8**, 579-621 (1990).
88. C. B. Pettinelli, D. E. McFarlin, Adoptive transfer of experimental allergic encephalomyelitis in SJL/J mice after in vitro activation of lymph node cells by myelin basic protein: requirement for Lyt 1+ 2- T lymphocytes., *Journal of Immunology* **127**, 1420-3 (1981).
89. B. Pöllinger et al., Spontaneous relapsing-remitting EAE in the SJL/J mouse: MOG-reactive transgenic T cells recruit endogenous MOG-specific B cells., *The Journal of Experimental Medicine* **206**, 1303-16 (2009).
90. J. Goverman et al., Transgenic mice that express a myelin basic protein-specific T cell receptor develop spontaneous autoimmunity., *Cell* **72**, 551-60 (1993).
91. T. G. Forsthuber et al., T cell epitopes of human myelin oligodendrocyte glycoprotein identified in HLA-DR4 (DRB1*0401) transgenic mice are encephalitogenic and are presented by human B cells., *Journal of Immunology* **167**, 7119-25 (2001).
92. K. Kawamura et al., Hla-DR2-restricted responses to proteolipid protein 95-116 peptide cause autoimmune encephalitis in transgenic mice., *The Journal of Clinical Investigation* **105**, 977-84 (2000).
93. P. Das et al., Complementation between specific HLA-DR and HLA-DQ genes in transgenic mice determines susceptibility to experimental autoimmune encephalomyelitis., *Human Immunology* **61**, 279-89 (2000).
94. L. S. Madsen et al., A humanized model for multiple sclerosis using HLA-DR2 and a human T-cell receptor., *Nature Genetics* **23**, 343-7 (1999).

95. J. A. Quandt et al., Unique clinical and pathological features in HLA-DRB1*0401-restricted MBP 111-129-specific humanized TCR transgenic mice., *The Journal of Experimental Medicine* **200**, 223-34 (2004).
96. B. Bielekova et al., Encephalitogenic potential of the myelin basic protein peptide (amino acids 83-99) in multiple sclerosis: results of a phase II clinical trial with an altered peptide ligand., *Nature Medicine* **6**, 1167-75 (2000).
97. B. Bielekova et al., Expansion and functional relevance of high-avidity myelin-specific CD4+ T cells in multiple sclerosis., *Journal of Immunology* **172**, 3893-904 (2004).
98. J. M. van Noort et al., The small heat-shock protein alpha B-crystallin as candidate autoantigen in multiple sclerosis., *Nature* **375**, 798-801 (1995).
99. S. S. Ousman et al., Protective and therapeutic role for alphaB-crystallin in autoimmune demyelination., *Nature* **448**, 474-9 (2007).
100. K. Banki et al., Oligodendrocyte-specific expression and autoantigenicity of transaldolase in multiple sclerosis., *The Journal of Experimental Medicine* **180**, 1649-63 (1994).
101. G. Krishnamoorthy et al., Myelin-specific T cells also recognize neuronal autoantigen in a transgenic mouse model of multiple sclerosis., *Nature Medicine* **15**, 626-32 (2009).
102. F. Forooghian, R. K. Cheung, W. C. Smith, P. O'Connor, H.-M. Dosch, Enolase and arrestin are novel nonmyelin autoantigens in multiple sclerosis., *Journal of Clinical Immunology* **27**, 388-96 (2007).
103. T. Olsson et al., Autoreactive T lymphocytes in multiple sclerosis determined by antigen-induced secretion of interferon-gamma., *The Journal of Clinical Investigation* **86**, 981-5 (1990).
104. J. Correale et al., Patterns of cytokine secretion by autoreactive proteolipid protein-specific T cell clones during the course of multiple sclerosis., *Journal of Immunology* **154**, 2959-68 (1995).
105. B. Hemmer et al., Cytokine phenotype of human autoreactive T cell clones specific for the immunodominant myelin basic protein peptide (83-99)., *Journal of Neuroscience Research* **45**, 852-62 (1996).
106. H. S. Panitch, R. L. Hirsch, A. S. Haley, K. P. Johnson, Exacerbations of multiple sclerosis in patients treated with gamma interferon., *Lancet* **1**, 893-5 (1987).
107. M. A. Kroenke, T. J. Carlson, A. V. Andjelkovic, B. M. Segal, IL-12- and IL-23-modulated T cells induce distinct types of EAE based on histology, CNS chemokine profile, and response to cytokine inhibition., *The Journal of Experimental Medicine* **205**, 1535-41 (2008).
108. J. S. Tzartos et al., Interleukin-17 production in central nervous system-infiltrating T cells and glial cells is associated with active disease in multiple sclerosis., *The American Journal of Pathology* **172**, 146-55 (2008).

109. V. Brucklacher-Waldert, K. Stuermer, M. Kolster, J. Wolthausen, E. Tolosa, Phenotypical and functional characterization of T helper 17 cells in multiple sclerosis., *Brain* **132**, 3329-41 (2009).
110. B. Cannella, C. S. Raine, The adhesion molecule and cytokine profile of multiple sclerosis lesions., *Annals of Neurology* **37**, 424-35 (1995).
111. R. A. Sobel, M. E. Mitchell, G. Fondren, Intercellular adhesion molecule-1 (ICAM-1) in cellular immune reactions in the human central nervous system., *The American Journal of Pathology* **136**, 1309-16 (1990).
112. K. Rössler et al., Expression of leucocyte adhesion molecules at the human blood-brain barrier (BBB)., *Journal of Neuroscience Research* **31**, 365-74 (1992).
113. A. Flügel et al., Migratory activity and functional changes of green fluorescent effector cells before and during experimental autoimmune encephalomyelitis., *Immunity* **14**, 547-60 (2001).
114. D. Franciotta, M. Salvetti, F. Lolli, B. Serafini, F. Aloisi, B cells and multiple sclerosis., *Lancet Neurology* **7**, 852-8 (2008).
115. S. L. Hauser et al., B-cell depletion with rituximab in relapsing-remitting multiple sclerosis., *The New England Journal of Medicine* **358**, 676-88 (2008).
116. C. F. Lucchinetti, W. Brück, M. Rodriguez, H. Lassmann, Distinct patterns of multiple sclerosis pathology indicates heterogeneity on pathogenesis., *Brain Pathology* **6**, 259-74 (1996).
117. J. E. Simpson, J. Newcombe, M. L. Cuzner, M. N. Woodroffe, Expression of monocyte chemoattractant protein-1 and other beta-chemokines by resident glia and inflammatory cells in multiple sclerosis lesions., *Journal of Neuroimmunology* **84**, 238-49 (1998).
118. J. W. Prineas, J. S. Graham, Multiple sclerosis: capping of surface immunoglobulin G on macrophages engaged in myelin breakdown., *Annals of Neurology* **10**, 149-58 (1981).
119. D. van Rossum, S. Hilbert, S. Strassenburg, U.-K. Hanisch, W. Brück, Myelin-phagocytosing macrophages in isolated sciatic and optic nerves reveal a unique reactive phenotype., *Glia* **56**, 271-83 (2008).
120. P. D. Murray et al., Perforin-dependent neurologic injury in a viral model of multiple sclerosis., *The Journal of Neuroscience* **18**, 7306-14 (1998).
121. S. Pouly, B. Becher, M. Blain, J. P. Antel, Interferon-gamma modulates human oligodendrocyte susceptibility to Fas-mediated apoptosis., *Journal of Neuropathology and Experimental Neurology* **59**, 280-6 (2000).
122. W. E. Biddison et al., Chemokine and matrix metalloproteinase secretion by myelin proteolipid protein-specific CD8+ T cells: potential roles in inflammation., *Journal of Immunology* **158**, 3046-53 (1997).
123. M. A. Friese et al., Acid-sensing ion channel-1 contributes to axonal degeneration in autoimmune inflammation of the central nervous system., *Nature Medicine* **13**, 1483-9 (2007).

124. D. Pitt, P. Werner, C. S. Raine, Glutamate excitotoxicity in a model of multiple sclerosis., *Nature Medicine* **6**, 67-70 (2000).
125. J. W. McDonald, S. P. Althomsons, K. L. Hyrc, D. W. Choi, M. P. Goldberg, Oligodendrocytes from forebrain are highly vulnerable to AMPA/kainate receptor-mediated excitotoxicity., *Nature Medicine* **4**, 291-7 (1998).
126. G. Lovas, N. Szilágyi, K. Majtényi, M. Palkovits, S. Komoly, Axonal changes in chronic demyelinated cervical spinal cord plaques., *Brain* **123** (Pt 2, 308-17 (2000).
127. P. Patrikios et al., Remyelination is extensive in a subset of multiple sclerosis patients., *Brain* **129**, 3165-72 (2006).
128. H. A. Arnett et al., TNF alpha promotes proliferation of oligodendrocyte progenitors and remyelination., *Nature Neuroscience* **4**, 1116-22 (2001).
129. J. L. Mason, K. Suzuki, D. D. Chaplin, G. K. Matsushima, Interleukin-1beta promotes repair of the CNS., *The Journal of Neuroscience* **21**, 7046-52 (2001).
130. M. Kerschensteiner et al., Activated human T cells, B cells, and monocytes produce brain-derived neurotrophic factor in vitro and in inflammatory brain lesions: a neuroprotective role of inflammation?, *The Journal of Experimental Medicine* **189**, 865-70 (1999).
131. C. Stadelmann et al., BDNF and gp145trkB in multiple sclerosis brain lesions: neuroprotective interactions between immune and neuronal cells?, *Brain* **125**, 75-85 (2002).
132. R. A. Linker et al., Functional role of brain-derived neurotrophic factor in neuroprotective autoimmunity: therapeutic implications in a model of multiple sclerosis., *Brain* **133**, 2248-63 (2010).
133. J. W. Prineas et al., Multiple sclerosis. Pathology of recurrent lesions., *Brain* **116** (Pt 3, 681-93 (1993).
134. W. Brück, C. Lucchinetti, H. Lassmann, The pathology of primary progressive multiple sclerosis., *Multiple Sclerosis* **8**, 93-7 (2002).
135. C. Lucchinetti et al., Heterogeneity of multiple sclerosis lesions: implications for the pathogenesis of demyelination., *Annals of Neurology* **47**, 707-17 (2000).
136. J. W. Peterson, L. Bö, S. Mörk, A. Chang, B. D. Trapp, Transected neurites, apoptotic neurons, and reduced inflammation in cortical multiple sclerosis lesions., *Annals of Neurology* **50**, 389-400 (2001).
137. L. Bø, C. A. Vedeler, H. Nyland, B. D. Trapp, S. J. Mørk, Intracortical multiple sclerosis lesions are not associated with increased lymphocyte infiltration., *Multiple Sclerosis* **9**, 323-31 (2003).
138. M. H. Barnett, J. W. Prineas, Relapsing and remitting multiple sclerosis: pathology of the newly forming lesion., *Annals of Neurology* **55**, 458-68 (2004).
139. C. M. Poser et al., New diagnostic criteria for multiple sclerosis: guidelines for research protocols., *Annals of Neurology* **13**, 227-31 (1983).

140. G. A. Schumacher et al., Problems of experimental trials of therapy in multiple sclerosis: report by the panel on the evaluation of experimental trials of therapy in multiple sclerosis., *Annals of the New York Academy of Sciences* **122**, 552-68 (1965).
141. W. I. McDonald et al., Recommended diagnostic criteria for multiple sclerosis: guidelines from the International Panel on the diagnosis of multiple sclerosis., *Annals of Neurology* **50**, 121-7 (2001).
142. C. H. Polman et al., Diagnostic criteria for multiple sclerosis: 2010 revisions to the McDonald criteria., *Annals of Neurology* **69**, 292-302 (2011).
143. H. F. McFarland, Examination of the role of magnetic resonance imaging in multiple sclerosis: A problem-orientated approach., *Annals of Indian Academy of Neurology* **12**, 254-63 (2009).
144. H. F. McFarland et al., Using gadolinium-enhanced magnetic resonance imaging lesions to monitor disease activity in multiple sclerosis., *Annals of Neurology* **32**, 758-66 (1992).
145. R. D. Davenport, D. F. Keren, Oligoclonal bands in cerebrospinal fluids: significance of corresponding bands in serum for diagnosis of multiple sclerosis., *Clinical Chemistry* **34**, 764-5 (1988).
146. H. Brønnum-Hansen, N. Koch-Henriksen, E. Stenager, Trends in survival and cause of death in Danish patients with multiple sclerosis., *Brain* **127**, 844-50 (2004).
147. B. Runmarker, O. Andersen, Prognostic factors in a multiple sclerosis incidence cohort with twenty-five years of follow-up., *Brain* **116** (Pt 1, 117-34 (1993).
148. C. Confavreux, G. Aimard, M. Devic, Course and prognosis of multiple sclerosis assessed by the computerized data processing of 349 patients., *Brain* **103**, 281-300 (1980).
149. J. H. Noseworthy, C. Lucchinetti, M. Rodriguez, B. G. Weinshenker, Multiple sclerosis., *The New England Journal of Medicine* **343**, 938-52 (2000).
150. H. Lassmann, W. Brück, C. F. Lucchinetti, The immunopathology of multiple sclerosis: an overview., *Brain Pathology* **17**, 210-8 (2007).
151. A. Compston, A. Coles, Multiple sclerosis., *Lancet* **372**, 1502-17 (2008).
152. C. Confavreux, S. Vukusic, Age at disability milestones in multiple sclerosis., *Brain* **129**, 595-605 (2006).
153. C. Confavreux, S. Vukusic, T. Moreau, P. Adeleine, Relapses and progression of disability in multiple sclerosis., *The New England Journal of Medicine* **343**, 1430-8 (2000).
154. J. W. Prineas, R. O. Barnard, E. E. Kwon, L. R. Sharer, E. S. Cho, Multiple sclerosis: remyelination of nascent lesions., *Annals of Neurology* **33**, 137-51 (1993).
155. A. J. Thompson et al., Primary progressive multiple sclerosis., *Brain* **120** (Pt 6, 1085-96 (1997).

156. I. Screpanti et al., Steroid sensitivity of thymocyte subpopulations during intrathymic differentiation. Effects of 17 beta-estradiol and dexamethasone on subsets expressing T cell antigen receptor or IL-2 receptor., *Journal of Immunology* **142**, 3378-83 (1989).
157. C. Paul, C. Bolton, Inhibition of blood-brain barrier disruption in experimental allergic encephalomyelitis by short-term therapy with dexamethasone or cyclosporin A., *International Journal of Immunopharmacology* **17**, 497-503 (1995).
158. D. Teitelbaum, A. Meshorer, T. Hirshfeld, R. Arnon, M. Sela, Suppression of experimental allergic encephalomyelitis by a synthetic polypeptide., *European Journal of Immunology* **1**, 242-8 (1971).
159. P. W. Duda, M. C. Schmier, S. L. Cook, J. I. Krieger, D. A. Hafler, Glatiramer acetate (Copaxone) induces degenerate, Th2-polarized immune responses in patients with multiple sclerosis., *The Journal of Clinical Investigation* **105**, 967-76 (2000).
160. P. Putheti, M. Soderstrom, H. Link, Y.-M. Huang, Effect of glatiramer acetate (Copaxone) on CD4+CD25high T regulatory cells and their IL-10 production in multiple sclerosis., *Journal of Neuroimmunology* **144**, 125-31 (2003).
161. T. Ziemssen, T. Kümpfel, W. E. F. Klinkert, O. Neuhaus, R. Hohlfeld, Glatiramer acetate-specific T-helper 1- and 2-type cell lines produce BDNF: implications for multiple sclerosis therapy. Brain-derived neurotrophic factor., *Brain* **125**, 2381-91 (2002).
162. I. M. S. S. Group, Interferon beta-1b is effective in relapsing-remitting multiple sclerosis. I. Clinical results of a multicenter, randomized, double-blind, placebo-controlled trial. The IFNB Multiple Sclerosis Study Group., *Neurology* **43**, 655-61 (1993).
163. P. A. Calabresi, L. A. Stone, C. N. Bash, J. A. Frank, H. F. McFarland, Interferon beta results in immediate reduction of contrast-enhanced MRI lesions in multiple sclerosis patients followed by weekly MRI., *Neurology* **48**, 1446-8 (1997).
164. L. A. Stone et al., The effect of interferon-beta on blood-brain barrier disruptions demonstrated by contrast-enhanced magnetic resonance imaging in relapsing-remitting multiple sclerosis., *Annals of Neurology* **37**, 611-9 (1995).
165. V. Brinkmann et al., The immune modulator FTY720 targets sphingosine 1-phosphate receptors., *The Journal of Biological Chemistry* **277**, 21453-7 (2002).
166. S. Mandala et al., Alteration of lymphocyte trafficking by sphingosine-1-phosphate receptor agonists., *Science* **296**, 346-9 (2002).
167. T. H. M. Pham, T. Okada, M. Matloubian, C. G. Lo, J. G. Cyster, S1P1 receptor signaling overrides retention mediated by G alpha i-coupled receptors to promote T cell egress., *Immunity* **28**, 122-33 (2008).
168. L. Kappos et al., A placebo-controlled trial of oral fingolimod in relapsing multiple sclerosis., *The New England Journal of Medicine* **362**, 387-401 (2010).
169. L. Kappos et al., Oral fingolimod (FTY720) for relapsing multiple sclerosis., *The New England Journal of Medicine* **355**, 1124-40 (2006).

170. V. Rothhammer et al., Th17 lymphocytes traffic to the central nervous system independently of α 4 integrin expression during EAE., *The Journal of Experimental Medicine* (2011), doi:10.1084/jem.20110434.
171. L. Kappos et al., Efficacy and safety of oral fumarate in patients with relapsing-remitting multiple sclerosis: a multicentre, randomised, double-blind, placebo-controlled phase IIb study., *Lancet* **372**, 1463-72 (2008).
172. G. Comi et al., Effect of laquinimod on MRI-monitored disease activity in patients with relapsing-remitting multiple sclerosis: a multicentre, randomised, double-blind, placebo-controlled phase IIb study., *Lancet* **371**, 2085-92 (2008).
173. P. W. O'Connor et al., A Phase II study of the safety and efficacy of teriflunomide in multiple sclerosis with relapses., *Neurology* **66**, 894-900 (2006).
174. H. Babbe et al., Clonal expansions of CD8(+) T cells dominate the T cell infiltrate in active multiple sclerosis lesions as shown by micromanipulation and single cell polymerase chain reaction., *The Journal of Experimental Medicine* **192**, 393-404 (2000).
175. B. Bielekova et al., Regulatory CD56(bright) natural killer cells mediate immunomodulatory effects of IL-2/alpha-targeted therapy (daclizumab) in multiple sclerosis., *Proceedings of the National Academy of Sciences of the United States of America* **103**, 5941-6 (2006).
176. B. Bielekova et al., Effect of anti-CD25 antibody daclizumab in the inhibition of inflammation and stabilization of disease progression in multiple sclerosis., *Archives of Neurology* **66**, 483-9 (2009).
177. B. Bielekova et al., Humanized anti-CD25 (daclizumab) inhibits disease activity in multiple sclerosis patients failing to respond to interferon beta., *Proceedings of the National Academy of Sciences of the United States of America* **101**, 8705-8 (2004).
178. M. Keegan et al., Relation between humoral pathological changes in multiple sclerosis and response to therapeutic plasma exchange., *Lancet* **366**, 579-82.
179. D. Shan, J. A. Ledbetter, O. W. Press, Signaling events involved in anti-CD20-induced apoptosis of malignant human B cells., *Cancer Immunology, Immunotherapy* **48**, 673-83 (2000).
180. N. Di Gaetano et al., Complement activation determines the therapeutic activity of rituximab in vivo., *Journal of Immunology* **171**, 1581-7 (2003).
181. D. Flieger, S. Renoth, I. Beier, T. Sauerbruch, I. Schmidt-Wolf, Mechanism of cytotoxicity induced by chimeric mouse human monoclonal antibody IDEC-C2B8 in CD20-expressing lymphoma cell lines., *Cellular Immunology* **204**, 55-63 (2000).
182. K. Hawker et al., Rituximab in patients with primary progressive multiple sclerosis: results of a randomized double-blind placebo-controlled multicenter trial., *Annals of Neurology* **66**, 460-71 (2009).
183. R. Martin, A. Lutterotti, S. Miller, Use of modified cells for the treatment of multiple sclerosis. (2011).

184. T. Guillaume, D. B. Rubinstein, M. Symann, Immune reconstitution and immunotherapy after autologous hematopoietic stem cell transplantation., *Blood* **92**, 1471-90 (1998).
185. R. K. Burt et al., Treatment of autoimmune disease by intense immunosuppressive conditioning and autologous hematopoietic stem cell transplantation., *Blood* **92**, 3505-14 (1998).
186. G. L. Mancardi et al., Autologous hematopoietic stem cell transplantation suppresses Gd-enhanced MRI activity in MS., *Neurology* **57**, 62-8 (2001).
187. R. K. Burt et al., Hematopoietic stem cell transplantation for progressive multiple sclerosis: failure of a total body irradiation-based conditioning regimen to prevent disease progression in patients with high disability scores., *Blood* **102**, 2373-8 (2003).
188. G. Comi et al., Guidelines for autologous blood and marrow stem cell transplantation in multiple sclerosis: a consensus report written on behalf of the European Group for Blood and Marrow Transplantation and the European Charcot Foundation. BMT-MS Study Group., *Journal of Neurology* **247**, 376-82 (2000).
189. M. S. Freedman et al., The therapeutic potential of mesenchymal stem cell transplantation as a treatment for multiple sclerosis: consensus report of the International MSCT Study Group., *Multiple Sclerosis* **16**, 503-10 (2010).
190. C. M. Rice et al., Safety and feasibility of autologous bone marrow cellular therapy in relapsing-progressive multiple sclerosis., *Clinical Pharmacology and Therapeutics* **87**, 679-85 (2010).
191. B. Yamout et al., Bone marrow mesenchymal stem cell transplantation in patients with multiple sclerosis: a pilot study., *Journal of Neuroimmunology* **227**, 185-9 (2010).
192. E. Brand-Schieber, P. Werner, Calcium channel blockers ameliorate disease in a mouse model of multiple sclerosis., *Experimental Neurology* **189**, 5-9 (2004).
193. D. A. Bechtold et al., Axonal protection achieved in a model of multiple sclerosis using lamotrigine., *Journal of Neurology* **253**, 1542-51 (2006).
194. B. Breuer et al., A randomized, double-blind, placebo-controlled, two-period, crossover, pilot trial of lamotrigine in patients with central pain due to multiple sclerosis., *Clinical Therapeutics* **29**, 2022-30 (2007).
195. M. Sakurai, I. Kanazawa, Positive symptoms in multiple sclerosis: their treatment with sodium channel blockers, lidocaine and mexiletine., *Journal of the Neurological Sciences* **162**, 162-8 (1999).
196. A. D. Goodman et al., Sustained-release oral fampridine in multiple sclerosis: a randomised, double-blind, controlled trial., *Lancet* **373**, 732-8 (2009).
197. T. Smith, A. Groom, B. Zhu, L. Turski, Autoimmune encephalomyelitis ameliorated by AMPA antagonists., *Nature Medicine* **6**, 62-6 (2000).
198. C. Paul, C. Bolton, Modulation of blood-brain barrier dysfunction and neurological deficits during acute experimental allergic encephalomyelitis by the N-methyl-D-aspartate receptor antagonist memantine., *The Journal of Pharmacology and Experimental Therapeutics* **302**, 50-7 (2002).

199. H. Ehrenreich et al., Exploring recombinant human erythropoietin in chronic progressive multiple sclerosis., *Brain* **130**, 2577-88 (2007).
200. Y. Sagot, R. Vejsada, A. C. Kato, Clinical and molecular aspects of motoneurone diseases: animal models, neurotrophic factors and Bcl-2 oncoprotein., *Trends in Pharmacological Sciences* **18**, 330-7 (1997).
201. K. Steinbach et al., Nogo-receptors NgR1 and NgR2 do not mediate regulation of CD4 T helper responses and CNS repair in experimental autoimmune encephalomyelitis., *PLoS One* **6**, e26341 (2011).
202. M. Reindl et al., Serum and cerebrospinal fluid antibodies to Nogo-A in patients with multiple sclerosis and acute neurological disorders., *Journal of Neuroimmunology* **145**, 139-47 (2003).
203. C. S. Raine, L. B. Barnett, A. Brown, T. Behar, D. E. McFarlin, Neuropathology of experimental allergic encephalomyelitis in inbred strains of mice., *Laboratory Investigation* **43**, 150-7 (1980).
204. P. Y. Paterson, D. G. Drobish, M. A. Hanson, A. F. Jacobs, Induction of experimental allergic encephalomyelitis in Lewis rats., *International Archives of Allergy and Applied Immunology* **37**, 26-40 (1970).
205. H. M. Wiśniewski, a B. Keith, Chronic relapsing experimental allergic encephalomyelitis: an experimental model of multiple sclerosis., *Annals of Neurology* **1**, 144-8 (1977).
206. L. Massacesi et al., Active and passively induced experimental autoimmune encephalomyelitis in common marmosets: a new model for multiple sclerosis., *Annals of Neurology* **37**, 519-30 (1995).
207. J. Freund, The mode of action of immunologic adjuvants., *Bibliotheca Tuberculosea* , 130-48 (1956).
208. S. D. Miller, W. J. Karpus, T. S. Davidson, Experimental autoimmune encephalomyelitis in the mouse., *Current Protocols in Immunology* **Chapter 15**, Unit 15.1 (2010).
209. C. Feurer, D. E. Prentice, S. Cammisuli, Chronic relapsing experimental allergic encephalomyelitis in the Lewis rat., *Journal of Neuroimmunology* **10**, 159-66 (1985).
210. S. Amor, P. a. Smith, B. 't Hart, D. Baker, Biozzi mice: of mice and human neurological diseases., *Journal of Neuroimmunology* **165**, 1-10 (2005).
211. D. O. Willenborg, Experimental allergic encephalomyelitis in the Lewis rat: studies on the mechanism of recovery from disease and acquired resistance to reinduction., *Journal of Immunology* **123**, 1145-50 (1979).
212. S. B. Su et al., Essential role of the MyD88 pathway, but nonessential roles of TLRs 2, 4, and 9, in the adjuvant effect promoting Th1-mediated autoimmunity., *Journal of Immunology* **175**, 6303-10 (2005).
213. M. A. Friese et al., The value of animal models for drug development in multiple sclerosis., *Brain* **129**, 1940-52 (2006).

214. K. P. Johnson et al., Copolymer 1 reduces relapse rate and improves disability in relapsing-remitting multiple sclerosis: results of a phase III multicenter, double-blind placebo-controlled trial. The Copolymer 1 Multiple Sclerosis Study Group., *Neurology* **45**, 1268-76 (1995).
215. J. W. Gregersen et al., Functional epistasis on a common MHC haplotype associated with multiple sclerosis., *Nature* **443**, 574-7 (2006).
216. M. A. Friese et al., Opposing effects of HLA class I molecules in tuning autoreactive CD8+ T cells in multiple sclerosis., *Nature Medicine* **14**, 1227-35 (2008).
217. H. Waldner, M. Collins, V. K. Kuchroo, Activation of antigen-presenting cells by microbial products breaks self tolerance and induces autoimmune disease., *The Journal of Clinical Investigation* **113**, 990-7 (2004).
218. J. J. Lafaille, K. Nagashima, M. Katsuki, S. Tonegawa, High incidence of spontaneous autoimmune encephalomyelitis in immunodeficient anti-myelin basic protein T cell receptor transgenic mice., *Cell* **78**, 399-408 (1994).
219. G. Krishnamoorthy, H. Lassmann, H. Wekerle, A. Holz, Spontaneous opticospinal encephalomyelitis in a double-transgenic mouse model of autoimmune T cell/B cell cooperation., *The Journal of Clinical Investigation* **116**, 2385-92 (2006).
220. K. Berer et al., Commensal microbiota and myelin autoantigen cooperate to trigger autoimmune demyelination., *Nature* **479**, 538-541 (2011).
221. J. Yuan, S. Shaham, S. Ledoux, H. M. Ellis, H. R. Horvitz, The *C. elegans* cell death gene *ced-3* encodes a protein similar to mammalian interleukin-1 beta-converting enzyme., *Cell* **75**, 641-52 (1993).
222. D. J. McConkey, Biochemical determinants of apoptosis and necrosis., *Toxicology Letters* **99**, 157-68 (1998).
223. R. J. Davis, Signal transduction by the JNK group of MAP kinases., *Cell* **103**, 239-52 (2000).
224. R. J. Davis, MAPKs: new JNK expands the group., *Trends in Biochemical Sciences* **19**, 470-3 (1994).
225. M. Karin, Y. Cao, F. R. Greten, Z.-W. Li, NF-kappaB in cancer: from innocent bystander to major culprit., *Nature Reviews Cancer* **2**, 301-10 (2002).
226. B. Binétruy, T. Smeal, M. Karin, Ha-Ras augments c-Jun activity and stimulates phosphorylation of its activation domain., *Nature* **351**, 122-7 (1991).
227. D. A. Brenner, M. O'Hara, P. Angel, M. Chojkier, M. Karin, Prolonged activation of jun and collagenase genes by tumour necrosis factor-alpha., *Nature* **337**, 661-3 (1989).
228. E. Gulbins et al., FAS-induced apoptosis is mediated via a ceramide-initiated RAS signaling pathway., *Immunity* **2**, 341-51 (1995).
229. L. Scorrano, S. J. Korsmeyer, Mechanisms of cytochrome c release by proapoptotic BCL-2 family members., *Biochemical and Biophysical Research Communications* **304**, 437-44 (2003).

230. K. Schulze-Osthoff, D. Ferrari, M. Los, S. Wesselborg, M. E. Peter, Apoptosis signaling by death receptors., *European Journal of Biochemistry* **254**, 439-59 (1998).
231. O. Micheau, J. Tschopp, Induction of TNF receptor I-mediated apoptosis via two sequential signaling complexes., *Cell* **114**, 181-90 (2003).
232. C. Scaffidi, S. Kirchhoff, P. H. Krammer, M. E. Peter, Apoptosis signaling in lymphocytes., *Current Opinion in Immunology* **11**, 277-85 (1999).
233. L. Lartigue et al., Caspase-independent mitochondrial cell death results from loss of respiration, not cytotoxic protein release., *Molecular Biology of the Cell* **20**, 4871-84 (2009).
234. O. Korkina, A. Degterev, in *Wiley Encyclopedia of Chemical Biology*, (2008).
235. P. G. Munder, E. Ferber, M. Modolell, H. Fischer, The influence of various adjuvants on the metabolism of phospholipids in macrophages., *International Archives of Allergy and Applied Immunology* **36**, 117-28 (1969).
236. P. G. Munder, M. Modolell, E. Ferber, H. Fischer, Phospholipids in quartz-damaged macrophages., *Biochemische Zeitschrift* **344**, 310-3 (1966).
237. K. Burdzy, P. G. Munder, H. Fischer, O. Westphal, Increase in the phagocytosis of peritoneal macrophages by lysolecithin., *Zeitschrift für Naturforschung. Teil B* **19**, 1118-20 (1964).
238. P. G. Munder, M. Modolell, Adjuvant induced formation of lysophosphatides and their role in the immune response., *International Archives of Allergy and Applied Immunology* **45**, 133-5 (1973).
239. R. Andreesen et al., Selective destruction of human leukemic cells by alkyllysophospholipids., *Cancer Research* **38**, 3894-9 (1978).
240. R. Andreesen, M. Modolell, P. G. Munder, Selective sensitivity of chronic myelogenous leukemia cell populations to alkyllysophospholipids., *Blood* **54**, 519-23 (1979).
241. M. Modolell, R. Andreesen, W. Pahlke, U. Brugger, P. G. Munder, Disturbance of phospholipid metabolism during the selective destruction of tumor cells induced by alkyllysophospholipids., *Cancer Research* **39**, 4681-6 (1979).
242. G. S. Tarnowski et al., Effect of lysolecithin and analogs on mouse ascites tumors., *Cancer Research* **38**, 339-44 (1978).
243. M. R. Berger, P. G. Munder, D. Schmähl, O. Westphal, Influence of the alkyllysophospholipid ET-18-OCH₃ on methylnitrosourea-induced rat mammary carcinomas., *Oncology* **41**, 109-13 (1984).
244. G. Kny, thesis, University of Freiburg (1969).
245. I. Pascher, S. Sundell, H. Eibl, K. Harlos, The single crystal structure of octadecyl-2-methyl-glycero-phosphocholine monohydrate. A multilamellar structure with interdigitating head groups and hydrocarbon chains., *Chemistry and Physics of Lipids* **39**, 53-64 (1986).
246. W. R. Vogler et al., Autologous bone marrow transplantation in acute leukemia with marrow purged with alkyllysophospholipid., *Blood* **80**, 1423-9 (1992).

247. W. R. Vogler et al., A phase II trial of autologous bone marrow transplantation (ABMT) in acute leukemia with edelfosine purged bone marrow., *Advances in Experimental Medicine and Biology* **416**, 389-96 (1996).
248. W. R. Vogler, A. C. Olson, S. Okamoto, L. B. Somberg, L. Glasser, Experimental studies on the role of alkyl lysophospholipids in autologous bone marrow transplantation., *Lipids* **22**, 919-24 (1987).
249. H. Eibl, C. Unger, Hexadecylphosphocholine: a new and selective antitumor drug., *Cancer Treatment Reviews* **17**, 233-42 (1990).
250. F. Mollinedo, R. Martínez-Dalmau, M. Modolell, Early and selective induction of apoptosis in human leukemic cells by the alkyl-lysophospholipid ET-18-OCH₃., *Biochemical and Biophysical Research Communications* **192**, 603-9 (1993).
251. L. Diomedea et al., Induction of apoptosis in human leukemic cells by the ether lipid 1-octadecyl-2-methyl-rac-glycero-3-phosphocholine. A possible basis for its selective action., *International Journal of Cancer* **53**, 124-30 (1993).
252. C. Gajate et al., Intracellular triggering of Fas, independently of FasL, as a new mechanism of antitumor ether lipid-induced apoptosis., *International Journal of Cancer* **85**, 674-82 (2000).
253. F. Mollinedo et al., Selective induction of apoptosis in cancer cells by the ether lipid ET-18-OCH₃ (Edelfosine): molecular structure requirements, cellular uptake, and protection by Bcl-2 and Bcl-X(L)., *Cancer Research* **57**, 1320-8 (1997).
254. C. Gajate, F. Mollinedo, The antitumor ether lipid ET-18-OCH₃ induces apoptosis through translocation and capping of Fas/CD95 into membrane rafts in human leukemic cells., *Blood* **98**, 3860-3 (2001).
255. A. H. van der Luit, M. Budde, P. Ruurs, M. Verheij, W. J. van Blitterswijk, Alkyl-lysophospholipid accumulates in lipid rafts and induces apoptosis via raft-dependent endocytosis and inhibition of phosphatidylcholine synthesis., *The Journal of Biological Chemistry* **277**, 39541-7 (2002).
256. K. Fujiwara, L. W. Daniel, E. J. Modest, C. A. Wallen, Relationship of cell survival, drug dose, and drug uptake after 1-O-octadecyl-2-O-methyl-rac-glycero-3-phosphocholine treatment., *Cancer Chemotherapy and Pharmacology* **34**, 472-6 (1994).
257. R. L. van der Bend et al., Identification of a putative membrane receptor for the bioactive phospholipid, lysophosphatidic acid., *The EMBO Journal* **11**, 2495-501 (1992).
258. G. L. May et al., Plasma membrane lipid composition of vinblastine sensitive and resistant human leukaemic lymphoblasts., *International Journal of Cancer* **42**, 728-33 (1988).
259. D. R. Hoffman, L. H. Hoffman, F. Snyder, Cytotoxicity and metabolism of alkyl phospholipid analogues in neoplastic cells., *Cancer Research* **46**, 5803-9 (1986).
260. C. C. Geilen et al., Uptake, subcellular distribution and metabolism of the phospholipid analogue hexadecylphosphocholine in MDCK cells., *Biochimica et Biophysica Acta* **1211**, 14-22 (1994).

261. W. J. van Blitterswijk, H. Hilkmann, G. A. Storme, Accumulation of an alkyl lysophospholipid in tumor cell membranes affects membrane fluidity and tumor cell invasion., *Lipids* **22**, 820-3 (1987).
262. R. A. Zoeller, M. D. Layne, E. J. Modest, Animal cell mutants unable to take up biologically active glycerophospholipids., *Journal of Lipid Research* **36**, 1866-75 (1995).
263. S. R. Vink, A. H. van der Luit, J. B. Klarenbeek, M. Verheij, W. J. van Blitterswijk, Lipid rafts and metabolic energy differentially determine uptake of anti-cancer alkylphospholipids in lymphoma versus carcinoma cells., *Biochemical Pharmacology* **74**, 1456-65 (2007).
264. F. Muñoz-Martínez, C. Torres, S. Castanys, F. Gamarro, The anti-tumor alkylphospholipid perifosine is internalized by an ATP-dependent translocase activity across the plasma membrane of human KB carcinoma cells., *Biochimica et Biophysica Acta* **1778**, 530-40 (2008).
265. F. Muñoz-Martínez, C. Torres, S. Castanys, F. Gamarro, CDC50A plays a key role in the uptake of the anticancer drug perifosine in human carcinoma cells., *Biochemical Pharmacology* **80**, 793-800 (2010).
266. J. M. Clement, C. Kent, CTP:phosphocholine cytidyltransferase: insights into regulatory mechanisms and novel functions., *Biochemical and Biophysical Research Communications* **257**, 643-50 (1999).
267. A. H. van der Luit et al., A new class of anticancer alkylphospholipids uses lipid rafts as membrane gateways to induce apoptosis in lymphoma cells., *Molecular Cancer Therapeutics* **6**, 2337-45 (2007).
268. K. P. Boggs, C. O. Rock, S. Jackowski, Lysophosphatidylcholine attenuates the cytotoxic effects of the antineoplastic phospholipid 1-O-octadecyl-2-O-methyl-rac-glycero-3-phosphocholine., *The Journal of Biological Chemistry* **270**, 11612-8 (1995).
269. A. H. Van Der Luit, M. Budde, M. Verheij, W. J. Van Blitterswijk, Different modes of internalization of apoptotic alkyl-lysophospholipid and cell-rescuing lysophosphatidylcholine., *The Biochemical Journal* **374**, 747-53 (2003).
270. S. F. Zerp et al., Alkylphospholipids inhibit capillary-like endothelial tube formation in vitro: antiangiogenic properties of a new class of antitumor agents., *Anti-Cancer Drugs* **19**, 65-75 (2008).
271. T. Tsutsumi, A. Tokumura, S. Kitazawa, Undifferentiated HL-60 cells internalize an antitumor alkyl ether phospholipid more rapidly than resistant K562 cells., *Biochimica et Biophysica Acta* **1390**, 73-84 (1998).
272. C. Gajate, F. Gonzalez-Camacho, F. Mollinedo, Involvement of raft aggregates enriched in Fas/CD95 death-inducing signaling complex in the antileukemic action of edelfosine in Jurkat cells., *PLoS One* **4**, e5044 (2009).
273. H. Sprong, P. van der Sluijs, G. van Meer, How proteins move lipids and lipids move proteins., *Nature Reviews Molecular Cell Biology* **2**, 504-13 (2001).
274. K. P. Boggs, C. O. Rock, S. Jackowski, Lysophosphatidylcholine and 1-O-octadecyl-2-O-methyl-rac-glycero-3-phosphocholine inhibit the CDP-choline pathway of phosphatidylcholine synthesis at the CTP:phosphocholine cytidyltransferase step., *The Journal of Biological Chemistry* **270**, 7757-64 (1995).

275. B. Ramos, M. El Mouedden, E. Claro, S. Jackowski, Inhibition of CTP:phosphocholine cytidyltransferase by C(2)-ceramide and its relationship to apoptosis., *Molecular Pharmacology* **62**, 1068-75 (2002).
276. K. P. Boggs, C. O. Rock, S. Jackowski, Lysophosphatidylcholine attenuates the cytotoxic effects of the antineoplastic phospholipid 1-O-octadecyl-2-O-methyl-rac-glycero-3-phosphocholine., *The Journal of Biological Chemistry* **270**, 11612-8 (1995).
277. K. Boggs, C. O. Rock, S. Jackowski, The antiproliferative effect of hexadecylphosphocholine toward HL60 cells is prevented by exogenous lysophosphatidylcholine., *Biochimica et Biophysica Acta* **1389**, 1-12 (1998).
278. I. Baburina, S. Jackowski, Apoptosis triggered by 1-O-octadecyl-2-O-methyl-rac-glycero-3-phosphocholine is prevented by increased expression of CTP:phosphocholine cytidyltransferase., *The Journal of Biological Chemistry* **273**, 2169-73 (1998).
279. M. H. M. van der Sanden, M. Houweling, D. Duijsings, A. B. Vaandrager, L. M. G. van Golde, Inhibition of phosphatidylcholine synthesis is not the primary pathway in hexadecylphosphocholine-induced apoptosis., *Biochimica et Biophysica Acta* **1636**, 99-107 (2004).
280. E. Gulbins et al., FAS-induced apoptosis is mediated via a ceramide-initiated RAS signaling pathway., *Immunity* **2**, 341-51 (1995).
281. W. J. van Blitterswijk, A. H. van der Luit, R. J. Veldman, M. Verheij, J. Borst, Ceramide: second messenger or modulator of membrane structure and dynamics?, *The Biochemical Journal* **369**, 199-211 (2003).
282. T. Nieto-Miguel et al., Endoplasmic reticulum stress in the proapoptotic action of edelfosine in solid tumor cells., *Cancer Research* **67**, 10368-78 (2007).
283. B. A. Wagner, G. R. Buettner, C. P. Burns, Increased generation of lipid-derived and ascorbate free radicals by L1210 cells exposed to the ether lipid edelfosine., *Cancer Research* **53**, 711-3 (1993).
284. L. A. Smets, H. Van Rooij, G. S. Salomons, Signalling steps in apoptosis by ether lipids., *Apoptosis* **4**, 419-27 (1999).
285. A. S. Vrablic, C. D. Albright, C. N. Craciunescu, R. I. Salganik, S. H. Zeisel, Altered mitochondrial function and overgeneration of reactive oxygen species precede the induction of apoptosis by 1-O-octadecyl-2-methyl-rac-glycero-3-phosphocholine in p53-defective hepatocytes., *The FASEB Journal* **15**, 1739-44 (2001).
286. H. Puthalakath et al., ER stress triggers apoptosis by activating BH3-only protein Bim., *Cell* **129**, 1337-49 (2007).
287. G. A. Ruiters, S. F. Zerp, H. Bartelink, W. J. van Blitterswijk, M. Verheij, Alkyllysophospholipids activate the SAPK/JNK pathway and enhance radiation-induced apoptosis., *Cancer Research* **59**, 2457-63 (1999).
288. C. Gajate, A. Santos-Beneit, M. Modolell, F. Mollinedo, Involvement of c-Jun NH2-terminal kinase activation and c-Jun in the induction of apoptosis by the ether phospholipid 1-O-octadecyl-2-O-methyl-rac-glycero-3-phosphocholine., *Molecular Pharmacology* **53**, 602-12 (1998).

289. T. Nieto-Miguel, C. Gajate, F. Mollinedo, Differential targets and subcellular localization of antitumor alkyl-lysophospholipid in leukemic versus solid tumor cells., *The Journal of Biological Chemistry* **281**, 14833-40 (2006).
290. T. Nieto-Miguel, C. Gajate, F. González-Camacho, F. Mollinedo, Proapoptotic role of Hsp90 by its interaction with c-Jun N-terminal kinase in lipid rafts in edelfosine-mediated antileukemic therapy., *Oncogene* **27**, 1779-87 (2008).
291. W. Kugler et al., MAP kinase pathways involved in glioblastoma response to erucylphosphocholine., *International Journal of Oncology* **25**, 1721-7 (2004).
292. M. Verheij et al., Requirement for ceramide-initiated SAPK/JNK signalling in stress-induced apoptosis., *Nature* **380**, 75-9 (1996).
293. E. Goillot et al., Mitogen-activated protein kinase-mediated Fas apoptotic signaling pathway., *Proceedings of the National Academy of Sciences of the United States of America* **94**, 3302-7 (1997).
294. B. W. Zanke et al., The stress-activated protein kinase pathway mediates cell death following injury induced by cis-platinum, UV irradiation or heat., *Current Biology* **6**, 606-13 (1996).
295. S. Kharbanda et al., Translocation of SAPK/JNK to mitochondria and interaction with Bcl-x(L) in response to DNA damage., *The Journal of Biological Chemistry* **275**, 322-7 (2000).
296. H. Aoki et al., Direct activation of mitochondrial apoptosis machinery by c-Jun N-terminal kinase in adult cardiac myocytes., *The Journal of Biological Chemistry* **277**, 10244-50 (2002).
297. L. W. Daniel et al., Ether lipids inhibit the effects of phorbol diester tumor promoters., *Lipids* **22**, 851-5 (1987).
298. Z. Kiss, K. S. Crilly, Alkyl lysophospholipids inhibit phorbol ester-stimulated phospholipase D activity and DNA synthesis in fibroblasts., *FEBS Letters* **412**, 313-7 (1997).
299. L. Lucas, R. Hernández-Alcoceba, V. Penalva, J. C. Lacal, Modulation of phospholipase D by hexadecylphosphorylcholine: a putative novel mechanism for its antitumoral activity., *Oncogene* **20**, 1110-7 (2001).
300. P. Drings et al., Final evaluation of a phase II study on the effect of edelfosine (an ether lipid) in advanced non-small-cell bronchogenic carcinoma., *Onkologie* **15**, 375-382 (1992).
301. F. Mollinedo, Antitumour ether lipids: proapoptotic agents with multiple therapeutic indications, *Expert Opinion on Therapeutic Patents* **17**, 385-405 (2007).
302. S. R. Vink et al., Phase I and pharmacokinetic study of combined treatment with perifosine and radiation in patients with advanced solid tumours., *Radiotherapy and Oncology* **80**, 207-13 (2006).
303. P. G. Munder, O. Westphal, Antitumoral and other biomedical activities of synthetic ether lysophospholipids., *Chemical Immunology* **49**, 206-35 (1990).

304. A. Klein-Franke, P. G. Munder, Alkyllysophospholipid prevents induction of experimental allergic encephalomyelitis, *Journal of Autoimmunity* **5**, 83-91 (1992).
305. V. Achterberg, G. Gercken, Cytotoxicity of ester and ether lysophospholipids on *Leishmania donovani* promastigotes., *Molecular and Biochemical Parasitology* **23**, 117-22 (1987).
306. C. Gajate, F. Mollinedo, Biological activities, mechanisms of action and biomedical prospect of the antitumor ether phospholipid ET-18-OCH₃ (edelfosine), a proapoptotic agent in tumor cells., *Current Drug Metabolism* **3**, 491-525 (2002).
307. F. Mollinedo, C. Gajate, S. Martín-Santamaría, F. Gago, ET-18-OCH₃ (edelfosine): a selective antitumour lipid targeting apoptosis through intracellular activation of Fas/CD95 death receptor., *Current Medicinal Chemistry* **11**, 3163-84 (2004).
308. W. J. van Blitterswijk, M. Verheij, Anticancer alkylphospholipids: mechanisms of action, cellular sensitivity and resistance, and clinical prospects., *Current Pharmaceutical Design* **14**, 2061-74 (2008).
309. H. Nakano, M. Yanagita, M. D. Gunn, CD11c(+)B220(+)Gr-1(+) cells in mouse lymph nodes and spleen display characteristics of plasmacytoid dendritic cells., *The Journal of experimental medicine* **194**, 1171-8 (2001).
310. Y. Han, Q. Guo, M. Zhang, Z. Chen, X. Cao, CD69⁺ CD4⁺ CD25⁻ T cells, a new subset of regulatory T cells, suppress T cell proliferation through membrane-bound TGF-β1., *Journal of Immunology* **182**, 111-20 (2009).
311. M. Schmied et al., Apoptosis of T lymphocytes in experimental autoimmune encephalomyelitis. Evidence for programmed cell death as a mechanism to control inflammation in the brain., *The American Journal of Pathology* **143**, 446-52 (1993).
312. C. Cabaner et al., Induction of apoptosis in human mitogen-activated peripheral blood T-lymphocytes by the ether phospholipid ET-18-OCH₃: Involvement of the Fas receptor/ligand system, *British Journal of Pharmacology* , 813-825 (1999).
313. M. van Engeland, F. C. Ramaekers, B. Schutte, C. P. Reutelingsperger, A novel assay to measure loss of plasma membrane asymmetry during apoptosis of adherent cells in culture., *Cytometry* **24**, 131-9 (1996).
314. D. W. Huang, B. T. Sherman, R. A. Lempicki, Systematic and integrative analysis of large gene lists using DAVID bioinformatics resources., *Nature Protocols* **4**, 44-57 (2009).
315. P. Serrano-Fernández et al., Time course transcriptomics of IFNβ1 drug therapy in multiple sclerosis., *Autoimmunity* **43**, 172-8 (2010).
316. K. Agematsu et al., Generation of plasma cells from peripheral blood memory B cells: synergistic effect of interleukin-10 and CD27/CD70 interaction., *Blood* **91**, 173-80 (1998).
317. S. Jacquot, T. Kobata, S. Iwata, Chikao Morimoto, S. F. Schlossman, CD154/CD40 and CD70/CD27 interactions have different and sequential functions in T cell-dependent B cell responses, *Journal of Immunology* **159**, 2652-2657 (1997).

318. R. Andreesen, M. Modolell, H. U. Weltzien, P. G. Munder, Alkyl-lysophospholipid induced suppression of human lymphocyte response to mitogens and selective killing of lymphoblasts., *Immunobiology* **156**, 498-508 (1980).
319. D. Chabannes, B. Ryffel, J.-F. Borel, SRI 62-834 , a cyclic ether analogue of the phospholipid ET-18-OCH₃ displays long-lasting beneficial effect in chronic relapsing experimental allergic encephalomyelitis in the Lewis rat. Comparison with Cyclosporin and (Val²)-dihydrocyclosporin effects in, *Journal of Autoimmunity* , 199-211 (1992).
320. J. Kovarik, D. Chabannes, J. F. Borel, Immunoregulation and drug treatment in chronic relapsing experimental allergic encephalomyelitis in the Lewis rat, *International Journal of Immunopharmacology* **17**, 255-263 (1995).
321. D. Baker, J. K. O'Neill, S. Amor, M. A. Khamashta, J. L. Turk, Inhibition of the chronic relapsing experimental allergic encephalomyelitis in the mouse by the alkyl-lysophospholipid ET-18-OCH₃, *International Journal of Immunopharmacology* **13**, 385-392 (1991).
322. R. J. De Boer, D. Homann, A. S. Perelson, Different dynamics of CD4⁺ and CD8⁺ T cell responses during and after acute lymphocytic choriomeningitis virus infection., *Journal of Immunology* **171**, 3928-35 (2003).
323. J. K. Whitmire et al., CD40-CD40 ligand costimulation is required for generating antiviral CD4 T cell responses but is dispensable for CD8 T cell responses., *Journal of Immunology* **163**, 3194-201 (1999).
324. M. Kopf et al., OX40-deficient mice are defective in Th cell proliferation but are competent in generating B cell and CTL Responses after virus infection., *Immunity* **11**, 699-708 (1999).
325. S. J. Szabo et al., Distinct effects of T-bet in TH1 lineage commitment and IFN-gamma production in CD4 and CD8 T cells., *Science* **295**, 338-42 (2002).
326. T. M. Kündig et al., Duration of TCR stimulation determines costimulatory requirement of T cells., *Immunity* **5**, 41-52 (1996).
327. G. Iezzi, K. Karjalainen, A. Lanzavecchia, The duration of antigenic stimulation determines the fate of naive and effector T cells., *Immunity* **8**, 89-95 (1998).
328. S. M. Kaech, E. J. Wherry, R. Ahmed, Effector and memory T-cell differentiation: implications for vaccine development., *Nature Reviews Immunology* **2**, 251-62 (2002).
329. R. Bhamra et al., Activity, pharmacokinetics and tissue distribution of TLC ELL-12 (liposomal antitumor ether lipid) in rats with transplantable, s.c. methylnitrosourea-induced tumors., *Anti-Cancer Drugs* **14**, 481-6 (2003).
330. J. Kötting, N. W. Marschner, W. Neumüller, C. Unger, H. Eibl, Hexadecylphosphocholine and octadecyl-methyl-glycero-3-phosphocholine: a comparison of hemolytic activity, serum binding and tissue distribution., *Progress in Experimental Tumor Research* **34**, 131-42 (1992).
331. A. Estella-Hermoso de Mendoza et al., Antitumor alkyl ether lipid edelfosine: tissue distribution and pharmacokinetic behavior in healthy and tumor-bearing immunosuppressed mice., *Clinical Cancer Research* **15**, 858-64 (2009).

332. B. L. McRae, C. L. Vanderlugt, M. C. Dal Canto, S. D. Miller, Functional evidence for epitope spreading in the relapsing pathology of experimental autoimmune encephalomyelitis., *The Journal of Experimental Medicine* **182**, 75-85 (1995).
333. C. L. Vanderlugt, S. D. Miller, Epitope spreading in immune-mediated diseases: implications for immunotherapy., *Nature Reviews Immunology* **2**, 85-95 (2002).
334. H. Wekerle, C. Linington, H. Lassmann, R. Meyermann, Cellular immune reactivity within the CNS, *Trends in Neurosciences* **8**, 271-277 (1986).
335. A. J. Coles et al., Monoclonal antibody treatment exposes three mechanisms underlying the clinical course of multiple sclerosis., *Annals of Neurology* **46**, 296-304 (1999).
336. A. Ben-Nun, H. Wekerle, I. R. Cohen, The rapid isolation of clonable antigen-specific T lymphocyte lines capable of mediating autoimmune encephalomyelitis., *European Journal of Immunology* **11**, 195-9 (1981).
337. H. Wekerle, K. Kojima, J. Lannes-Vieira, H. Lassmann, C. Linington, Animal models., *Annals of Neurology* **36 Suppl**, S47-53 (1994).
338. V. Viglietta, C. Baecher-Allan, H. L. Weiner, D. A. Hafler, Loss of functional suppression by CD4+CD25+ regulatory T cells in patients with multiple sclerosis., *The Journal of Experimental Medicine* **199**, 971-9 (2004).
339. J. Haas et al., Reduced suppressive effect of CD4+CD25high regulatory T cells on the T cell immune response against myelin oligodendrocyte glycoprotein in patients with multiple sclerosis., *European Journal of Immunology* **35**, 3343-52 (2005).
340. M. J. McGeachy, L. A. Stephens, S. M. Anderson, Natural recovery and protection from autoimmune encephalomyelitis: contribution of CD4+CD25+ regulatory cells within the central nervous system., *Journal of Immunology* **175**, 3025-32 (2005).
341. X. Zhang, IL-10 is involved in the suppression of experimental autoimmune encephalomyelitis by CD25+CD4+ regulatory T cells, *International Immunology* **16**, 249-256 (2004).
342. P. Yu et al., Functions against experimental allergic encephalomyelitis upon activation with cognate antigen 1, *The Journal of Immunology* (2005).
343. R. K. Gershon, K. Kondo, Cell interactions in the induction of tolerance: the role of thymic lymphocytes., *Immunology* **18**, 723-37 (1970).
344. Y. Chen, V. K. Kuchroo, J. Inobe, D. A. Hafler, H. L. Weiner, Regulatory T cell clones induced by oral tolerance: suppression of autoimmune encephalomyelitis, *Science* **265**, 1237-1240 (1994).
345. H. Groux et al., A CD4+ T-cell subset inhibits antigen-specific T-cell responses and prevents colitis., *Nature* **389**, 737-42 (1997).
346. B. Charlton, K. J. Lafferty, The Th1/Th2 balance in autoimmunity., *Current Opinion in Immunology* **7**, 793-8 (1995).
347. C. L. Langrish et al., IL-23 drives a pathogenic T cell population that induces autoimmune inflammation., *The Journal of Experimental Medicine* **201**, 233-40 (2005).

348. B. Becher, B. G. Durell, R. J. Noelle, Experimental autoimmune encephalitis and inflammation in the absence of interleukin-12, *Journal of Clinical Investigation* **110**, 493-497 (2002).
349. D. J. Cua et al., Interleukin-23 rather than interleukin-12 is the critical cytokine for autoimmune inflammation of the brain., *Nature* **421**, 744-8 (2003).
350. D. Sun et al., Myelin antigen-specific CD8+ T cells are encephalitogenic and produce severe disease in C57BL/6 mice., *Journal of Immunology* **166**, 7579-87 (2001).
351. W. F. Hickey, B. L. Hsu, H. Kimura, T-lymphocyte entry into the central nervous system., *Journal of Neuroscience Research* **28**, 254-60 (1991).
352. K. Chiba et al., FTY720, a novel immunosuppressant possessing unique mechanisms. I. Prolongation of skin allograft survival and synergistic effect in combination with cyclosporine in rats., *Transplantation Proceedings* **28**, 1056-9 (1996).
353. T. Fujita et al., Potent immunosuppressants, 2-alkyl-2-aminopropane-1,3-diols., *Journal of Medicinal Chemistry* **39**, 4451-9 (1996).
354. D. Oz-Arslan et al., IL-6 and IL-8 release is mediated via multiple signaling pathways after stimulating dendritic cells with lysophospholipids., *Journal of Leukocyte Biology* **80**, 287-97 (2006).
355. H. Rosen, E. J. Goetzl, Sphingosine 1-phosphate and its receptors: an autocrine and paracrine network., *Nature Reviews Immunology* **5**, 560-70 (2005).
356. M. C. Dieu et al., Selective recruitment of immature and mature dendritic cells by distinct chemokines expressed in different anatomic sites., *The Journal of Experimental Medicine* **188**, 373-86 (1998).
357. S. Yanagihara, E. Komura, J. Nagafune, H. Watarai, Y. Yamaguchi, EBI1/CCR7 is a new member of dendritic cell chemokine receptor that is up-regulated upon maturation., *Journal of immunology (Baltimore, Md. : 1950)* **161**, 3096-102 (1998).
358. F. Sallusto et al., Rapid and coordinated switch in chemokine receptor expression during dendritic cell maturation., *European Journal of Immunology* **28**, 2760-9 (1998).
359. K. Reif et al., Balanced responsiveness to chemoattractants from adjacent zones determines B-cell position., *Nature* **416**, 94-9 (2002).
360. V. N. Ngo, H. L. Tang, J. G. Cyster, Epstein-Barr virus-induced molecule 1 ligand chemokine is expressed by dendritic cells in lymphoid tissues and strongly attracts naive T cells and activated B cells., *The Journal of experimental medicine* **188**, 181-91 (1998).
361. F. Sallusto, D. Lenig, R. Förster, M. Lipp, A. Lanzavecchia, Two subsets of memory T lymphocytes with distinct homing potentials and effector functions., *Nature* **401**, 708-12 (1999).
362. B. Arnold, R. Reuther, H. U. Weltzien, Distribution and metabolism of synthetic alkyl analogs of lysophosphatidylcholine in mice., *Biochimica et Biophysica Acta* **530**, 47-55 (1978).

363. R. A. Read, E. E. Moore, F. A. Moore, V. S. Carl, A. Banerjee, Platelet-activating factor-induced polymorphonuclear neutrophil priming independent of CD11b adhesion., *Surgery* **114**, 308-13 (1993).
364. M. Chignard, J. P. Le Couedic, M. Tence, B. B. Vargaftig, J. Benveniste, The role of platelet-activating factor in platelet aggregation., *Nature* **279**, 799-800 (1979).
365. J. T. O'Flaherty et al., 1-O-Alkyl-sn-glycerol-3-phosphorylcholines: a novel class of neutrophil stimulants., *The American Journal of Pathology* **103**, 70-8 (1981).
366. M. T. Alonso et al., Dissociation of the effects of the antitumour ether lipid ET-18-OCH₃ on cytosolic calcium and on apoptosis., *British Journal of Pharmacology* **121**, 1364-8 (1997).
367. S. D. Miller, E. J. McMahon, B. Schreiner, S. L. Bailey, Antigen presentation in the CNS by myeloid dendritic cells drives progression of relapsing experimental autoimmune encephalomyelitis., *Annals of the New York Academy of Sciences* **1103**, 179-91 (2007).
368. T. Takahashi et al., Immunologic self-tolerance maintained by CD25+CD4+ naturally anergic and suppressive T cells: induction of autoimmune disease by breaking their anergic/suppressive state., *International immunology* **10**, 1969-80 (1998).
369. A. M. Thornton, E. M. Shevach, CD4+CD25+ immunoregulatory T cells suppress polyclonal T cell activation in vitro by inhibiting interleukin 2 production., *The Journal of Experimental Medicine* **188**, 287-96 (1998).
370. a M. Thornton, E. M. Shevach, Suppressor effector function of CD4+CD25+ immunoregulatory T cells is antigen nonspecific., *Journal of Immunology* **164**, 183-90 (2000).
371. C.-T. Huang et al., Role of LAG-3 in regulatory T cells., *Immunity* **21**, 503-13 (2004).
372. S. Sakaguchi, Naturally arising CD4+ regulatory t cells for immunologic self-tolerance and negative control of immune responses., *Annual Review of Immunology* **22**, 531-62 (2004).
373. F. Fallarino et al., The combined effects of tryptophan starvation and tryptophan catabolites down-regulate T cell receptor zeta-chain and induce a regulatory phenotype in naive T cells., *Journal of Immunology* **176**, 6752-61 (2006).
374. B. L. McRae, S. D. Miller, Fine specificity of CD4+ T cell responses to the dominant encephalitogenic PLP 139-151 peptide in SJL/J mice., *Neurochemical Research* **19**, 997-1004 (1994).
375. R. Zeine, T. Owens, Loss rather than downregulation of CD4+ T cells as a mechanism for remission from experimental allergic encephalomyelitis., *Journal of Neuroimmunology* **44**, 193-8 (1993).
376. M. A. Friese, L. Fugger, Autoreactive CD8+ T cells in multiple sclerosis: a new target for therapy?, *Brain* **128**, 1747-63 (2005).
377. R. A. Linker et al., EAE in beta-2 microglobulin-deficient mice: axonal damage is not dependent on MHC-I restricted immune responses., *Neurobiology of Disease* **19**, 218-28 (2005).

378. G. Das, S. Sheridan, C. A. Janeway, The Source of Early IFN- γ That Plays a Role in Th1 Priming, *Animals* (2011).
379. S.-J. Liu et al., Induction of a distinct CD8 Tnc17 subset by transforming growth factor-beta and interleukin-6., *Journal of Leukocyte Biology* **82**, 354-60 (2007).
380. S. Takeda, H. R. Rodewald, H. Arakawa, H. Bluethmann, T. Shimizu, MHC class II molecules are not required for survival of newly generated CD4+ T cells, but affect their long-term life span., *Immunity* **5**, 217-28 (1996).
381. T. Brocker, Survival of mature CD4 T lymphocytes is dependent on major histocompatibility complex class II-expressing dendritic cells., *The Journal of Experimental Medicine* **186**, 1223-32 (1997).
382. J. Kirberg, A. Berns, H. von Boehmer, Peripheral T cell survival requires continual ligation of the T cell receptor to major histocompatibility complex-encoded molecules., *The Journal of Experimental Medicine* **186**, 1269-75 (1997).
383. L. Vivien, C. Benoist, D. Mathis, T lymphocytes need IL-7 but not IL-4 or IL-6 to survive in vivo., *International Immunology* **13**, 763-8 (2001).
384. J. T. Tan et al., IL-7 is critical for homeostatic proliferation and survival of naive T cells., *Proceedings of the National Academy of Sciences of the United States of America* **98**, 8732-7 (2001).
385. B. Ernst, D. S. Lee, J. M. Chang, J. Sprent, C. D. Surh, The peptide ligands mediating positive selection in the thymus control T cell survival and homeostatic proliferation in the periphery., *Immunity* **11**, 173-81 (1999).
386. C. Viret, F. S. Wong, C. a Janeway, Designing and maintaining the mature TCR repertoire: the continuum of self-peptide:self-MHC complex recognition., *Immunity* **10**, 559-68 (1999).
387. T. Kondo et al., Dendritic cells signal T cells in the absence of exogenous antigen., *Nature Immunology* **2**, 932-8 (2001).
388. P. Revy, M. Sospedra, B. Barbour, A. Trautmann, Functional antigen-independent synapses formed between T cells and dendritic cells., *Nature Immunology* **2**, 925-31 (2001).
389. C. Gajate et al., Intracellular triggering of Fas aggregation and recruitment of apoptotic molecules into Fas-enriched rafts in selective tumor cell apoptosis., *The Journal of Experimental Medicine* **200**, 353-65 (2004).
390. Z. Kiss, K. S. Crilly, Alkyl lysophospholipids inhibit phorbol ester-stimulated phospholipase D activity and DNA synthesis in fibroblasts, *FEBS Letters* **412**, 313-317 (1997).
391. Y. Devary, R. A. Gottlieb, L. F. Lau, M. Karin, Rapid and preferential activation of the c-jun gene during the mammalian UV response., *Molecular and Cellular Biology* **11**, 2804-11 (1991).
392. Y. Manome et al., Coinduction of c-jun gene expression and internucleosomal DNA fragmentation by ionizing radiation., *Biochemistry* **32**, 10607-13 (1993).

393. E. Bossy-Wetzel, L. Bakiri, M. Yaniv, Induction of apoptosis by the transcription factor c-Jun., *The EMBO Journal* **16**, 1695-709 (1997).
394. T. Smeal, B. Binetruy, D. A. Mercola, M. Birrer, M. Karin, Oncogenic and transcriptional cooperation with Ha-Ras requires phosphorylation of c-Jun on serines 63 and 73., *Nature* **354**, 494-6 (1991).
395. A. X. Liu, W. Du, J. P. Liu, T. M. Jessell, G. C. Prendergast, RhoB alteration is necessary for apoptotic and antineoplastic responses to farnesyltransferase inhibitors., *Molecular and Cellular Biology* **20**, 6105-13 (2000).
396. H. S. Ko, S. M. Fu, R. J. Winchester, D. T. Yu, H. G. Kunkel, Ia determinants on stimulated human T lymphocytes. Occurrence on mitogen- and antigen-activated T cells., *The Journal of Experimental Medicine* **150**, 246-55 (1979).
397. A. Lanzavecchia, E. Roosnek, T. Gregory, P. Berman, S. Abrignani, T cells can present antigens such as HIV gp120 targeted to their own surface molecules., *Nature* **334**, 530-2 (1988).
398. J. M. LaSalle, K. Ota, D. a Hafler, Presentation of autoantigen by human T cells., *Journal of Immunology* **147**, 774-80 (1991).
399. F. Di Rosa et al., HLA class II molecules transduce accessory signals affecting the CD3 but not the interleukin-2 activation pathway in T blasts., *Human Immunology* **38**, 251-60 (1993).
400. E. Schooten, P. Klous, P. J. van den Elsen, T. M. Holling, Lack of MHC-II expression in activated mouse T cells correlates with DNA methylation at the CIITA-PIII region., *Immunogenetics* **57**, 795-9 (2005).
401. G. Roos, W. E. Berdel, Sensitivity of human hematopoietic cell lines to an alkyl-lysophospholipid-derivative., *Leukemia Research* **10**, 195-202 (1986).
402. O. Engebraaten, R. Bjerkgvig, M. E. Berens, Effect of alkyl-lysophospholipid on glioblastoma cell invasion into fetal rat brain tissue in vitro., *Cancer Research* **51**, 1713-9 (1991).
403. P. Principe, C. Sidoti, P. Braquet, Tumor cell kinetics following antineoplastic ether phospholipid treatment., *Cancer Research* **52**, 2509-15 (1992).
404. P. Principe, C. Sidoti, H. Coulomb, C. Broquet, P. Braquet, Tumor cell kinetics following long-term treatment with antineoplastic ether phospholipids., *Cancer Detection and Prevention* **18**, 393-400 (1994).
405. K. Fujiwara, E. J. Modest, C. A. Wallen, Cell kill and cytostasis by ET-18-OCH₃ and heat., *Anticancer Research* **15**, 1333-8.
406. M. Lohmeyer, P. Workman, Growth arrest vs direct cytotoxicity and the importance of molecular structure for the in vitro anti-tumour activity of ether lipids., *British Journal of Cancer* **72**, 277-86 (1995).
407. M. Y. Pushkareva, A. S. Janoff, E. Mayhew, Inhibition of cell division but not nuclear division by 1-O- octadecyl-2-O-methyl-Sn-glycero-3-phosphocholine., *Cell Biology International* **23**, 817-28 (1999).

408. G. A. Storme et al., Antiinvasive effect of racemic 1-O-octadecyl-2-O-methylglycero-3-phosphocholine on MO4 mouse fibrosarcoma cells in vitro., *Cancer Research* **45**, 351-7 (1985).
409. F. Mollinedo, C. Gajate, S. Martín-Santamaría, F. Gago, ET-18-OCH₃ (edelfosine): a selective antitumour lipid targeting apoptosis through intracellular activation of Fas/CD95 death receptor., *Current Medicinal Chemistry* **11**, 3163-84 (2004).
410. D. B. Herrmann, H. a Neumann, Cytotoxic ether phospholipids. Different affinities to lysophosphocholine acyltransferases in sensitive and resistant cells., *The Journal of Biological Chemistry* **261**, 7742-7 (1986).
411. C. Kent, Regulation of phosphatidylcholine biosynthesis., *Progress in Lipid Research* **29**, 87-105 (1990).
412. H. Tronchère, M. Record, F. Tercé, H. Chap, Phosphatidylcholine cycle and regulation of phosphatidylcholine biosynthesis by enzyme translocation., *Biochimica et Biophysica Acta* **1212**, 137-51 (1994).
413. C. Kent, Eukaryotic phospholipid biosynthesis., *Annual Review of Biochemistry* **64**, 315-43 (1995).
414. I. Baburina, S. Jackowski, Apoptosis triggered by 1-O-octadecyl-2-O-methyl-rac-glycero-3-phosphocholine is prevented by increased expression of CTP:phosphocholine cytidyltransferase., *The Journal of Biological Chemistry* **273**, 2169-73 (1998).
415. K. Maly et al., Interference of new alkylphospholipid analogues with mitogenic signal transduction., *Anticancer Drug Design* **10**, 411-25 (1995).
416. D. Strassheim, S. H. Shafer, S. H. Phelps, C. L. Williams, Small cell lung carcinoma exhibits greater phospholipase C-beta1 expression and edelfosine resistance compared with non-small cell lung carcinoma., *Cancer Research* **60**, 2730-6 (2000).
417. X. Lu, G. Arthur, The differential susceptibility of A427 and A549 cell lines to the growth-inhibitory effects of ET-18-OCH₃ does not correlate with the relative effects of the alkyl-lysophospholipid on the incorporation of fatty acids into cellular phospholipids., *Cancer Research* **52**, 2813-7 (1992).
418. X. Lu, G. Arthur, Perturbations of cellular acylation processes by the synthetic alkyl-lysophospholipid 1-O-octadecyl-2-O-methylglycero-3-phosphocholine do not correlate with inhibition of proliferation of MCF7 and T84 cell lines., *Cancer Research* **52**, 2806-12 (1992).
419. X. Zhou, G. Arthur, Effect of 1-O-octadecyl-2-O-methyl-glycerophosphocholine on phosphatidylcholine and phosphatidylethanolamine synthesis in MCF-7 and A549 cells and its relationship to inhibition of cell proliferation., *European Journal of Biochemistry* **232**, 881-8 (1995).
420. J. M. González-Navajas, J. Lee, M. David, E. Raz, Immunomodulatory functions of type I interferons, *Nature Reviews Immunology* , 1-11 (2012).
421. V. Brinkmann, T. Geiger, S. Alkan, A. Heusser, C. H., Interferon α increases the frequency of interferon γ -producing human CD4 + T cells, *Journal of Experimental Medicine* **178**, 1655-63 (1993).

422. B. L. P. Cousens et al., Two roads diverged: interferon α / β - and interleukin 12-mediated pathways in promoting T cell interferon γ responses during viral infection, *The Journal of Experimental Medicine* **189**, 1315–1327 (1999).
423. M.-L. Santiago-Raber et al., Type-I interferon receptor deficiency reduces lupus-like disease in NZB mice., *The Journal of experimental medicine* **197**, 777-88 (2003).
424. I. Tassioulas et al., Amplification of IFN- α -induced STAT1 activation and inflammatory function by Syk and ITAM-containing adaptors., *Nature Immunology* **5**, 1181-9 (2004).
425. L. G. M. van Baarsen et al., Pharmacogenomics of interferon-beta therapy in multiple sclerosis: baseline IFN signature determines pharmacological differences between patients., *PLoS One* **3**, e1927 (2008).
426. F. Sellebjerg et al., Gene expression analysis of interferon-beta treatment in multiple sclerosis., *Multiple Sclerosis* **14**, 615-21 (2008).
427. J. Hilpert et al., Biological response genes after single dose administration of interferon beta-1b to healthy male volunteers., *Journal of Neuroimmunology* **199**, 115-25 (2008).
428. M. K. Singh et al., Gene expression changes in peripheral blood mononuclear cells from multiple sclerosis patients undergoing beta-interferon therapy., *Journal of the Neurological Sciences* **258**, 52-9 (2007).
429. P. A. Muraro et al., Decreased integrin gene expression in patients with MS responding to interferon-beta treatment., *Journal of Neuroimmunology* **150**, 123-31 (2004).
430. O. C. Micali et al., Silencing of the XAF1 gene by promoter hypermethylation in cancer cells and reactivation to TRAIL-sensitization by IFN- β ., *BMC Cancer* **7**, 52 (2007).
431. S. Stürzebecher et al., Expression profiling identifies responder and non-responder phenotypes to interferon-beta in multiple sclerosis., *Brain* **126**, 1419-29 (2003).
432. L. Thyrell et al., Mechanisms of Interferon- α induced apoptosis in malignant cells, *Oncogene* (2002), doi:10.1038/sj/onc/1205179.
433. C. Selleri et al., Involvement of Fas-mediated apoptosis in the inhibitory effects of interferon- α in chronic myelogenous leukemia., *Blood* **89**, 957-64 (1997).
434. S. a Buechner et al., Regression of basal cell carcinoma by intralesional interferon- α treatment is mediated by CD95 (Apo-1/Fas)-CD95 ligand-induced suicide., *The Journal of Clinical Investigation* **100**, 2691-6 (1997).
435. A. Takaoka et al., Integration of interferon- α /beta signalling to p53 responses in tumour suppression and antiviral defence., *Nature* **424**, 516-23 (2003).
436. C. Porta et al., Interferons α and γ induce p53-dependent and p53-independent apoptosis, respectively., *Oncogene* **24**, 605-15 (2005).
437. M. Chawla-Sarkar, D. W. Leaman, E. C. Borden, Preferential induction of apoptosis by interferon (IFN)-beta compared with IFN- α 2: correlation with TRAIL/Apo2L induction in melanoma cell lines., *Clinical Cancer Research* **7**, 1821-31 (2001).

438. M. Comabella et al., Genome-wide scan of 500,000 single-nucleotide polymorphisms among responders and nonresponders to interferon beta therapy in multiple sclerosis., *Archives of Neurology* **66**, 972-8 (2009).
439. D. Wallach et al., Tumor necrosis factor receptor and Fas signaling mechanisms., *Annual Review of Immunology* **17**, 331-67 (1999).
440. M. R. Sprick et al., FADD/MORT1 and caspase-8 are recruited to TRAIL receptors 1 and 2 and are essential for apoptosis mediated by TRAIL receptor 2., *Immunity* **12**, 599-609 (2000).
441. J. Wang, H. J. Chun, W. Wong, D. M. Spencer, M. J. Lenardo, Caspase-10 is an initiator caspase in death receptor signaling., *PNAS* **98**, 13884-8 (2001).

9 Acknowledgments

Ich bedanke mich bei Prof. Dr. Roland Martin für die Möglichkeit, dass ich diese Arbeit im Institut für Neuroimmunologie und klinische Multiple Sklerose-Forschung (inims) des Zentrums für Molekulare Neurobiologie Hamburg, Universitätsklinikum Hamburg-Eppendorf (UKE) anfertigen konnte. Prof. Dr. Roland Martin und Prof. Dr. Axel R. Zander danke ich für die interessante Themenstellung und die erfahrene Unterstützung.

Ich möchte mich zudem bei Prof. Dr. Roland Martin für die hervorragende Betreuung, die gewährte wissenschaftliche Freiheit und das persönliche Engagement sowie die freundschaftliche Zusammenarbeit bedanken. Prof. Dr. Roland Martin danke ich auch für die Erstellung des Dissertationsgutachtens.

Prof. Dr. Matthias Kneussel danke ich für die Bereitschaft, die vorliegende Arbeit zu begutachten.

Ich bedanke mich herzlich bei Dr. Sabine Fleischer und Katja Husen für ihr großes Engagement für die Mitarbeiter des inims.

Mein großer Dank gilt zudem Dr. Karin Steinbach für die wertvolle Unterstützung, die freundschaftliche Zusammenarbeit und dafür, dass sie stets für mich ansprechbar war.

Ich danke allen Mitarbeitern des inims für das freundschaftliche Arbeitsklima, die gute Zusammenarbeit und Kollegialität sowie die lebhaften Diskussionen. Insbesondere danke ich Dr. Stefan Gold als Ansprechpartner für Fragen der Statistik, Benjamin Schattling für Diskussionen von Fragen der Immunhistochemie und Vera Rosbroj für die Unterstützung bei der Durchführung des Microarray-Versuchs.

PD Dr. Claudia Lange danke ich für viele hilfreiche Diskussionen und ihre Unterstützung auf dem Feld der therapeutischen Anwendung von mesenchymalen Stammzellen.

Ich bedanke mich bei Dr. Benjamin Otto und Kristin Klätschke für die wertvolle Unterstützung bei der Durchführung und Analyse des Microarray-Experiments. Dr. Christian Bernreuther danke ich dafür, dass er immer für mich ansprechbar war für Fragen der Histologie. Ich danke ihm ebenfalls für die Erstellung von Paraffin-Schnitten und histologischen Färbungen.

Ganz besonders bedanke ich mich bei meiner Familie, meinen Eltern, meinem Bruder und Ulrike, die mich immer unterstützt haben. Ich möchte mich auch bedanken bei allen Freundinnen und Freunden, die ich im Laufe dieser Arbeit kennen lernen durfte. Nicht zuletzt seid Ihr es, die den bisweilen erlebten Stress so gering erscheinen lasst in Anbetracht der gemeinsamen Zeit.